J Bruce Gemmell

Studies of VHMS-related alteration: geochemical and mineralogical vectors to ore

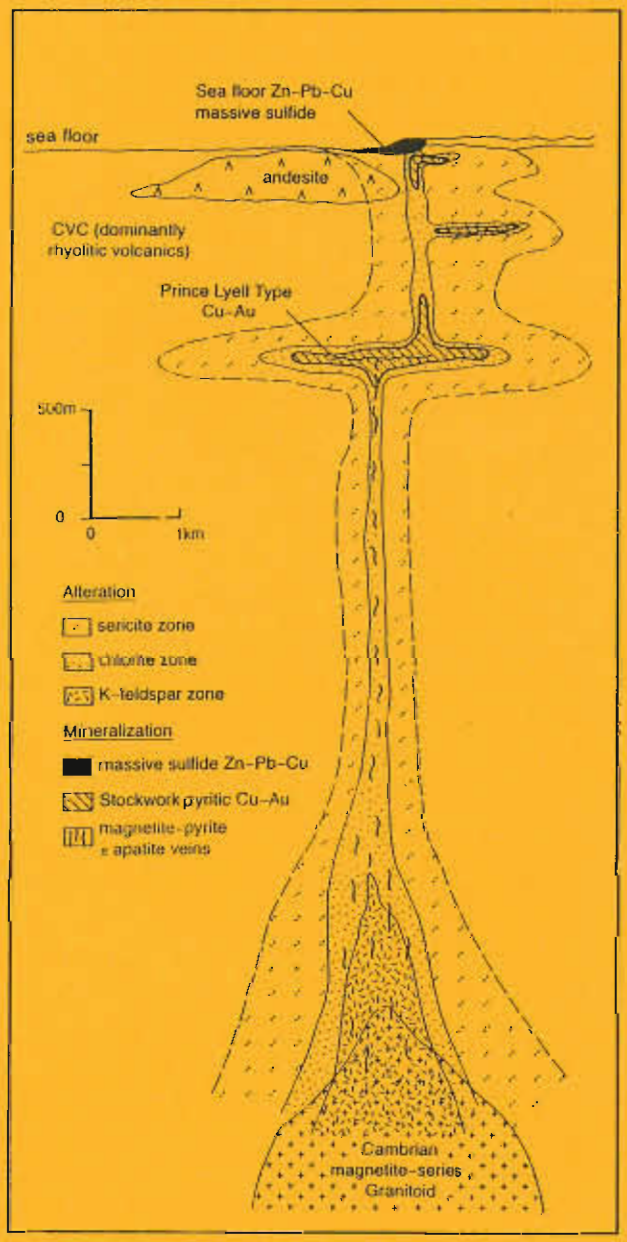

AMIRA/ARC project P439

Report 1
November 1995

Centre for Ore Deposit and Exploration Studies
University of Tasmania

Studies of VHMS-related alteration: geochemical and mineralogical vectors to ore

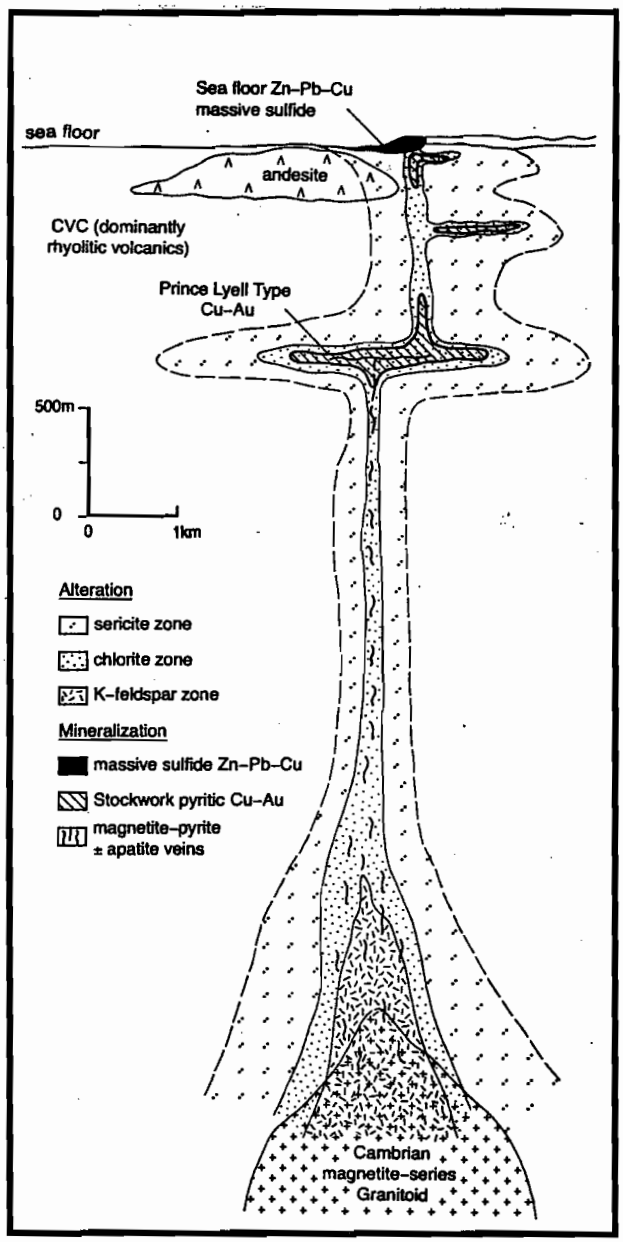

AMIRA/ARC project P439

Report 1
November 1995

Centre for Ore Deposit and Exploration Studies
University of Tasmania

Contents

Structure and Management of the Project

Introduction

Volcanic-hosted massive sulphide deposits (VHMS) provide a significant contribution to the total zinc, copper, lead, silver and gold production in Australia and continue to be a major target for most base metal explorers. However, due to the geological complexity of ancient submarine volcanic terrains, new VHMS deposits are becoming extremely difficult to discover, especially deposits that are buried more than a few tens of metres below the surface. To complement the conventional multidisciplinary approach utilising geology, geophysics and geochemistry, a new attack to the problem is proposed here which involves the integration of volcanic facies analysis with alteration geochemical and mineral chemical studies to develop a set of vectors to guide explorers toward ore-grade mineralisation. The research will concentrate on three productive submarine volcanic belts in Australia: the Mount Read Volcanics (MRV) in western Tasmania, the Mount Windsor Volcanics (MWV) in northern Queensland, and the Archean Murchison volcanic province in western Australia.

Project objectives

1. To characterise the mineralogy and geochemistry for the various styles of hydrothermal alteration throughout the Mount Read Volcanics (MRV) and the Mount Windsor Volcanics (MWV). This will be based on mapping supported by whole-rock and trace element geochemistry, mineral chemistry, REE and stable isotope geochemistry.
2. To determine the relationship between geochemical alteration patterns and sub-volcanic intrusions that are coeval with VHMS formation.
3. To undertake case studies of alteration halos related to specific VHMS deposits with particular emphasis on hangingwall alteration, and the relationship between alteration patterns and volcanic facies.
4. To develop a set of vectors towards ore, based on the regional studies and ore deposit specific studies, that can be applied in the exploration for VHMS deposits in submarine volcanic sequences throughout Australia. The vector matrix will include whole-rock, trace element, mineral chemistry, REE, isotope and volcanic facies factors.

Research framework

As there has been considerable research on alteration mineralogy and geochemistry of VHMS systems, our research is not to repeat previous work but to break new ground, utilising a multi-disciplinary approach at both the regional volcanic belt scale and selected ore deposit scale, with emphasis on selective geochemical techniques.

The project consists of three research modules as outlined on page 2.

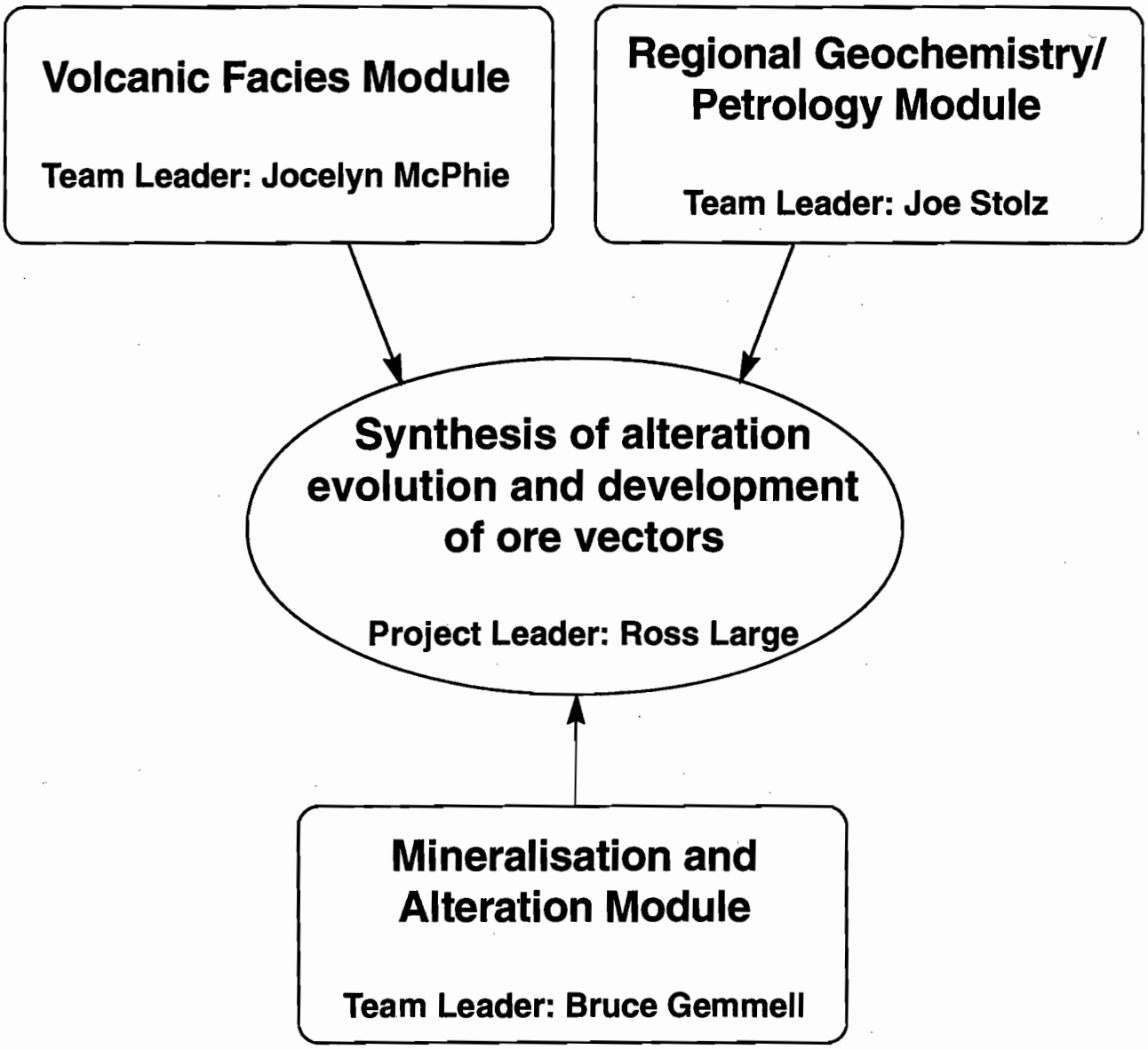
Volcanic Facies Module
Team Leader: Jocelyn McPhie
Regional Geochemistry/ Petrology Module
Team Leader: Joe Stolz
Synthesis of alteration evolution and development of ore vectors
Project Leader: Ross Large
Mineralisation and Alteration Module
Team Leader: Bruce Gemmell

This report

This is the first major progress report on the project and covers the first six-month period from May to October 1995. Very good progress has been achieved in all three modules.

1. Volcanic Facies

- Jocelyn McPhie provides an overview of the structure and objectives of the module.
- Matthew White reports on the volcanic facies and alteration in the Tyndall Group of the Mount Read Volcanics (MRV).
- Cathyrn Gifkins provides a preliminary report on the Mount Black Volcanics in the Rosebery area.

2. Regional geochemistry/petrology module

- Joe Stolz provides an overview of the structure and objectives of the module.
- Nathan Duhig discusses the geochemical database for the MRV and preliminary interpretations.
- Ross Large describes a recent model for the importance of the Cambrian granites to mineralisation in the MRV.
- Bill Wyman provides a preliminary report on the granitoids and associated alteration in the Mt Lyell-Darwin area.
- Joe Stolz gives an update on the volcanic geochemistry for the Mount Windsor Volcanics (MWV), QLD and the Benambra Volcanics, VIC.

3. Mineralisation and alteration

- Bruce Gemmell provides an overview of the structure and objectives of the module.
- Bruce Gemmell describes the Pearce-Element Ratio lithogeochemical research and hangingwall alteration study at the Hellyer deposit, Tasmania.
- Ross Large discusses the proposed Rosebery carbonate case study and potential research at the Henty deposit, Tasmania.
- Karin Orth and Anthea Hill describe their research on the carbonate alteration at Rosebery.
- Anthea Hill and Holger Paulick report on progress to date on the volcanic facies and alteration at the Thalanga deposit, Queensland.
- Mark Doyle provides an update on the volcanic facies and alteration research at the Highway Reward deposit, Queensland.

Important data and interpretations are already emerging from this project which will have implications for exploration and will be discussed in detail at the November meeting. Progress in the first six months of the project has been very encouraging and I would like to acknowledge the excellent work by the CODES research team and the cooperation provided by the sponsor companies.

Ross Large
Director

Volcanic Facies Module: An outline of aims and objectives

J. McPhie and R.L. Allen
Centre for Ore Deposit and Exploration Studies, Geology Department, University of Tasmania

This module has two principal aims:

- to provide a geological framework, based on regional- and deposit-scale volcanic facies analysis, for companion studies of alteration related to volcanic-hosted massive sulfide (VHMS) deposits;
- to establish the textural, mineralogical and compositional changes that accompany cooling, hydration, devitrification, compaction and lithification of glassy volcanic rocks emplaced in submarine environments, especially glassy or partly glassy lavas, intrusions and pumice-rich deposits.

Facies architecture of submarine volcanic successions

The principal volcanic facies present in submarine volcanic sequences are:

1. Silicic, intermediate and mafic lavas and domes. Pillow lavas (commonly andesitic or basaltic) are critical indicators of submarine emplacement.
2. A variety of syn-eruptive volcaniclastic deposits. Two main types are typically present. One is dominated by non-vesicular to poorly vesicular, originally glassy juvenile clasts and is related to the emplacement of lavas and domes. The other type contains abundant pumice, and is produced by large-volume, explosive silicic eruptions.
3. Largely conformable syn-volcanic intrusions. These include high aspect ratio dome-shaped intrusions (cryptodomes) and sheet-like sills and sill complexes.

Because sedimentation and volcanism are synchronous in these settings, the volcanic lithofacies are typically interbedded with sedimentary lithofacies such as pelagic and hemi-pelagic mudstone and turbidites. The sedimentary lithofacies association may also include important but thin and laterally discontinuous chemical/hydrothermal exhalative facies such as chert or carbonate. Correlation depends on volcanic facies that are strictly extrusive, produced in large volumes, erupted infrequently, emplaced rapidly and widespread. Mass-flow emplaced units generated from large explosive eruptions are thus the best stratigraphic markers in the entire facies architecture.

One of many, important recent advances is the recognition that significant additions to the architecture of submarine volcanic sequences may remain subsurface, in the form of syn-volcanic sills, cryptodomes and other intrusions. Positive identification of these depends heavily on upper contacts that are demonstrably intrusive (locally cross-cutting stratigraphy; induration or alteration of the host) and evidence that the host sequence was unconsolidated (presence of peperite; deformation or destruction of bedding). Their role in initiating or modifying hydrothermal systems that exhale at the seafloor has yet to be fully explored.

Syn-volcanic intrusions and peperite are a characteristic component of the facies architecture of both ancient and modern, submarine volcanic successions (Allen 1992; McPhie and Allen 1992; McPhie et al. 1993), many of which are hosts to massive sulfide mineralisation. The coincidence arises not because the intrusions necessarily play a role in ore deposition (although they might, e.g. Boulter 1993), but because such mineralisation occurs in submarine volcanic successions in which syn-volcanic intrusions are an integral part.

This working model for the volcanic facies architecture of submarine volcanic successions (Fig. 1; McPhie and Allen 1992) has yet to be integrated with models for the distribution and character of alteration facies.

An understanding of volcanic facies architecture is critical for the correct interpretation of the stratigraphic, structural and temporal relationships of VHMS deposits, and hence also for the correct interpretation of alteration and mineralisation processes. Submarine volcanic successions are inherently complex and within one succession, there may be enormous variety in the geometry and character of the volcanic facies and hence, in potential VHMS-ore forming environments. This is amply illustrated in the Mount Read Volcanics by the contrasts between the volcanic facies that host the Rosebery–Hercules Hellyer deposits (Figs 2, 3). In addition to a generally applicable model of submarine volcanic facies architecture, it is thus imperative to develop deposit-specific facies architecture models that adequately deal with the diversity volcanic host successions.

Recent research in the Mount Read Volcanics suggests that volcanic facies strongly influence the distribution and character of hydrothermal alteration assemblages associated with VHMS deposits (Allen and Cas 1990; Allen and Hunns 1990; Gemmell and Large 1992; Large 1992; Waters and Wallace 1992). For example, alteration developed in pumice-rich footwall sequences to the Rosebery–Hercules VHMS deposits is typically pervasive and extensive (strike length of several km) and involved very early, syn-depositional and diagenetic changes which strongly

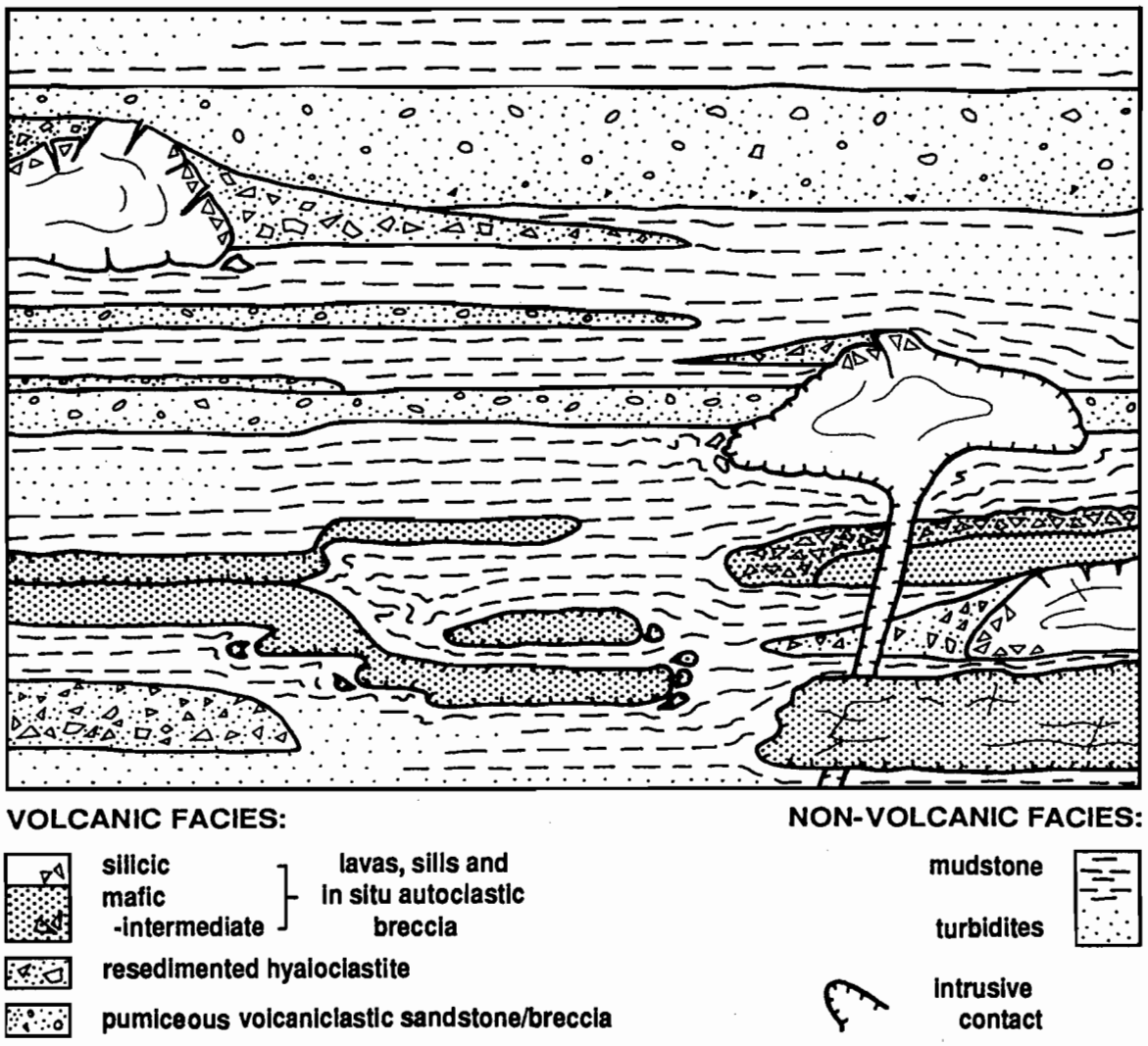

Figure 1. Schematic facies architecture of submarine volcanic sequences. Typically there are considerable regional variations in relative proportions of lavas, sills and volcaniclastic facies, and in volcanic versus non-volcanic facies. Modified from McPhie and Allen (1992).

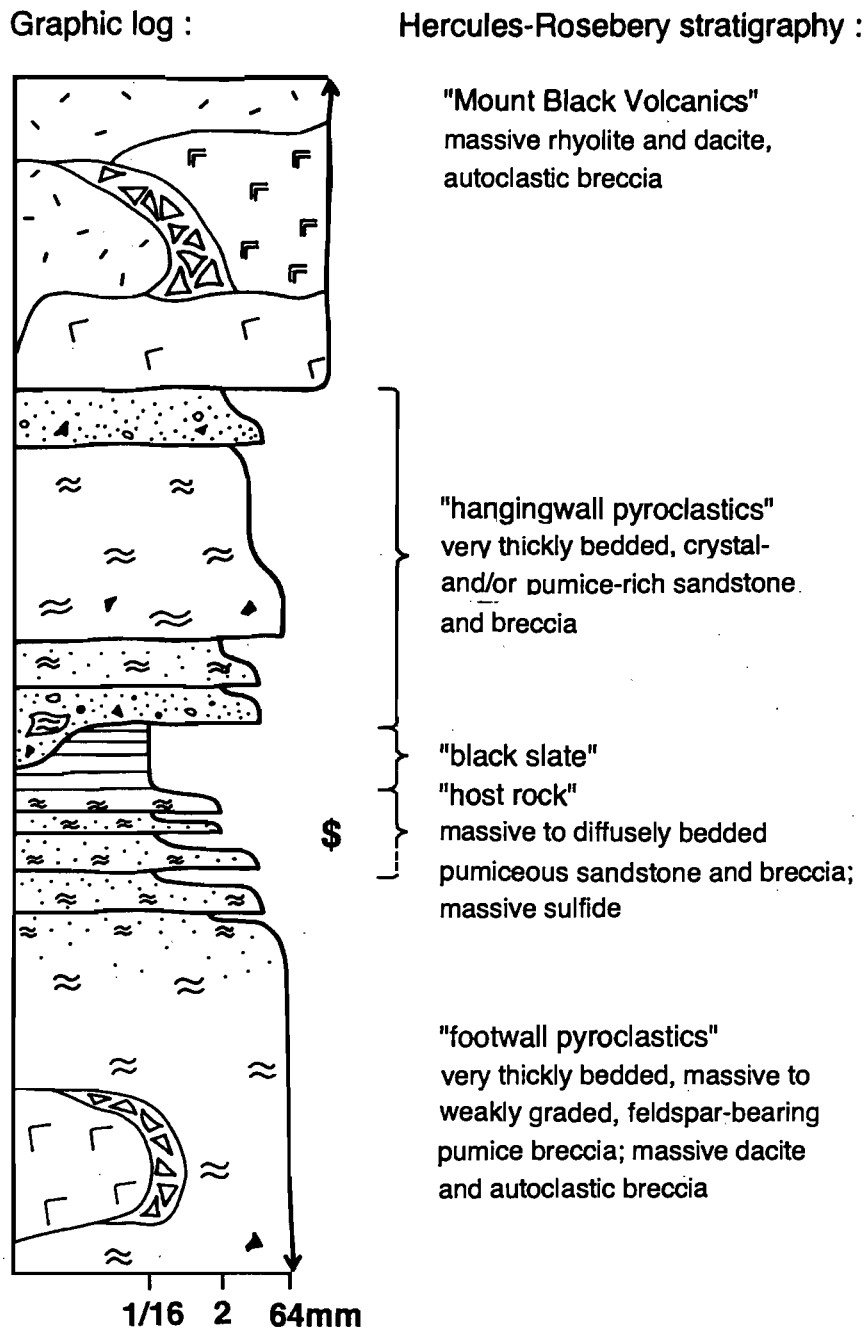

Figure 2. Simplified graphic log of the host succession to the Rosebery–Hercules VHMS deposit. The total thickness of the section illustrated here is ~ 2000 m. From McPhie et al. (1993).

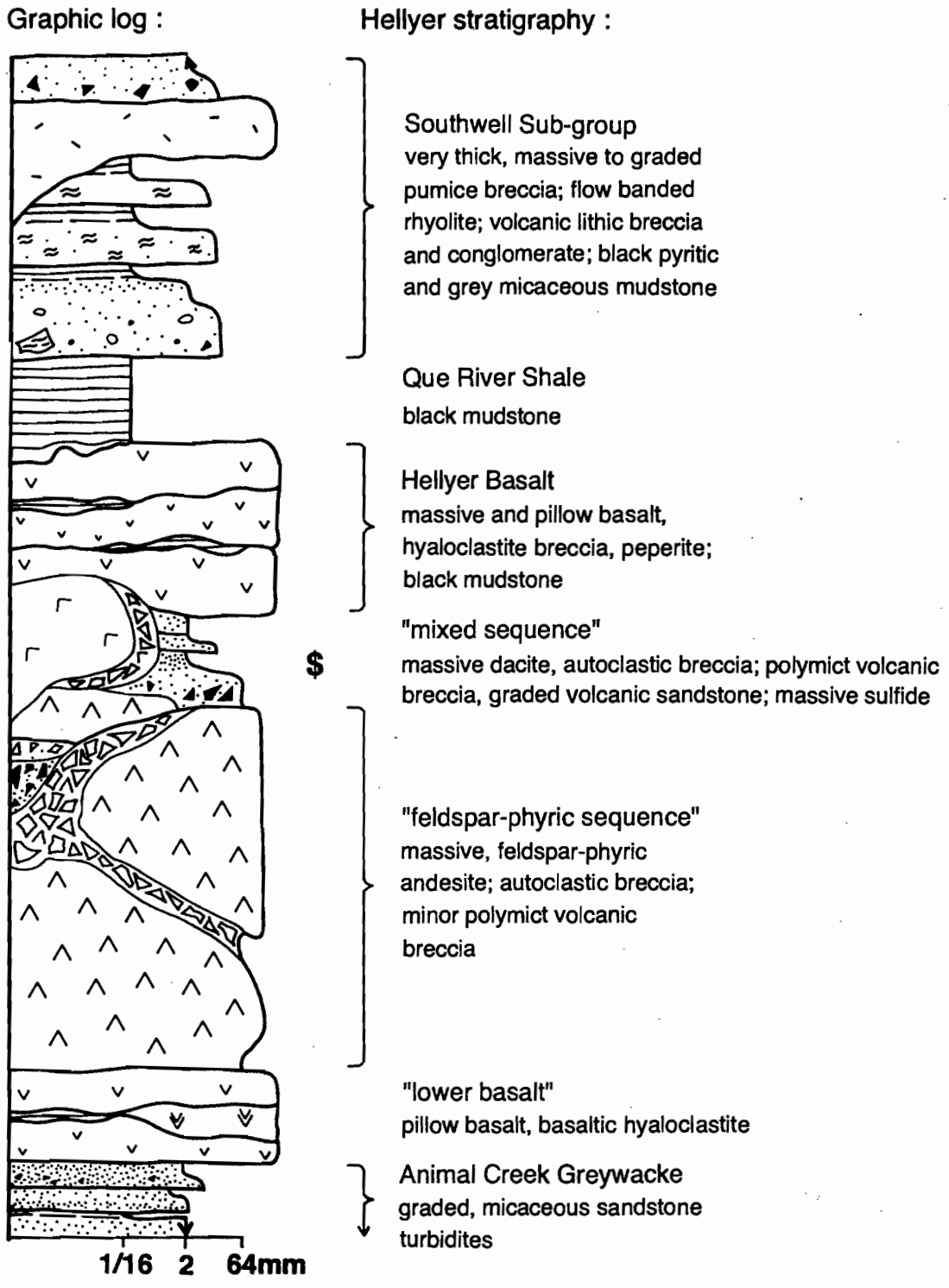

Figure 3. Simplified graphic log of the host succession to the Hellyer VHMS deposit. The total thickness of the section illustrated here is ~ 2400 m. From McPhie et al. (1993).

influenced later hydrothermal alteration. Two–phase alteration is common, with phyllosilicate versus feldspar being the dominant phases and controlling whether pre-existing textures are preserved or destroyed. It also appears that sub-seafloor replacement styles of mineralisation are favoured by pumice-rich footwall sequences (Large 1992).

In contrast, at Hellyer where the footwall comprises lavas, intrusions and related autoclastic breccia there is a well-defined alteration pipe that has considerable vertical dimensions (>500 m) but narrow lateral extent (McArthur 1989; Gemmell and Large 1992). Alteration is strongly controlled by original fractures in coherent facies and in situ autoclastic breccia, or by the distribution of matrix to clasts in resedimented breccia. Sea-floor mound and sub-seafloor vein styles of mineralisation are evidently favoured in volcanic successions dominated by lavas and intrusions.

Early textural modification of glassy volcanic facies

Lavas, high level intrusions and volcaniclastic deposits, especially those emplaced in submarine environments, are commonly initially glassy or partly glassy, and highly permeable and porous because of the presence of abundant fractures (e.g. perlitic fractures, quench fractures), inter-granular pores and/or vesicles. Once formed both the texture and composition of volcanic glass may be partially or completely modified by a variety of processes, such as crystallisation during cooling (above the glass transition temperature), hydration, devitrification and compaction. The rate at which these modifications proceed is in general accelerated by the presence of water and by elevated temperature. It is thus expected that glass-rich submarine volcanic successions, including those that host massive sulfide deposits, will be affected by textural and compositional modification prior to and/or synchronous with any alteration specifically related to VHMS ore-forming hydrothermal activity.

In most ancient and lithified submarine volcanic successions, only relict glass remains. In general, the original glass has been converted to more stable mineral assemblages accompanied by variable degrees of textural modification. The conversion of fresh glass to relict glass is expected to result in profound changes in porosity and permeability, composition, texture and mineralogy, and to simultaneously affect both the chemistry and circulation of pore fluids. We predict that the conversion will involve a pattern comprising a series of stages controlled by temperature, pressure and the chemical environment. Numerous studies have focussed on present-day alteration assemblages and their distribution in relation to VHMS deposits (e.g. Gemmell and Large 1992). Our concern here is to monitor textural evolution beginning with fresh unaltered glass (both pumiceous and non-vesicular) through steps comprising crystallisation, hydration, devitrification, seafloor alteration, compaction and lithification, all of which may precede VHMS-related hydrothermal alteration. An appreciation of the early stages in textural modification of glassy volcanic rocks is critical in correct evaluation of the exploration significance of particular alteration textures and assemblages.

Participants and projects

Jocelyn McPhie and Rod Allen (Leaders): Textural evolution of glassy lavas, intrusions and pumice-rich rocks in submarine environments; facies architecture of submarine volcanic successions that host VHMS deposits.

Matt White (PhD): Alteration processes and volcanic facies in the Tyndall Group, Mount Read Volcanics, western Tasmania.

Andrew Jones (MSc): Volcanic facies architecture, alteration and mineralisation in the Anthony Basin, western Tasmania.

Cathryn Gifkins (PhD): Textural evolution and alteration processes in glassy lavas, intrusions and pumice-rich rocks: Mount Black Volcanics, western Tasmania, and the Green Tuff, Japan.

Mark Doyle (PhD): An intrusive–extrusive dome complex in the Mount Windsor Volcanics at Highway–Reward, Queensland: relationships between facies architecture, alteration and VHMS mineralisation.

Holger Paulick (PhD): A comparison of volcanic facies architecture and alteration styles in felsic and mafic volcanic host sequences to massive sulfide deposits: Thalanga, Queensland and Teutonic Bore, Western Australia.

References

Allen, R.L., 1992. Reconstruction of the tectonic, volcanic and sedimentary setting of strongly deformed Zn–Cu massive sulfide deposits at Benambra, Victoria. *Economic Geology* 87: 825–854.

Allen, R.L. and Cas, R.A.F., 1990. The Rosebery controversy: distinguishing prospective submarine ignimbrite-like units from true subaerial ignimbrites in the Rosebery–Hercules ZnCuPb massive sulphide district, Tasmania. *Geological Society of Australia Abstracts* 25: 31–32.

Allen, R.L. and Hunns, S.R., 1990. Excursion Guide E1. The Mount Read Volcanics and related ore deposits. 10th Aust Geol Conv, Hobart: 15-27.

Boulter, C.A., 1993. High-level peperitic sills at Rio Tinto, Spain: implications for stratigraphy and mineralisation. *Transactions of the Institute of Mining and Metallurgy B: Applied Earth Science* 102: B30-B38.

Gemmell, J.B. and Large, R.R., 1992. Stringer system and alteration zones underlying the Hellyer volcanic-hosted massive sulfide deposit, Tasmania, Australia. *Economic Geology* 87: 620-649.

Large, R.R., 1992. Australian volcanic-hosted massive sulfide deposits: features, styles and genetic models. *Economic Geology* Geol 87: 471–510.

McArthur, G.J., 1989. Hellyer. *In* C.F. Burrett and E.L. Martin (eds): *GEOLOGY AND MINERAL DEPOSITS OF TASMANIA: Geological Society of Australia Special Publication* 15: 144–148.

McPhie, J. and Allen, R.L., 1992. Facies architecture of mineralised submarine volcanic sequences: Cambrian Mount Read Volcanics, western Tasmania. *Economic Geology* 87: 587–596.

McPhie, J., Doyle, M. and Allen, R., 1993. *VOLCANIC TEXTURES. A GUIDE TO THE INTERPRETATION OF TEXTURES IN VOLCANIC ROCKS.* Centre for Ore Deposit and Exploration Studies, Hobart: 198 pp.

Waters, J.C. and Wallace, D.B., 1992. Volcanology and sedimentology of the host succession to the Hellyer and Que River volcanic-hosted massive sulfide deposits, northwestern Tasmania. *Economic Geology* 87: 650–666.

Volcanic facies and alteration in the Cambrian Tyndall Group, Mount Read Volcanics, western Tasmania

Matthew J. White
Centre for Ore Deposit and Exploration Studies, Geology Department, University of Tasmania

Introduction

This report describes the principal lithofacies and alteration assemblages in the Tyndall Group. Genetic models for distinctive albite+quartz and chlorite alteration textures in the crystal-rich volcaniclastic sandstone facies are also considered. This work is part of an ARC-funded PhD project on the Tyndall Group, and lies outside the AMIRA project.

When volcanic deposits form, they develop textures that reflect the primary physical processes and chemical conditions that were operating at that time. After deposition, volcanic deposits can be subjected to a variety of post-depositional processes, including devitrification, hydration, diagenetic alteration, diagenetic compaction, hydrothermal alteration, metamorphism and tectonic deformation. The primary textures may be overprinted or modified by these secondary processes. The intensity of secondary replacement will be controlled in part by the primary composition of the rocks. For example, glass will undergo changes more readily than other, more stable components (e.g. crystals). The chemical composition may also be modified by post-depositional processes (e.g hydrothermal alteration). Because volcanic textures evolve through time, textural analysis of ancient volcanic deposits requires an understanding of both the primary and secondary processes that may have occurred.

The Tyndall Group

The Tyndall Group occurs in the upper part of the Mount Read Volcanics, conformably overlain in places by the Late Cambrian to Early Ordovician Owen Conglomerate, and has variable basal contact relationships to older MRV rocks (Corbett, 1992). In areas close to Cambrian granite, part of the Tyndall Group contains angular to rounded granite clasts, indicating a post-granite age, whereas the older lithostratigraphic units in the MRV are intruded by the Cambrian granites (Corbett, 1992).

The Tyndall Group forms a narrow discontinuous belt of exposures which extend from near Mount Darwin in the south, to Moxon Saddle. Correlates of the Tyndall Group occur in the northern parts of the Mount Read Volcanics: (1) around the Cradle Mountain Link Road in the upper part of the Mount Charter Group (Mount Cripps Subgroup, Corbett, 1992); (2) in the Mount Cattley to Mount Tor area (Pemberton and Vicary, 1988); (3) in the Winterbrook area (Pemberton and Vicary, 1989) (Fig. 2.2.); (4) in other parts of the Western volcanosedimentary sequences (e.g. Pinnacles area, McKibben, 1993). The thickness of the Tyndall Group varies regionally from approximately 1300 m in the Cradle Mountain Link Road area to approximately 450 m at Comstock (assuming minimal fault repetitions and disruptions). Relatively thin and incomplete sequences of the Tyndall Group also occur in places (e.g. Mount Lyell Mill area).

Tyndall Group stratigraphy

The Tyndall Group is a dominantly submarine, volcano-sedimentary succession that occurs in the upper part of the Mount Read Volcanics, western Tasmania. The internal stratigraphy of the Tyndall Group is relatively complex, comprising a wide variety of lithofacies including crystal- and lithic-

rich volcaniclastic breccia, conglomerate and sandstone, welded ignimbrite, rhyolite, laminated mudstone and carbonate. Problems with the previously defined stratigraphic nomenclature prompted development of a new stratigraphic scheme, based on detailed facies analysis of major Tyndall Group exposures in the central Mount Read Volcanics (White and McPhie, in press). The Tyndall Group is divided into two formations, the Comstock Formation and the overlying Zig Zag Hill Formation. The Comstock Formation is further subdivided into the Lynchford Member and the overlying Mount Julia Member. This stratigraphic scheme is based on regional lithological variations, which largely reflect different provenance characteristics.

Comstock Formation: Lynchford Member

The Lynchford Member forms the lower part of the Comstock Formation and comprises four main facies: (1) quartz-poor crystal ± lithic volcaniclastic sandstone; (2) carbonate; (3) laminated mudstone/sandstone; (4) volcaniclastic lithic breccia. The character of the lower contact (to older underlying rocks) appears to be conformable in some areas (e.g. Anthony Road, Comstock), but is undefined in other areas due to poor exposure.

Quartz-poor crystal-rich volcaniclastic sandstone is the most common facies in the Lynchford Member and comprises abundant crystals and crystal fragments (35–70%) (largely plagioclase and lesser clinopyroxene, titanomagnetite, ± ilmenite, ± quartz) and angular felsic to mafic volcanic lithic clasts. The crystal composition suggests an andesitic to dacitic volcanic provenance. The crystal-rich volcaniclastic sandstone is interpreted to be deposited from high-density turbidity currents and/or debris flows in a below-storm-wave-base submarine depositional environment (*cf.* Lowe, 1982).

Carbonates also occur in the Lynchford member comprising creamy white to pink/purple massive recrystallised calcite ± hematite. In places the carbonates are strongly foliated and contain patches of sericite-chlorite alteration. In one Comstock drill hole (C50), the main carbonate unit contains shallow marine fossils including trilobites, small echinoderm plates, hyolithids, gastropods and inarticulate brachiopods, indicating a shallow marine depositional environment (Jago et al., 1972).

Laminated mudstone and sandstone generally overlies the carbonate units, and in other areas they occur as lenses within quartz-poor crystal-rich volcaniclastic deposits. The fine-grained deposits of the Lynchford Member comprise normally graded beds and laminae (cm to 10's of cm thick) that are laterally continuous in outcrop. They are interpreted to be deposited from low-density turbidity currents and/or by suspension sedimentation in a below-storm-wave-base environment (*cf.* Lowe, 1982). The Lynchford Member also contains massive units of finely-laminated black mudstone up to tens of metres thick (e.g. Anthony Road area) that probably represent pelagic sedimentation.

Volcaniclastic lithic breccia units occur in some areas (e.g. Comstock area), intercalated with laminated mudstone and sandstone deposits. These units are generally several metres thick and normally graded. They are dominated by pebble- to cobble-size, angular, quartz-feldspar porphyritic volcanic clasts and intraclasts of laminated mudstone, in a crystal-rich matrix and/or grey mud-rich matrix. These units are interpreted to be subaqueous mass-flow deposits.

Comstock Formation: Mount Julia Member

The Mount Julia Member is relatively quartz-rich (rhyolitic to dacitic) and comprises four main facies: (1) crystal-rich volcaniclastic sandstone; (2) normally graded volcaniclastic breccia-sandstone units; (3) welded ignimbrite; (4) coherent rhyolite. Minor laminated mudstone/sandstone units (as described above) also occur in the Mount Julia Member in places.

Crystal-rich volcaniclastic sandstone (CRVS) is the most common facies in the Mount Julia Member and comprises a closed framework of dominantly plagioclase and quartz (and minor titanomagnetite, ± ilmenite, ± hornblende, ± clinopyroxene) crystals and crystal fragments (35–70%) in a fine-grained altered matrix. Minor pebble- to cobble-size, angular to rounded lithic fragments (dominantly felsic volcanic clasts) also occur in places. The fine-grained altered matrix in the CRVS facies forms pink (albite+quartz-rich) and green (chlorite-rich) bands and wispy pseudoclastic textures in many areas that are dominantly subparallel to regional bedding. The preservation of unwelded bubble-wall shards in albite+quartz-rich domains in some samples suggests

that the matrix was originally vitric ash. The CRVS facies form laterally extensive, thick (tens of metres to >100 m thick), massive units interpreted to be deposited from voluminous, crystal-rich, more or less steady, high-density turbidity currents and/or debris flows (*cf.* Lowe, 1982).

Normally graded volcaniclastic lithic breccia/sandstone deposits also occur in the Mount Julia Member. They comprise volcaniclastic lithic breccia near the base grading up into massive CRVS, with laminated fine-grained sandstone ± mudstone at the top, and are interpreted to be subaqueous mass-flow units, deposited in a below-storm-wave-base environment.

Welded ignimbrite is present in the Mount Julia Member in the Zig Zag Hill, Comstock, Anthony Road, and Cradle Mountain Link Road areas (White and McPhie, in press). The ignimbrites comprise more or less evenly distributed, subhedral to euhedral crystals and crystal fragments (quartz, plagioclase, sparse altered ferromagnesian phases; 10–30%), and minor felsic volcanic lithic clasts in a fine-grained, devitrified and quartz-feldspar ± hematite altered, purple-brown coloured matrix. The matrix contains abundant moderately to strongly welded, cuspate- and platey-shaped bubble wall shards. The shards are most strongly deformed around crystal and lithic grains. The ignimbrite occurrences also contain abundant chlorite-altered, wispy-shaped, spherulitic clasts, commonly defining a eutaxitic foliation. These are interpreted as relict compacted pumice clasts or fiamme. The ignimbrites were deposited from hot pyroclastic flows.

Coherent rhyolite and associated breccia occurs in the Mount Julia Member around the Henty Canal to Moxon Saddle area. The rhyolite is generally pink to white, coarsely porphyritic (5–15% quartz-feldspar) and in places shows well-developed flow banding and open flow folding. Volcaniclastic breccia deposits consisting of angular pebble- to cobble-size pink rhyolite clasts in a quartz-, feldspar-, lithic-bearing sandy matrix occur within and overlying the rhyolite sequence. These volcaniclastic breccias probably represent both autoclastic breccia and redeposited autoclastic breccia deposits. The rhyolite sequence is interpreted as a lava dome complex, made up of multiple lavas and possible intrusions. It was probably emplaced subaqueously as it is underlain and overlain by other subaqueous deposits.

Zig Zag Hill Formation

The Zig Zag Hill Formation consists of massive, normally graded and less commonly inversely graded, polymict volcaniclastic conglomerate and sandstone beds containing very uncommon units of laminated and graded mudstone and sandstone. In the Anthony Road area near Newton Creek, the Zig Zag Hill Formation contains minor occurrences of pink, flow banded and flow folded rhyolite, similar to those further north in the Henty Canal area, in the underlying Mount Julia Member.

Polymict volcaniclastic conglomerate and sandstone commonly occurs as massive or normally graded units ranging from boulder/cobble, clast-supported conglomerate through matrix-supported pebble conglomerate and/or pebbly sandstone, to massive and/or diffusely stratified sandstone. The clast population in these rocks is diverse, comprising dominantly quartz-feldspar (felsic) porphyritic volcanic clasts, with minor sedimentary intraclasts, metamorphic basement-derived quartzite, granite, feldspar-ferromagnesian (intermediate) porphyritic clasts and undifferentiated altered clasts. The clasts are dominantly subrounded to well-rounded, indicating reworking prior to deposition. The polymict volcaniclastic conglomerate and sandstone deposits are interpreted to have been deposited from high-density turbidity currents (and/or debris flows) in a submarine below-wave-base depositional environment (*cf.* Lowe, 1982). This facies is conformably overlain by the Owen Conglomerate in places.

Palaeovolcanology

The first stage of Comstock Formation sedimentation (Lynchford Member) reflects subaqueous (syn-eruptive) redeposition of pyroclastic debris generated from an adjacent subaerial to shallow marine, andesitic to dacitic, explosive volcanic terrane. Fine-grained turbidites, massive mudstone units, lithic breccia units and massive carbonates also accumulated in the basin during this time. The overlying Mount Julia Member was generated by subaqueous (syn-eruptive) redeposition of pyroclastic debris, sourced from an adjacent subaerial to shallow marine, rhyolitic to dacitic, explosive volcanic terrane.

Subaqueous rhyolite lava dome complexes also developed on the sea floor during this stage. The overlying Zig Zag Hill Formation records post-eruptive erosion and reworking of the subaerial to shallow marine source areas (probably in response to tectonic uplift), supplying a large proportion of polymict, epiclastic debris to the marine basin. The palaeogeography envisaged for the Tyndall Group comprises a marine setting that is adjacent to an active subaerial to shallow water volcanic terrane.

Post-depositional alteration

Post-depositional alteration in the Tyndall Group has led to the development of secondary minerals and textures. The most distinctive secondary textures in the Tyndall Group occur in the crystal-rich volcaniclastic sandstone facies (CRVS) of the Comstock Formation. These textures have been commented on by many previous workers (e.g. Solomon, 1964; Corbett et al., 1974), but are still poorly understood. They consist of domains of pink, polycrystalline albite+quartz alteration and green, chlorite-rich alteration of the matrix, forming bedding-parallel bands and wispy pseudoclastic textures. In this section, the alteration textures in the crystal-rich volcaniclastic sandstone facies are described, and genetic models are considered.

Alteration mineral assemblages and textures in the CRVS facies

The CRVS facies comprises 35–70% crystals and crystal fragments (largely quartz and plagioclase), and minor pebbly lithics, in a fine-grained matrix of secondary minerals consisting of quartz, albite and chlorite with minor sericite, calcite, Fe-Ti oxides (magnetite, titanomagnetite, ilmenite, hematite), sphene, epidote and actinolite/tremolite. The matrix probably originally contained a large proportion of vitric ash, as rare unwelded bubble wall shard textures are observed in the matrix. The alteration is considered to be a 'pervasive-selective' style of alteration. It is pervasive as it occurs throughout the CRVS facies on a regional scale, but is also selective as it has mainly replaced the fine-grained vitric-rich matrix. The alteration assemblage is commonly domainal in character, forming pink, albite+quartz-rich zones and green, chlorite-rich zones. In some areas, however, the alteration assemblage is more randomly distributed.

Banding textures

In the CRVS facies, domainal, pink albite+quartz-rich and green chlorite-rich alteration of the matrix commonly occurs as laterally continuous rhythmic bands (2–10 cm thick) within massive crystal-rich sandstone. The pink bands are rich in albite and quartz but also contain minor chlorite, sericite, opaque alteration minerals, ± epidote, ± calcite, ± actinolite/tremolite. The green bands are rich in chlorite but also contain minor albite, quartz, sericite and opaque alteration minerals, ±epidote, ± calcite, ± actinolite/tremolite. The albite + quartz-altered and chlorite-altered banding textures occur regionally in the CRVS facies and are well exposed at Comstock, Zig Zag Hill, along the Anthony Road and at the Mount Lyell Mill area. Weakly banded varieties also occur in the Cradle Mountain Link Road area and at Lynchford. The bands are laterally continuous for several metres to tens of metres in areas of good exposure, and are largely subparallel to regional bedding.

Discontinuous, bedding-parallel, wispy, chlorite-altered bands also occur within albite + quartz-altered CRVS, forming a pseudoclastic texture that resembles fiamme in welded ignimbrites. In addition, thin (0.2–1 cm), discontinuous, chlorite-altered bands surrounded by pink albite + quartz alteration occur within fine grained sandstone at the top of thick, normally-graded CRVS units on the Anthony Road. These thin chlorite bands are similar to bedding-parallel stylolitic textures in the pumice-rich volcaniclastic units in the Rosebery–Hercules area (McPhie et al., 1993). In some areas the bedding-parallel alteration bands are oblique to the regional Devonian cleavage.

The main features of the albite+quartz and chlorite alteration banding textures are:

(1) the secondary minerals have been derived from alteration of a formerly glassy ash matrix;

(2) the alteration assemblages are of regional extent, but are confined to CRVS facies in the Tyndall Group;

(3) the domainal alteration bands and wisps are mostly bedding-parallel, and are laterally continuous for up to tens of metres in places;

(4) the bands are oblique to cleavage attitudes in some areas.

Alteration haloes around lithics

Distinctive pink albite + quartz alteration halos surrounding pebble size lithic clasts occur in the CRVS facies (and associated volcaniclastic lithic breccia facies). The pink alteration halos extend up to 10 cm outward from the clasts as spherical shaped albite+quartz alteration rinds set in green chlorite + quartz + albite-altered CRVS. The clasts consist of angular to well rounded, felsic volcanic and fine-grained cherty, pebble to cobble size clasts.

Planar alteration features

Planar, pink albite + quartz-altered zones were observed in the Anthony Road section. These 'vein-like' features are typically oriented in two directions at an angle of approximately 90° to each other, and at a moderately high angle to bedding. The planar features are 1–5 cm wide and occur within pervasive, light green coloured chlorite + quartz + albite-altered massive CRVS. The planar nature of the albite-quartz alteration zones suggests that they may have formed by the passage of fluids along joints.

Possible origins of the albite + quartz and chlorite alteration

In this section, possible origins for the albite+quartz and chlorite alteration assemblages are discussed. These interpretations are based on textural observations and are unsupported by fluid inclusion and stable isotope studies, which are required to accurately determine the physio-chemical conditions during the alteration event(s). Detailed geochemical studies are beyond the scope of this project.

Devonian regional metamorphism

The alteration in the CRVS facies is comprised of quartz, albite, chlorite and minor sericite, calcite, Fe-Ti oxides and actinolite/tremolite. This mineral assemblage is typical of lower greenschist facies regional metamorphic rocks. Eastoe et al. (1987) proposed that the banded and mottled pink and green domains in the Comstock Formation ('post-ore' rocks) were a product of Devonian regional greenschist metamorphism, rather than Cambrian hydrothermal alteration, which is recorded in the 'pre-ore' volcanic rocks (Mount Read Volcanics) close to volcanic-hosted massive sulfide (VHMS) deposits. Regional metamorphism in the Mount Read Volcanics occurred during the Devonian (Tabberabberan) orogeny (Williams et al., 1989), which also produced regional scale folding and associated cleavages. Eastoe et al. (1987) proposed that the "post-ore"volcanic rocks (e.g. Tyndall Group) retained most of their primary mineralogy until the Devonian, when albite, chlorite, calcite, sphene and epidote were formed by metamorphic processes. Reactions probably did not proceed to completion, allowing primary minerals (including ferromagnesian phases) to be preserved. In Eastoe et al.'s (1987) model, metamorphism did not affect the pre-existing chemical composition of the rocks on a regional scale, but redistribution of Na, Ca, Mg, and Fe occurred on a mesoscopic scale, producing the mottles and bands marked by recrystallised albite, epidote, and chlorite.

Greenschist facies rocks are generally completely recrystallised, with prominent foliations and lineations. They are the products of repeated penetrative deformation and greenschist facies metamorphism. The mineralogy of the CRVS facies of the Tyndall Group is consistent with lower greenschist facies metamorphism, but abundant primary components survived the alteration event in the CRVS and a schistose fabric is not developed. This is interpreted to be inconsistent with a metamorphic origin for the domainal albite+quartz and chlorite alteration in the CRVS. In addition, regional metamorphism is generally not heterogeneous in nature. It is more likely that alteration assemblages in the CRVS facies developed relatively early, and were overprinted by the low-grade (sub-greenschist?) Devonian regional metamorphic event.

Hydrothermal origin

A Cambrian hydrothermal origin for the albite + quartz and chlorite alteration is possible, provided fluid flow was diffuse (due to the lack of well-defined veins and regional alteration halos). Diffuse fluid flow would be possible while the sandstones were unconsolidated. After lithification, fluid flow (and hydrothermal alteration) would mostly be fracture-controlled. The regional distribution of albite + quartz and chlorite alteration is more consistent with a diagenetic or regional metamorphic origin. In addition, the low intensity of alteration in the CRVS facies is not consistent with proximity to hydrothermal centres associated with hydrothermal mineralisation. The

volcanic facies that host the hydrothermal massive sulfide deposits in the Mount Read Volcanics generally show marked depletion in Na_2O and CaO and an increase in K_2O and MgO (Stoltz, 1992). In contrast, the CRVS is rich in Na (as albite) and therefore is probably not associated with the typical VHMS-style hydrothermal alteration which is more common in older lithostratigraphic units of the Mount Read Volcanics.

Diagenetic alteration and compaction model

Diagenetic alteration and compaction has been proposed as the major process responsible for the formation of chlorite-sericite lenses in feldspar-quartz altered pumice breccia deposits in the Rosebery-Hercules area (Allen and Cas, 1990). The altered pumice breccia is comprised of dark, phyllosilicate-rich lenses generally 1–5 cm long that are aligned roughly parallel to regional bedding, set in pale-coloured quartz + K-feldspar + albite alteration. The dark lenses consist of flattened pumice material and resemble fiamme in welded pyroclastic deposits. However, pumice in the feldspar-quartz altered zones has preserved delicate, unflattened, undeformed pumice and glass shard textures, implying that the rocks are unwelded. The pumiceous units have sharp bases, very thick (10's m) massive or graded lower parts and thin finer stratified upper parts suggesting deposition from cold, water-supported mass flows in a submarine environment, below wave base (Allen and Cas 1990).

Allen and Cas (1990) suggested that the pumice breccias were heterogeneously altered soon after deposition, and the phyllosilicate altered pumice patches were flattened by bedding-parallel diagenetic compaction, and by tectonic deformation, resulting in false welded fiamme textures. The uncompacted pumice and shards in the quartz-feldspar altered domains indicate that the deposits were originally unwelded, and that quartz + K-feldspar + albite alteration occurred prior to cleavage development, and prior to the conclusion of diagenetic compaction (Allen, 1990; Allen and Cas, 1990; McPhie et al., 1993). It is uncertain whether quartz, K-feldspar and albite were the first alteration minerals formed, or whether they replaced an earlier alteration mineral such as zeolite. Elements such as Na, K, Al, Si which were necessary to form the widespread quartz+K-feldspar + albite alteration, were probably derived from the dissolution of volcanic glass at clast contacts during diagenetic compaction, and/or from upward migration of elements liberated by diagenetic or hydrothermal leaching of glass deeper in the pile (McPhie et al., 1993). Textural evidence that is consistent with early dissolution of glassy clasts is the widespread occurrence of bedding-parallel, spaced, stylolite-type dissolution foliation. This foliation is interpreted as a diagenetic compaction fabric, and has been crenulated by the Devonian regional cleavage (McPhie et al., 1993).

A diagenetic alteration and compaction model is favoured for the CRVS facies in the Tyndall Group, because it contains similar alteration minerals and textures to the pumice breccias at Rosebery–Hercules. In both cases, alteration has involved the replacement of originally vitric material (i.e. pumice and glass shards). The CRVS facies of the Comstock Formation was buried by coarse-grained deposits of the Zig Zag Hill Formation and Owen Conglomerate, deposited during the Late Cambrian to Early Ordovician (Corbett, 1992). Increased lithostatic pressures and temperatures would have resulted in compaction and fluid expulsion, causing devitrification and/or diagenetic alteration of reactive components (e.g. volcanic glass). The glassy ash matrix in the CRVS was ideal for relatively early diagenetic alteration, as glass is reactive in sub-seafloor environments (Masuda et al., 1992). Seawater was the most likely pore fluid, and would have facilitated diagenetic alteration by acting as the transport medium, carrying dissolved substances to sites of precipitation.

The discontinuous bedding-parallel wispy chlorite-altered bands in albite + quartz-altered CRVS (pseudoclastic textures) probably developed as a consequence of diagenetic alteration of the glassy ash matrix, occurring contemporaneously with diagenetic compaction. The laterally continuous, bedding-parallel, albite-quartz-altered and chlorite-altered bands may have also have developed by this process, however, the rhythmical nature of the banding suggests that an additional feature (e.g. primary compositional layering or diffuse bedding) may have had some control on the distribution of alteration minerals. In this case, the movement of diagenetic fluids may have been controlled by permeable zones along diffuse bedding planes.

The development of chlorite-altered, bedding-parallel, stylolitic features in the fine grained upper portions of some of the normally graded CRVS units may be related to an increase in the proportion of glassy ash material at the top of the unit. Mass flow deposits generally concentrate dense components at the base and middle portions of the flow, while less dense and finer components should be concentrated at the top. Diagenetic alteration and compaction of the upper glass-rich zones may have responsible for forming these stylolitic textures.

The physical and chemical conditions of the early diagenetic phase are not known, and detailed geochemical studies (e.g. fluid inclusion studies, stable isotope analyses, high-precision mineral analyses) are recommended to fully characterise the alteration event(s). The Devonian lower greenschist metamorphic event is also poorly constrained and requires further work.

Conclusions

The main stratigraphic units in the Tyndall Group (Lynchford and Mount Julia Members of the Comstock Formation and the Zig Zag Hill Formation) each contain one or more lithofacies. The Lynchford Member of the Comstock Formation contains abundant quartz-poor crystal-rich volcaniclastic sandstone and breccia units that are generally more andesitic to dacitic in composition relative to the rest of the Tyndall Group. This member also contains laminated mudstone/sandstone and minor carbonate units. The overlying Mount Julia Member of the Comstock Formation contains abundant quartz-rich rhyolitic to dacitic crystal-rich volcaniclastic sandstone and lithic breccia units, and also contains coherent rhyolite and minor welded ignimbrite. The overlying Zig Zag Hill Formation contains mostly polymict volcaniclastic lithic conglomerate and sandstone. These stratigraphic units are regionally extensive and can be correlated across a large part of the central Mount Read Volcanics.

The Comstock Formation largely reflects sub-aqueous (syn-eruptive) redeposition of pyroclastic debris generated from an adjacent subaerial to shallow marine, explosive volcanic terrane. The overlying Zig Zag Hill Formation largely records post-eruptive erosion and reworking of the subaerial to shallow marine source areas (probably in response to tectonic uplift), supplying a large proportion of polymict, epiclastic debris to the marine basin.

The post-depositional alteration in the CRVS facies of the Comstock Formation consist of secondary albite, quartz, chlorite, and minor sericite, calcite, Fe-Ti oxides, sphene, epidote and actinolite/tremolite. The secondary minerals are mostly products of alteration of a glassy ash-rich matrix. Primary crystal components of the CRVS (e.g. plagioclase, quartz, clinopyroxene, amphibole) have only undergone partial alteration but are generally well preserved. Pink (albite + quartz-rich) and green (chlorite-rich) alteration domains are common in the CRVS forming laterally continuous rhythmic bands (2–10 cm thick), and as discontinuous wispy domains, within massive crystal-rich sandstone. The domainal albite+quartz and chlorite alteration bands and wispy textures are dominantly bedding-parallel, and similar to those documented by Allen and Cas (1990) in the pumice breccia units at Rosebery–Hercules. The bands were probably formed by diagenetic alteration and compaction during burial.

References

Allen, R.L., 1990. Subaqueous welding, or alteration, diagenetic compaction and tectonic dissolution? *Abstracts IAVCEI International Volcanological Congress*, Mainz, Germany.

Allen, R.L. and Cas, R.A.F., 1990. The Rosebery controversy: distinguishing prospective submarine ignimbrite-like units from true subaerial ignimbrites in the Rosebery–Hercules ZnCuPb massive sulphide district, Tasmania. *Geological Society of Australia Abstracts* 25: 31–32.

Corbett, K.D., 1992. Stratigraphic-volcanic setting of massive sulfide deposits in the Cambrian Mount Read Volcanics, Tasmania. *Economic Geology* 87: 564–586.

Corbett, K.D., Reid, K.O., Corbett, E.B., Green, G.R., Wells, K. and Sheppard, N.W., 1974. The Mount Read Volcanics and Cambrian–Ordovician relationships at Queenstown, Tasmania. *Journal of the Geological Society of Australia* 21: 173–186.

Eastoe, C.J., Solomon, M. and Walshe, J.L., 1987. District-scale alteration associated with massive sulfide deposits in the Mount Read Volcanics, western Tasmania. *Economic Geology* 82: 1239–1258.

Jago, J.B., Reid, K.O., Quilty, P.G., Green, G.R. and Daily, B., 1972. Fossiliferous Cambrian limestone from within the Mt Read Volcanics, Mount Lyell mine area, Tasmania. *Journal of the Geological Society of Australia* 19: 379–382.

Lowe, D.R., 1982. Sediment gravity flows: II. depositional models with special reference to the deposits of high-density turbidity currents. *Journal of Sedimentary Petrology* 52: 279–297.

Masuda, H., Tanaka, H., Gamo, T., O'Neil, J.R., Peacor, D.R. and Jiang, W-T., 1992. Formation of authigenic smectite and

zeolite and associated element behaviour during early diagenesis of volcanic ash in the Nankai Trough, Japan, ODP leg 131. *In* Kharaka and Maest (eds): *WATER-ROCK INTERACTION*. Balkeme, Rotterdam: 1659–1662.

McKibben, J.A.J., 1993. The geology and geochemistry of the North Pinnacles Ridge, western Tasmania. Unpublisged BSc (Hons) thesis, University of Tasmania, Hobart.

McPhie. J,, Doyle, M, and Allen, R., 1993. *VOLCANIC TEXTURES: A GUIDE TO THE INTERPRETATION OF TEXTURES IN VOLCANIC ROCKS*. Centre for Ore Deposit and Exploration Studies.

Pemberton, J. and Vicary, M.J., 1988. Geology of the Mt Cattley–Mt Tor area, 1:25 000 Map 8. Geological Survey of Tasmania, Department of Mines, Hobart.

Pemberton, J. and Vicary, M.J., 1989. Geology of the Winterbrook–Moina area, 1:25 000 Map 9. Geological Survey of Tasmania, Department of Mines, Hobart.

Solomon, M., 1964. Spilites, keratophyres and the Rosebery, Mt Lyell ores. Unpublished PhD thesis, University of Tasmania, Hobart.

Stoltz, J., 1992. Compositional and textural alteration of volcanic rocks. Master of Economic Geology coursework manual 10. Centre for Ore Deposit and Exploration Studies, Hobart.

White, M.J. and McPhie, J., in press. Stratigraphy and palaeo-volcanology of the Cambrian Tyndall Group, Mount Read Volcanics, western Tasmania. *Australian Journal of Earth Sciences*.

Williams, E., McClenaghan, M.P. and Collins, P.L.F., 1989. Mid-Palaeozoic deformation, granitoids and ore deposits. *In* Burrett C.F. and Martin E.L. (eds): *GEOLOGY AND MINERAL RESOURCES OF TASMANIA*. *Geological Society of Australia Special Publication* 15: 238–292.

Subaqueous silicic volcanism in the Mount Black Volcanics, western Tasmania

Cathryn Clare Gifkins
Centre for Ore Deposit and Exploration Studies, Geology Department, University of Tasmania

Introduction

This report outlines the proposed research plan for the study of alteration in pumiceous rocks and work to date within the Mount Black Volcanics (MBV). The project is intended to enhance our understanding of the styles and distribution of the alteration facies within a silicic submarine volcanic succession. How are the alteration facies controlled by the primary volcanic facies, and why? Particular emphasis is being placed on the alteration of pumiceous deposits in order to produce a model for their textural, mineralogical and chemical evolution. Pumice-rich rocks are commonly misinterpreted or overlooked and yet they host a number of submarine massive sulphide deposits including Rosebery and Hercules in Western Tasmania (Allen and Hunns, 1990). In order to provide better genetic exploration models for similar deposits in pumice rich sequences we need to be able to define the textural and mineralogical alteration that occurs as a result of different processes, that is seafloor and diagenetic alteration compared with hydrothermal alteration and metamorphism.

The MBV are a 500 m to several kilometres thick sequence of volcanics located in the northern part of the Cambrian Mount Read Volcanic Belt in Western Tasmania. Occurring between the Henty Fault Zone and the Rosebery–Hercules sequence, the MBV extend northwards from Mount Read to Pieman Road and Lake Rosebery. They are a package of feldspar phyric massive, flow banded and flow brecciated lavas and sills of generally dacitic composition with minor rhyolite and andesite. Variable proportions of pumiceous material are interbedded in the sequence and the entire package has been intruded by a series of mafic dykes. They have been chosen as a study area because they dominate the northern Central Volcanic Complex (CVC) of the Mount Read Volcanics and yet very little previous work has been completed on these rocks despite the concentration of exploration around Rosebery, Hercules and Pinnacles. There is significant potential to increase our understanding of the regional geology, volcanic facies and relationships in the northern Mount Read belt and the hangingwall hydrothermal alteration associated with the major VHMS deposits of Rosebery and Hercules.

The MBV have previously been considered to be younger than the Rosebery–Hercules sequence, however their similarity to the feldspar phyric Rosebery–Hercules footwall sequence is quite marked.The main difference is that the MBV contain more lavas and intrusives than massflow units while the footwall is predominantly pumiceous massflow deposits. Based on this observation Allen (1994) suggested that the MBV are a fault repetition of the Rosebery footwall and that as a result there may be potential for the Rosebery and Hercules ore horizons to be repeated to the east of the proposed Mt Black thrust fault. The MBV are mainly in fault contact with the hangingwall, however several authors (Warmeant, 1990; Lees, 1987; Allen, 1991) have also reported conformable or sheared contacts at depth near the Rosebery mine and south of Hercules. To test the hypothesis that the MBV may be a repetition of the footwall this contact needs to be further investigated and the nature of the fault determined.

Research Proposal

The proposed aims of this project are;

1. To understand the styles and distribution of alteration facies within the Mount Black Volcanics. This will be achieved by
   - defining the local facies and stratigraphy.
   - defining the alteration facies, styles and associations.
   - comparing the facies architecture and alteration with an undeformed, less altered analogue in the Miocene Kuroko District, Japan.
2. To establish the textural, mineralogical and compositional changes attendant upon the deposition, compaction and lithification, alteration and deformation of pumice rich volcanic rocks. This will be achieved by determining the textural, mineralogical and geochemical differences of pumiceous samples which have undergone different degrees and styles of alteration. The five steps defined in this study are;
   (i) fresh unaltered subaerial pumice, Taupo Volcanic Zone, NZ.
   (ii) Seafloor altered pumice, Manus Basin, PNG.
   (iii) Diagenetically altered submarine pumice, Kuroko District, Japan.
   (iv) Lithified compacted submarine pumice breccia, Berserker Beds, Qld.
   (v) Devitrified, hydrothermally altered, lithified and deformed pumice, Rosebery footwall and MBV, western Tasmania.

   Samples will be collected from these localities and polished slabs, thin sections and geochemistry will be used to identify the textures, mineralogy and chemistry of each stage.
3. Comparing the MBV with other parts of the northern CVC. In particular with the Rosebery–Hercules footwall pumice breccias. To define the contact between the hangingwall and the MBV. Is it all faulted or partly conformable?

The Mount Black Volcanics

There are a number of principal volcanic facies within the MBV and their proportions vary across strike. In the eastern succession coherent dacitic to andesitic lavas and sills dominate the stratigraphy as can be seen in the graphic log of MBD3 (Fig. 1) from the eastern flank of Mount Black, while alternatively in the western section the facies and alteration relationships are far more complex, with abundant interbedded pumiceous massflows and autoclastic or hyaloclastic breccias. The graphic log of 128R (Fig. 2) shows the typically complex interbedding and intrusive relationships between the principal facies. The complex nature of these relationships reflects the coeval emplacement of shallow sills and extrusion of lavas which have very similar mineralogy. It would be reasonable to expect that bodies may be both partly intrusive and vary along strike to extrusive.

The Rosebery and Henty faults dominate the local geology (Fig. 3). They are major reverse faults that dip inward under the volcanics. The Rosebery sequence is believed to be on the eastern limb of a regional anticline which extends for 20 km from Hercules to Pinnacles. The Sterling Valley Andesites are in the core of and on the western limb of another regional anticline which extends from the north of Mount Block and is truncated by the Henty Fault. There are some variations on this theme suggesting local parasitic folds. The large scale regional structures have a shallow northerly plunge and strike N–NE.The MBV represent a large open syncline, with bedding and younging facing east near the Mount Black Fault and west in and near the Sterling Valley Volcnics.

Textural variation within the units may be primary, secondary (alteration, deformation and devitrification) or both. All the units appear variably modified and the style and intensity of alteration appears to be affected by the nature of the primary volcanic unit, ie the intensity of alteration in coherent versus autobrecciated lavas can be very different.

Stratigraphy

A generalised stratigraphy (Fig. 4) has been interpreted for the MBV and Sterling Valley Volcanics based on a number of diamond drill holes and three traverses between the Henty Fault Zone and the Rosebery–Hercules sequence. At the base of the sequence are the Sterling Valley volcanics. These are an approximately 1 km thick package of normally graded, basaltic to dacitic clastic massflow units, minor siltstone, and numerous basaltic to dacitic sills. The lavas and sills are dominantly massive blue-

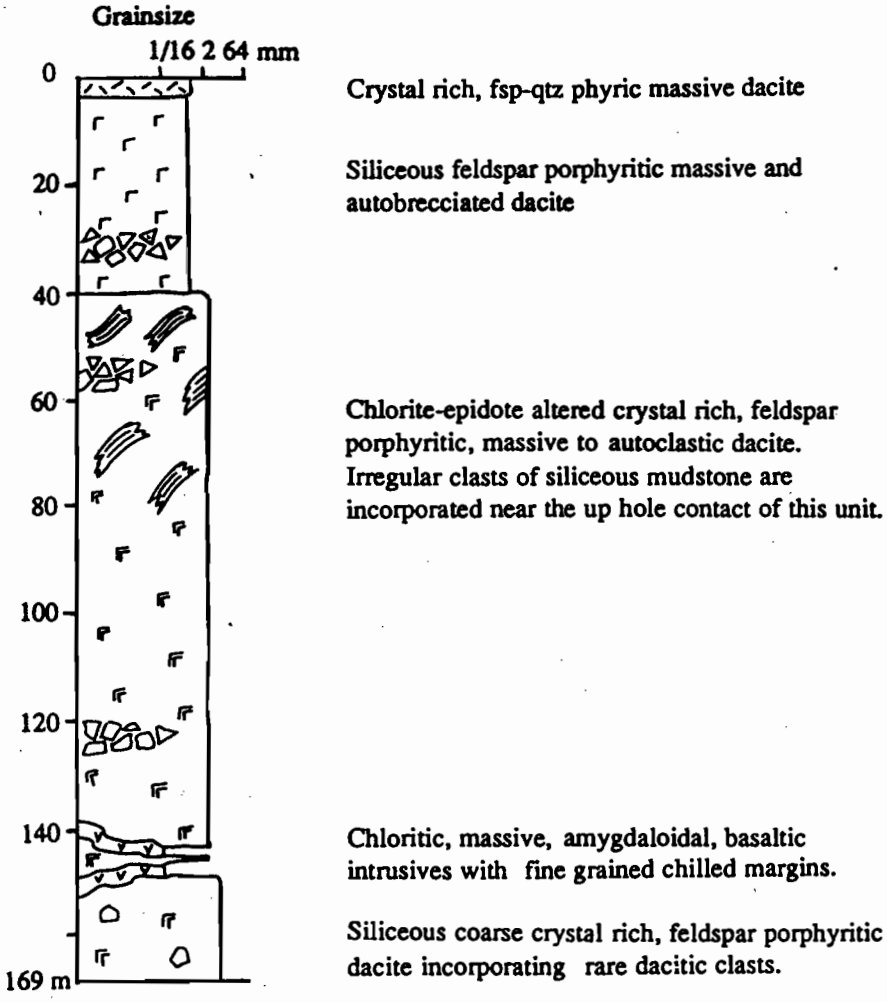

Figure 1. Graphic log of MBD3, from the eastern flank of Mount Black.

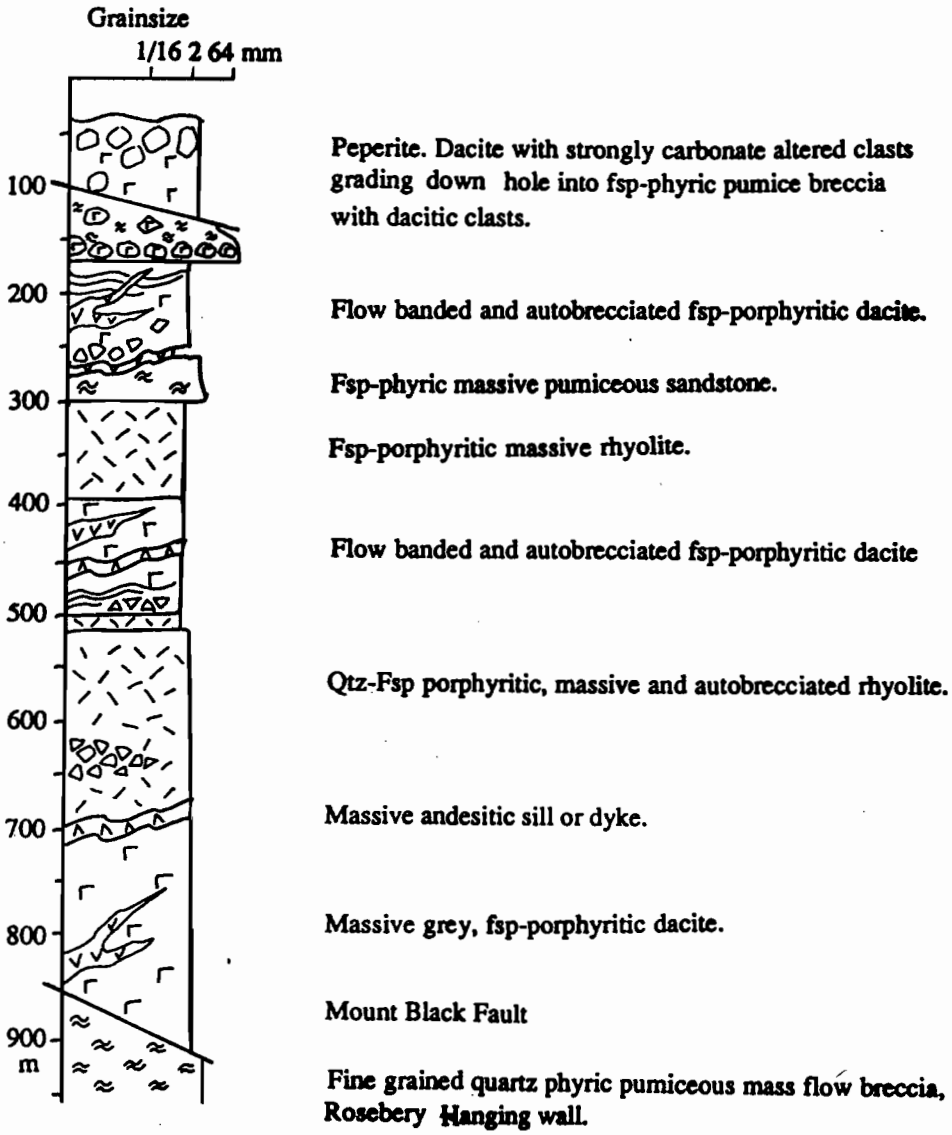

Figure 2. Graphic log of 128R, from the western side of Mount Black.

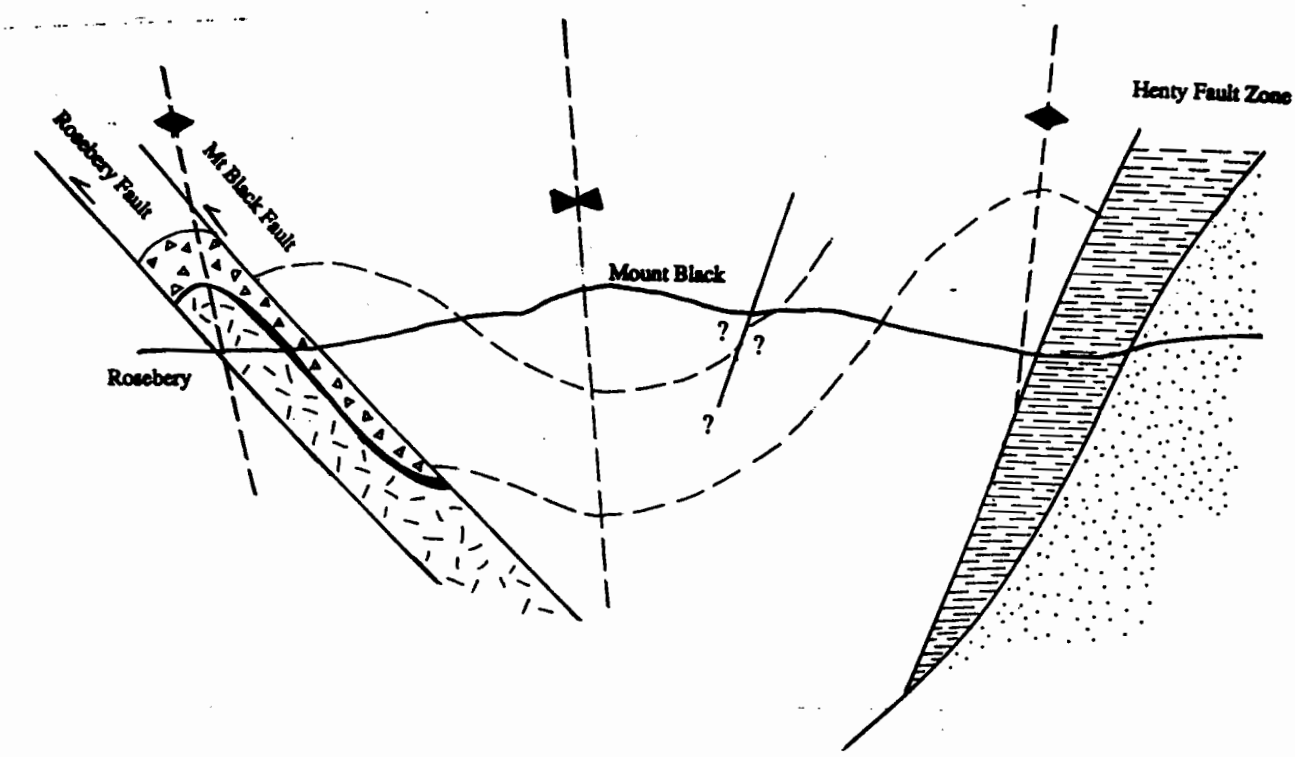

Figure 3. East–west structural cross section from Rosebery to Tullah along the Murchison Highway in western Tasmania.

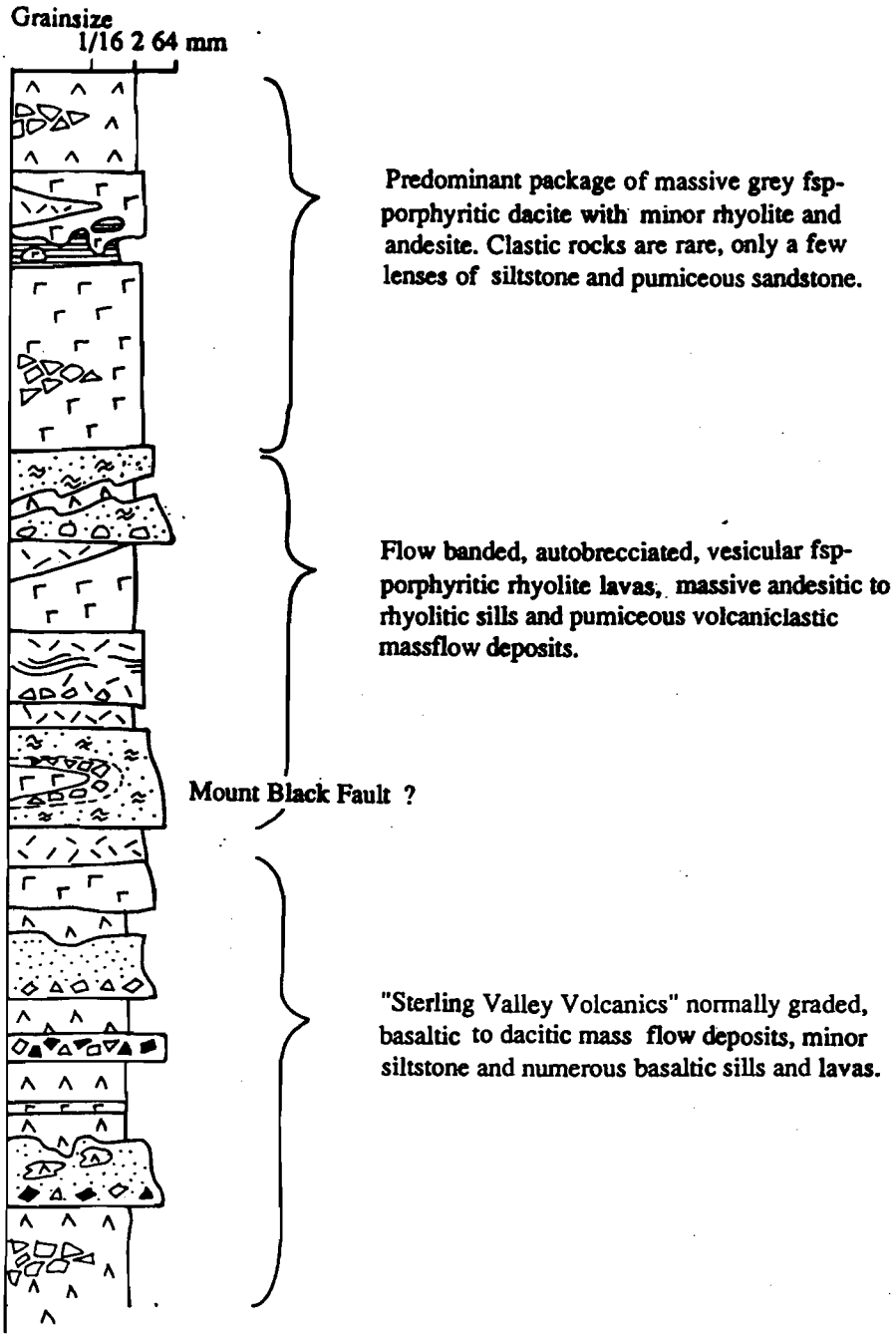

Figure 4. Summarised stratigraphic log of the Sterling Valley volcanics and Mount Black Volcanics.

green andesites, with pyroxene and feldspar phenocrysts. The groundmass is variably altered and rarely displays perlitic fracturing. There are a minor number of dacites and rhyolites identical to those in the MBV. The massflows vary from monomictic to polymictic packages of angular porphyritic lava clasts of basaltic to dacitic composition and rarely rhyolitic. These deposits also contain abundant angular and broken feldspar crystals and a in a chloritic matrix.

Conformably overlying the Sterling Valley Volcanics is the MBV. The base of the MBV is dominated by flow banded, autobrecciated, vesicular feldspar porphyritic rhyolite lavas, lesser massive andesitic to rhyolitic sills and pumiceous volcaniclastic massflow deposits (Fig. 4). The bulk of the MBV comprises massive red-brown to grey feldspar porphyritic dacite with minor rhyolite and andesite. More rarely are interbedded reworked pumiceous sandstones and volcaniclastic siltstones.

Rhyolitic to andesitic lavas and sills in the MBV typically have euhedral feldspar phenocrysts of 1–3 mm diameter which often form glomeroporphyritic aggregates in a siliceous groundmass which may show snowflake, spherulitic, or perlitic textures. Vesicles are commonly filled with chlorite, calcite and quartz. The margins of units may be marked by peperite textures and sedimentary clasts which have mixed with the lava as it flowed over or intruded into wet sediment. Individual units are largely defined by the size and abundance of the phenocrysts. Autobrecciation is commonly preserved, often fragments are incorporated within the moving coherent lava flow or sill or maybe reworked and deposited by sedimentary processes, that is massflows. The autoclastic breccias typically consist of fine grained blocky lava fragments which vary from massive, aphanitic, to perlitic strongly feldspar porphyritic to flow banded. They vary from matrix supported aggregates of blocky rotated clasts to clast supported breccias with jigsaw fit textures to coherent bodies. The clasts in these breccias are either quench fragmented (hyaloclastite) or flow brecciated (autobreccia) which formed at the margins of a coherent body as it migrated.

Thick massflow deposits of feldspar porphyritic pumice debris vary in composition from rhyolitic to dacitic and the clasts are commonly fibrous tube pumice. They commonly contain broken and euhedral feldspar and quartz crystals and fine grained blocky flow banded to massive porphyritic lava clasts. The pumice breccias are always strongly altered probably as a result of their high initial porosity.

There are only limited occurrences of fine sediment. It is commonly siliceous pale grey siltstone or mudstone, and displays a number of sedimentary structures including cross-bedding, fine laminations, flame structures and loading structures. These units have been deposited by turbidites and can be used as evidence for the below wave base environment of deposition in many parts of the sequence.

The entire sequence has been intruded by abundant basaltic sills and dykes. They form irregular often branching dark green sills and dykes cross-cutting contacts. They are fine grained, massive and a trachytic texture of feldspar and pyroxene laths can be observed in some of the coarser samples. They commonly contain calcite, chlorite and quartz filled amygdales and are rarely more than one metre wide. These dykes and sills have very irregular disruptive intrusive contacts and sheared margins suggesting that they have preferentially taken up strain during deformation.

Volcanic Architecture and Environment

The mode of fragmentation, transportation and environment of deposition of the MBVs and the Sterling Valley Volcanics are indicated by their facies associations and stratigraphic relationships.

The oldest package here is the Sterling Valley Volcanics which may represent a structural relic of a large submarine mafic volcano that was active early in the eruptive history of the CVC. This volcano was predominantly basaltic but also produced more fractionated magmas which were extruded into the submarine environment. Quenching of the hot lava as it was extruded or flowed into the marine environment brecciated the lava and this debris was redeposited down slope by massflow events. The base of the volcano has been removed by displacement along the Henty Fault.

This was followed by a period of complex extrusion and shallow intrusion of coherent felsic lavas and sills coeval with the deposition of pumiceous massflow units. Evidence of subaqueous

emplacement and deposition of these units is abundant and includes the presence of subaqueous facies (mudstone), normally graded clastic deposits, fine laminations and cross bedding indicating below wave base conditions (turbidites) and also supportive but not diagnostic is the lack of true welding. Although the pumiceous units were ultimately deposited in quiet deep subaqueous conditions this does not imply that the source was also subaqueous. The pumiceous units are the result of pyroclastic eruption of siliceous vesicular magma and because of the confining hydrostatic pressures in deep water it is in fact most likely that the source was either shallow marine or sub aerial (Cas and Wright, 1987).

The extrusion and syn-volcanic intrusion of a thick pile of intermediate lavas and sills was the dominant episode and followed the deposition of siliceous pyroclastic units and lavas/sills. Some of this material was quench fragmented or autobrecciated and redeposited down slope by massflow. Much of the debris however remained insitu or was deposited on the flanks of a moving flow. This large volume episode which dominates the MBVs may represent a period of intermediate lava dome or cryptodome formation.

The final volcanic event was the intrusion of the mafic dykes and sills which are part of the Henty Dyke Swarm.

References

Allen, R.L., 1994. Volcanic Facies analysis indicates large pyroclastic eruptions, sill complexes, synvolcanic grabens, and subtle thrusts in the Cambrian "Central Volcanic Complex" volcanic centre, western Tasmania. *In* Cooke, D.R. and Kitto, P.A. (Eds): *CONTENTIOUS ISSUES IN TASMANIAN GEOLOGY. Geological Society of Australia Abstracts* 39: 41–44.

Allen, R.L., 1991. Structure, stratigraphy and volcanology of the Rosebery – Hercules Zn–Pb–Cu–Au massive sulphide district, Tasmania: Results 1988–1990. Report to Pasminco Exploration Mining Rosebery.

Allen, R.L. and Hunns, S.R., 1990. Excursion guide E1. The Mount Read Volcanics and related ore deposits. 10th Australian Geological Convention, Hobart: 15–27.

Lees, T.C., 1987. Geology and mineralisation of the Rosebery–Hercules area, Tasmania. Unpublished MSc thesis, University of Tasmania.

Warmeant, P.J., 1990. The geology, geochemistry and mineralisation of the Mount Black Volcanics. Unpublished BSc Honours thesis, University of Tasmania.

Regional Geochemistry/Petrology Module

Team members

Joe Stolz
Nathan Duhig
Mike Roach
Bill Wyman
Garry Davidson
Tony Crawford
Dave Cooke

Module components

- Production of a geochemical database for the Mount Read and Mount Windsor volcanic belts linked to geology via a GIS (Nathan Duhig/ Mike Roach).
  This will involve compilation of descriptive information, and geochemical and isotopic data for volcanic rocks (altered and unaltered) from theses, company and government work into a single coherent database. The database will be merged with the digitised geology for these belts so that regional trends in the alteration geochemistry can be assessed relative to geological features of interest.

- Characterisation of the least altered volcanic suites within the Mount Read and Mount Windsor volcanic belts (Tony Crawford/Joe Stolz).
  This will extend previous work done in these belts and involve collection and analysis of additional rock samples to provide a better coverage of the volcanic belts. An appreciation of the range of unaltered volcanic compositions is essential to evaluate the geochemical effects of alteration. Additional outcomes should include confirmation of presently recognised suites and possible identification of additional suites that may prove useful in understanding stratigraphic relationships, and in locating potential mineralised horizons.

- Regional alteration patterns and vectors (Bill Wyman, Garry Davidson).
  This part of the project involves an analysis of the relationships of alteration patterns (mineralogy, chemistry and textures) to intrusives and the various volcanic facies. It will include:
  - the regional sampling traverses
  - alteration patterns around Cambrian granitoids
  - alteration in lavas and domes
  - alteration in volcaniclastic rocks
  - geochemistry of exhalites

- Interpretation of the databases for the Mount Read and Mount Windsor volcanic belts in terms of hydrothermal fluid flow patterns and ore genesis. This will include fluid–rock computer simulations to develop geochemical models to aid in understanding the processes involved in hydrothermal alteration (Dave Cooke).

- Fertile and barren volcanic belts (Joe Stolz).
  This will involve using the geochemical database assembled in this project, and additional data for silicic volcanics from various belts to assess the criteria that have been applied in the Archean of Canada to distinguish belts that are fertile with respect to VHMS deposits from those with low potential.

GIS Report

Nathan Duhig
Centre for Ore Deposit and Exploration Studies, Geology Department, University of Tasmania

Summary

This progress report summarises work to date compiling the Western Tasmania GIS database. A total of 537 located samples, all with whole-rock analyses, most with differing ranges of trace elements and some with rare-earth elements make up four separate tables in ArcInfo. These samples are yet to be combined with any data from project sponsors or the released Industry, Safety and Mines (ISM) data. Preliminary plots, showing the distribution of samples and some manipulation of the data are also presented.

Introduction

GIS can be a very powerful tool for data analysis and interpretation. A large amount of geochemical data of Mount Read Volcanics has been collected over the years and exists in different forms. For any regional alteration study to be meaningful, these disparate data bases must be drawn together before data analysis and interpretation can be undertaken.

Geochemistry database format

The database has the same format as ISM's ROCKCHEM whole rock database. This in turn was based upon the PETCHEM DATA SET of AGSO. The database is divided into four linked tables; RCHEM.SAM, RCHEM.MAJ, RCHEM.TRC and RCHEM.REE, containing sample, major element, trace element, and rare earth element data, respectively.

Data sources

Geochemical data for the Mount Read Volcanics exists in several forms: ISM has a large database of their own and open file data, some of which has recently been released; company databases, which usually contain proprietary data from mining leases and tenements that have been held for long periods of time; some researchers have collected databases of analyses which range in degrees of usefulness, usually a factor of how well the samples are located; AMIRA Project 84/P210 Controls on Gold and Silver Grades in Volcanogenic Sulphide Deposits, produced an excellent set of located analyses; and unpublished Honours and post-graduate theses. The latter two sources have been the main contributors to this project's database to this stage of its development.

The geology exists on two levels: the 1:500 000 state coverage and the 1:100 000 Mount Read Volcanics compilation map (Corbett and McNeill, 1988). The latter has been digitised as part of this project. As mentioned earlier, ISM recently released the eastern (with respect to the Mount Read belt), Charter, Block, Tullah, Selina and Tyndall 1:25 000 sheets, but these, as with the data released with them, are yet to be incorporated into this project. Some of these contain more outcropping Proterozoic than Paleozoic geology, so their current usefulness would be limited.

Data entry and problems

Where possible, data already in spreadsheets was sought to minimise manual data entry. For the AMIRA Project 84/P210 data, the geochemical data

was found on old Macintosh discs in the CODES storeroom. The other fields had to be entered manually. Some researchers had copies of their students' data but otherwise data from theses was either scanned or entered manually, depending upon the amount of data. Much of the descriptive and location data is present in the Geology Department catalogue, some of which is also contained in Excel spread sheets. However, individual catalogues range in quality, and considerable time was spent trying to resolve problems, some of which were unresolvable. Other problems included data which had been normalised to 100%, but often the loss on ignition values were absent. Phil Robinson's meticulous record keeping was a valuable aid in some of these cases.

Distribution of samples

Figure 1 shows the distribution of samples north of Macquarie Harbour (this excludes two beach boulders of granite from Elliott Bay). There are obvious holes in the distribution of samples. For example, some areas where there is known to be data in the Geology Department, such as Mount Lyell, Pinnacles-High Point, Hercules-Mount Read. Some of this data was avoided as ISM has entered it into their database. Other data was presumed to be contained in company databases (especially around Rosebery-Hercules and Hellyer-Que River), to which this project may be granted access at some stage.

There is a problem at the moment with multiple samples from single drill holes as they are all assigned the collar coordinates for their position. In one case, 20 samples are reported from the one hole. This obviously under-represents the number of samples in the database shown on Figure 1.

Examples of GIS applications to whole-rock geochemistry

Figure 2 shows a very straightforward example for the area around Rosebery, where there is the densest concentration of surface samples, mainly from Naschwitz (1985). The plot shown splits the samples on the basis of whether SiO_2 is greater or less than 70%. Figure 3 discriminates the rocks of rhyolitic composition on the basis Ti:Zr. Figure 4 takes this one step further by discriminating altered rhyolites as those with $Na_2O < 1$. These simple plots demonstrate the ease with which a large database can be manipulated. Once the database is more comprehensive, it will be straightforward for the lithogeochemists to refine these basic plots and make much more complex queries of the database.

Conclusions

The western Tasmania wholerock geochemistry database compilation is progressing well. There are more samples from theses to add and other databases to integrate with the current one. The preliminary plots give an indication of the potential of GIS to interrogate large databases.

References

Corbett, K.D. & McNeill, A., 1988. Map 6. Geological compilation map of the Mount Read Volcanics and associated rocks. Hellyer to South Darwin Peak. Geological Survey of Tasmania, Hobart.

Naschwitz, W., 1985. Geochemistry of the Rosebery ore deposit. Unpublished PhD thesis, Geology Department, University of Tasmania.

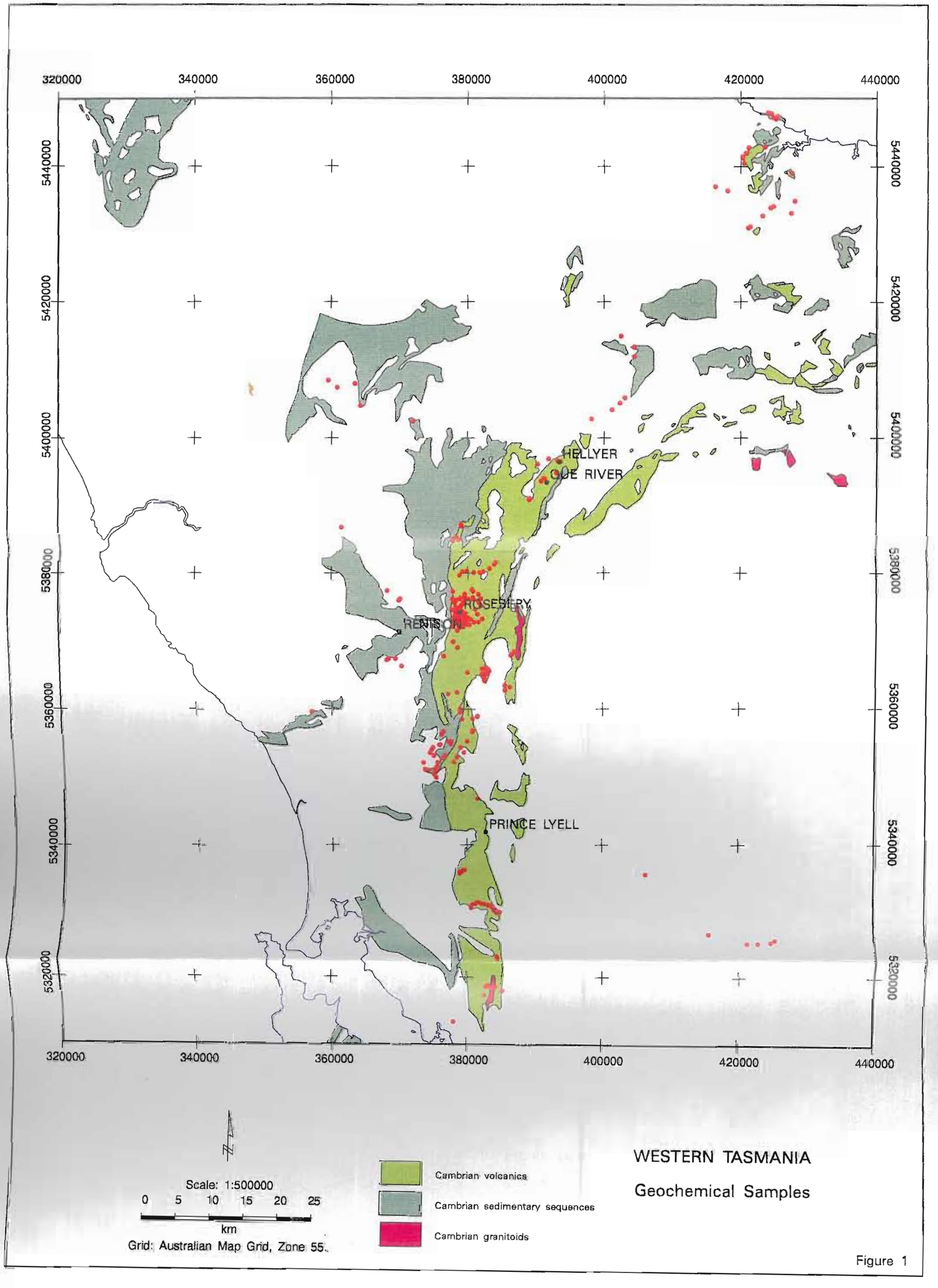
320000
340000
360000
380000
400000
420000
440000
5440000
5420000
5400000
5380000
5360000
5340000
5320000
HELLYER
QUE RIVER
ROSEBERY
RENISON
PRINCE LYELL
Scale: 1:500000
0 5 10 15 20 25
km
Grid: Australian Map Grid, Zone 55.
Cambrian volcanics
Cambrian sedimentary sequences
Cambrian granitoids
WESTERN TASMANIA
Geochemical Samples

Figure 1

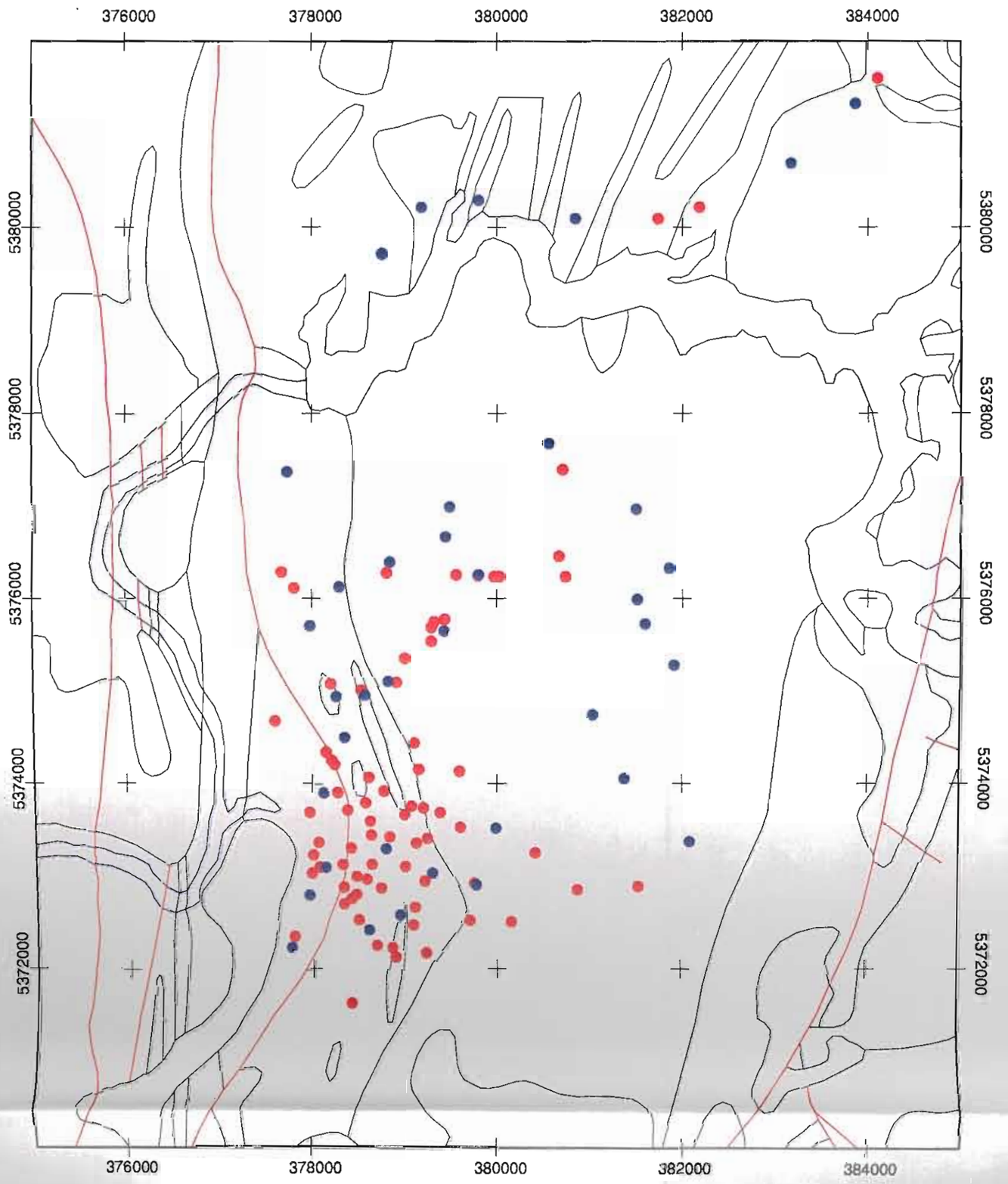

Scale: 1:50000

0 500 1000 1500 2000 2500

m

Grid: Australian Map Grid, Zone 55.

SiO2 > 70%

SiO2 <= 70%

ROSEBERY AREA

Geochemical Samples

Figure 2

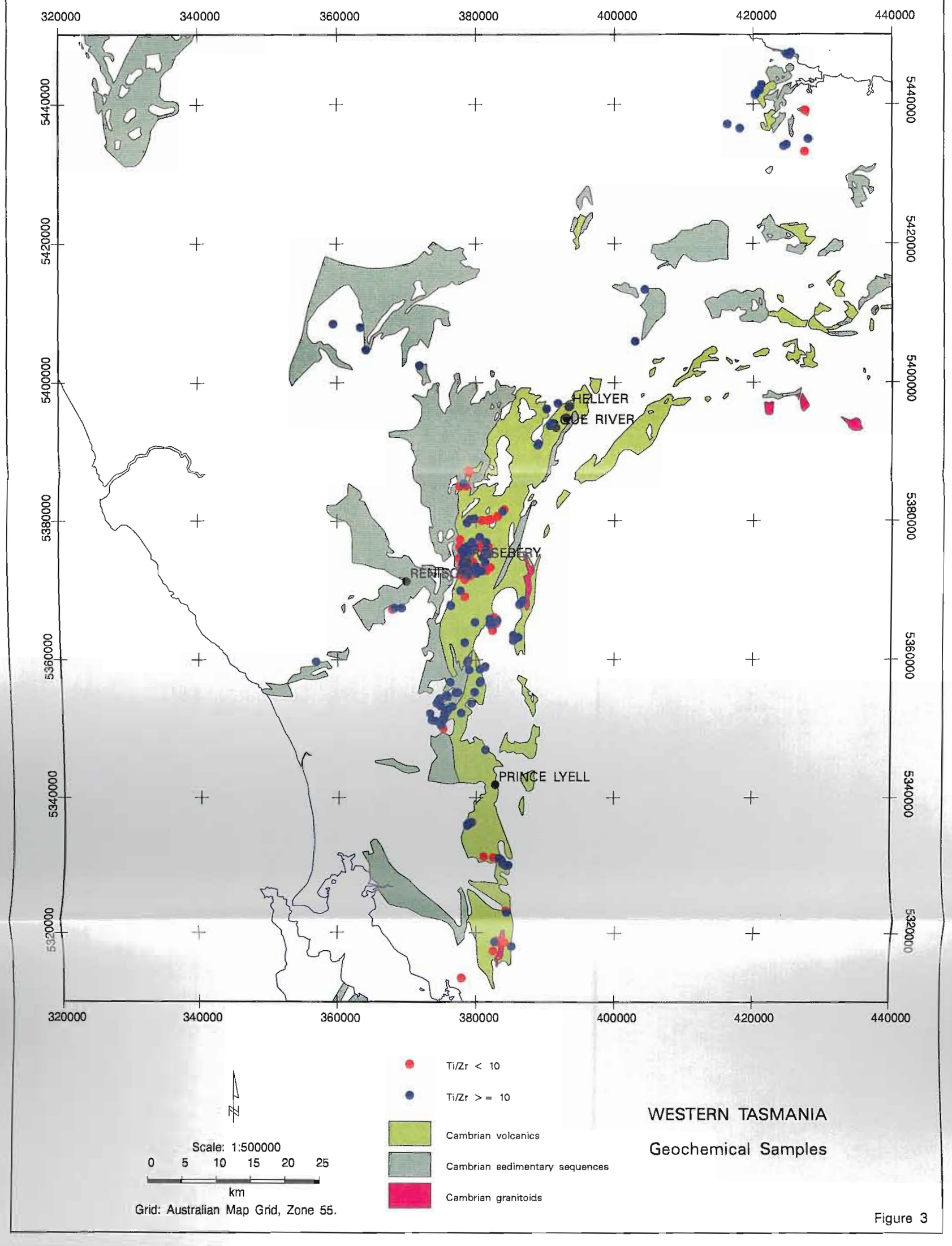

WESTERN TASMANIA

Geochemical Samples

Figure 3

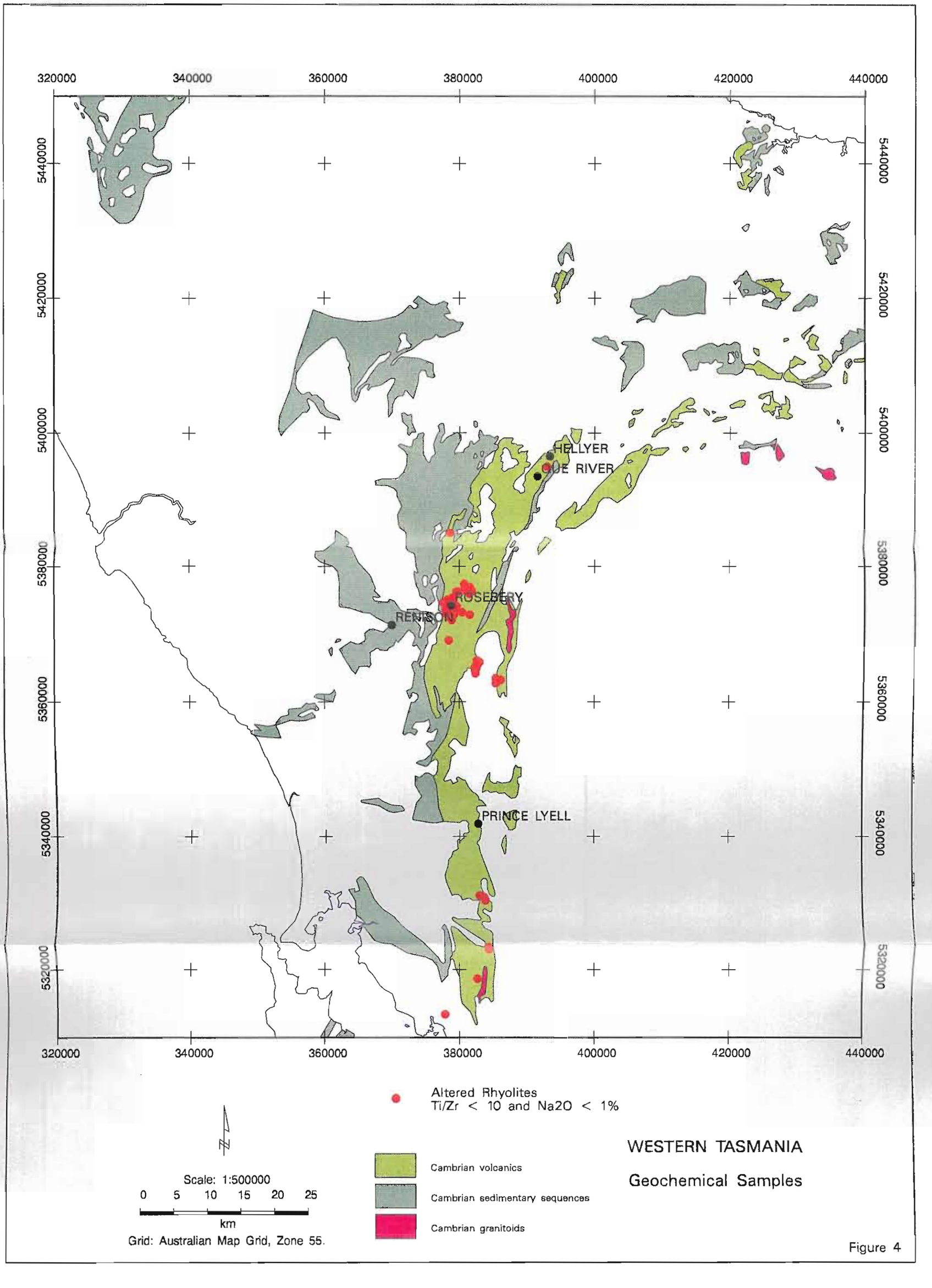
320000
340000
360000
380000
400000
420000
440000
5440000
5420000
5400000
5380000
5360000
5340000
5320000
HELLYER
QUE RIVER
ROSEBERY
RENISON
PRINCE LYELL
Altered Rhyolites
Ti/Zr < 10 and Na2O < 1%
Cambrian volcanics
Cambrian sedimentary sequences
Cambrian granitoids
Scale: 1:500000
0 5 10 15 20 25
km
Grid: Australian Map Grid, Zone 55.
WESTERN TASMANIA
Geochemical Samples

Figure 4

EVALUATION OF THE ROLE OF CAMBRIAN GRANITES IN THE GENESIS OF WORLD–CLASS VHMS DEPOSITS IN TASMANIA

Ross Large[1], Mark Doyle[1], Ollie Raymond[2], David Cooke[1], Andrew Jones[1] and Lachlan Heasman[1]

(accepted for publication in *Ore Geology Reviews*, 1966)

An analysis of the distribution, composition and alteration zonation of Cambrian granites which intrude the Mt Read Volcanics of western Tasmania provides evidence that there may have been a direct input of magmatic fluids containing Fe, Cu, Au and P to form the copper–gold volcanic-hosted massive sulphide (VHMS) mineralisation in the Mt Lyell district.

Interpretation of regional gravity and magnetic data indicates that a narrow discontinuous body of Cambrian granite (2–4 km wide) extends along the eastern margin of the Mt Read Volcanic belt for over 60 km. The Cambrian granites are altered magnetite series types which show enrichment in barium and potassium, and contrast markedly with the fractionated ilmenite series Devonian granites related to tin mineralisation elsewhere in the Dundas Trough.

Copper mineralisation occurs in a linear zone above the apex of the buried Cambrian granite body at the southern end of the belt, from Mt Darwin to the Mt Lyell district over a strike length of 25 km. Gold and zinc mineralisation are concentrated higher in the volcanic stratigraphy more distant from the granite. Overlapping zones of alteration extend from the granite into the surrounding volcanic rocks. An inner zone of k-feldspar alteration is overprinted by chlorite alteration, which passes outwards into sericite alteration. Magnetite ± pyrite ± chalcopyrite ± apatite mineralisation is concentrated in the chlorite alteration zone as veins and low grade disseminations. The Mt Lyell copper–gold stringer and disseminated mineralisation is hosted in felsic volcanic rocks 1 to 2 km west of the interpreted buried granite position. Magnetite – apatite ± pyrite veins in the Prince Lyell deposit at Mt Lyell are very similar to the veins in the halo of the granite, further south, and provide evidence for magmatic fluid input during the formation of the copper–gold VHMS deposits.

A model involving deeply penetrating convective seawater, mixing with a magmatic fluid released from the Cambrian granites, best explains the features of VHMS mineralisation in the Mt Lyell district.

1. Introduction

There has been considerable debate over the past 25 years on the role of granitic magmas during the generation of volcanic-hosted massive sulphide (VHMS) deposits. Some workers (eg. Urabe & Sato 1978, Henley & Thornley 1979, Sawkins & Kowalik 1981 and Stanton 1985, 1990) have argued for a direct input of volatiles and metals from the magma to form the ore solutions, while others (eg. Kajiwara 1973, Spooner & Fyfe 1973, Ohmoto & Rye 1974, Solomon 1976, Large 1977 and Stolz & Large 1992) have argued that the granites have acted as heat engines, driving seawater convection causing metals to be leached from the volcanic rocks stratigraphically below the massive sulphide deposits. In this paper, we provide evidence for a genetic link between granites and VHMS mineralisation in the Mt Read Volcanic belt of Western Tasmania (Fig. 1), and suggest that the granites may have provided important contributions of metal to the ore-forming fluid, especially Fe, Cu, Au and P.

2. Previous Work

The studies presented here build upon the thirty-year program of research led by Mike Solomon, investigating the genesis of massive sulphide deposits in the Mt Read Volcanics. Solomon (1976) was one of the first workers to evaluate and quantify the seawater convection model for massive sulphide genesis. His work showed that metals for the Rosebery and Mt Lyell deposits in western Tasmania could be sourced through leaching by seawater convective cells with a size of about 70 km²,

[1] Centre for Ore Deposit & Exploration Studies, University of Tasmania, GPO Box 252C, Hobart, Tasmania, 7001, Australia.
[2] AGSO, PO Box 378, Canberra, ACT, 2601, Australia.

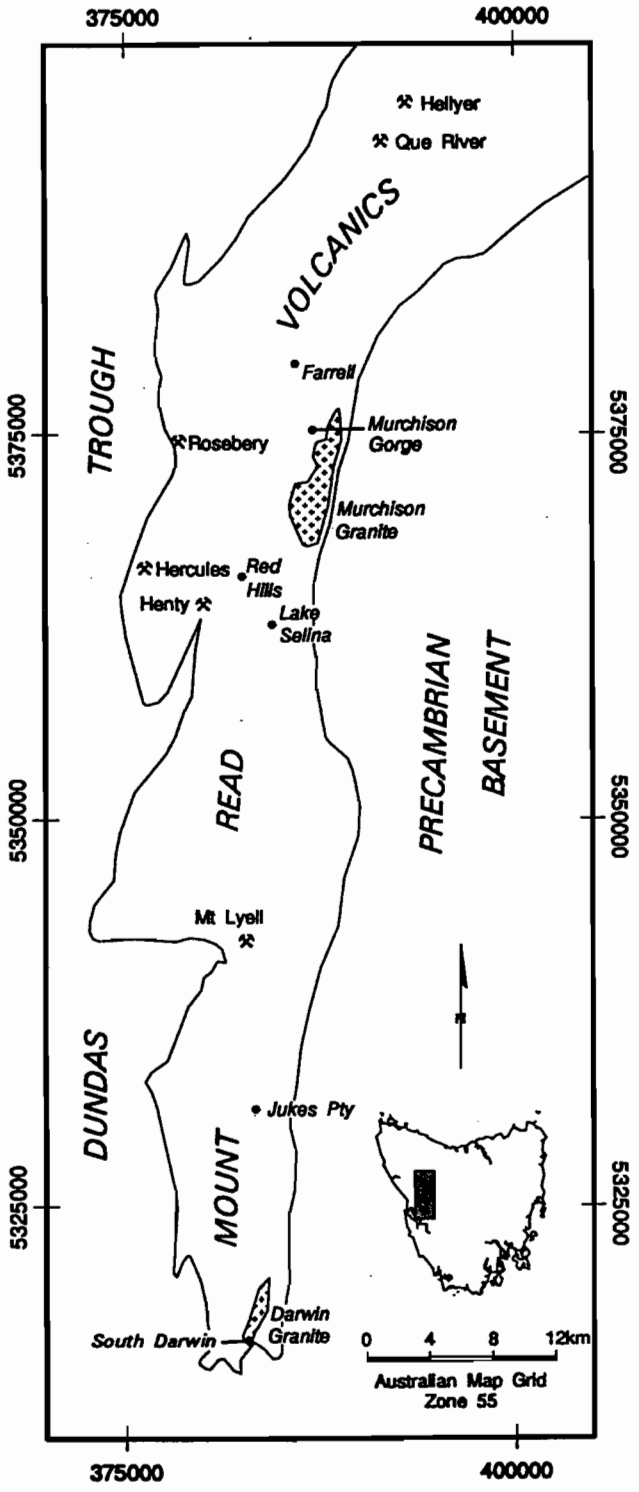

Figure 1: Extent of the Mt Read Volcanics in western Tasmania, showing outcrops of Murchison and Darwin Granites, and locations of major VHMS deposits, and prospects.

penetrating to depths of 4–5 km below the deposits. Subsequent work by Solomon and his students (Polya et al. 1986 and Eastoe et al. 1987) suggested a relationship between granite emplacement, district scale alteration, seawater circulation and VHMS mineralisation. Their work highlighted a relationship between hydrothermal alteration and sulphur isotope zonation around the granites which was interpreted to demonstrate a seawater sulphur source for the deep convective ore fluid. The critical section for their study was the Murchison Gorge area (Fig. 1), which exposed a continuous section from the Cambrian granite through altered volcanic rocks to the Farrell slates, host to the Farrell Pb–Zn mineralisation and correlated with the Rosebery ore horizon (Polya et al. 1986).

However, subsequent mapping by Corbett (1989) suggested that the Cambrian granite in the Murchison Gorge had intruded Tyndall Group volcanic rocks, which were substantially younger than the host volcanic sequence to the Rosebery massive sulphide deposits, thus precluding the granites as heat engines for the ore fluid. A second blow to their theory was delivered by Gulson (1986), who showed with Pb-isotope studies that the Farrell Pb–Zn mineralisation at the top of the alteration system in the Murchison Gorge, was Devonian rather than Cambrian in age as proposed by Polya et al. (1986). Subsequently Taheri & Green (1990) demonstrated, using a range of geological and geochemical techniques, that the nearby Lakeside Au–As–Sn deposit was also related to Devonian granites. Consequently the Cambrian granite-related seawater convective theory of Solomon's team (Polya et al. 1986 and Eastoe et al. 1987) based on the Murchison Gorge section was discounted, and the Tasmanian Cambrian granites have been essentially ignored as a critical element of ore genesis models for the past seven years. However, our recent research in the southern section of the Mt Read Volcanics has led to a re-evaluation of the role of granites in VHMS genesis, especially in the Mt Lyell district.

3. Factors Linking Granites to VHMS Mineralisation in Western Tasmania

3.1 Distribution of granites and mineralisation

Two narrow bodies of Cambrian granite (Murchison Granite and Darwin Granite) have intruded the eastern margin of the Central Volcanic Complex (CVC) in the Mt Read Volcanics (Fig. 1). Based only on these two exposures, there appears to be no clear relationship between granite location and massive sulphide distribution throughout the volcanic belt (Fig. 1).

Regional aeromagnetic surveys of the Mt Read Volcanics (Fig. 2) indicate a strong elongate magnetic

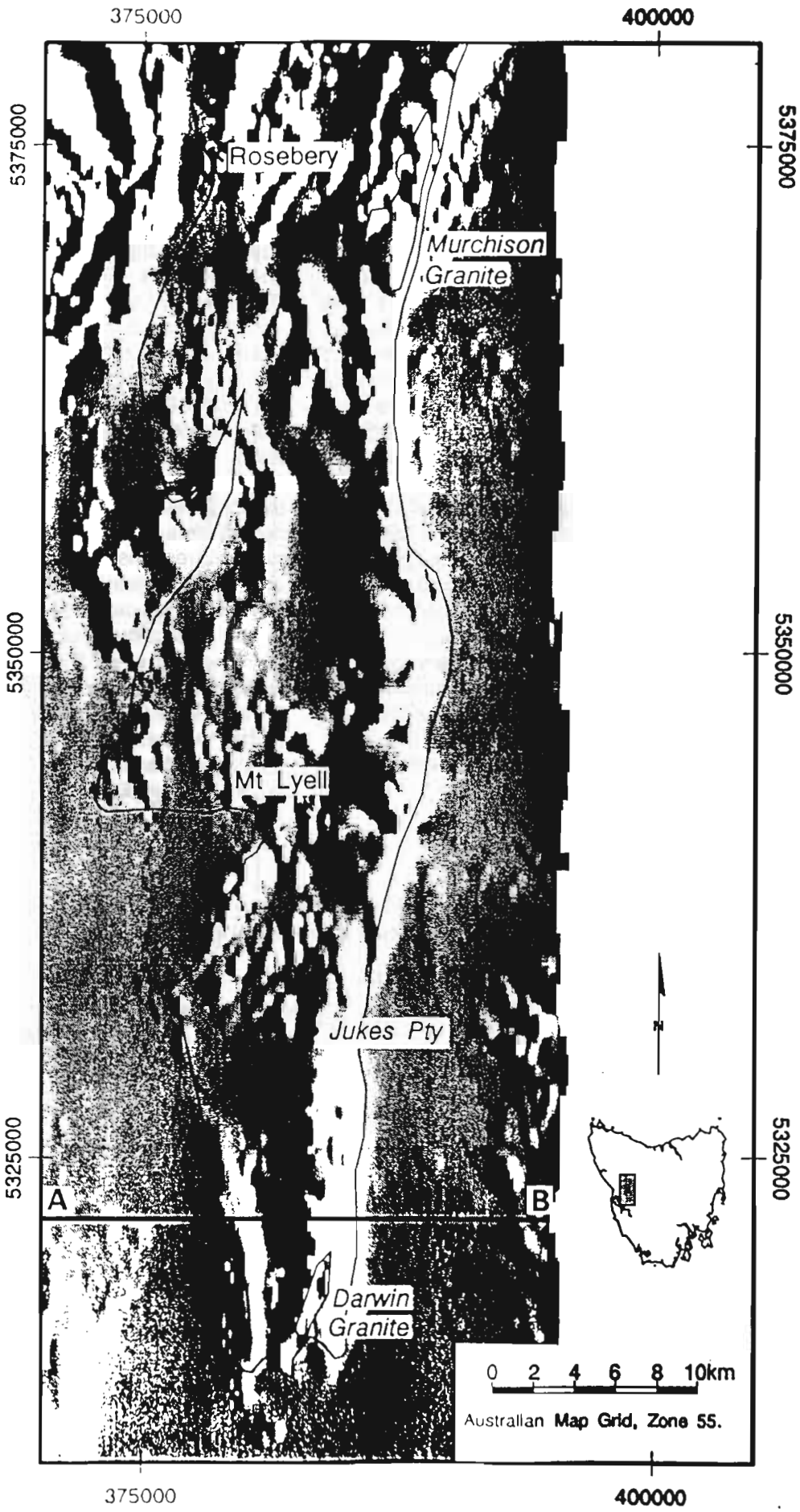

Figure 2: Total magnetic intensity grey scale image of the Mt Read Volcanics with artificial sun angle from the east. The line of magnetic anomalies along the eastern margin of the volcanic belt are related to the Cambrian granites and associated alteration zone. Data from Mineral Resources Tasmania Survey, 1981.

anomaly over the outcrop area of the Darwin Granite. This anomaly relates to magnetite veining and alteration within and along the margins of the granite, as discussed in detail later in this paper. Immediately north of the Darwin Granite, a discontinuous belt of similar magnetic anomalies extends for over 60 km merging with a complex anomaly over the Murchison Granite (Fig. 2). Computer modelling of gravity and magnetic data along this zone has enabled the subsurface position of the granite to be estimated (Leaman & Richardson 1989, Payne 1991). The granite geophysical models are based on the fact that the Cambrian granites are significantly less dense and more magnetic than the Central Volcanic Complex rocks which they intrude. The granites show a density contrast of –0.04 gm/cc and magnetic susceptibility of 0.002 to 0.004 cgs units, compared with 0.0001 cgs units for the CVC rhyolites (Table 1). Recent studies by Heasman (in prep.) indicate that the magnetite-bearing alteration zone adjacent to the Murchison Granite, has magnetic susceptibility values over a wide range, from 0.03 to 0.0003 cgs units (Table 1). Similar results have been obtained over the alteration zone at Jukes Pty (Fig. 1). Due to the variable magnetic nature of the altered volcanic rocks surrounding and, in particular, vertically above the granite, it is difficult to accurately model the depth to the top of the granite. However, estimates of the horizontal width of the subsurface granite are considered to be fairly reliable.

Gravity and magnetic modelling of an E–W section 5 km north of the Darwin Granite shows a vertically oriented lenticular body of granite about 2 km wide with depth to top of about 1 km (Fig. 3). Similar E–W geophysical models at intervals along the belt indicate that the narrow granite body is semi-continuous along the eastern side of the Central Volcanic Complex from South Darwin to the Murchison Gorge (Fig. 4). The basic assumptions and limitations of 2D modelling of this type are discussed by Leaman & Richardson (1989).

A significant problem in interpreting the continuity of the subsurface granite is caused by the presence of detrital magnetite in certain volcaniclastic units of the Tyndall Group. This means the average magnetic susceptibility of the Tyndall Group volcanic rocks fall within the range of the Cambrian granite values (Table 1). Consequently, at certain localities along the interpreted extent of the Cambrian granite it is not possible to positively distinguish between the magnetic response from buried Tyndall volcanic rocks and buried granite. Although this causes problems in interpreting the detailed position of the buried granite in certain localities (eg. east of Mt Lyell) it is not considered to effect the overall interpretation of the regional north–south extent of the granite body.

The relationship between the interpreted extent of the subsurface granite and the distribution of copper, gold and zinc mineralisation in the district is shown in Figure 5. Important features to note include:

Table 1: Density and magnetic susceptibility data used in the geophysical modelling (Fig. 3). Compiled from the Mineral Resources Tasmania data-base supplemented with data from Payne (1992) and this study.

Rock Unit	Label *	Density contrast	Magnetic Susceptibility (cgs)
Cambrian granite	Cgr	2.64	0.002 → 0.004
Granite-related alteration	Alt	2.60	0.0003 → 0.03
Central Volcanic Complex	Cvc	2.68	0.0001
Tyndall Group	Ctyn	2.70	0.002
Eastern Quartz Phyric Sequence	Cqps	2.68	0.001
Western Sequence	Cws	2.66	0.0002
Owen Group	Ow	2.63	0.00005
Gordon Group	Ogl	2.81	0.0001
Siluro-Devonian	S-D	2.66	0.00001
Tertiary	Ts	2.14	0.0001
Precambrian	PreC	2.67	0.0003
Dundas undefined	Cvs	2.68	0.0005
Dundas Basalt	Cba	2.77	0.001

* The labels are those used in Figure 3.

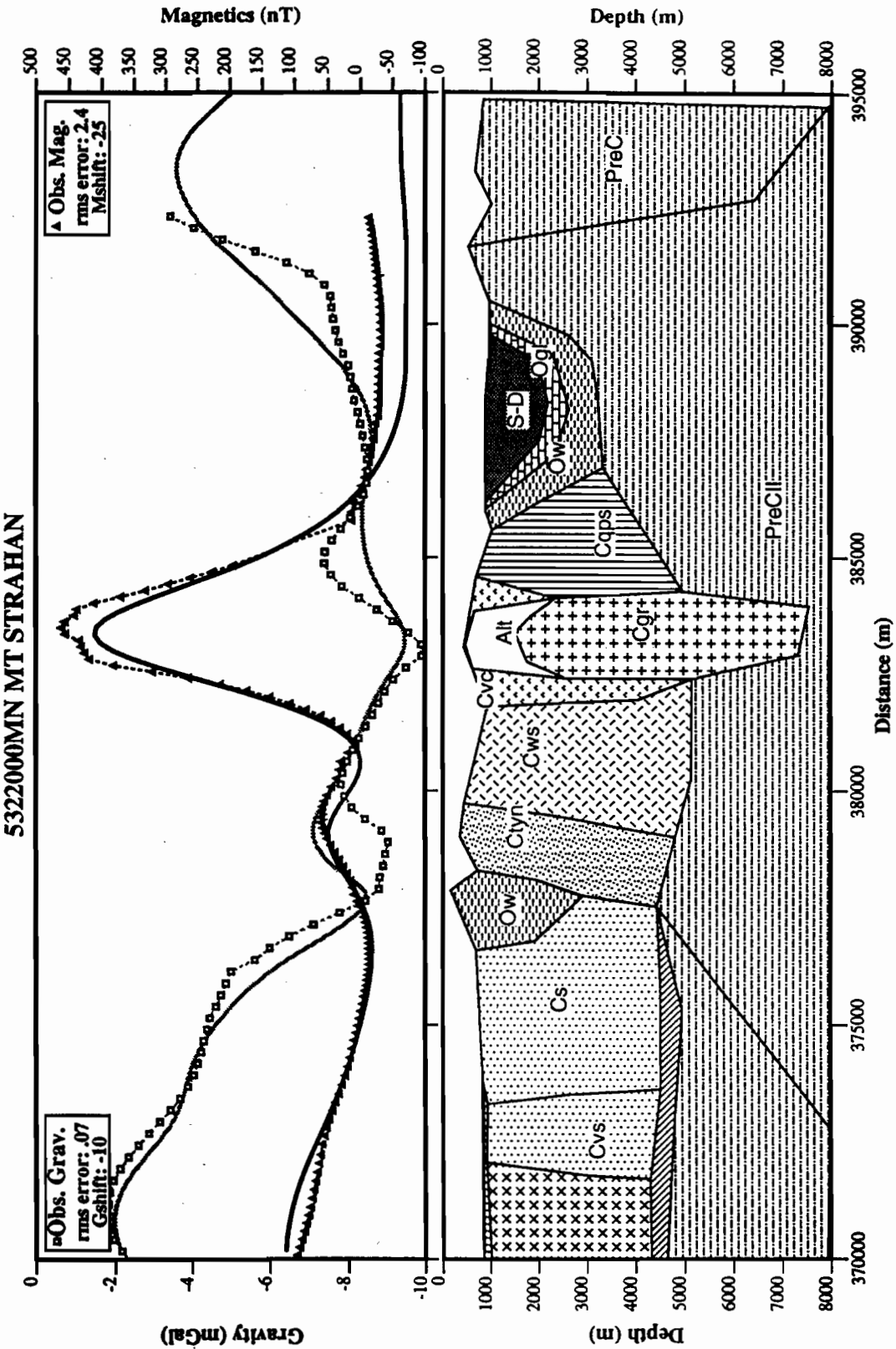

Figure 3: 2D gravity and magnetic model of geology along line A-B shown in figure 2. The modelling program Model 2D, Version 2.1 from Roache, 1991, was employed to interpret the subsurface geology. Density and magnetic susceptibility data used in the model are given in Table 1.

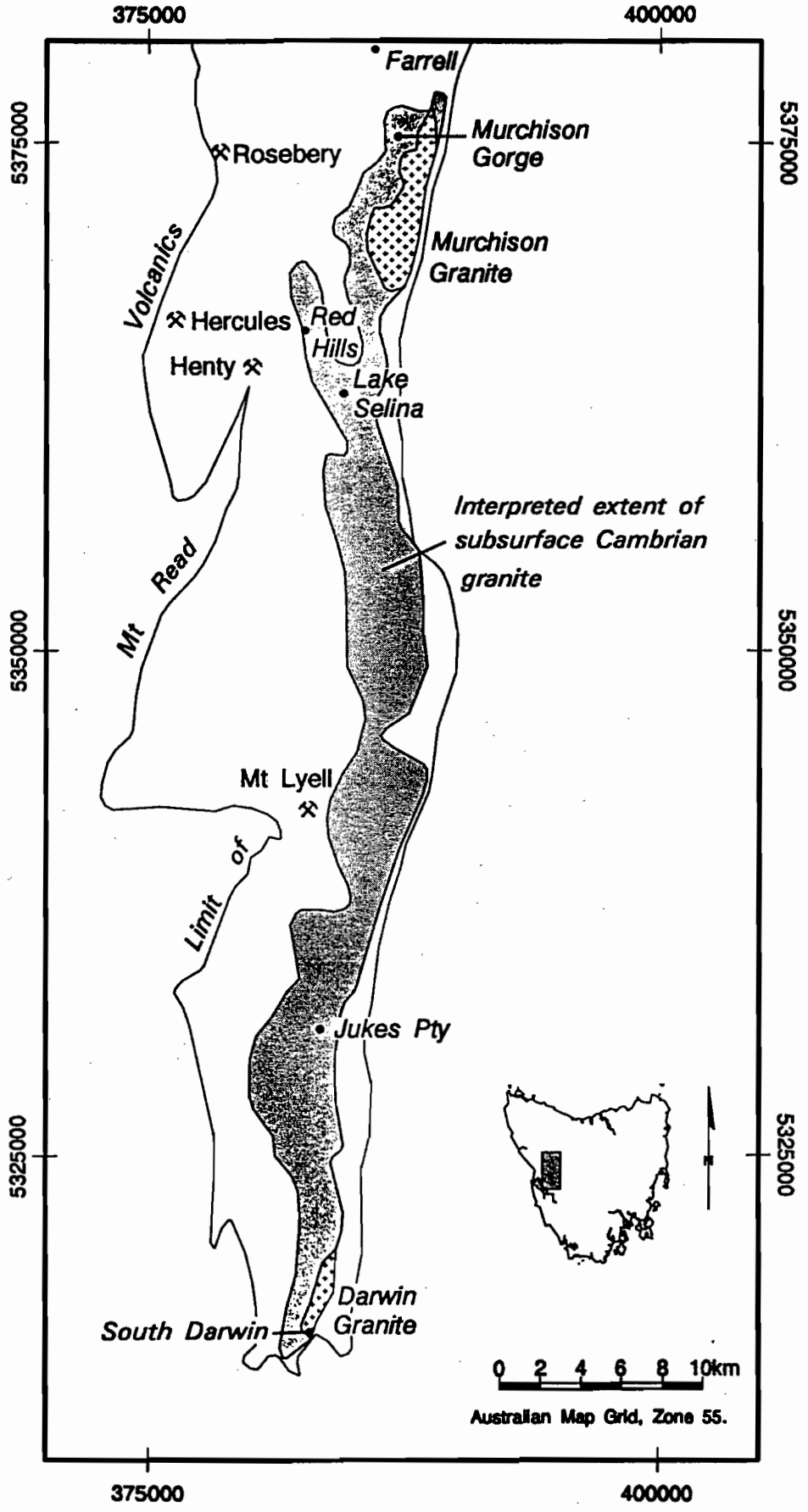

Figure 4: Interpreted position of sub-surface Cambrian granite based on modelling of gravity and magnetic data (compiled from Leaman and Richardson, 1989; Payne, 1991 and this study).

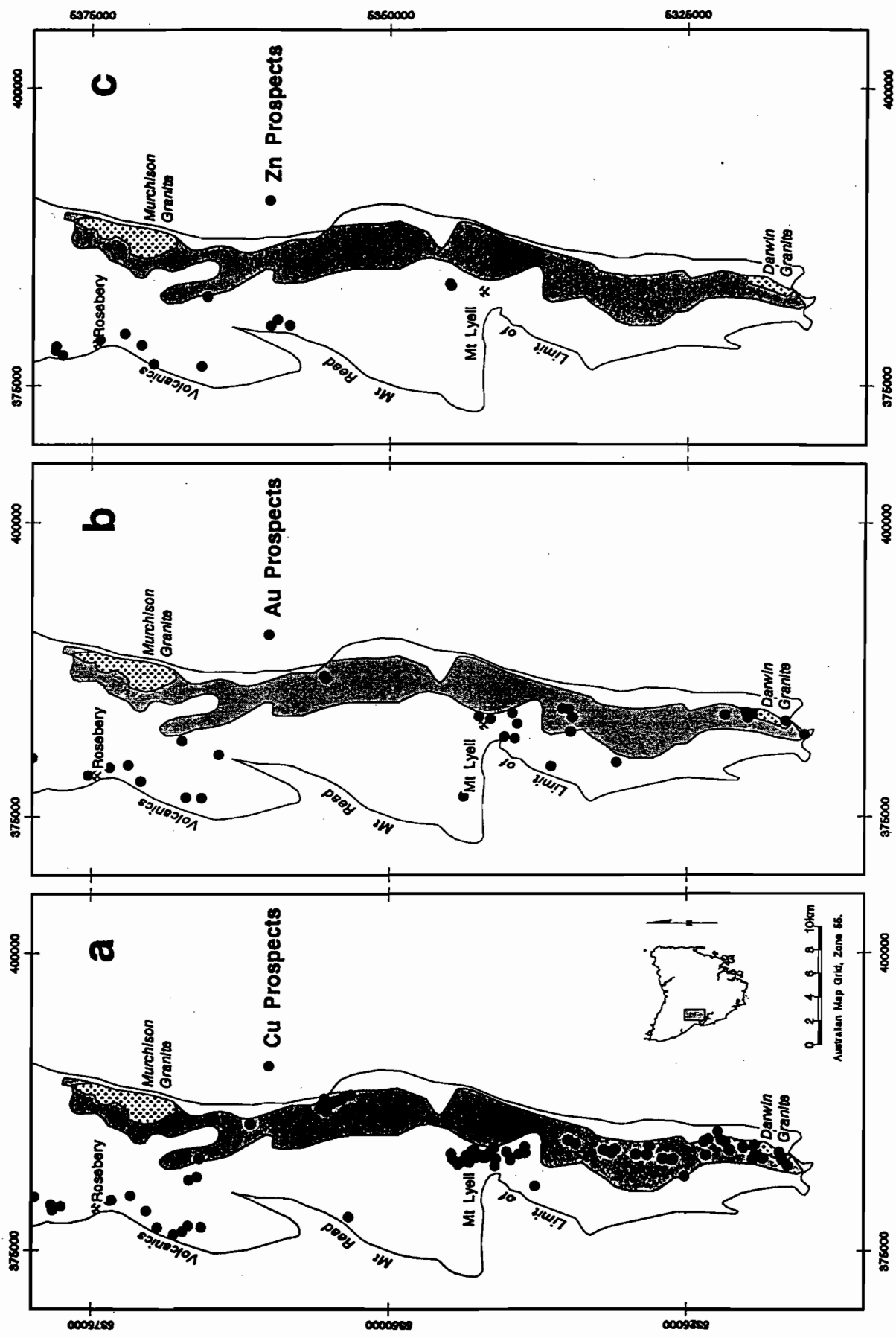

Figure 5: Position of copper, gold and zinc deposits and prospects relative to the subsurface granite in the Mt Read Volcanics. Prospect locations are taken from the MIRLOC data base, Mineral Resources of Tasmania.

(i) Copper distribution: shows a clear relation to the granite. A line of copper prospects lies over the northern extent of the Darwin Granite and continues north to the Mt Lyell Cu–Au mineral field (Fig. 5a). At Mt Lyell the copper deposits appear to lie 1–2 km west of the interpreted western margin of the subsurface granite.

(ii) Gold distribution: A few gold prospects lie over the granite in the Mt Darwin area, but most of the gold deposits lie in a zone west of the granite and "copper-line". In other words, gold is concentrated further from the granite in the stratigraphically overlying volcanic rocks.

(iii) Zinc distribution: zinc (and lead) deposits are absent from the southern end of the belt, and are concentrated in the north-western sector, in the higher volcanic stratigraphy west of the granite.

Overall, there is a regional zonation of metals from copper to gold to zinc (lead) passing west and north, away from the granite to higher stratigraphic levels in the Central Volcanic Complex (Fig. 5).

3.2. Timing of granites and mineralisation

Stratiform massive sulphide mineralisation in the Mt Read Volcanics is primarily hosted by the Central Volcanic Complex. Previous mapping by Corbett (1989) suggested that the Murchison Granite intruded the Tyndall Group Volcanics, which unconformably overlie the Central Volcanic Complex, and is therefore younger than the massive sulphide deposits. However, later work (eg. Corbett 1992) has revised this interpretation, and recent dating by Perkins & Walshe (1992) has confirmed that the Murchison Granite has an age of 501 ± 5.7 Ma (Ar/Ar on hornblende), the same age as the host rocks to the massive sulphide deposits (494.9 ± 4.3 to 503.2 ± 3.8 Ma). In addition, the Darwin Granite is unconformably overlain by the Tyndall Group, and clasts of magnetite-veined Darwin Granite can be observed in the basal Tyndall Group conglomerates (Jones 1993).

3.3. Composition of the granites

Recent studies by Abbott (1992) and Jones (1993) indicate that the Murchison and Darwin granites are strongly altered, high-K, magnetite series granites, following the classification of Ishihara (1981). The high degree of alteration precludes the use of the I/S classification of White & Chappell (1983). The Murchison Granite varies in composition from diorite to granite (58–78 wt % SiO_2, Fig. 6) while the Darwin Granite is composed of two highly fractionated phases (Jones 1993), with SiO_2 content from 74–78 wt % (Fig. 6). The K_2O content of the granites varies up to 8 wt % (Fig. 7), and the barium content is anomalously high (up to 3,000 ppm). Some of the K_2O and Ba enrichment is due to hydrothermal alteration.

Crawford et al. (1992) have undertaken a detailed study of the geochemistry of the Mt Read Volcanics, dividing the belt into three calc-alkaline suites and two tholeiitic suites based on major, minor and REE geochemistry. They consider that the Murchison and Darwin granites have geochemical affinities with the voluminous Suite I medium to high K calc-alkaline volcanic rocks, including rhyolitic to andesitic lavas from the Central volcanic Complex and Tyndall Group. Selected whole rock and trace element analyses of the granites are given in Table 2. A database of 58 whole-rock and trace element analyses is available from the first author on request.

The classification of these granites as magnetite-series is based on their high magnetic susceptibility (demonstrated by the aeromagnetic patterns, Figure 2) and their high Fe_2O_3/FeO ratios (generally greater than 0.5). A comparison between the Tasmanian Devonian ilmenite-series tin granites and the Cambrian granites in terms of their Fe_2O_3/FeO ratios is shown in Figure 8. Some of the scatter in Fe_2O_3/FeO ratios in Figure 8 is related to variable alteration of the granite samples. However the least altered samples, such as sample 76943 in Table 2, show an Fe_2O_3/FeO ratio of between 1 and 3 and clearly fall within the magnetite-series field. The common association of magnetite-series granites with copper–gold mineralisation and fractionated ilmenite-series granites with tin mineralisation (Ishihara, 1981) is compatible with the compositions shown on Figure 8, and consistent with a relationship between the Cambrian magnetite-series granites of the Mt Read Volcanics and the copper–gold mineralisation at Mt Lyell.

3.4. Alteration zonation around the Cambrian granites

Well-developed zones of hydrothermal alteration have been mapped around the margins of the Murchison and Darwin granites. Polya et al. (1986) noted that the Murchison Granite has suffered potassic alteration, chloritization and late calcite-epidote alteration. They recorded a zonation in alteration mineralogy from the western margin (top?) of the granite, up through the volcanic section to the Farrell slates (about 2.5 km of stratigraphic section) as follows: potassic zone (K-feldspar, chlorite, epidote, calcite, pyrite, magnetite); epidote zone (epidote, chlorite, calcite, magnetite); chlorite zone (chlorite, sericite, albite, calcite); sericite zone (dominantly sericite, quartz). Eastoe et al. (1987) and Jones (1993) record potassic, chloritic and sericitic phases of alteration in the Darwin Granite and the Central Volcanic Complex to the immediate west and north

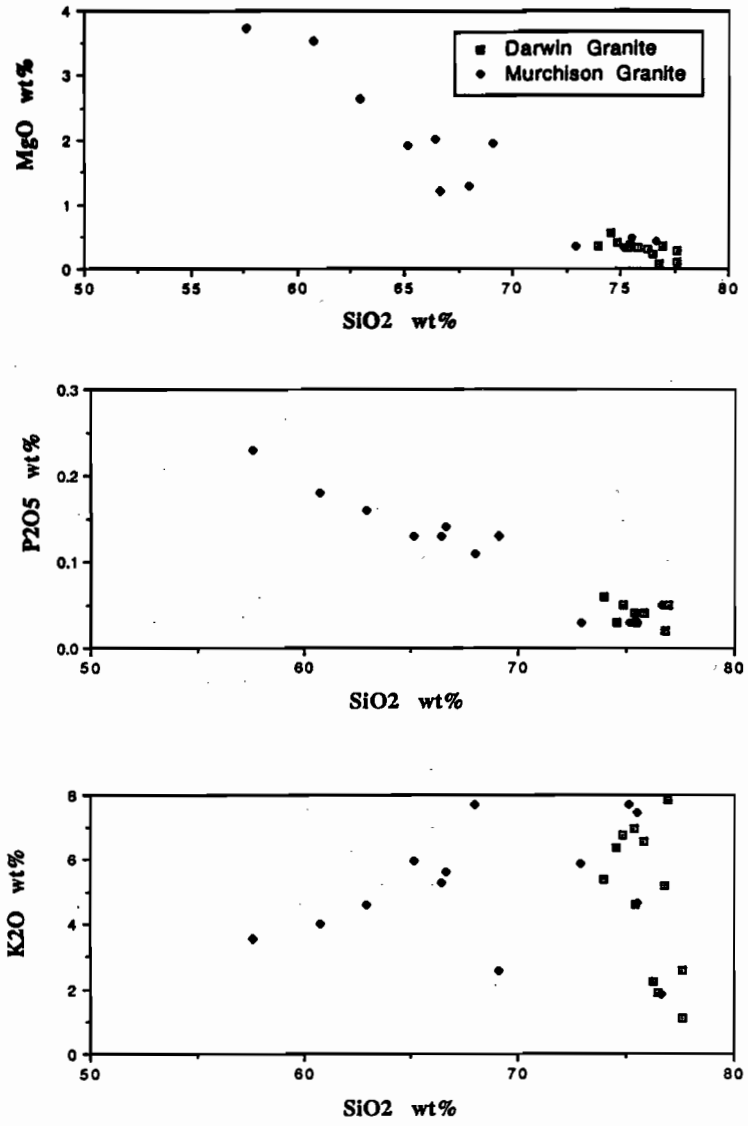

Figure 6: Harker diagrams for selected elements (MgO, P_2O_5, K_2O) of analyses from the Murchison and Darwin granites.

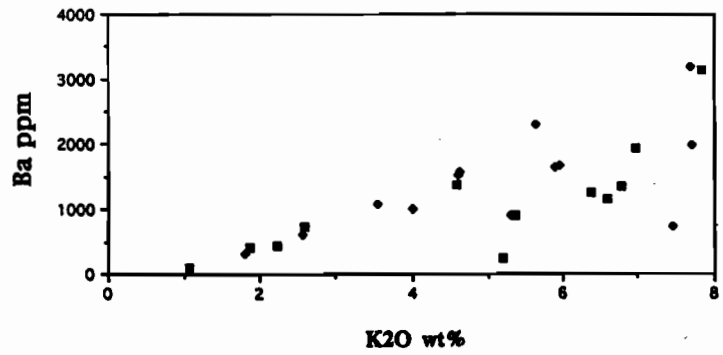

Figure 7: K_2O versus Ba for the Murchison and Darwin granites.

Table 2: Analyses of selected samples of Cambrian granitoids from the Mt Read Volcanics

Field No*	AT050	AT013	AT053	GS2	GS6	GS5
Sample No**	76943	76964	76941	78322	78324	78447
Source	Murchison Granite	Murchison Granite	Murchison Granite	Darwin Granite	Darwin Granite	Darwin Granite
References	Abbott (1992)	Abbott (1992)	Abbott (1992)	Jones (1993)	Jones (1993)	Jones (1993)
SiO_2	57.65	67.93	75.51	76.93	74.83	76.23
TiO_2	0.87	0.45	0.27	0.19	0.19	0.26
Al_2O_3	15.53	13.97	12.16	12.45	13.60	13.54
FeO	3.12	1.36	0.68	0.81	0.41	0.81
Fe_2O_3	4.50	1.89	0.72	1.81	1.49	1.45
MnO	1.21	0.09	0.07	0.01	0.01	0.10
MgO	3.73	1.28	0.47	0.35	0.40	0.30
CaO	5.14	1.16	0.94	0.05	0.09	0.18
Na_2O	3.32	0.89	2.97	0.19	2.20	2.95
K_2O	3.54	7.68	4.64	7.84	6.77	2.23
P_2O_5	0.23	0.11	0.03	0.05	0.05	<0.02
LOI	2.24	2.59	1.15	1.76	1.36	2.57
Total	100.58	99.62	99.68	100.77	100.08	98.14
Ni	9	5	1	3	5	3
Cr	40	18	bd	2	2	4
V	188	81	11	20	16	4
Sc	nd	nd	nd	4	2	<2
Zr	166	179	258	124	128	190
Nb	13	21	11	11	12	20
Y	29	31	18	22	12	7
Sr	421	98	183	59	67	75
Rb	145	336	139	211	200	116
Ba	1087	3191	1578	3152	1348	444
Th	10	30	21	35	38	44
U	2.6	8	4.3	10.4	6.9	2.6
Pb	145	336	139	327	6	19
Zn	203	121	42	309	22	50
Cu	26	21	3	93	10	10

* = Field numbers reported in Abbott (1992) and Jones (1993)
** = Sample numbers are those catalogued in University of Tasmania collection
nd = not determined
bd = below detection level

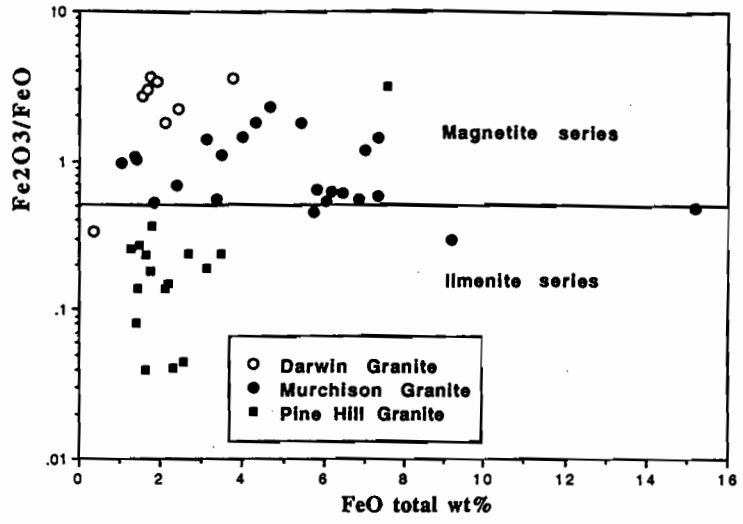

Figure 8: Fe_2O_3/FeO ratio plot for Cambrian Murchison and Darwin Granites compared with the Devonian Pine Hill Granite. Note that the majority of data for the Cambrian granites plot in the magnetite-series field of Ishihara (1981) while the tin related Pine Hill granite plots in the ilmenite-series field.

of the granite. Although no clear regional zones of alteration were defined, Eastoe et al. (1987) notes that the alteration assemblages are similar to those around the contact of the Murchison Granite, and are considered to relate to hydrothermal fluid circulation associated with granite emplacement and cooling. Magnetite and tourmaline veins and breccias are localised within and adjacent to the Darwin Granite, demonstrating that magmatic-hydrothermal fluids were exsolved from the granite during crystallisation.

At three other localities along the magnetic anomaly zone above the inferred granite "batholith" (Jukes Pty, Red Hills and Lake Selina, Fig. 2), extensive zones of mineralogically similar hydrothermal alteration with associated pyrite ± magnetite ± chalcopyrite mineralisation have been recorded (Eastoe et al. 1987, Hunns 1987, Doyle 1990, and Jenkins 1991). The best exposed section of alteration has been mapped by Doyle (1990) along the Jukes Road and King Tunnel cutting, east–west through the Central Volcanic Complex, at the Jukes Pty copper–gold prospect (Fig. 2). A diagrammatic section along the road is shown in Figure 9. This section incorporates mapping from the King Tunnel, 500 m below the road section. The geology of the section is dominated by altered rhyolitic to dacitic lavas of the Central Volcanic Complex, which are faulted against the Eastern quartz phyric sequence and unconformably overlain to the east by rhyolitic volcaniclastic rocks and lavas of the Tyndall Group.

Alteration of the volcanic rocks is zonally arranged, with intense pink K-feldspar alteration surrounded and overprinted by chlorite ± dolomite alteration, which passes outwards to a zone of pervasive sericite ± quartz alteration. Magnetite veins and patchy disseminations occur throughout the K-feldspar and chlorite alteration zones, with two main assemblages observed (Doyle 1990). Examples of slabbed rock samples from the major alteration zones are shown in figures 10A to 10D. Magnetite–pyrite ± tourmaline ± scheelite veins are extensively developed in the K-feldspar zone, while magnetite ± apatite–pyrite–chalcopyrite ± gold veins are developed in the strongly chloritic regions. The similarity of these alteration zones to those observed at the margins of the Murchison and Darwin granites supports the magnetic and gravity interpretation (Fig. 3) which indicates that granite is present at a depth of about 1 km below surface at this locality.

In summary, detailed mapping and petrography along the eastern margin of the Mt Read Volcanics, covering the line of granite extending from the Murchison Gorge to Mt Darwin (Polya et al. 1986, Eastoe et al. 1987, Hunns 1987, Doyle 1990, Jenkins 1991, and Jones 1993), indicates that the Cambrian granites are extensively altered and surrounded by a zonal arrangement of alteration as follows:

(i) K-feldspar zone (Z1) — pink K-feldspar alteration, with associated magnetite veins and disseminations extend from the outer parts of the granite into the surrounding volcanic rocks.

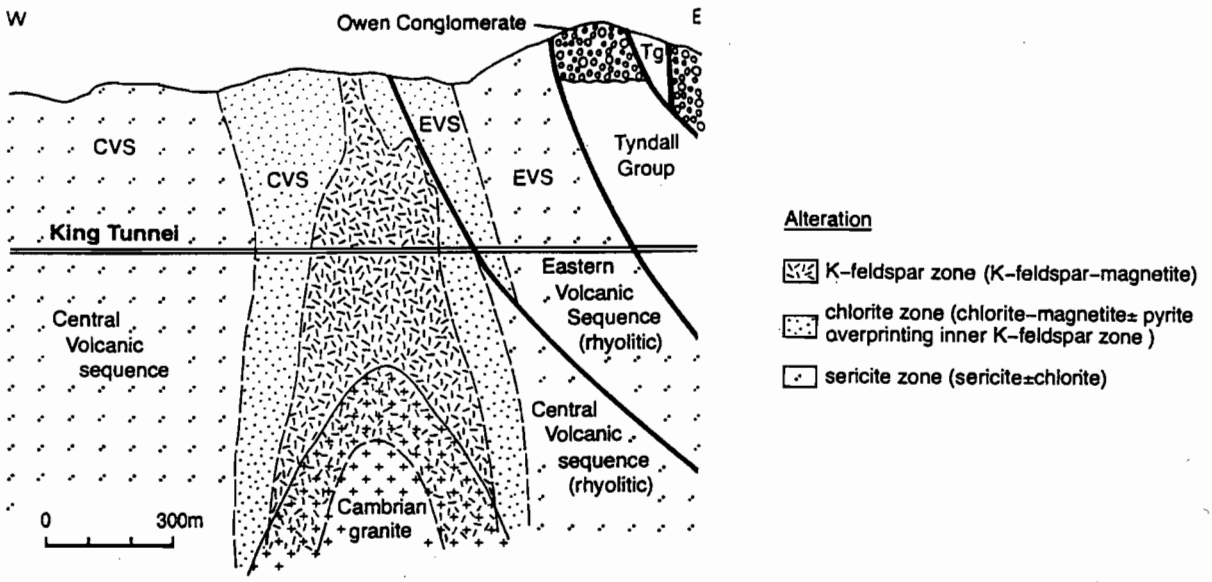

Figure 9: A generalised section along the Jukes Road and King Tunnel showing geological relations and alteration zonation. The section line is shown on figure 4. The granite position is interpreted from the gravity and magnetic modelling (Fig. 3).

(ii) Chlorite zone (Z2) — an overlapping shell of chlorite–dolomite–magnetite ± apatite ± pyrite–chalcopyrite alteration overprints and extends outwards from the K-feldspar zone.

(iii) Sericite zone (Z3) — a sericite ± chlorite ± pyrite assemblage forms a distal alteration zone which extends outwards overprinting the unaltered volcanic rocks.

The defined lateral extent (or radius) of these overlapping alteration shells varies from about 500 m at Jukes Pty to over 2 km in the Murchison Gorge.

3.5. The magnetite–apatite association

The strongest evidence for a link between the Cambrian granites and VHMS Cu–Au mineralisation in the Mt Read Volcanics is provided by the occurrence of magnetite–apatite ± Cu–Au veins and patchy disseminated mineralisation both within the chloritic alteration halo of the granites and within the centre of the Prince Lyell ore deposit in the Mt Lyell VHMS district. Hendry (1981) reported the presence of a phosphatic unit within the Prince Lyell orebody, on 14 level, which contained pyrite, magnetite, barite, apatite and other rare earth phosphate minerals. He suggested that the pyrite, phosphates and magnetite were deposited from seafloor hydrothermal exhalative activity during volcanism. Raymond (1992) recorded a large zone of magnetite–apatite stockwork vein and disseminated mineralisation at Prince Lyell (Fig. 11). The magnetite–apatite mineralisation occurs principally as elongate lenses to irregular semi-massive bodies of magnetite, up to 1–2 m wide, with large accessory pink apatite crystals (1 mm to 50 mm diameter) associated with chlorite and minor pyrite alteration (Fig. 10E, F). Stockwork veins of magnetite ± apatite–chlorite are associated with the elongate magnetite lenses and may be surrounded by zones of disseminated magnetite ± apatite. Throughout the copper ore bodies at Prince Lyell, minor veinlets of pyrite–chalcopyrite commonly display accessory apatite ± magnetite.

Trace element compositions (high Ti, V and REE) and magnetite $d^{18}O$ values of around 4 per mil led Raymond (1992) to conclude that the magnetite–apatite mineralisation was of magmatic origin. The presence of similar magnetite–apatite veins within the Darwin Granite (Jones 1993) and in the chlorite alteration zone surrounding the granite at Lake Selina (Hunns 1987) and Jukes Pty (Doyle 1990) supports this conclusion and suggests that the magnetite–apatite mineralisation at Mt Lyell is sourced from the nearby Cambrian Granite.

The correlation between magnetite and apatite within the hydrothermal systems of the region is supported by geochemical correlation data for FeO(total) and P_2O_5 shown in Figure 12. On this plot,

the Cambrian granites show a linear correlation between P_2O_5 and FeO(total) with the more dioritic compositions showing the greatest P_2O_5 enrichment, and the more felsic, potassic-altered granites showing P_2O_5 depletion. In comparison, the chlorite and sericite-altered volcanic rocks adjacent to the Cambrian Granite at Lake Selina generally show FeO enrichment with P_2O_5 values of < 0.2 wt %, except for a few samples (highlighted in Figure 12) which carry magnetite–apatite veins and show both FeO and P_2O_5 enrichment. Altered volcanic samples from the Mt Lyell orebody show considerable enrichment in both P_2O_5 and FeO, with P_2O_5 values varying from 0.2 wt % up to 0.8 wt %. Note that the magnetite–apatite veined volcanic rocks from the Lake Selina alteration zone adjacent to the southern extension of the Murchison Granite plot in the same field as the altered volcanic rocks from the Mt Lyell orebody.

A positive correlation is also observed between copper and P_2O_5 in the Mt Lyell orebody (Fig. 13) suggesting that the magnetite–apatite assemblage at Mt Lyell was part of the copper mineralisation event. Raymond (1992) concluded that on the basis of textural evidence and grade distribution that the magnetite–apatite mineralisation occurred late in the development of the Prince Lyell deposit. However the occurrence of minor magnetite and apatite in pyrite–chalcopyrite-bearing veins throughout the ores indicates that the magnetite–apatite event overlapped in space and time with the copper–gold mineralisation event.

4. Discussion

The data presented above on the distribution, timing, composition and alteration of the Cambrian granites provides strong indirect evidence that they had an important role to play in the genesis of the VHMS deposits in the Mt Read Volcanics. The common occurrence of magnetite ± apatite veins and alteration within, and surrounding, the Cambrian granites, and within the Prince Lyell copper–gold deposits indicates that magmatic fluids were likely to be involved in the genesis of the Mt Lyell deposits. The Mt Lyell field contains both stringer-style copper–gold deposits such as Prince Lyell (with magnetite–apatite assemblages) and separate stratiform lead–zinc–copper deposits such as Comstock, and Tasman and Crown Lyell Extended. Most previous workers (eg. Solomon, 1976 and Walshe and Solomon, 1981) consider that the Cu–Au and Pb–Zn–Cu deposits formed as part of the same hydrothermal system, where the Cu–Au stringer-style formed large zones of stratiform subsurface replacement and the Pb–Zn–Cu massive sulphides formed by contemporaneous seafloor exhalation or mound development (Large, 1992).

Based on the results of this study combined with previous work by Solomon and his co-workers (Solomon 1976, Walshe & Solomon 1981, Polya et al. 1986, Eastoe et al. 1987 and Solomon et al. 1988), it is now possible to present a preliminary model for the genesis of the Mt Lyell Cu–Au deposits and related Pb–Zn–Cu massive sulphides of the Mt Read Volcanics (Fig. 14).

Details of the model are:

(i) A linear zone of magnetite-series Cambrian granites intruded the eastern margin of the Central Volcanic Complex of the Mt Read Volcanics, probably along a major north–south marginal fault structure, or series of faults;

(ii) Seawater convection was established through the volcanic sequence surrounding the granites as proposed by Solomon (1976) and Eastoe et al. (1987) leading to the development of a series of overlapping alteration zones extending out from the granite;

(iii) Early magmatic hydrothermal fluid emanations produced the inner zones of K-feldspar ± magnetite alteration. Later mixing between magmatic and seawater derived fluids produced the overprinting chlorite and sericite zones surrounding the K-feldspar zone.

(iv) Continued magmatic hydrothermal fluid release resulted in magnetite ± apatite vein development and related minor copper–gold mineralisation in the chlorite zone surrounding the granites.

(v) Major copper–gold deposition occurred at distances of 1–2 km from the granite as the mixed magmatic-seawater fluid precipitated overlapping zones of pyrite–chalcopyrite and magnetite–apatite in permeable volcanic rocks below the seafloor. Minor seafloor exhalation led to the formation of Pb–Zn–Cu massive sulphide mounds stratigraphically above the Cu–Au deposits.

The Cambrian Granite is not considered to be the sole source of elements which constitute the Mt Lyell orebodies. The inner zones of copper and gold enrichment close to the granite (eg. Jukes Pty.) implies a magmatic source for these metals. Phosphorous and iron, which contribute to the magnetite–apatite veins within and around the granite, and within the Mt Lyell orebodies, are also likely to be magmatic contributions. However, previous studies by Green et al. (1981) and Solomon et al. (1988) indicate that sulphur in the ores is probably a mixture of sulphur derived from the granites and host volcanic sequence, and reduced sulphate from deep convective seawater. They demonstrate that sulphur isotope variations in the massive sulphide ores (7–15 per mil) are similar to those in the granite alteration systems (8–17 per mil), and therefore the source of sulphur for both systems is probably the same. A recent study of

sulphur isotopes in the Murchison Granite, utilising a laser microprobe for S-isotope analysis at the Central Science Laboratory, University of Tasmania, indicates (based on 24 analyses) that isolated pyrite disseminations from samples throughout the granite have $d^{34}S$ values of 10–17 per mil, with 50% of the data from 14–17 per mil (Large, in prep). Heavy sulphur isotopes of this type are incompatible with a magmatic source and can only be explained by reduction of sulphate derived from penetration of seawater deep into the core of the granite. Thus, although some elements in the VHMS hydrothermal systems may be of magmatic origin (eg. Cu, Au, P_2O_5), other elements (eg. S) are largely derived from reduced seawater, and other more soluble metals (eg. Pb, Zn, Ag) may be derived due to leaching from the volcanic pile by the convective seawater/magmatic fluid mixture.

4.1. Alternative Sources of Phosphorous

The least altered granodiorite samples of the Murchison Granite contain about 0.2 wt % P_2O_5, while the potassic altered granite (>5 wt % K_2O) is considerably depleted in P_2O_5 with values from 0.02 to 0.15 wt % P_2O_5. This suggests the possibility that the magmatic-hydrothermal K-feldspar alteration event was accompanied by leaching of phosphorous from the granite, thus providing a source for the P_2O_5 concentrated in apatite–magnetite veins in the distal chlorite alteration and related copper ore deposits. Generally the Mount Read Volcanics contain low levels of P_2O_5 (0.16 to 0.17 wt % P_2O_5); however, the Suite II andesites and Suite III basalts defined by Crawford et al. (1992) contain elevated P_2O_5 levels from 0.19 to 1.0 wt % P_2O_5. Phosphorous-rich hornblende andesites of Suite II occur within the volcanic sequence containing the Mt Lyell deposits (eg. Comstock, Corbett 1992), and provide an alternative source for the P_2O_5 found in the mineralisation.

A research program utilising isotope zonation studies (O, H, C, S, Sr and Pb) around the granites and the Suite II andesites is currently underway to assist in resolving the source of individual components related to the ores.

5. Conclusions

Cambrian granites of the Mt Read Volcanics form a thin (2–4 km wide), semi-continuous, linear body extending for over 60 km along the eastern margin of the volcanic belt from Mt Darwin to the Murchison Gorge. At the southern end of the belt, copper mineralisation occurs in magnetite–pyrite ± apatite veins which are concentrated along the granite contacts and granite apex. This line of copper prospects in the Darwin–Jukes area extends northwards into the Mt Lyell mineral district, where Cu–Au and Cu–Pb–Zn massive sulphide deposits are located 1–2 km west of the inferred granite position. Regionally, there is zonation of metals with respect to the granite; copper deposits lie closest to the granite, followed by gold ± copper and then zinc–lead ± copper in more distant locations in the higher volcanic stratigraphy to the west. In parallel with the metal zonation there is a consistent pattern of alteration zonation related to the linear zone of granites. An inner zone of K-feldspar ± magnetite alteration is overprinted by an intermediate zone of chlorite–magnetite ± apatite ± pyrite alteration, which merges laterally with a distal zone of sericite alteration. A magnetite–apatite stockwork vein system in the centre of the Mt Lyell deposit shows similar geochemical characteristics to the magnetite ± apatite veins and alteration surrounding the Cambrian granites and indicates that Cambrian granite-related fluids were probably involved in the genesis of the Mt Lyell deposits. A preliminary model has been developed which involves mixing of deep penetrating convective seawater within magmatic fluid released from fractionated phases of the magnetite-series Cambrian granites to produce sub-seafloor volcanogenic Cu–Au deposits and contemporaneous seafloor Zn–Pb mound-style massive sulphide deposits in the upper part of the Central Volcanic Complex in the Mt Lyell district.

Figure 10 (on opposite page): Photographs of hand specimens of granite and alteration lithologies: A: Cambrian Darwin granite containing a black magnetite vein; B: Chlorite (c) forming a vein-network overprinting intensley K-feldspar altered dacite, Jukes Pty Prospect; C: Pervasively K-feldspar altered dacite (k) containing zones of intense K-feldspar alteration (K) cut by chlorite veins (c), Jukes Pty Prospect; D: Hydraulic breccia in which magnetite (m) separates jigsaw-fit dacite clasts, Jukes Pty Prospect; E: Lozenge-shaped domains of apatite (a) are separated by magnetite (m) containing minor pyrite (arrow), Prince Lyell orebody, Mt Lyell; F: Chlorite-apatite altered volcanic containing a dismembered pyrite (arrow) and apatite (a) vein, Prince Lyell orebody, Mt Lyell.

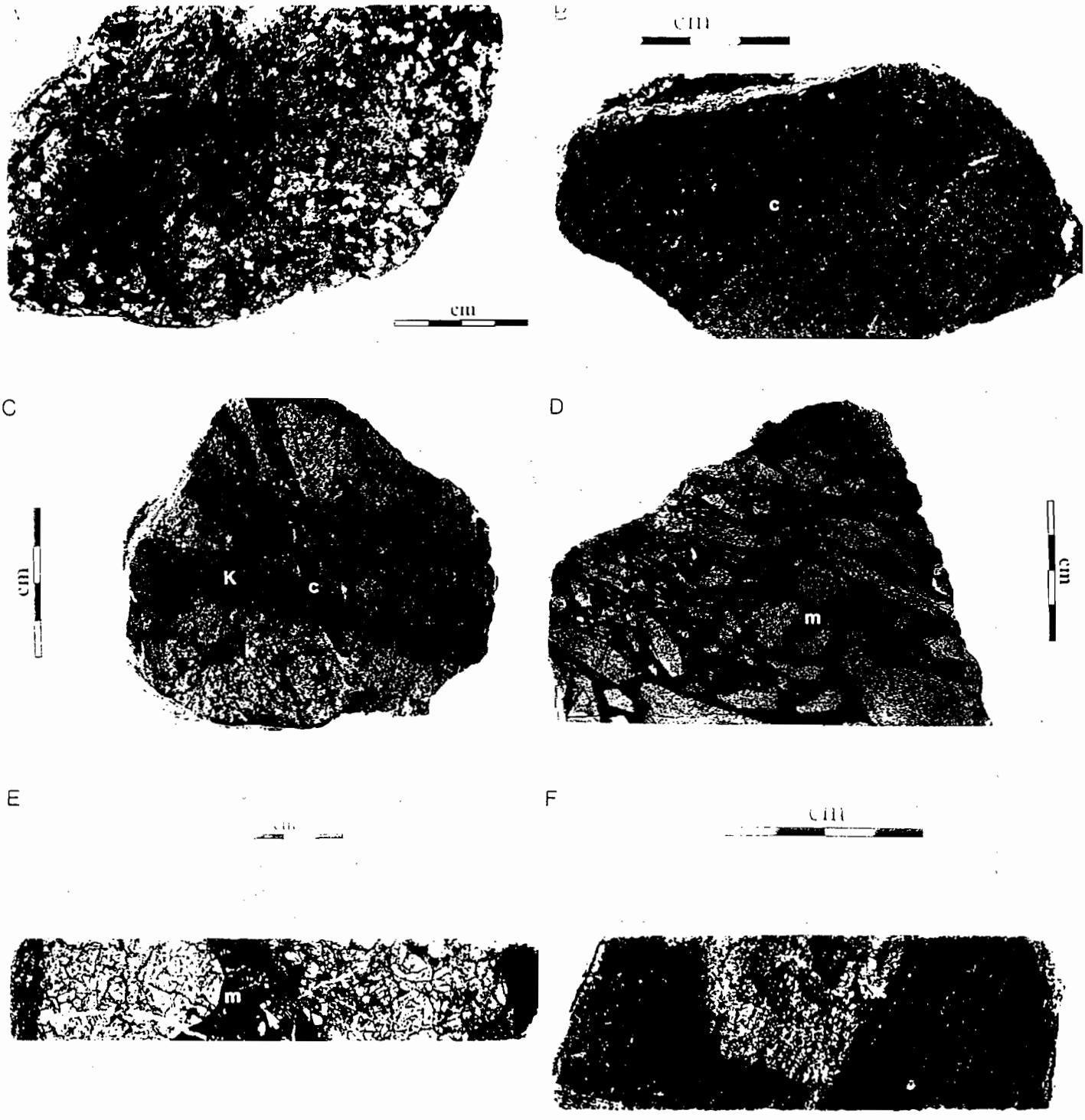
B
cm
c
cm
C
cm
K
c
D
m
cm
E
m
F
cm

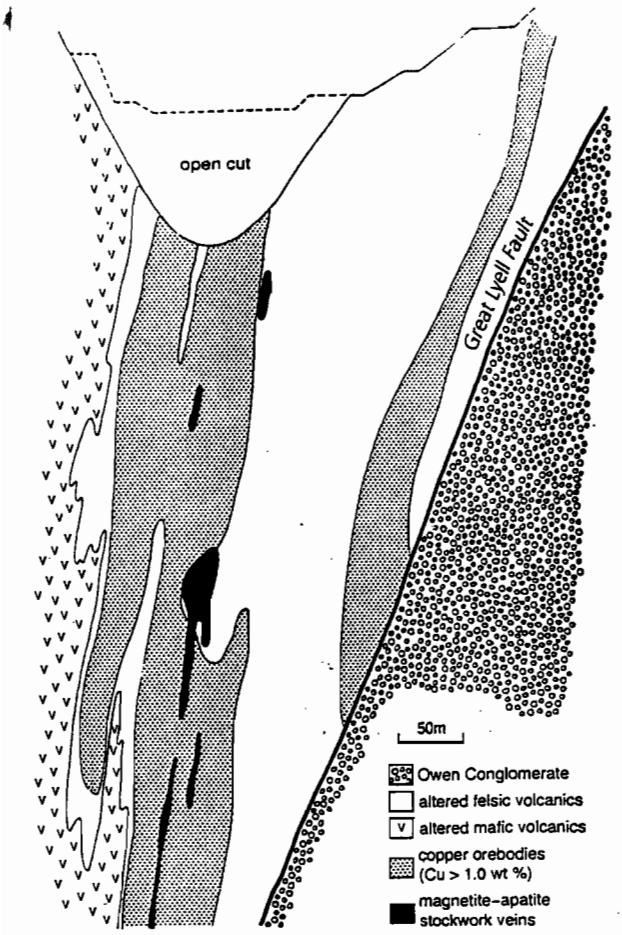

Figure 11: Cross-section of the Prince Lyell deposit showing the relationship of the magnetite-apatite stockwork zone to the copper orebodies.

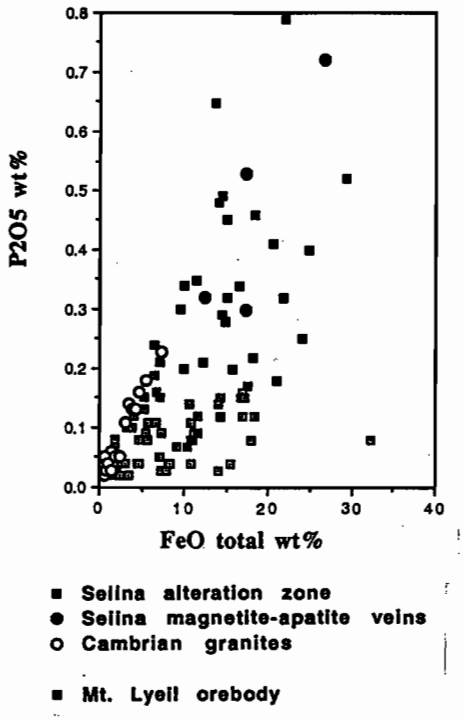

Figure 12: Total iron as FeO versus P_2O_5 for granites (Table 1), altered volcanic rocks from Lake Selina (S. Hunns, unpublished data), and the Mt Lyell copper orebodies (Raymond, 1992).

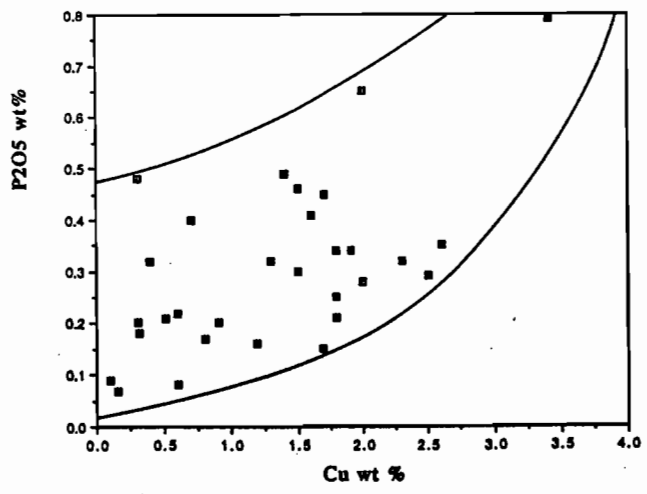

Figure 13: Cu versus P_2O_5 for altered felsic volcanic host rocks to the Prince Lyell copper orebodies (data from Raymond, 1992).

6. Acknowledgments

Discussions with various academic and industry geologists on the genesis of the Mt Lyell deposits and Cambrian granites have contributed to development of this paper; in particular David Leaman, Joe Stolz, Ben Payne, Scott Halley, Tony Crawford, Mike Solomon and Ron Berry. Permission to use geochemical data for Cambrian granites from the Mineral Resources Tasmania data-base, and from Steve Hunns for unpublished analyses on the Lake Selina Prospect, is also gratefully acknowledged. Thanks also to Michael Roach for generation of the Arcinfo geology/geophysics overlay diagrams. Comments by the two *Ore Geology Reviews* reviewers led to considerable improvement in the paper.

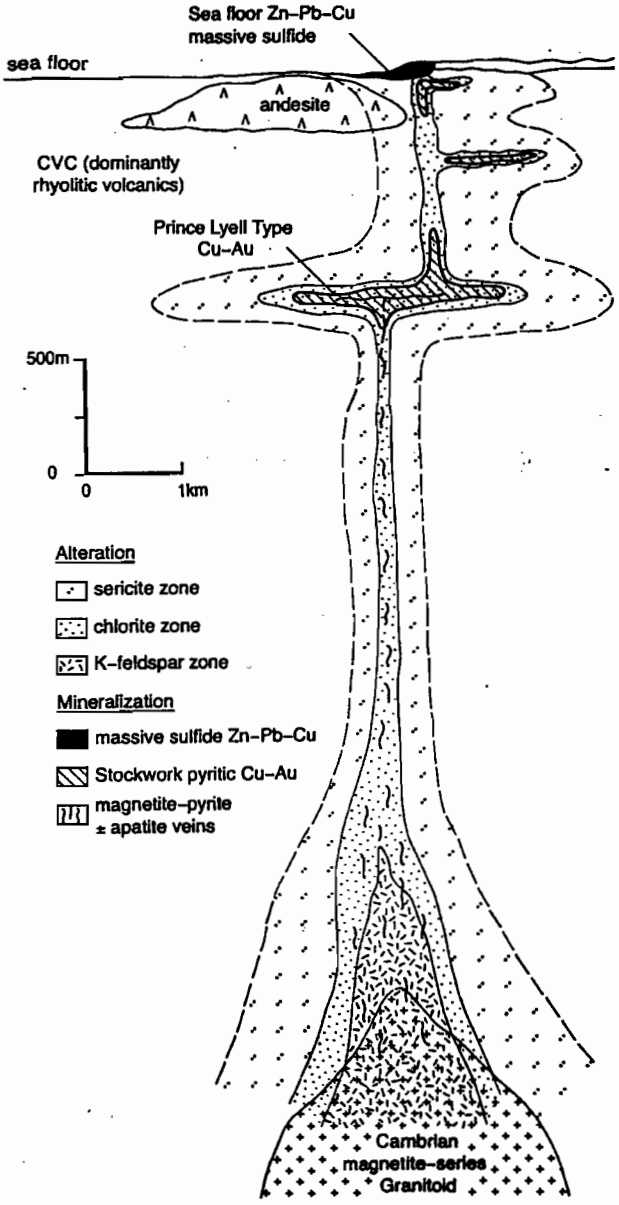

Figure 14: Preliminary geology-alteration model for the hydrothermal system related to the Mt Lyell VHMS deposits.

7. References

Abbott, P.D.B., 1992. Geology of a barite–galena occurrence exposed in the Anthony Power Development Tunnel, western Tasmania. Unpubl. Honours Thesis, University of Tasmania, 62p.

Corbett, K.D., 1989. Stratigraphy, palaeogeography and geochemistry of the Mt Read Volcanics, In: C.F. Burrett & E.L. Martin (Editors), Geology and Mineral Resources of Tasmania. Geol. Soc. Aust. Spec. Publ., 15: 86-119.

Corbett, K.D., 1992. Stratigraphic-volcanic setting of massive sulfide deposits in the Cambrian Mount Read Volcanics, Tasmania. Econ. Geol., 87: 564–586.

Crawford, A.J., Corbett, K.D. & Everard, J.L., 1992. Geochemistry of the Cambrian volcanic-hosted massive sulfide-rich Mount Read Volcanics, Tasmania, and some tectonic implications. Econ. Geol., 87: 597–619.

Doyle, M.G., 1990. The geology of the Jukes Proprietary prospect, Mt Read Volcanics. Unpubl. Honours Thesis, Univ. Tas., 114p.

Eastoe, C.J., Solomon, M. & Walshe, J.L., 1987. District-scale alteration associated with massive sulfide deposits in the Mt Read Volcanics, western Tasmania. Econ. Geol., 82: 1239–1258.

Green, G.R., Solomon, M. & Walshe, J.L., 1981. The formation of the volcanic-hosted massive sulfur ore deposit at Rosebery, Tasmania. Econ. Geol., 76: 304–338.

Gulson, B.L., 1986. Lead isotopes in mineral exploration: Developments in Economic Geology, 23, Elsevier, Amsterdam, 2450.

Hendry, D.A.F., 1981. Chlorites, phengites and siderites from the Prince Lyell Ore Deposit, Tasmania, and the origin of the deposit. Econ. Geol., 76: 285–303.

Henley, R.W. & Thomley, P., 1979. Some geothermal aspects of polymetallic massive sulfide information. Econ. Geol., 74: 1600–1612.

Hunns, S.R., 1987. Mineralisation of the Lake Selina prospect. Unpubl. Masters Qualifying Thesis, Univ. Tas.

Ishihara, S., 1981. The Granitoid Series and Mineralisation. Econ. Geol., Seventy-fifth Anniv. Vol., 458–484.

Jenkins, D.R., 1991. Volcanology, mineralisation and alteration of the Red Hills, western Tasmania: Unpubl. Honours Thesis, Univ. Tas., 90p.

Jones, A.T., 1993. The geology, geochemistry and structure of the Mt Darwin – South Darwin Peak area, western Tasmania. Unpubl. Honours Thesis, Univ. Tas., 120p.

Kajiwara, U., 1973. Significance of cyclic seawater as a possible determination of rock alteration facies in the earth's crust. Geochem. J., 7: 23–36.

Large, R.R., 1977. Chemical evolution and zonation of massive sulfide deposits in volcanic terrains. Econ. Geol., 72: 549–572.

Large, R.R., 1992. Australian volcanic-hosted massive sulfide deposits: features, style and genetic models: Econ. Geol., 87: 471–510.

Leaman, D.E. & Richardson, R.G., 1989. The granites of west and north-west Tasmania — a geophysical interpretation. Geol. Surv. Bull. 66, Tas. Dept. Mines, Hobart, 146p.

Ohmoto, H. & Rye, R.P., 1974. Hydrogen and oxygen isotopic compositions of fluid inclusions in the Kuroko deposits, Japan. Econ. Geol., 69: 947–953.

Payne, B., 1991. Geophysical interpretation of the Mt Sedgewick–Red Hills area, western Tasmania. Unpubl. Honours thesis, Univ. Tas., 107p.

Perkins, C. & Walshe, J.L., 1993. Geochronology of the Mt Read Volcanics, Tasmania, Australia. Econ. Geol., 88: 1176–1197.

Polya, D.A., Solomon, M., Eastoe, C.J. & Walshe, J.L., 1986. The Murchison Gorge, Tasmania — a possible cross-section through a Cambrian massive sulfide system. Econ. Geol., 76: 1341–1355.

Raymond, O., 1992. Geology and mineralisation of the Southern Prince Lyell Deeps, Queenstown, Tasmania: Unpubl. MSc Thesis, Univ. Tas., 161p.

Sawkins, F.J. & Kowalik, J., 1981. The source of ore metals at Buchans: Magmatic versus leaching models. Geol. Assoc. Canada Spec. Pap., 22: 255–267.

Solomon, M., 1976. "Volcanic" massive sulphide deposits and their host rocks — a review and an explanation. In: K.A. Wolf (Editor), Handbook of strata-bound and stratiform ore deposits: II: Regional studies and specific deposits. Amsterdam. Elsevier, 231–50.

Solomon, M., Eastoe, C.J., Walshe, J.L. & Green, G.R., 1988. Mineral deposits and sulfur isotope abundances in the Mt Read Volcanics between Que River and Mt Darwin, Tasmania. Econ. Geol., 83: 1307–1328.

Spooner, E.T.C. & Fyfe, W.S., 1973. Sub-sea floor metamorphism, heat and mass transfer. Contr. Min. Pet., 42: 287–304.

Stanton, R.L., 1985. Stratiform ores and geological processes: Roy. Soc. N.S.W., 118: 77–100.

Stanton, R.L., 1990. Magmatic evolution and the ore type-lava type affiliations of volcanic exhalative ores. Austral. Inst. Min. Met., Monog., 15: 101–107.

Stolz, A.J. & Large, R.R., 1992. Evaluation of the source rock control on precious metal grades in volcanic-hosted massive sulfide deposits from western Tasmania. Econ. Geol., 87: 720–738.

Urabe, T. & Sato, T., 1978. Kuroko deposits of the Kosaka mine, northeast Honshu, Japan — products of submarine hot springs on the Miocene sea floor. Econ. Geol., 73: 161–179.

Walshe, J.L. & Solomon, M., 1981. An investigation into the environment of formation of the volcanic-hosted Mount Lyell copper deposits using geology, mineralogy, stable isotopes, and a six-component chlorite solid solution model: Econ. Geol., 76: 246–284.

White, A.J.R. & Chappell, B.W., 1983. Granitoid types and their distribution in the Lachlan Fold Belt, south-eastern Australia. Geol. Soc. Am. Mem., 159: 21–34.

Cambrian granites in western Tasmania and their association to volcanic-hosted copper–gold-bearing massive sulfide deposits

Bill Wyman

Centre for Ore Deposit and Exploration Studies, Geology Department, University of Tasmania

The role of granitic magmas in VHMS genesis has been widely debated in the literature, most recently by Large et al. (in press), and earlier by Stanton (1985, 1990), Sawkins and Kowalik (1981), Stoltz and Large (1992), Large (1977) and Solomon (1976). Many others have argued these issues as well. Two primary schools of thought exist: (l) The granites act as a heat engine driving circulation systems which leach the metals and other components from the overlying volcanic pile by sea-water convection; (2) In addition to heat transfer, the granites supply magmatic components, primarily metals, directly to the ore forming solutions. Magmatic components possibly supplied by the granites include Cu, Au, Mo, Sn, and W. This work is directly focused on gathering and interpreting data in an attempt to critically evaluate and try to resolve this issue in Western Tasmania.

Andesitic Volcanics are associated with the VHMS mineralisation at Que River, Hellyer and Comstock and with the volcanic-hosted disseminated sulfide deposit (VHDS) at Prince Lyell. The Prince Lyell and Comstock deposits are associated with the Suite II rocks and are hosted in the Suite I rocks of Crawford et al. (1992). Que River and Hellyer are Hosted in Suite I rocks and are immediately overlain by Suite III rocks. Crawford et al. also point out that Suite II and Suite III rocks appear to have been erupted contemporaneously. It therefore appears that there may be a genetic link as well as a spatial association with mineralisation and the andesitic rocks. This study will also gather data in an attempt to shed some light on this association and possible genetic links between the andesites, rhyolites and granites.

This study will focus on the area beginning at the Darwin granite in the south and extending north to the Mount Lyell Field. Limited sampling and field work will be conducted in areas of outcropping granites at Lake Selina and the Murchison granite and results will be compared with those from the study area.

Objectives of the research

Establish the source of ore forming fluids involved in the generation of Cambrian Cu–Au and Pb–Zn–Ag mineralisation in western Tasmania and determine the extent of mixing between various fluid types.

Evaluate the regional extent of hydrothermal alteration associated with the Cambrian granites in the Mt. Read volcanic belt. The project will attempt to establish if a link exists between the alteration in and around the granites and the hydrothermal alteration around the VHMS deposits. The approach to this problem will be to examine the link between the apatite–magnetite association in alteration associated with the Cambrian granites, the Jukes prospect, and the Mount Lyell Field.

Determine the chemical changes in the volcanic host rocks, induced by hydrothermal alteration associated with Cu–Au mineralisation. This study will focus on the Jukes Prospect and comparisons will be drawn with the Prince Lyell deposit.

Attempt to evaluate the relationship of hornblende–andesites, which appear to be coeval with some of the VHMS deposits, and the hydrothermal alteration within the CVC

Establish if magmatic fluids were involved in the generation of large submarine Cu–Au volcanic hosted disseminated sulfide deposits such as Prince Lyell in the Mount Lyell Field.

Establish the genetic link between the granites and the volcanics (andesitic or felsic) associated with VHMS deposits within the Central Volcanic Complex (CVC).

Research plan

The proposed research has three components: (1) field mapping; (2) geochemical analysis; and, if necessary, (3) limited geophysical modeling.

Field mapping

The field portion of the program will involve detailed geologic mapping of the area between the Darwin granite and the Garfield andesite (Fig. 1). The objective will be to detail the composition and characteristics of the various phases of granitic intrusion. This will provide the context for samples of granite that will be collected for geochemical analysis. Further, geological mapping will be extended from the granite into the surrounding volcanics with emphasis on alteration styles and characteristics. The mapping will extend to the Garfield hornblende–andesite. Structural modification to stratigraphy will be carefully evaluated. The geological mapping will carefully examine the alteration associated with both the Cambrian granites and the hornblende andesites.

Limited geological mapping and sampling of selected Cambrian andesites in the Mount Lyell area will also be undertaken. These units strike directly into the Mount Lyell Field and are lost in surface mapping due to the intensity of sericite–pyrite alteration within the field.

Geochemical analysis

Geochemical studies will comprise and important aspect of the project. The following proposed analytical studies will be reviewed as the project progresses. The objective will be to track geochemical changes in both whole rocks and alteration as they change with distance from the granites or andesites. These changes may be useful vectors to assist in future exploration efforts.

Sulfur isotope analysis of pyrite will be undertaken. Pyrites will be obtained from within the granites and andesites through the alteration assemblages and into the selected VHMS deposits. The selected deposits include Prince Lyell, Jukes Pty, Lyell Consols, East Darwin, and other small prospects on the Jukes–Darwin Ridge. Particular emphasis will be given to pyrite equilibrium with magnetite in the apatite/magnetite veins. Establishing pyrite–magnetite equilibrium or non-equilibrium is important in constraining the hydrothermal fluid characteristics. Other workers have already established the seawater contribution of sulfur. This work will focus on evaluating how far magmatic sulfur can be detected from the granites and andesites and determine the regime of mixed sulfur sources.

Oxygen isotopes will be analyzed from K-feldspar, sericite, magnetite, chlorite, and carbonates. $\delta^{18}O$ values will be traced from within the granite through the various alteration styles to the VHMS deposits if possible. $\delta^{18}O$ values of samples of magnetite in the apatite/magnetite veins will be compared to samples collected within the granites and various alteration assemblages and within various VHMS deposits. The objective of this will be to establish the extent of mixing between magmatic and non-magmatic fluids in the veins.

Various chemical ratios, including Fe/Mg, Ti/Zr, and Fe/Ti, will be calculated from mineral chemistry and compared. Sampling will focus on alteration in the volcanic host rocks and apatite/magnetite veins within the granites, volcanics, and feeders to the VHMS deposits

Limited carbon and hydrogen isotope analysis of carbonates will be conducted to systematically evaluate isotopic zonation around the Darwin granite, and trace fluid sources in the Mt Darwin–Jukes–Mount Lyell Field.

Whole rock geochemistry (major, minor, trace elements, and REE) will be determined on granites, andesites, unaltered volcanics(to establish background), and altered volcanics. Chemical zonation of alteration styles around the Darwin granite will be assessed by whole-rock geochemical analysis. Further low level gold analysis will be undertaken to supplement the previous AMIRA data base.

This study will not only focus on elements considered to be "immobile" such as Ti, Zr, Y, Nb, P and the REE but will also examine mobile elements that may be concentrated or depleted during hydrothermal alteration and may therefore be useful vectors in exploration.

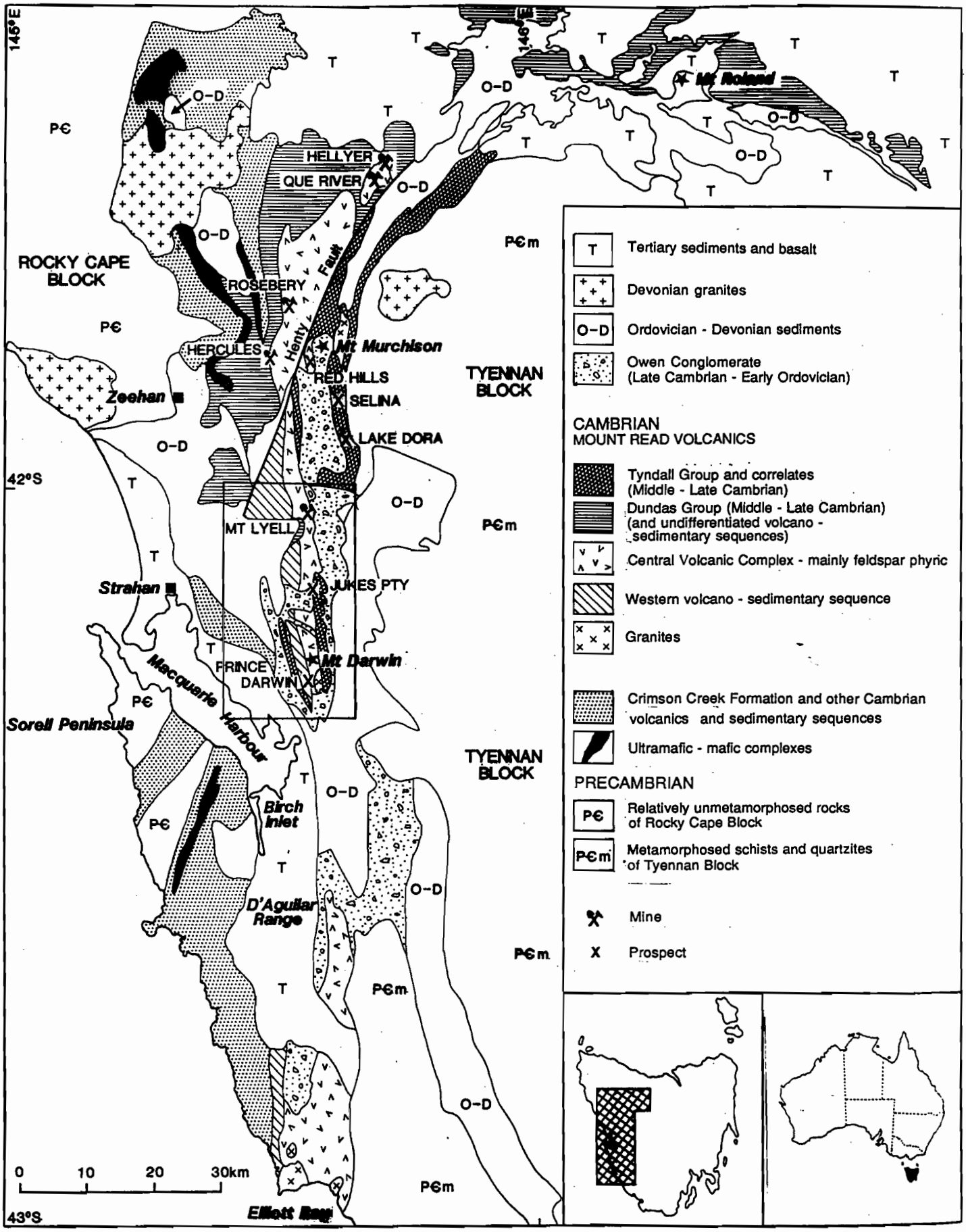
145°E
145°
42°S
43°S
0 10 20 30km
ROCKY CAPE BLOCK
TYENNAN BLOCK
TYENNAN BLOCK
HELLYER
QUE RIVER
ROSEBERY
HERCULES
Henty Fault
Mt Murchison
RED HILLS
SELINA
LAKE DORA
MT LYELL
JUKES PTY
Mt Darwin
PRINCE DARWIN
Zeehan
Strahan
Macquarie Harbour
Sorell Peninsula
Birch Inlet
D'Aguilar Range
Elliott Bay
Mt Roland
T
O-D
P€
P€m
Tertiary sediments and basalt
Devonian granites
Ordovician - Devonian sediments
Owen Conglomerate
(Late Cambrian - Early Ordovician)
CAMBRIAN
MOUNT READ VOLCANICS
Tyndall Group and correlates
(Middle - Late Cambrian)
Dundas Group (Middle - Late Cambrian)
(and undifferentiated volcano - sedimentary sequences)
Central Volcanic Complex - mainly feldspar phyric
Western volcano - sedimentary sequence
Granites
Crimson Creek Formation and other Cambrian volcanics and sedimentary sequences
Ultramafic - mafic complexes
PRECAMBRIAN
Relatively unmetamorphosed rocks of Rocky Cape Block
Metamorphosed schists and quartzites of Tyennan Block
Mine
Prospect

Rare-earth element chemistry of apatites will be determined from the Jukes–Mt Darwin and Lake Selina–Murchison area. Results will be compared to the data available from Mount Lyell to see if the same geochemical characteristics exist throughout the study area.

Limited geophysical modelling

Geophysical data suggest that the Cambrian granites underlie most of the 100 km long belt of Mount Read volcanics. Extensive magnetic and gravity interpretations have been done by (Leaman and Richardson, 1989; Payne, 1991). This work will be critically examined and re-modeled as necessary to eliminate possible effects of magnetite bearing volcanics.

Progress to date

The Jukes Pty Prospect is located approximately 9 km south of Queenstown. The prospect is a small Cu–Au prospect that is cut by the Hydroelectric Commission of Tasmania (HEC) road to the Crotty Dam. The Jukes prospect has been the subject of work by others most recently being Doyle (1990), and White (1975). This road cut provides an excellent opportunity to examine a small Cu–Au system hosted in Central Volcanic Complex rocks in cross section. As part of this project over 100 ten-metre-long chip samples were collected along a 5.7 km traverse along the Jukes Road. Rock chip and whole rock samples were collected at 500 m intervals outside the prospect and at 10 m intervals within the prospect. To date 87 selected chip samples and 32 selected hand specimens have been analysed. From the rocks collected on the above traverse, 65 thin sections have been prepared.

A comment about sample preparation: The chip samples mentioned above represent an entire 10 m interval in most cases and do not consist only of pristine un weathered clean rock. They may contain not only the dominant lithology but weathered rock, soil, sulfides and minor float debris. It is believed that the characteristics of the dominant lithology will over-ride minor impurities that result from this ìcontaminationî. Because of the sensitivity of the analytical procedures, however, 32 selected hand specimens were crushed and all oxidized/weathered/sulfide pieces were hand picked and removed. A comparison of the two sets of data is presented on the "immobile" element plots (SiO_2 vs distance, TiO_2 vs distance, P_2O_5 vs distance, and Ti/Zr).

Almost 350 m directly below the Jukes Road is the King River Tunnel operated by the HEC. Rocks exposed in this tunnel would give an excellent cross-section deeper in the system that formed the Jukes mineralisation. Unfortunately the tunnel is in use and has mostly been "rockcreted" in areas of interest. All is not lost, however. Geoff Green at the Tasmania Mines Department (now Industry, Safety and Mines, ISM) spent several days in the tunnel in 1988 prior to flooding and he and his crew gathered approximately 80 rock samples over about a 2 km section below Jukes. Unfortunately they did not create a geological map but all of the rocks collected by ISM are now in our possession. Crushed pulps from these rocks, which had been kept in sealed plastic bags and are in excellent condition have also been received. Selected samples of these rocks will be analysed for the geochemical suite of minerals of interest and thin sections will be prepared as necessary. Data from the Jukes road and the King River Tunnel can then be combined to create an excellent geochemical cross-section through the Jukes Pty mineralised system.

As part of this project it was necessary to create a geochemical database of all previous work in the area. This database is now almost complete. Selected samples from the work of various authors were reanalysed to fill in data gaps or to re-analyse elements where previous results were questionable.

Samples from Oliver Raymond's MSc thesis on the Prince Lyell deposit were reanalysed at the University of Tasmania to fill in missing elements and to re-analyse elements where previous results were in question. This data set is now complete and results can be compared to other rocks in the MRV.

Darwin Granite samples, from Andrew Jones Honours thesis, have also been recovered from archives and re-analysed to fill in gaps in his data set. This data set is now complete.

Some of the results of the Jukes road geochemistry and comparisons with MRV geology will be presented and discussed.

References

Crawford, A.J., Corbett, K.D. and Everard, J.L., 1992. Geochemistry of the Cambrian volcanic-hosted massive sulfide-rich Mount Read Volcanics, Tasmania, and some tectonic implications. *Economic Geology* 87: 597–619

Doyle, M.G., 1990. The geology of the Jukes Proprietary prospect, Mt. Read Volcanics. Unpubl. Honours Thesis, Univ. Tas.: 114p.

Large, R.R., 1977. Chemical evolution and zonation of massive sultide deposits in volcanic terrains. *Economic Geology* 72: 549–572.

Large, R.R., 1992. Australian volcanic-hosted massive sulfide deposits: features, styles and genetic models. *Economic Geology* 87: 471–510

Large, R.R., Doyle, M., Raymond, O., Cooke, D., Jones, A. and Heasman, L., 1995. Evaluation of the Role of Cambrian Granites in the Genesis of World Class VHMS Deposits in Tasmania. In press, Ore Geology Reviews.

Leaman, D.E. and Richardson, R.G., 1989. The granites of west and north-west Tasmania, a geophysical interpretation: *Geological Survey Bulletin* 66. Tas. Dept. Mines, Hobart: 146 pp.

Sawkins, F.J., and Kowalik, J., 1981. The source of ore metals at Bucans: Magmatic versus leaching models. *Geol. Assoc. Canada Spec. Pap.* 22: 255–267.

Solomon, M., 1976. Volcanic massive sulfide deposits and their host rocks — a review and an explanation. *In* K.A. Wolf (Ed.): *Handbook of strata-bound and stratiform ore deposits: II Regional studies and specific deposits.* Amsterdam. Elsevier: 231–250.

Stanton, R.L., 1985. Stratiform ores and geological processes. *Roy. Soc. NSW* 118: 77–100.

Stanton, R.L., 1990. Magmatic evolution and the ore type-lava type affiliations of volcanic exhalative ores. *Austr. Inst. Min. Met. Mon.* 15: 101–107.

Stoltz, A.J. and Large, R.R., 1992. Evolution of the source rock control on precious metal grades in volcanic-hosted massice sulfide deposits from western Tasmania. *Economic Geology* 87: 720–738.

White, N.C., 1975. Cambrian volcanism and mineralisation, SW Tasmania. Unpubl. PhD thesis, Univ. Tas.

Geochemistry of the host volcanics to the Benambra massive sulfide deposits, Victoria, Australia, and the importance of silicic magmatism in VHMS mineralisation

A.J.Stolz [1], G.R. Davies [2] and R.L. Allen [3]

(submitted for publication in *Economic Geology*)

Abstract

The Wilga and Currawong Cu-Zn massive sulfide deposits are hosted by a deformed sequence of Upper Silurian basaltic to rhyolitic volcanics and sedimentary units. The broadly syn-volcanic mineralisation occurs immediately above a thick package of rhyolitic volcanics and volcaniclastic rocks (Thorkidaan Volcanics), and is overlain by relatively thin intercalated flows of basalt, andesite and dacite (Gibson's Folly Formation). The Thorkidaan Volcanics have $\varepsilon_{Nd(420Ma)}$ = –2.2 to –9.8 and are considered to have been derived by partial melting of older crustal rocks, whereas the basalt-andesite-dacite hangingwall sequence has $\varepsilon_{Nd(415Ma)}$ = –0.5 to +2.0 suggesting derivation from a relatively undepleted mantle source. Relatively high TiO_2 andesitic to dacitic rocks from the Bumble Creek area have $\varepsilon_{Nd(415)}$ = +5.2 to 5.9 suggesting affinities with Ordovician volcanics elsewhere in the Lachlan Fold Belt.

The Thorkidaan Volcanics display a limited silica range (73 to 79 wt.%), but have distinctive minor and trace element variations indicating a substantial fractionation history involving feldspar and several accessory phases. Major and trace element compositions of the basalt-andesite-dacite suite display regular variations consistent with a cogenetic relationship by fractional crystallisation. The basaltic rocks mostly have low TiO_2 (<0.8 wt.%) and other chemical characteristics such as high Zr/Nb and La/Nb which suggest formation in a subduction-related setting; probably an embryonic back-arc basin developed on stretched continental lithosphere, or in small pull-apart basins developed adjacent to a transtensional margin.

Consideration of the types of mineralisation associated with crustal, S-type granitoids, coupled with thermal constraints limiting the capacity of small bodies of silicic magma to initiate and sustain hydrothermal convection cells of reasonable size, suggests that in the absence of coeval mafic magmatism, S-type crustal-derived silicic volcanic packages are likely to be barren of VHMS deposits. Mineralisation occurs in association with mantle-derived basalt-andesite-dacite suites that either provide the necessary heat to facilitate leaching of the footwall volcanics, or contribute metal-rich hydrothermal solutions during fractional crystallisation, or both.

Introduction

Our understanding of the tectonic setting and depositional environment in which volcanic-hosted massive sulfide (VHMS) deposits form has been substantially enhanced as a result of recent studies of modern seafloor deposits (e.g. Halbach et al., 1989; Focquet et al., 1991). However, because of the restricted stratigraphic interval which is available for sampling in these modern deposits without drilling, they provide limited information about the nature and geochemical character of the host footwall and hangingwall volcanic packages, and their role in the mineralising process. Such information can be more readily obtained from ancient volcanic sequences that provide a stratigraphic cross-section due to folding and subsequent erosion, although stratigraphic relationships may be complicated by subsequent faulting.

In this study we examined the host sequences of the Wilga and Currawong VHMS deposits from northeastern Victoria, Australia. These Cu-Zn-rich massive sulfide deposits are hosted by Middle to Upper Silurian volcanics and sedimentary rocks of the Lachlan Fold Belt in southeastern Australia (Fig. 1). The Lachlan Fold Belt is part of the larger

1. Department of Geology, University of Tasmania, G.P.O. Box 252C, Hobart, Tasmania 7001, Australia.
2. Faculteit der Aardwetenschwappen, Vrije Universiteit Be Boelelaan 1085,1081 HV Amsterdam, The Netherlands.
3. Consultant, c/- Mortevein 57, 4085 Hundvag, Stavanger, Norway.

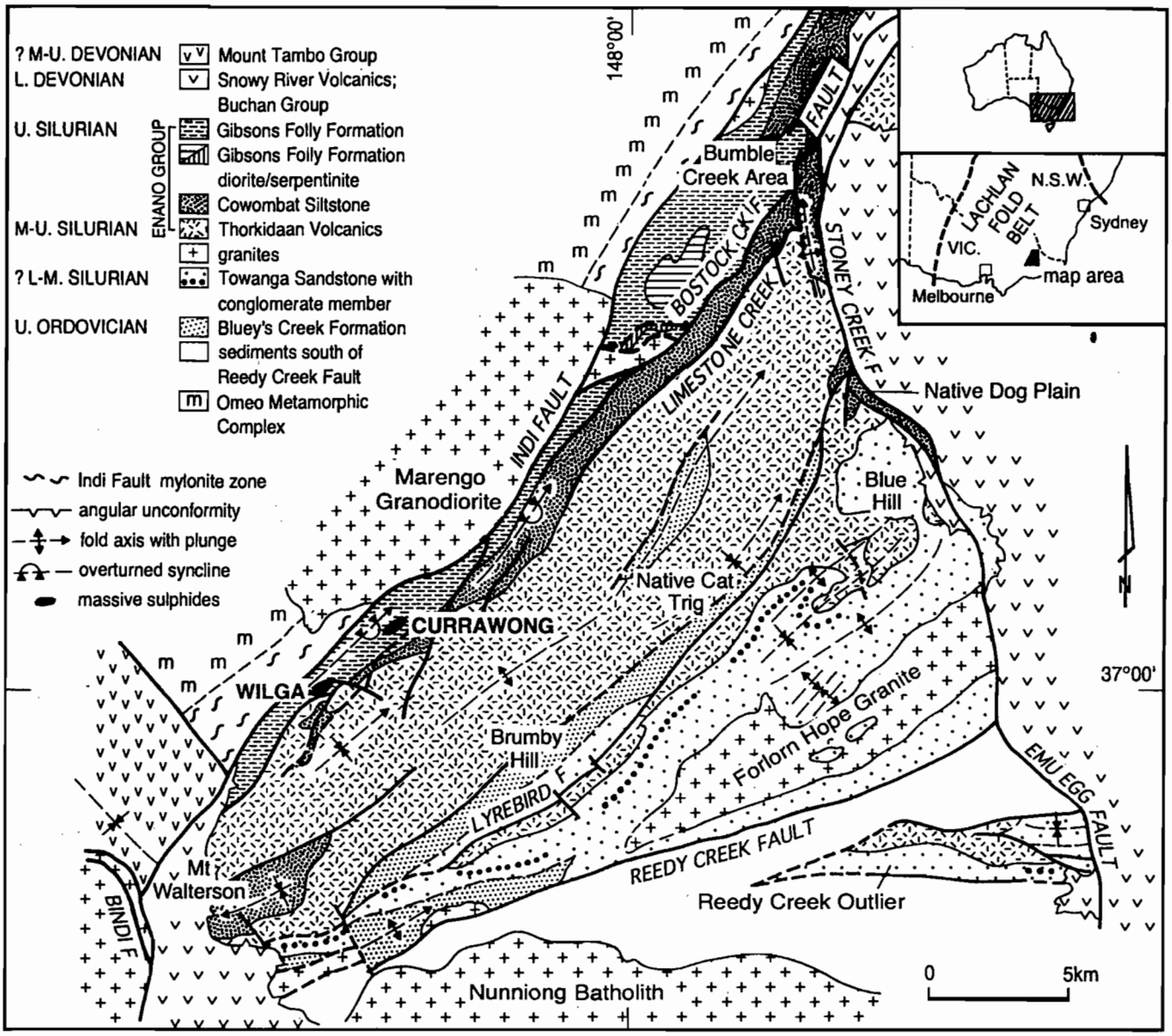

Fig. 1. Geological map of the Limestone Creek region, near Benambra, Victoria (modified after Allen, 1992) showing the locations of the Wilga and Currawong deposits and the distribution of their Middle to Upper Silurian volcano-sedimentary host rocks.

Palaeozoic Tasman Fold Belt system that extends along the greater part of the eastern margin of Australia, and within this belt there are a number of VHMS deposits ranging from Cambrian to Permian in age. The Woodlawn, Captains Flat and Currawang deposits also occur within rocks of Middle Silurian age in the Lachlan Fold Belt (Davis, 1990). The Wilga deposit has reserves of 3.97 Mt with 3.0 percent copper, 6.3 percent zinc, 23 g/t silver, and the Currawong deposit has an indicated resource of 9.5 Mt with 1.65 percent copper, 4.33 percent zinc, 0.86 percent lead, 38 g/t silver and 1.3 g/t gold (Macquarie Oil NL, 1987; Cox et al., 1990). Based on stratigraphic relationships the Wilga and Currawong deposits were regarded as essentially synvolcanic by Allen (1992). However, detailed textural and metal zonation studies of the Currawong deposit by Boden and Valenta (1995) suggest an origin by sub-seafloor replacement of porous volcaniclastic rocks rather than by seafloor exhalative processes.

This study seeks to clarify the relationships between the volcanism, mineralisation and the geodynamic setting at the time the massive sulphides were deposited. Specifically, geochemical and isotopic data for the volcanics are used to evaluate the likely source rocks for the magmatism, and to provide constraints on tectonic models for the host sequence at the time of mineralisation.

Regional Geology and Stratigraphy

The Wilga and Currawong Cu–Zn VHMS deposits are hosted by a strongly deformed Ordovician–Silurian volcano-sedimentary sequence that occurs as a series of northeast striking fault-bounded belts (Fig. 1; Allen, 1992). These rocks are overlain unconformably by a gently folded Devonian succession that includes the Snowy River Volcanics and the Mt Tambo Group, and they are intruded by several major granitoid intrusions of Silurian age. The stratigraphy of this region is discussed in detail elsewhere (VandenBerg et al., 1984; Allen, 1987; Allen and VandenBerg, 1988; Allen and Barr, 1990; Allen, 1992), and only a brief summary is presented here.

The oldest volcanics of interest in this study occurring within the footwall succession to the VHMS deposits are from the Bluey's Creek Formation. These include dacitic and rhyolitic lavas and sills which are associated with cherts (containing Late Ordovician conodonts), shales, mudstones and turbiditic sandstones, the latter including types rich in quartz and basaltic to andesitic volcaniclastic detritus (Allen, 1992). The precise age of these volcanics is not well constrained as they lie stratigraphically above the conodont-bearing units used to date the sequence. It is possible therefore that they represent an early manifestation of the subsequent, more voluminous silicic magmatism.

The Enano Group consists of the Middle-Upper Silurian Thorkidaan Volcanics, the Upper Silurian Cowombat Siltstone, and the Upper Silurian Gibson's Folly Formation. The Thorkidaan Volcanics comprise a 2–3 km thick package of porphyritic rhyolitic lavas and associated subvolcanic intrusives, with subordinate reworked volcaniclastic deposits. Many of the relatively altered, subaqueously deposited rhyolitic lavas display pseudo-pyroclastic textures which Allen (1987) interpreted as due to post-depositional alteration and tectonic processes. The rhyolitic lavas and subvolcanic intrusives are characterised by alkali feldspar, plagioclase, minor biotite, and partially resorbed quartz phenocrysts in a variably recrystallised spherulitic silicic groundmass. The intrusives, typified by the Currawong Porphyry (Allen, 1992) are, in general, more strongly porphyritic than the lavas.

The Gibson's Folly Formation which hosts the VHMS deposits is up to 500m thick and comprises a sequence of lenticular basalt, andesite and dacite lava flows with associated volcaniclastic rocks enclosed within a fine grained turbiditic sedimentary package. The stratigraphically lower parts of this sequence have been intruded by some porphyritic rhyolite bodies that appear to represent the final stages of the Thorkidaan silicic magmatism. In the Bumble Creek area (within the northern part of Fig. 1) dioritic plutons have intruded basaltic to dacitic volcanics that have previously been correlated with the Gibson's Folly Formation. This interpretation is based on the observation that they appear to occur along the regional strike extension of the host sequence (Fig. 1). However, many of these lithostratigraphic units are fault-bounded and the relatively high strain that has affected these rocks may have resulted in the juxtaposition of discrete unrelated volcanic packages.

The absolute ages of the Thorkidaan Volcanics and Gibson's Folly Formation are constrained by the inferred ages of the underlying and overlying unconformities, and a Late Silurian fossil age for the Cowombat Siltstone (Talent et al., 1975). The Lower Silurian Benambran orogeny resulted in strong folding of the Ordovician sedimentary units and development of the Omeo Metamorphic Complex which has a faulted contact with the western margin of the Cowombat Rift (Fig. 1). Uplift associated with deformation in the Middle Silurian (Crook et al., 1973) was a result of the Quidongan orogeny, followed soon after by the development of a series of extensional

basins (including the Cowombat Rift) in the Middle Silurian. The Upper Silurian Bindian orogeny marked the end of the host volcanism to the VHMS mineralisation, and resulted in a strong angular unconformity between the Middle Silurian Thorkidaan Volcanics and the overlying Lower Devonian Snowy River Volcanics (Vandenberg and O'Shea, 1981; Vandenberg et al., 1984).

Sampling and Analytical Techniques

Analytical data are presented in this paper for a suite of the least altered, coherent volcanic and intrusive units collected during a regional sampling program in the vicinity of the Wilga and Currawong massive sulfide deposits. The designation of samples to specific stratigraphic units is based on the mapping of Allen (1992). The majority of the samples from the Bluey's Creek Formation and Thorkidaan Volcanics were from outcrop, whereas a considerable proportion of samples from the comparatively poorly exposed Gibson's Folly Formation were obtained from drill core in the vicinity of the Wilga and Currawong deposits.

Samples were crushed initially in a jaw crusher, and a hand-picked sub-sample of chips free of vein material and vesicles was powdered in a tungsten carbide mill. Major and trace elements were determined on a Philips automated XRF spectrometer at the University of Tasmania using standard fused bead and pressed pellet techniques (Norrish and Chappell, 1977). Rare earth elements were determined by an ion-exchange-XRF technique at the University of Tasmania (Robinson et al., 1986). Precision of the REE analyses is typically in the range 1–4%, and 1–2% for Sm and Nd. Nd isotope ratios were measured on a Finnigan MAT 261 Thermal Ionisation Mass Spectrometer in the Faculteit der Aardweten-schwappen, Vrije Universiteit following chemical separation from 0.1g sample by standard ion-exchange techniques in the Geology Department, University of Tasmania (Stolz, 1995). Analyses are normalised to $^{146}Nd/^{144}Nd = 0.7219$, and during the course of the study the LaJolla standard gave $^{143}Nd/^{144}Nd = 0.511848 \pm 8$ (n=6). The routine total Nd blank was about 0.2 ng and no blank corrections were necessary.

Chemistry

Representative major and trace element analyses of volcanics from the footwall and hangingwall sequences (Tables 1 to 4) are grouped principally according to their stratigraphic designation. However, the volcanics in the Gibson's Folly Formation are split into two geochemically and geographically discrete suites. The major element analyses have been recalculated to 100% on an anhydrous basis to remove variations resulting from different loss on ignition values. Samples with obvious evidence of hydrothermal alteration have not been included in this study, although very weak sericitic alteration is present in many of the silicic volcanics. As the volcanics were all deposited in a subaqueous setting (Allen, 1992) and have subsequently experienced low grade (greenschist facies) regional metamorphism, a greater reliance has been placed on the immobile elements for interpretation of original magmatic affinities (MacLean and Barrett, 1993; Stolz, 1995).

Major and trace element data for the analysed volcanic samples indicate the existence of five distinctive rock suites within the stratigraphic package encompassing the Upper Ordovician Bluey's Creek Formation through to the Upper Silurian Gibson's Folly Formation. These suites correspond closely with their designated stratigraphic and geographic distribution. They include : (1) dacites and rhyolites from the Bluey's Creek Formation, (2) a relatively high-Ti and a low-Ti suite within the Thorkidaan Volcanics, (3) a basalt-andesite-dacite suite from the Gibson's Folly Formation, and (4) a high-Ti andesite-dacite suite from the Bumble Creek area (Fig. 1). A plot of Zr/TiO_2 versus Nb/Y (Fig. 2) for the analysed samples indicates these suites collectively span a broad and continuous range of compositions (from basalt to rhyolite), and all are characterised by relatively low Nb/Y values suggesting subalkaline affinities. In a plot of SiO_2 versus TiO_2 (Fig. 3) the separate suites show a series of strong negative correlations suggesting that silica concentrations have remained relatively unmodified during regional metamorphism. Nevertheless TiO_2 is used as the abscissa in most subsequent plots as it is less likely to have been mobilised and it also assists in discriminating the various suites in these plots.

Bluey's Creek Formation

These volcanics are dacitic to rhyolitic in terms of their variation in silica contents and Ti/Zr values (Table 1), and the least siliceous samples (~67 wt.% SiO_2) have relatively high ΣFe_2O_3, TiO_2, P_2O_5, Zr, V, Cr, Sc and Ni contents (Figs. 3 to 5) compared with the other siliceous volcanics in the area. These rocks are characterised by increasing Zr, Ce and U, and decreasing ΣFe_2O_3, P_2O_5 and trace transition element concentrations with decreasing TiO_2. They display a slight increase in Zr/Nb (17–25) with decreasing TiO_2 (Fig. 6) which is similar to the trend for the Gibson's Folly basalt-andesite-dacite suite, and they have relatively high Zr/Y values (Fig. 7) which tend to increase with decreasing TiO_2. The dacites and rhyolites have moderately

Table 1. Representative major and trace element analyses of volcanics from the Upper Ordovician Bluey's Creek Formation

	BEJ11	BEJ10	BEJ6	BEJ4	BEJ5	BEJ7	RLA/E54
SiO_2	66.79	66.88	70.78	71.78	73.98	74.26	74.56
TiO_2	0.79	0.74	0.56	0.52	0.34	0.33	0.33
Al_2O_3	15.83	15.70	14.09	13.68	13.40	13.49	13.48
Fe_2O_3#	5.04	5.12	4.53	4.01	3.14	3.27	2.74
MnO	0.08	0.08	0.08	0.08	0.03	0.03	0.03
MgO	2.41	2.40	2.03	1.70	0.75	0.99	0.93
CaO	2.60	2.72	1.75	2.23	0.90	0.65	0.68
Na_2O	5.01	4.59	3.23	3.68	4.19	4.53	4.98
K_2O	1.29	1.62	2.81	2.17	3.19	2.38	2.20
P_2O_5	0.15	0.15	0.13	0.13	0.08	0.07	0.07
Total *	100.00	100.00	100.00	100.00	100.00	100.00	100.00
LOI	2.03	2.00	1.85	1.51	1.04	1.44	1.10
Sc	16	14	13	13	12	14	13
V	127	112	83	87	27	27	27
Cr	41	53	14	13	3	2	3
Ni	16	20	5	6	2	1	1
Cu	47	35	31	29	3	1	1
Zn	77	46	60	57	40	34	33
Pb	6	16	16	11	4	3	3
Rb	34	39	69	59	94	51	52
Sr	193	216	142	137	103	95	85
Y	34	37	51	37	55	33	34
Zr	184	184	200	197	242	240	241
Nb	10	11	9	9	10	10	10
Ba	256	319	606	460	527	464	368
Th	14	15	13	12	14	11	14
U	3	4	3	3	4	3	3
La	27.6	28	28.5	21	31	24	25
Ce	58.5	58	61.9	45	52	53	54
Pr	6.96		8.04				
Nd	26.3	27	34.6	23	41	28	23
Sm	5.60		7.64				
Eu	1.28		1.42				
Gd	5.34		8.22				
Tb	1.02		1.37				
Dy	5.43		8.22				
Er	3.86		4.63				
Yb	2.76		3.97				
$(La/Yb)_N$	6.6		4.7				
Ti/Zr	25.7	24.1	16.8	15.8	8.4	8.2	8.2
Zr/Nb	19.0	16.9	22.4	23.0	23.5	25.3	23.6
Zr/Y	5.4	5.0	3.9	5.4	4.4	7.4	7.1

 # Total Fe as Fe_2O_3; * Analyses normalised to 100% anhydrous

Table 2. Representative major and trace element analyses of the Middle to Upper Silurian Thorkildaan Volcanics

	Low Ti-Zr Group									High Ti-Zr Group						
	B18/144	B52/114	B89/158	BEJ31B	RLAH18	BEJ21	BEJ1	BEJ12	RLAE25/J	B134/604	B95/113	B67/392	B66/394	B134/489	BEJ31	BEJ13
SiO_2	74.21	75.66	76.61	76.72	77.25	77.27	77.59	77.80	80.61	72.50	75.63	76.52	77.43	77.76	78.43	79.19
TiO_2	0.06	0.04	0.04	0.09	0.03	0.06	0.03	0.04	0.03	0.26	0.17	0.16	0.15	0.17	0.17	0.16
Al_2O_3	14.66	12.90	12.19	13.90	12.60	12.24	12.59	12.99	10.37	17.24	12.10	11.50	11.98	11.83	11.91	12.09
Fe_2O_3 #	0.68	1.22	1.01	0.87	0.85	0.67	0.98	0.64	0.30	1.35	2.41	3.75	2.10	2.23	1.97	0.73
MnO	0.01	0.01	0.01	0.02	0.02	0.01	0.02	0.01	<0.01	0.02	0.06	0.05	0.02	0.03	0.02	0.01
MgO	0.33	0.29	1.32	0.46	0.15	0.18	0.26	0.31	0.13	1.30	0.52	1.22	0.32	0.43	0.41	0.09
CaO	0.53	0.21	0.14	0.11	0.11	0.07	0.15	0.14	0.04	1.08	0.43	0.95	1.01	0.57	0.21	0.17
Na_2O	3.79	2.48	2.59	6.92	4.15	1.62	2.96	3.27	0.63	4.11	2.66	2.92	3.15	3.05	4.66	5.38
K_2O	5.88	7.18	6.06	0.90	4.61	7.85	5.38	4.77	7.46	2.11	5.59	2.90	3.80	3.89	1.99	2.15
P_2O_5	0.03	0.03	0.03	0.01	0.03	0.03	0.04	0.03	0.03	0.05	0.03	0.03	0.04	0.04	0.03	0.03
Total *	100.00	100.00	100.00	100.00	100.00	100.00	100.00	100.00	100.00	100.00	100.00	100.00	100.00	100.00	100.00	100.00
LOI	1.14	0.76	1.03	0.66	0.35	0.44	0.59	0.87	0.43	2.52	2.17	2.41	1.76	1.60	0.89	0.36
Sc	9	7	7	5	5	5	8	7	5	10	8	6	7	9	8	7
V	4	2	2	3	1	2	2	1	1	10	3	7	6	7	2	5
Cr	2	2	1	2	3	3	3	2	3	3	2	2	3	3	3	2
Ni	1	1	2	1	1	1	1	1	1	1	1	2	2	1	1	2
Cu	3	2	2	1	2	2	1	4	14	57	3	4	1	1	2	4
Zn	90	29	45	27	20	8	24	20	9	36	36	50	30	24	36	20
Pb	72	19	18	2	15	17	12	22	1	6	4	5	6	5	5	12
Rb	119	173	165	20	175	199	215	225	276	102	115	77	134	118	49	45
Sr	101	39	42	53	37	36	43	24	26	155	48	54	75	85	66	70
Y	52	49	53	34	53	43	56	112	42	30	44	35	34	39	60	30
Zr	96	59	87	105	50	69	59	57	44	194	192	115	128	118	229	155
Nb	9	10	8	9	9	6	10	10	8	10	7	6	7	7	10	8
Ba	1213	672	618	195	210	781	296	258	235	1937	613	482	514	490	446	449
Th	21	13	13	26	9	12	12	10	6	20	9	14	13	14	16	14
U	3	1	7	4	6	4	5	7	5	5	3	4	3	2	4	3
La	36	17	22	27.4	9	13	7.21	18.5	10	44.4	25	26	36	32	35	46
Ce	76	36	44	63.7	25	33	14.71	36.9	21	94.6	47	51	85	61	62	75
Pr				7.68			2.45	7.69		10.93						
Nd	33	16	21	28.5	14	15	9.21	35.1	11	42.1	23	22	30	26	32	39
Sm				5.46			3.52	12.48		8.07						
Eu				0.79			0.24	0.75		1.23						
Gd				4.98			4.27	17.9		7.34						
Tb				1.05			0.96	3.22		1.29						
Dy				6.25			7.17	19.0		6.66						
Er				4.30			5.49	10.48		3.30						
Yb				3.90			5.25	10.65		2.96						
$(La/Yb)_N$				4.6			0.9	1.2		9.6						
Ti/Zr	5.0	4.0	3.6	5.1	3.8	5.2	3.1	4.2	4.1	8.0	5.3	8.3	7.0	8.6	4.5	8.2
Zr/Nb	10.8	5.9	8.4	11.8	5.5	6.5	6.1	5.5	5.8	19.4	27.0	18.0	18.3	16.8	23.9	19.3
Zr/Y	1.9	1.2	1.3	3.1	0.9	1.6	1.0	0.5	1.1	6.5	4.4	3.3	3.7	3.0	3.8	5.2
Rb/Sr	1.172	4.424	4.433	0.373	4.766	5.500	4.961	9.205	10.902	0.659	2.368	1.440	1.781	1.397	0.738	0.645

Total Fe as Fe_2O_3; * Analyses normalised to 100% anhydrous

Table 3. Representative major and trace element analyses of volcanics from the Gibson's Folly Formation

	W171/67	B93/43	B44/27	B4/5	B99/59	B145/45	B148/191	B67/177	B135/111	B17/62	B138/28	B72/82	B175/43	B135/15	B145/32	B134/223	B67/148
SiO_2	51.88	55.62	56.55	56.76	59.95	63.85	65.12	68.49	68.67	68.92	70.67	72.62	73.60	74.16	74.50	74.96	78.67
TiO_2	0.80	0.63	0.74	0.76	0.78	0.61	0.60	0.52	0.50	0.44	0.36	0.30	0.39	0.25	0.24	0.23	0.36
Al_2O_3	18.36	17.26	17.77	17.58	15.66	15.46	15.32	18.10	14.66	15.04	13.43	14.57	13.80	13.55	13.12	13.42	12.57
Fe_2O_3 #	8.71	7.66	7.66	8.55	7.78	6.24	6.69	3.44	4.73	3.43	2.66	3.24	2.51	3.25	2.68	2.67	2.41
MnO	0.21	0.24	0.11	0.14	0.15	0.16	0.09	0.02	0.07	0.02	0.03	0.05	0.06	0.03	0.03	0.04	0.03
MgO	7.28	7.54	7.41	8.16	6.41	4.06	3.94	1.72	2.35	4.58	5.02	3.09	0.58	0.79	0.78	1.19	0.82
CaO	7.05	5.45	4.76	3.43	4.18	3.93	1.41	2.41	2.16	0.82	1.83	0.76	2.56	0.44	1.49	0.88	1.56
Na_2O	4.85	5.10	2.94	3.74	4.20	3.16	5.19	4.57	6.06	6.76	5.67	3.56	5.04	5.97	4.76	5.84	4.54
K_2O	0.94	0.35	1.76	0.60	0.76	2.40	1.10	0.62	0.48	0.11	0.20	1.71	1.15	1.48	2.15	0.74	0.95
P_2O_5	0.12	0.11	0.06	0.04	0.13	0.13	0.14	0.11	0.10	0.10	0.09	0.08	0.09	0.06	0.05	0.05	0.09
Total *	100.00	100.00	100.00	100.00	100.00	100.00	100.00	100.00	100.00	100.00	100.00	100.00	100.00	100.00	100.00	100.00	100.00
LOI	5.25	7.92	4.79	4.78	6.22	5.28	3.22	2.98	3.17	2.54	3.24	2.66	2.66	0.89	2.06	1.74	1.91
Sc	37	36	26	35	34	27	28	17	22	14	14	9	15	9	10	10	10
V	309	225	361	323	253	168	142	5	117	43	36	37	6	11	15	8	5
Cr	24	307	24	26	148	8	16	3	5	6	10	2	2	2	2	2	2
Ni	14	43	12	13	43	3	8	2	2	3	3	2	<1	1	1	2	<1
Cu	32	26	31	37	55	16	24	1	9	1	1	67	2	2	1	2	2
Zn	86	72	154	263	110	79	81	79	73	53	147	61	66	54	50	54	75
Pb	4	4	2	2	2	<1	5	3	3	6	6	5	2	4	1	2	2
Rb	23	15	60	26	32	60	35	16	11	3	5	44	24	25	42	19	21
Sr	232	157	131	116	125	65	92	271	116	128	109	56	135	136	66	72	154
Y	14	20	13	12	18	22	17	16	22	33	25	23	23	20	29	28	19
Zr	45	65	39	41	74	93	76	150	113	172	148	113	125	159	163	163	110
Nb	2	3	2	2	3	4	4	7	4	7	6	4	5	6	6	6	5
Ba	134	90	65	37	143	1252	142	171	240	48	73	391	651	564	546	243	261
Th	<1	1	1	1	3	3	2	5	3	9	6	5	4	6	6	6	3
U	<1	1	1	<1	1	3	1	<1	1	1	1	2	2	2	2	2	2
La	4.50	6	5	3.69	10	9	11.1	12	13.0	22	16	15	14	20.6	21	39	12
Ce	9.50	14	4	7.42	17	21	25.4	30	26.9	45	36	31	30	42.0	39	37	23
Pr	1.25			1.06			3.14		3.43					5.07			
Nd	5.98	7	4	4.62	8	10	13.9	16	14.5	21	19	14	16	21.3	16	18	12
Sm	1.70			1.56			2.97		3.59					4.74			
Eu	0.66			0.59			0.66		0.85					1.02			
Gd	2.11			1.80			2.96		3.60					4.14			
Tb	0.35			0.31			0.43		0.70					0.66			
Dy	2.37			2.09			2.94		3.60					3.94			
Er	1.60			1.60			1.66		2.08					2.62			
Yb	1.34			1.33			1.59		2.04					3.36			
$(La/Yb)_N$	2.2			1.6			4.6		3.3					4.1			
Ti/Zr	106.8	57.9	112.9	110.9	82.9	39.4	62.8	20.8	26.6	15.4	15.8	16.0	16.7	9.4	8.6	8.4	19.7
Zr/Nb	22.5	24.1	23.1	19.6	21.9	23.8	21.2	23.1	26.2	24.9	23.9	26.2	25.1	26.9	27.2	26.6	21.9
Zr/Y	3.2	3.3	3.0	3.5	4.0	4.2	4.5	9.3	5.1	5.2	5.6	4.6	5.4	8.1	5.6	5.9	5.9

Total Fe as Fe_2O_3; * Analyses normalised to 100% anhydrous

Table 4. Representative major and trace element analyses of volcanics and a dioritic intrusive from the Bumble Ck area

	BEJ28 Diorite	RLAK14b	BEJ26	BEJ22	BEJ23	BEJ25	BEJ24
SiO_2	48.81	54.23	57.54	58.22	62.10	63.35	65.05
TiO_2	0.87	1.57	0.87	1.37	1.29	1.12	1.06
Al_2O_3	16.91	17.13	17.44	16.04	15.05	15.01	14.42
Fe_2O_3 #	14.02	11.70	7.94	9.99	8.83	8.07	7.68
MnO	0.21	0.24	0.13	0.17	0.17	0.20	0.18
MgO	6.48	4.33	4.40	5.05	2.37	2.09	3.42
CaO	9.26	4.45	3.77	2.33	2.80	2.74	1.72
Na_2O	3.10	5.83	7.63	5.04	6.31	6.37	5.31
K_2O	0.16	0.24	0.12	1.59	0.86	0.78	0.96
P_2O_5	0.18	0.28	0.16	0.20	0.22	0.27	0.20
Total *	100.00	100.00	100.00	100.00	100.00	100.00	100.00
LOI	2.61	3.77	4.93	3.62	2.32	2.23	2.83
Sc	59	32	31	29	22	21	22
V	551	217	174	246	92	52	108
Cr	12	6	28	10	3	4	4
Ni	21	4	21	6	1	2	2
Cu	156	27	42	27	16	16	21
Zn	111	120	71	100	95	109	167
Pb	1	2	4	2	3	4	5
Rb	2	6	3	32	23	19	30
Sr	334	179	132	102	93	125	79
Y	15	40	38	47	44	50	47
Zr	12	106	155	141	148	161	152
Nb	1	3	5	4	4	4	5
Ba	44	102	105	277	184	198	189
Th	1	2	5	1	3	4	4
U	<1	1	1	1	1	1	1
La	2	7.54	12	8.74	11	11	16
Ce	9	19.7	26	22.1	25	25	32
Pr		2.83		3.25			
Nd	8	14.3	14	15.9	16	17	20
Sm		4.10		4.78			
Eu		1.42		1.40			
Gd		5.76		6.20			
Tb				1.05			
Dy		6.19		7.29			
Er		4.28		5.23			
Yb		3.86		4.85			
$(La/Yb)_N$		1.3		1.2			
Ti/Zr	431.1	89.1	33.6	58.2	52.3	41.7	41.8
Zr/Nb	9.3	35.2	33.0	35.3	36.1	37.4	32.3
Zr/Y	0.8	2.6	4.1	3.0	3.3	3.2	3.2

Total Fe as Fe_2O_3; * Analyses normalised to 100% anhydrous

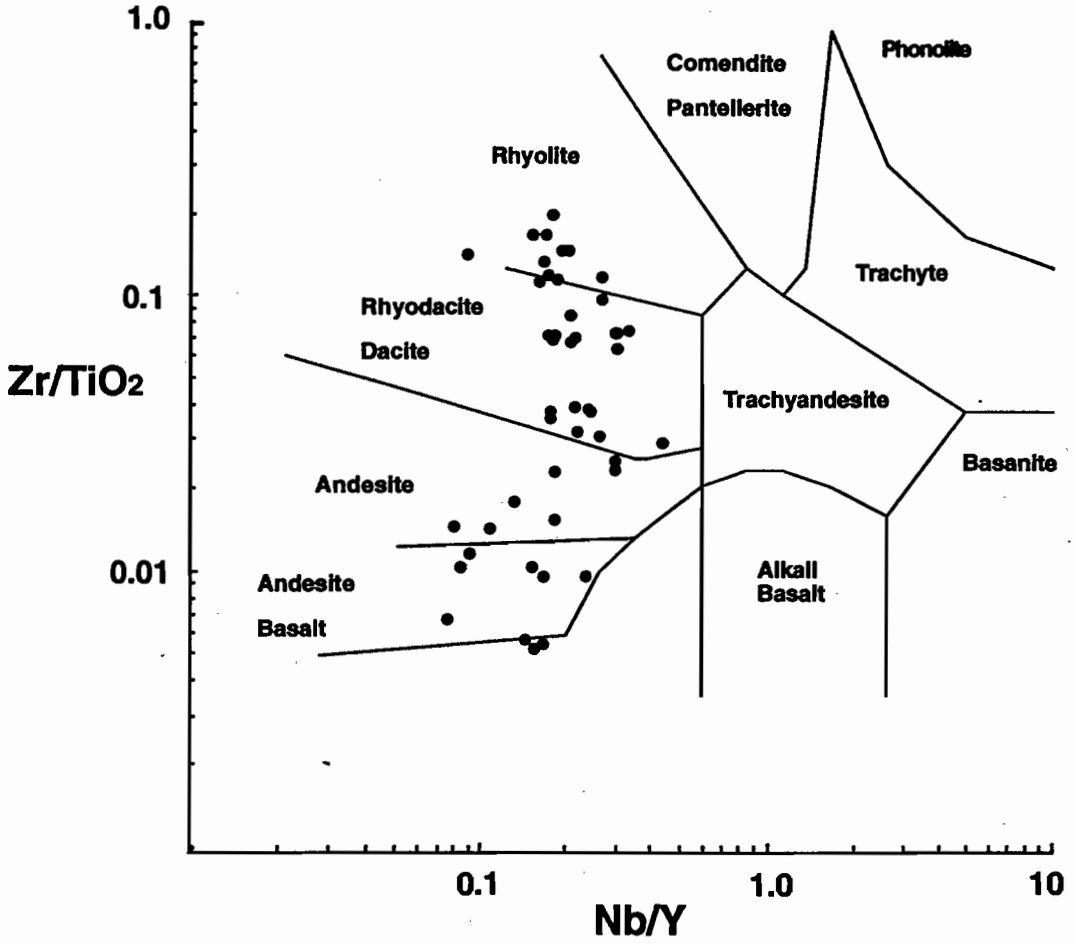

Fig. 2. Plot of Nb/Y versus Zr/TiO2 (after Winchester and Floyd, 1977) showing the complete range of compositions from the host volcanic package.

LREE enriched ($(La/Yb)_N$ = 4.7–6.6) chondrite-normalised REE patterns (Fig. 8) that are characterised by significant negative Eu anomalies.

Thorkidaan Volcanics

The Thorkidaan Volcanics are all rhyolites characterised by a restricted range of silica values (73–79 wt. %), but they can be divided (Fig. 3a) into a relatively low-Ti (<0.1 wt.% TiO_2) and a high-Ti suite (>0.15 wt.% TiO_2) that are distinguishable using a number of geochemical parameters. The high-Ti suite has higher ΣFe_2O_3, Sr, Zr, Zr/Y and Zr/Nb (Figs 3, 4), whereas the low-Ti suite has substantially higher Rb/Sr. Both suites have very low concentrations of P_2O_5, V, Cr, Ni and Sc that are typical for such silicic compositions. In plots of TiO_2 versus Zr, Th, Ce and Zr/Nb (Fig. 4, 6), the two suites display marked systematic decreases of these components over a relatively restricted range of TiO_2 concentrations, although depletion is more pronounced for the low-Ti suite. Moreover, the depletion trends are subparallel rather than contiguous suggesting that these volcanic suites developed as discrete magmatic series.

Both low- and high-Ti suites show a decrease in Zr/Y with decreasing TiO_2 that is most marked for the low-Ti suite, and despite the well known mobility of Rb and Sr during regional metamorphism, the low-Ti suite also shows a sharp increase in Rb/Sr with decreasing Zr/Y (Fig. 7). The high-Ti rhyolite suite is characterised by LREE enriched patterns with La ~ 100x chondrite, and a moderate negative Eu anomaly. The low-Ti rhyolites mostly have flatter patterns with variable overall enrichment in REE, and a marked negative Eu anomaly. Sample BEJ31B has a TiO_2 content that is transitional between the two groups,

and its REE pattern, although more similar to the high-Ti suite, displays some evidence of relative HREE enrichment compared with the other relatively Ti-rich sample (B134/604; Fig. 9).

Gibson's Folly Formation

In plots of SiO_2 versus ΣFe_2O_3 and TiO_2 (Fig. 3) the volcanics from the Gibson's Folly Formation display quite coherent variation trends over a broad range of silica concentrations (48–79 wt. % SiO_2) spanning basaltic to high-silica dacite compositions. This suite is also characterised by systematic increases in Zr, Th, U, LREE, and decreasing P_2O_5, Sc, V, Cr and Ni with decreasing TiO_2 (Figs. 4 & 5). The basaltic rocks have flat or slightly LREE enriched REE patterns with La ~ 10x chondrite (Fig. 10). The andesites and dacites display progressive overall enrichment in REE which is slightly greater for the LREE, and the most evolved high-silica dacitic rocks are characterised by slight negative Eu anomalies.

High-Ti Andesite–Dacite Suite

The Bumble Creek andesitic to dacitic volcanics can be distinguished from the Gibson's Folly Formation rocks by their substantially higher TiO_2, P_2O_5 and ΣFe_2O_3 for a given SiO_2 content (Fig. 3). The high-Ti suite also has higher Zr, and LREE, overlapping Th, U, Sc, and generally lower Cr, Ni and V than rocks of similar SiO_2 content from the Gibson's Folly Formation. In plots of TiO_2 versus Zr, V, Ce, U and Sc (Figs. 4 & 5, not all shown) the high-Ti andesite-dacite suite generally shows coherent variation trends that in many cases are transitional to the rocks of the Bluey's Creek Formation. The andesites of the high-Ti suite have almost flat REE profiles at ~ 20–30x chondrite with a slight negative Eu anomaly (Fig. 8).

Nd Isotope Data

Nd isotopes provide a useful method of characterising the source materials of ancient volcanic rocks due to the relatively robust behaviour of the REE during low grade regional metamorphism and sea-floor alteration (Whitford et al., 1989; Stolz, 1995). The Nd isotope analyses corrected for inferred age of emplacement (Table 5) suggest that the 4 chemically distinguishable suites of volcanics were derived from at least 3 isotopically discrete sources (Fig. 11). The dacites and rhyolites of the Bluey's Creek Formation have $e_{Nd(440Ma)}$ = –8.3 to –9.1. This is within the range of the Thorkidaan Volcanics which have $e_{Nd(420Ma)}$ = –2.2 to –9.8, but with 3 of the 4 analysed samples in the range $e_{Nd(420Ma)}$ = –5.1 to –9.8. In contrast the Gibson's Folly Formation basalts, andesites and dacites have $eNd_{(415Ma)}$ = +2.0 to –0.5, and the high-Ti Bumble Creek suite have $e_{Nd(415Ma)}$ = +5.2 to 5.9. It could be reasonably argued that the absolute ages for the various suites are not well constrained, and that the various phases of volcanism may have occurred over a much shorter time interval. However, recalculation of the e_{Nd} values at a single age results in very little change, and has no significant affect on the substantial differences in Nd isotopic signature that characterise these suites.

The relatively large negative e_{Nd} values of the silicic volcanics from the Bluey's Creek Formation and the Thorkidaan Volcanics closely overlap the ranges of values displayed by S- and I-type granitoids from the Lachlan Fold Belt (i.e $e_{Nd(400Ma)}$ = –6 to –10 and 0 to –9, respectively; McCulloch and Chappell, 1982). Some samples of the Bluey's Creek Formation have pseudomorphs after hornblende phenocrysts suggesting an affinity with the I-type suite, whereas the Thorkidaan Volcanics commonly contain biotite phenocrysts and hornblende is absent suggesting they are more closely affiliated with the S-type magmatism in the region. Whatever the specific source rocks for these volcanics were, their relatively unradiogenic Nd isotope signature suggests they had a relatively long-term LREE-enriched history, or that the magmas have assimilated a large proportion of a component with an old continental crustal Nd isotope signature.

The range in e_{Nd} values for the Gibson's Folly Formation is essentially identical to that of basaltic to rhyolitic volcanics of the Silurian Gundary Formation ($e_{Nd(426Ma)}$ = +2.3 to –0.6) from the Wollondilly Basin, eastern Lachlan Fold Belt (Fig. 12, Jones et al., 1995). The Wollondilly Basin is adjacent to the Hill End Trough which hosts the Woodlawn and Captains Flat VHMS deposits. The basalts from the Wollondilly Basin have some major and trace element differences to the Gibson's Folly Formation, but they appear to have been derived from an isotopically similar mantle source.

The high-Ti volcanics from the Bumble Creek area also have a distinctive isotopic signature ($e_{Nd(415Ma)}$ = +5.2 to 5.9) which is most similar to Ordovician volcanics that occur extensively in the Lachlan Fold Belt from Goonumbla to Orange in New South Wales ($e_{Nd(450Ma)}$ = +5.8 to 7.6; Sun and Wyborn, 1994). However, these Ordovician volcanics are dominantly shoshonitic and have a clear subduction-related geochemical signature characterised by relatively low TiO_2, Nb and Zr in mantle-normalised trace element plots (Wyborn, 1992).

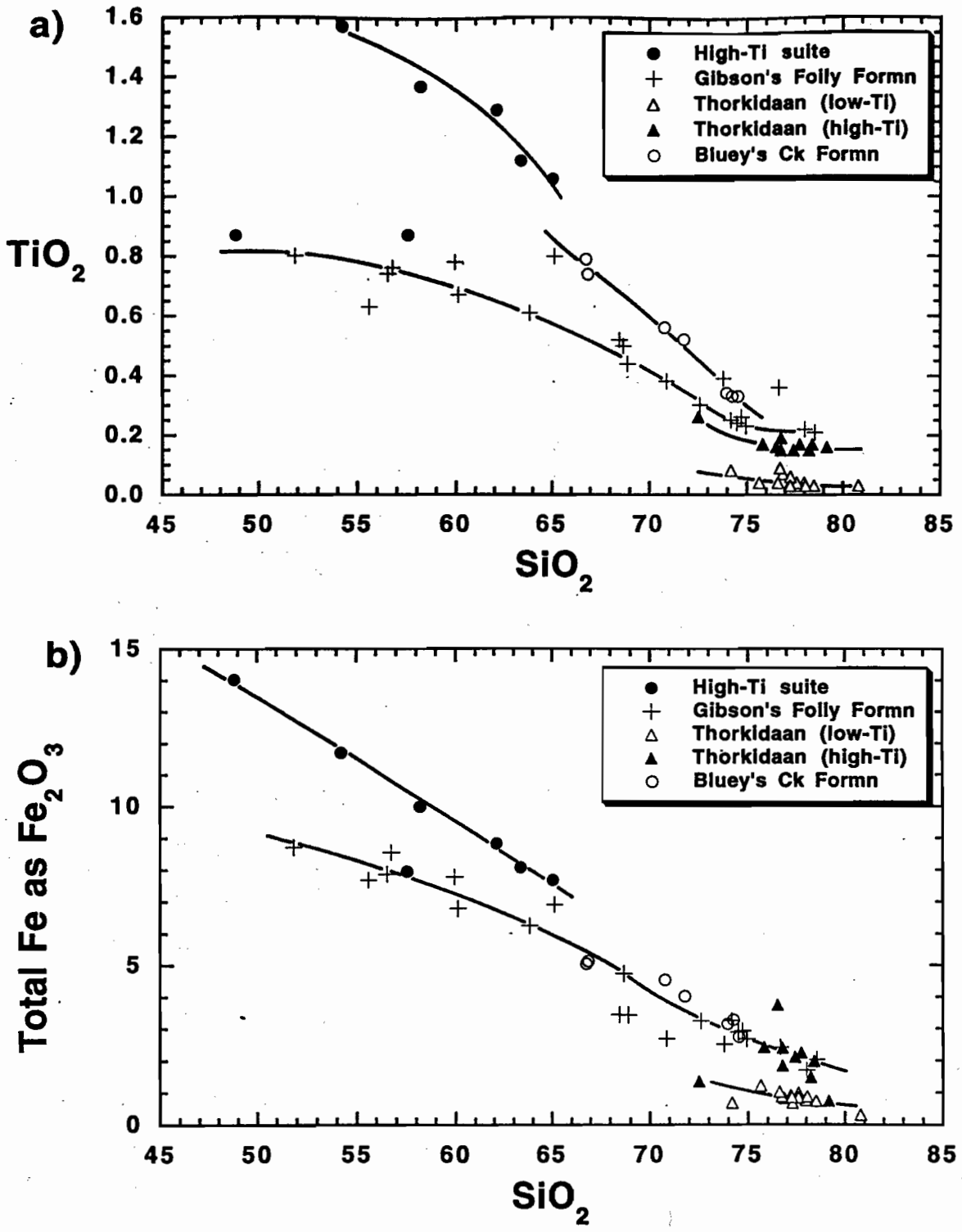

Fig. 3. Plots of (a) SiO_2 versus TiO_2, (b) SiO_2 versus ΣFe as Fe_2O_3 for the host volcanics.

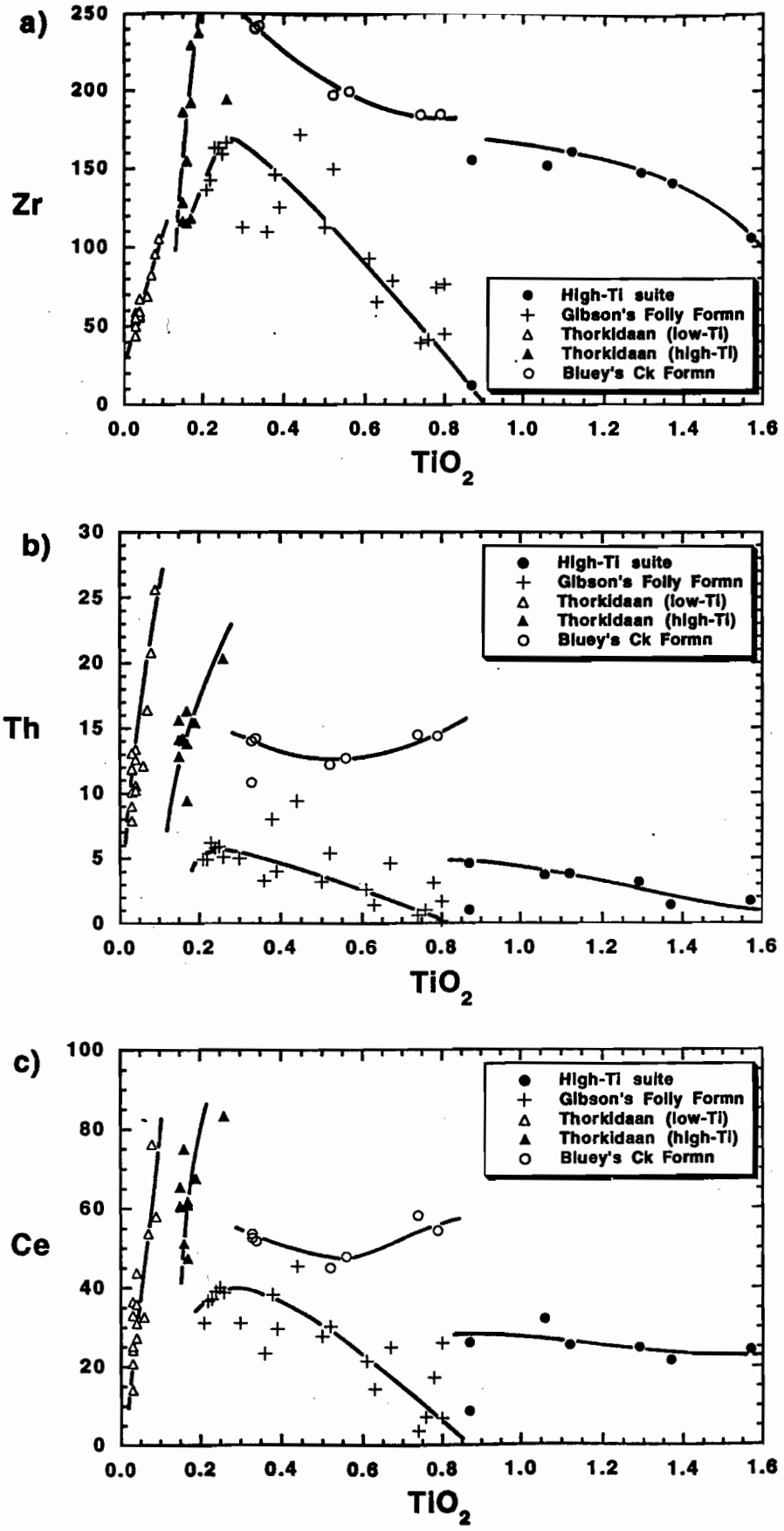

Fig. 4. Plots of (a) TiO_2 versus Zr, (b) TiO_2 versus Th, and (c) TiO_2 versus Ce for the host volcanics which highlight the marked high-field-strength element depletion in the Thorkidaan Volcanics with decreasing TiO_2.

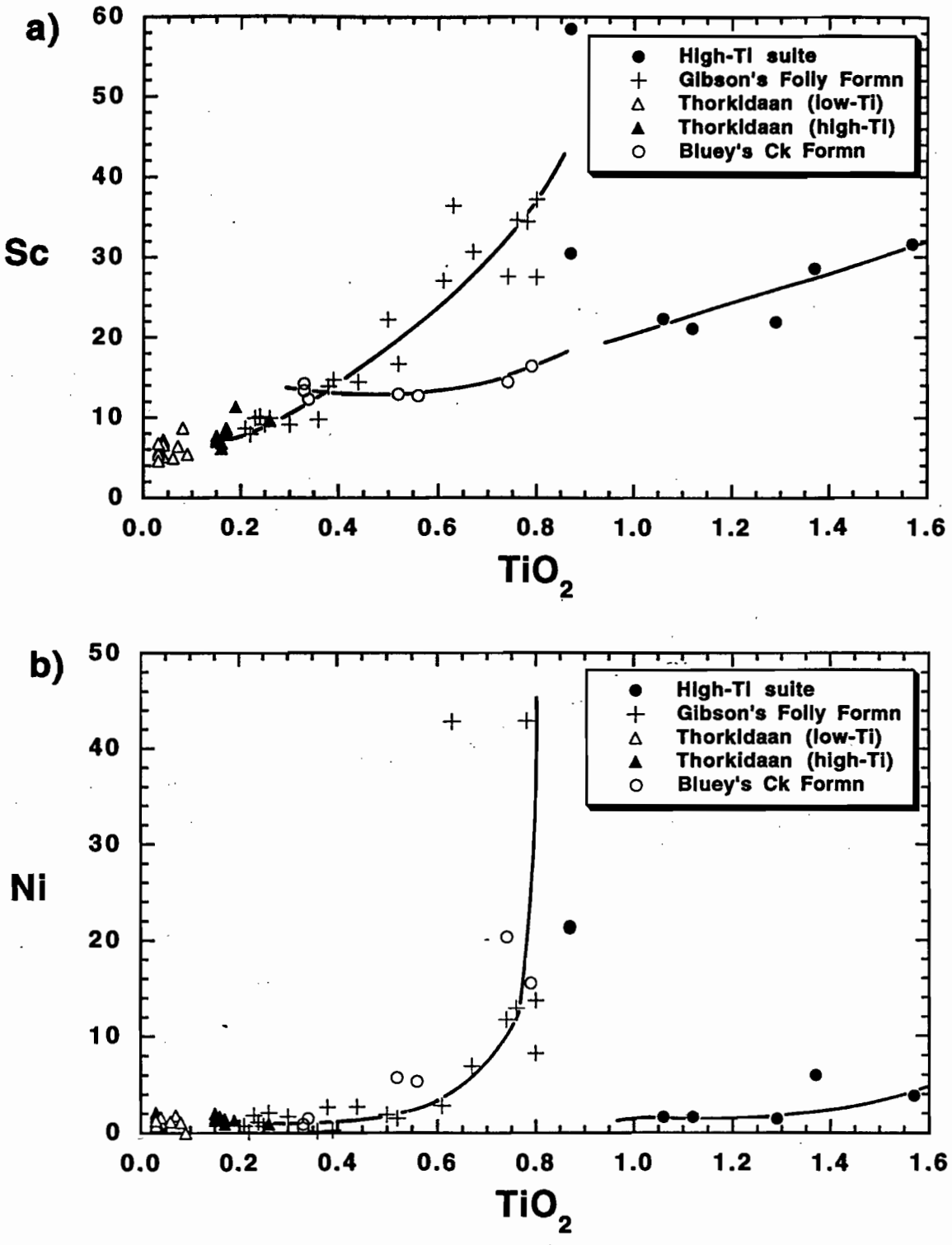

Fig. 5. Plots of a) TiO_2 versus Sc, and b) TiO_2 versus Ni for the host volcanics showing the trace transition element variations for the various suites.

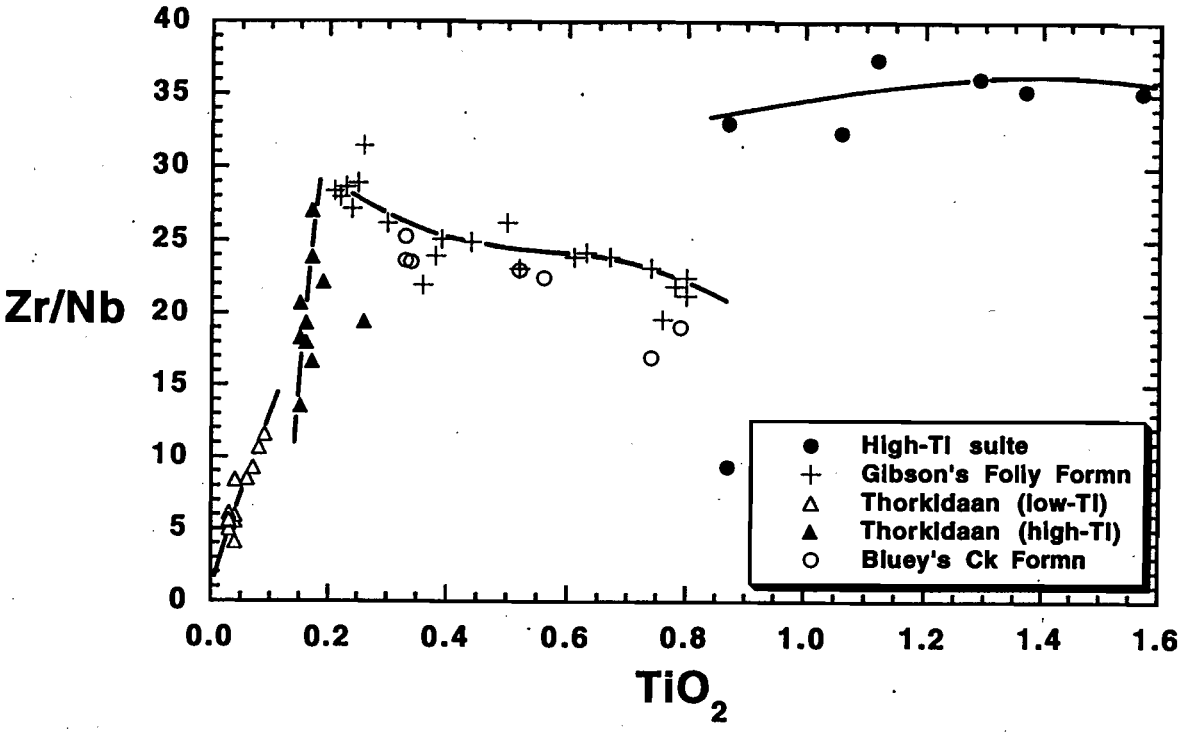

Fig. 6. Plot of TiO_2 versus Zr/Nb showing the different Zr/Nb values for the high-Ti and Gibson's Folly suites, and the marked decrease in Zr/Nb with TiO_2 for the Thorkidaan Volcanics.

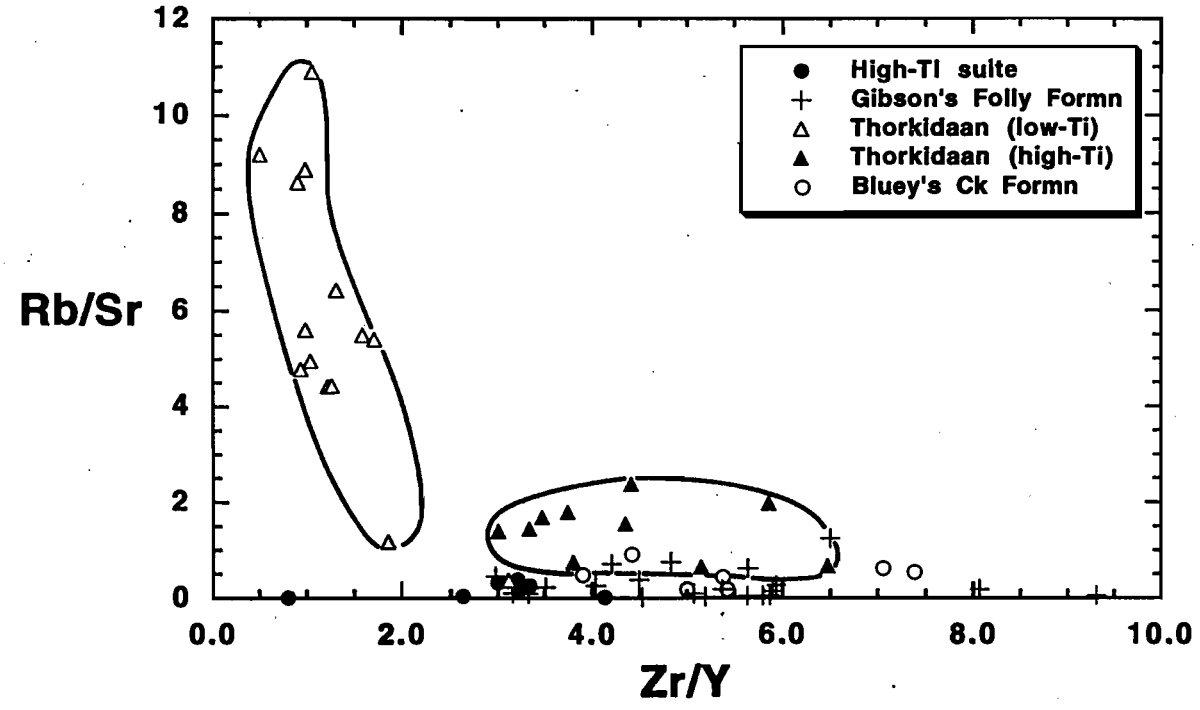

Fig. 7. Plot of Zr/Y versus Rb/Sr for the host volcanics which clearly distinguishes the low-Ti and high-Ti suites of the Thorkidaan Volcanics.

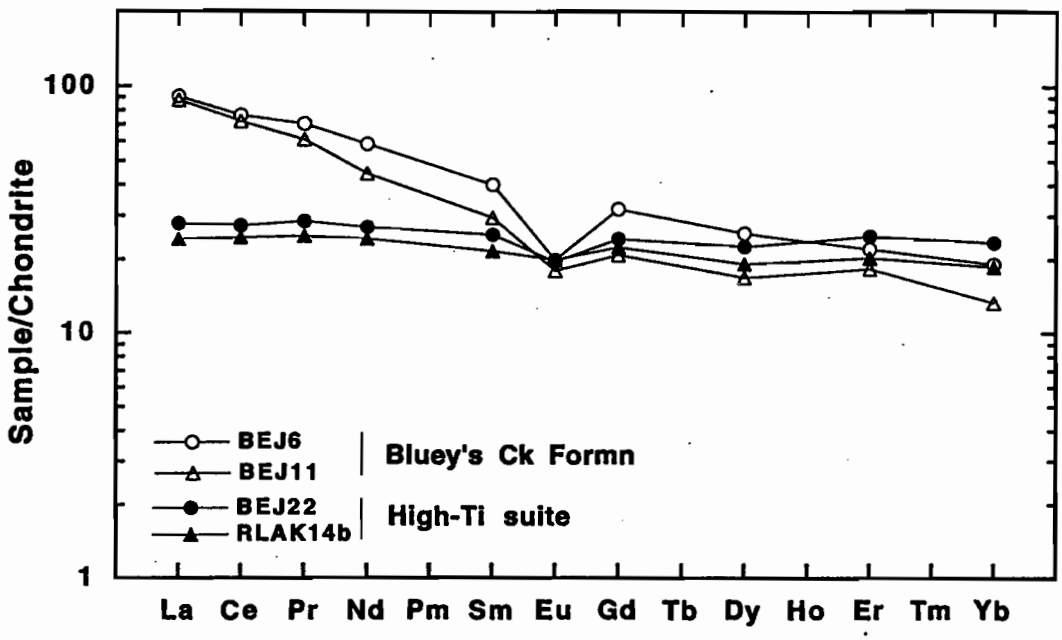

Fig. 8. Chondrite-normalised REE plots for the dacitic rocks from the Bluey's Creek Formation and the high-Ti suite andesites from the Bumble Creek area.

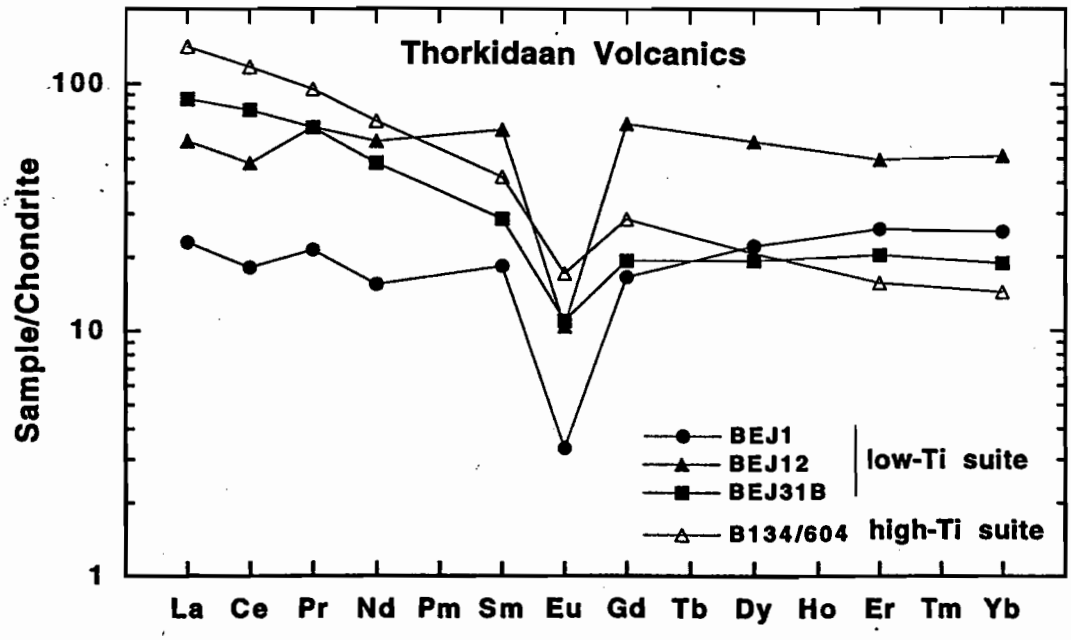

Fig. 9. Chondrite-normalised REE plots of the low- and high-Ti rhyolites from the Thorkidaan Volcanics.

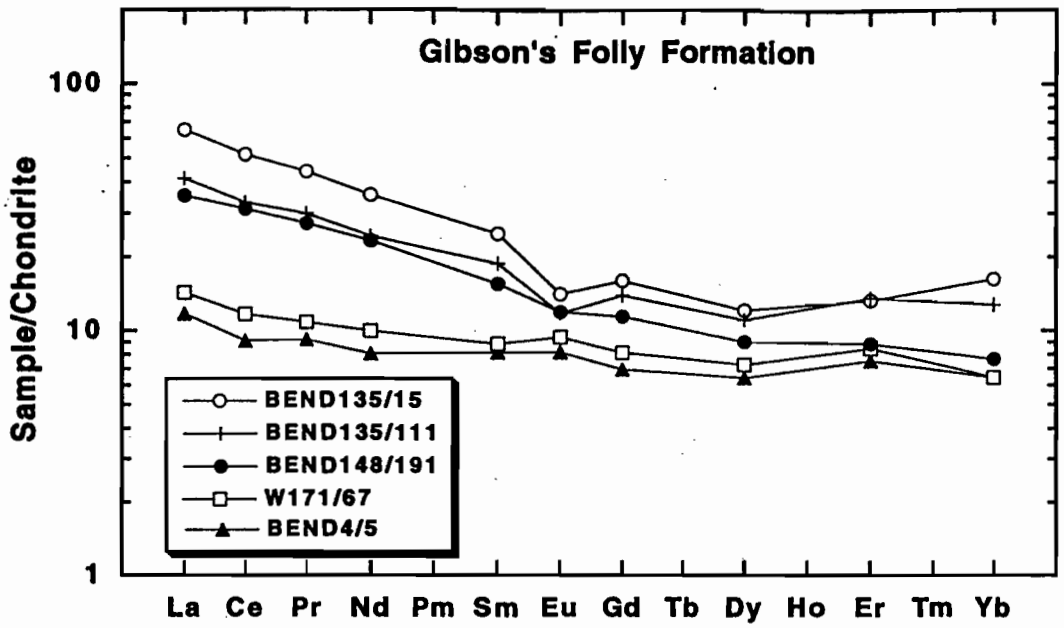

Fig. 10. Chondrite-normalised REE plots of the basalt, andesites and dacites from the Gibson's Folly Formation.

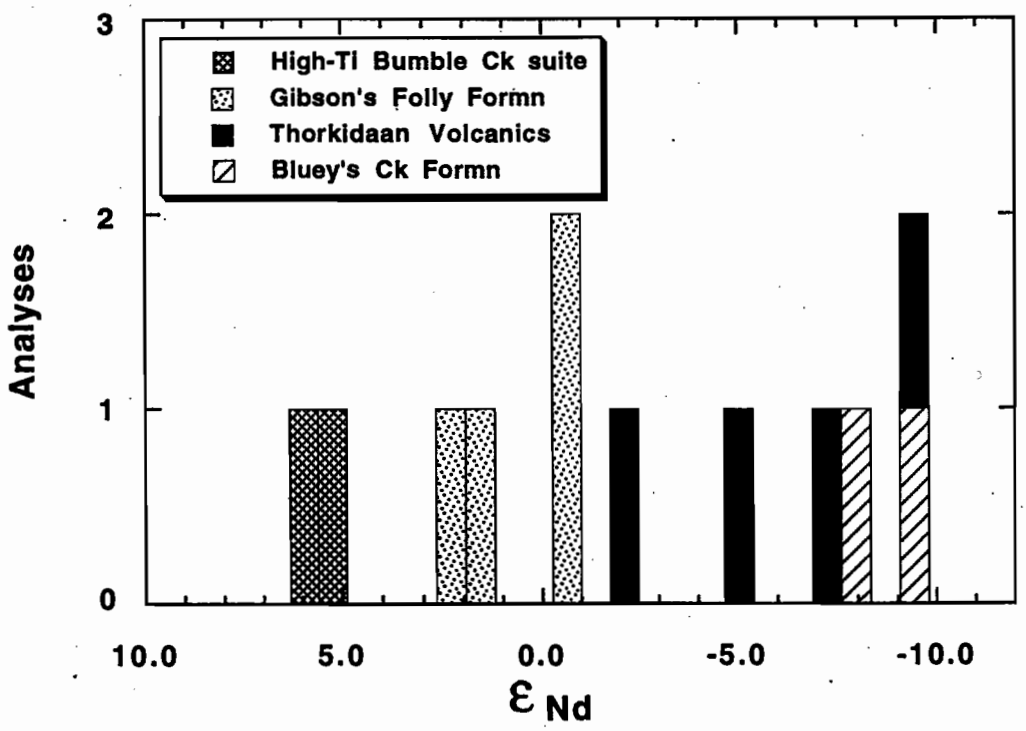

Fig. 11. A histogram showing the variability in ε_{Nd} values for the four major chemically distinguishable volcanic suites in the host sequence to the Wilga and Currawong VHMS deposits.

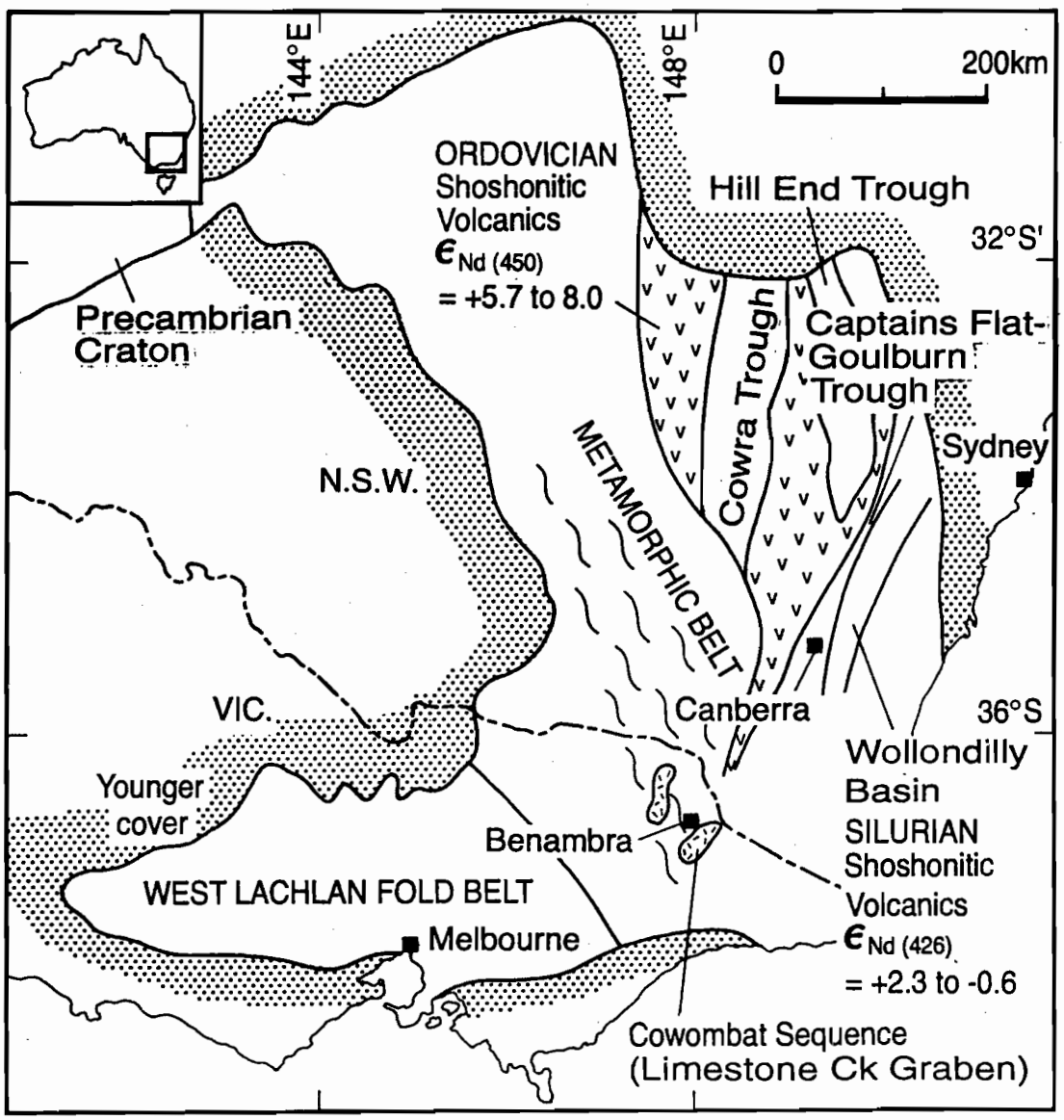

Fig. 12. Map of southeastern Australia showing the distribution of Ordovician volcanics and Silurian depositional basins within the Lachlan Fold Belt. Modified after Fergusson et al. (1986).

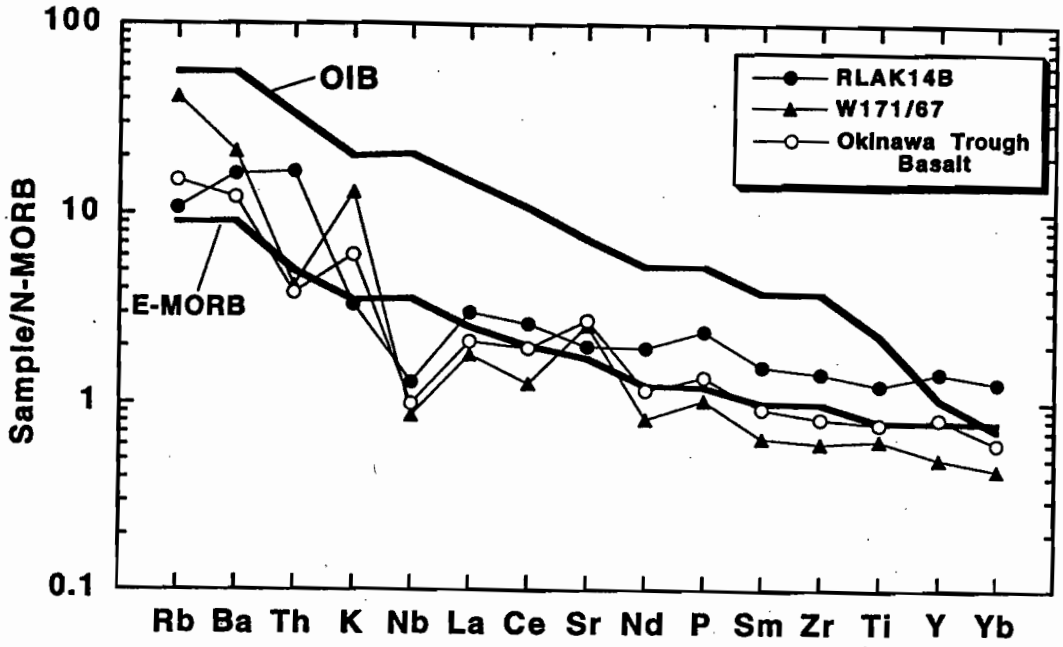

Fig. 13. A N-MORB normalised multi-element plot comparing typical E-MORB and OIB from Sun and McDonough (1989) with a basalt from the Gibson's Folly Formation and a typical modern back-arc basalt from the Okinawa Trough (Honma et al., 1991).

Table 5. Nd isotope data for the Benambra volcanics

		$^{147}Sm/^{144}Nd$	$(^{143}Nd/^{144}Nd)_m$	ε_{Nd} #
Bluey's Ck Formation				
BEJ6	Dacite	0.133506	0.512031 ± 4	−8.30
BEJ11	Dacite	0.128739	0.511974 ± 11	−9.14
Bumble Ck Volcanics				
BEJ22	Andesite	0.181804	0.512897 ± 12	5.85
RLAK14b	Andesite	0.173386	0.512841 ± 12	5.20
Thorkidaan Volcanics				
BEJ1	Rhyolite	0.231093	0.512232 ± 7	−9.78
BEJ12	Rhyolite	0.214990	0.512301 ± 8	−7.56
BEJ31B	Rhyolite	0.116265	0.512306 ± 6	−2.16
B134/604	Rhyolite	0.115901	0.512153 ± 4	−5.13
Gibsons Folly Formation				
W171/67	Basalt	0.171903	0.512544 ± 18	−0.52
B4/5	Andesite	0.195714	0.512621 ± 11	−0.28
B135/15	Dacite	0.134567	0.512570 ± 9	1.97
B135/111	Dacite	0.149715	0.512581 ± 4	1.38

ε_{Nd} values calculated assuming ages of 440 Ma for the Bluey's Ck Formation, 420Ma for the Thorkidaan Volcanics, and 415Ma for the Gibson's Folly Formation and Bumble Ck volcanics.

Discussion

Relationships within and between suites

The geochemical and isotopic data provide good constraints on the sources of the volcanics in the Benambra area, and also on the possible relationships within and between the suites. The generally coherent relationships displayed by the volcanics from the Gibson's Folly Formation in various plots, including SiO_2 versus ΣFe_2O_3 and TiO_2 (Fig. 3), and TiO_2 versus Zr, Th, Sc, Ni and Zr/Nb (Figs 4 to 6), together with the continuous range of compositions from basalt to high-silica dacite, suggest these rocks comprise a cogenetic suite. The systematic decreases in TiO_2, MgO, ΣFe_2O_3, CaO, P_2O_5, Cr, Ni and Sc with increasing SiO_2 which characterise the suite are consistent with well established fractionation trends for modern calcalkaline suites (Gill, 1981; Ewart, 1982). This interpretation is also supported by the systematic increase in ΣREE concentrations over the composition range basalt-dacite, with the latter also showing an increase in $(La/Yb)_N$ reflected in somewhat more LREE-enriched patterns, and slight negative Eu anomalies that reflect plagioclase fractionation. Fractionation in the early stages was most likely controlled by separation of olivine and pyroxene, followed by plagioclase and hornblende with minor Fe-Ti oxide and apatite in the andesitic to dacitic rocks. Metamorphic effects have largely obscured the evidence for these fractionating phases, although plagioclase is usually preserved (albeit albitised), and chloritic aggregates in some of the andesitic and dacitic rocks may be altered ferromagnesian phenocrysts. The similar $\varepsilon_{Nd(415Ma)}$ values for the basaltic, andesitic and dacitic rocks from the Gibson's Folly Formation (Table 5) provide additional strong support for their cogenesis and an origin by fractionation of a basaltic parent magma derived from a mantle characterised by a Bulk Earth Nd isotope signature.

The markedly different ε_{Nd} values of the Thorkidaan Volcanics compared with the Gibson's Folly Formation indicates that there is no genetic relationship between the two suites. This, coupled with the large volume of the silicic volcanics, and the absence of more basic and intermediate associates strongly suggests a separate origin for the Thorkidaan Volcanics by partial melting of pre-existing crustal rocks. Furthermore, their large negative ε_{Nd} values suggest a source with a substantial time-integrated history of LREE enrichment. The most likely source would be Proterozoic metamorphic middle to lower crust, although Ordovician sedimentary units derived by reworking exposed Precambrian basement material may also be appropriate. The two discrete suites within the Thorkidaan Volcanics evident from the chemical variation diagrams (Figs 4, 7) indicate that some fractionation of the silicic magma occurred in high-level magma chambers. The relatively low- and high-Ti suites appear to have evolved separately as their chemical variation trends are not continuous. The generally lower ΣFe_2O_3, TiO_2, Sr, Ba, Zr/Y, La/Yb and more pronounced negative Eu anomalies of the low-Ti Thorkidaan rhyolites suggests they have experienced the most extensive fractionation which was probably dominated by alkali feldspar and sodic plagioclase. Marked depletion of Zr, Th and the LREE, coupled with Y and HREE enrichment in both suites suggests trace element fractionation was controlled by accessory phases such as zircon and allanite. A number of studies (e.g. Miller and Mittlefehldt, 1982; Rapp and Watson, 1986; Wark and Miller, 1993) have demonstrated the strong control on the Zr, Th and REE concentrations of silicic melts by the fractionation of relatively minor quantities of these phases, the solubility of which is substantially decreased in high-silica rhyolites compared with less evolved magmas.

The ε_{Nd} values for the dacites and rhyolites of the Bluey's Creek Formation overlap those of the Thorkidaan Volcanics suggesting derivation from similar source materials. However, this suite is characterised by significantly higher TiO_2, Fe_2O_3, Al_2O_3, P_2O_5, Sc, V, Zr and lower Rb than the Thorkidaan rhyolites at similar SiO_2 contents. These differences, coupled with the contrasting I-type and S-type mineralogical characteristics of the Bluey's Creek rocks and Thorkidaan Volcanics, respectively, suggest they had different origins. The Bluey's Creek Formation rocks display a moderate range of compositions (66.8 to 74.6 wt.% SiO_2) characterised by coherent variation on chemical variation diagrams (Figs 3 to 6), and which appear broadly consistent with progressive fractional crystallisation involving separation of plagioclase, amphibole, magnetite and minor apatite from an andesitic melt. In plots of TiO_2 versus Zr, V, Ce, U and Sc (Figs 4, 5, not all shown) the high-Ti andesite-dacite suite from the Bumble Creek area generally show coherent variation trends that appear contiguous with the rocks of the Bluey's Creek Formation suggesting a cogenetic relationship between these suites. However, similar plots of TiO_2 versus Ni, Zr and Zr/Nb, (Figs 4 to 6) do not support this interpretation. In addition, the markedly different ε_{Nd} values of the two suites (Fig. 11) confirms their different sources and independent origins.

Early development of the Lachlan Fold Belt

The tectonic development of the Lachlan Fold Belt (LFB) during the early to mid- Palaeozoic has been extensively studied, yet many aspects of the early history remain controversial (e.g. Cas, 1983; Powell, 1984; Crawford et al., 1984; Scheibner, 1987; Collins and Vernon, 1992; Fergusson and Coney, 1992a). An excellent, relatively recent review of the geology and interpretations of the regional tectonic

development of the LFB is provided by Coney et al. (1990). The oldest rocks exposed in the LFB are Cambrian metabasalts that occur as a series of narrow, N–S trending fault bounded belts restricted to the western half of the LFB. These were originally interpreted as ensimatic crustal basement to the LFB developed in a back-arc basin (Crawford et al., 1984). However, probable Middle Cambrian correlatives from western Tasmania have been interpreted as part of a forearc volcanic package that was obducted on to the Proterozoic cratonic margin during a Middle Cambrian arc-continent collision (Berry and Crawford, 1988). This model may also be applicable to the Victorian greenstone packages, with their present configuration resulting from subsequent deformation.

A very thick and laterally uniform sequence of marine turbidites was deposited during the Ordovician and early Silurian. This may represent a huge submarine fan derived by erosion of the Late Proterozoic cratonic margin (Fergusson and Coney, 1992b) that was uplifted as a result of an arc-continent collision in the Middle Cambrian. In the eastern part of the LFB, extending from the New South Wales-Victorian border northward towards Parkes and Dubbo in New South Wales there are several belts of Ordovician volcanics and associated intrusives (Wyborn, 1992). The mafic types are dominated by shoshonitic compositions with a relatively depleted mantle-like Nd isotope signature ($\varepsilon_{Nd(480)} = 5–8$; Sun and Wyborn, 1994), but volumetrically subordinate tholeiitic basalts also occur in the southern part of the belt (Wyborn, 1992). In earlier tectonic models (Cas, 1983; Powell, 1984) these volcanics were interpreted as the remnants of an Ordovician volcanic arc (the Molong Arc), however Wyborn (1992) argued that they were more likely erupted in an extensional intraplate setting, and they were derived from oceanic mantle that had been metasomatised during an earlier (probably Cambrian) subduction event. The entire LFB sequence underwent substantial deformation as a result of the early Silurian Benambran Orogeny culminating in the development of the high-temperature, low-pressure Omeo Metamorphic Complex and associated syntectonic granitic magmatism.

Tectonic setting of the Silurian volcanics and VHMS deposits

The Middle Silurian to Late Devonian represents a period during which there was extensive silicic magmatism in the LFB, dominated by I- and S-type granitic intrusives (Chappell, 1984; Chappell et al., 1988), with subordinate but nevertheless substantial volumes of silicic volcanics and volcaniclastic rocks. During the Middle Silurian, a number of roughly N–S oriented elongate troughs developed in the eastern LFB (Fig. 12). These include the Cowra Trough, Hill End Trough, Wollondilly Basin and Captains Flat-Goulburn Trough in New South Wales, and the Wombat Creek Graben and Limestone Creek Graben in northeastern Victoria, the latter which hosts the Wilga and Currawong mineralisation. Other significant Silurian Cu-Zn-Pb VHMS deposits that occur in the Captains Flat-Goulburn Trough in southeastern New South Wales include the Woodlawn (McKay and Hazeldene, 1987) and Captains Flat deposits (Bain et al. 1987; Davis, 1990).

As with the tectonic history of the LFB during the Ordovician, there has been considerable debate about the presence or absence of an active arc in the eastern LFB during the Silurian. Powell (1984) proposed a model involving regional dextral shear in southeastern Australia associated with a transtensional boundary between the palaeo-Pacific plate and the eastern margin of Gondwana. This is considered to have resulted in lithospheric extension producing a series of narrow trough structures accompanied by bimodal basic and silicic magmatism. Scheibner (1974) and Degling et al. (1986) prefer a back-arc setting for the eastern LFB at this time with an arc and subduction zone located somewhere to the east of the present east coastline of Australia. The lack of obvious evidence for a constructional continental margin arc is a major short-coming of this model. However, a back-arc basin setting has also been proposed for the somewhat older (Cambrian) Mt Windsor Volcanic Belt in northern Queensland (Stolz, 1995) where the arc front deposits are no longer evident. The occurrence of the Middle Silurian silicic volcanics in narrow troughs clearly supports an extensional environment with crustal melting likely to be facilitated by intrusion of mafic magmatism generated as a result of lithospheric thinning and mantle upwelling. The predominance of silicic magmatism over more mafic volcanic products suggests that much of the mafic magmatic component may have solidified near the crust-mantle boundary underplating the lower crust.

The isotopic and chemical characteristics of the Silurian mafic volcanics from the LFB are not well documented, however the scattered literature data suggest significant variability. Middle Silurian basaltic to andesitic volcanics from the Gundary Formation in the Wollondilly Basin (Fig. 12; Jones et al., 1995) differ from the Gibson's Folly Formation basalts in that they are shoshonitic and are characterised by significantly higher K_2O, P_2O_5, Rb, Sr, Zr, Th, ΣREE and La/Yb at similar SiO_2, TiO_2, Al_2O_3, MgO, CaO. However, both suites have a distinctive subduction-related geochemical signature (negative Nb anomalies in N-MORB normalised plots, Fig. 13) and essentially identical ε_{Nd} values (i.e. 2.3 to –0.6 and 2.0 to –0.5), suggesting an isotopically similar mantle source

characterised by variable enrichment in large-ion-lithophile elements. The shoshonitic compositions of the basalts from the Wollondilly Basin appear to indicate an extension into the Silurian of the Ordovician shoshonitic volcanism, although their different Nd isotope characteristics indicate some source differences. The only relatively low Ti tholeiitic rocks in the LFB of possible Ordovician age that are broadly comparable with the Gibson's Folly suite, are the Gooandra Volcanics in southern New South Wales (Owen and Wyborn, 1979). However, Wyborn (1992) suggests these may be Early Silurian in age.

Mafic intrusives and eruptives are also closely associated with the Silurian Woodlawn, Captains Flat and Currawang VHMS deposits in southeastern New South Wales. At Woodlawn the mafic rocks are intrusive (dolerites), and although they post-date the mineralisation, their emplacement into unconsolidated sediment immediately overlying the deposit (McKay and Hazeldene, 1987) suggests they are only slightly younger. These intrusives have been correlated with pillow basalts that form the footwall to the Currawang Cu-Zn deposit that occurs approximately 10 km northwest of the Woodlawn deposit. The available data for Woodlawn mafic rocks (Petersen et al., 1977) indicate quite different compositions to the Gibson's Folly Formation. These rocks are characterised by relatively high TiO_2 (1.7 – 2.2 wt.%), P_2O_5 (0.32 – 0.43 wt.%), Zr (150 – 200ppm), Nb (9 – 14ppm), Cr (>250ppm) and Ni (>100ppm), and they are comparable with many intraplate tholeiitic rocks and flood basalts (cf. BSVP, 1981; Wilson, 1989). Some of these characteristics (e.g. high TiO_2) are also a feature of the Bumble Creek rocks, but the latter are generally more evolved and have significantly lower MgO, P_2O_5, Ni, Cr, Zr and Nb, and higher Al_2O_3, Y, and Zr/Nb. Unfortunately there are no published Nd isotope data available for the mafic rocks associated with the Woodlawn, Captains Flat and Currawang deposits, so it remains unknown if they were derived from a mantle with depleted isotopic characteristics similar to the Bumble Creek volcanics, or isotopically less depleted mantle similar to the other Silurian volcanics from the Cowombat Rift and the Wollondilly Basin.

The chemistry of the Gibson's Folly suite is consistent with its eruption in a continental back-arc setting similar to the Okinawa Trough which is currently developing on stretched continental lithosphere behind the Ryukyu Arc (Letouzey and Kimura, 1985). Comparison of the compositions of basaltic rocks from the Gibson's Folly Formation and the Okinawa Trough (Fig. 13) indicate very similar characteristics that are also similar to E-MORB (Sun and McDonough, 1988) with the exception of a significant relative depletion of Nb in the Gibson's Folly and Okinawa Trough rocks. This relative depletion in Nb is a distinctive feature of volcanics formed both at the arc front and during the early stages of back-arc basin development (Stern et al., 1990). The occurrence of active hydrothermal systems and modern massive sulphide deposits in the Okinawa Trough (Halbach et al., 1989) supports the appropriateness of the comparison with the Benambra volcanics, although the lack of evidence for the presence of a volcanic arc to the east of the Cowombat Rift during the Silurian remains problematic.

The very similar Nd isotope signatures of the Ordovician volcanics and the Bumble Creek volcanics suggests a link between the latter and the Ordovician volcanism which would be consistent with the presence of predominantly faulted contacts between the Bumble Creek volcanics and the established Silurian sequences. Earlier studies of the region suggested a closer affiliation of the Bumble Creek rocks with the Ordovician Nine Mile Creek Volcanics (Ramsay and Vandenberg, 1986), although in subsequent mapping they were regarded as lateral equivalents of the Gibson's Folly Formation due to their spatial association with limestones similar to those within the Enano Group to the southwest (Fig. 1; Allen, 1992). However, the Bumble Creek rocks are chemically somewhat different from both the Gibson's Folly Formation basalts and the Ordovician volcanics. A further possibility is that the Bumble Creek volcanics were derived from an evolving mantle source region shortly after the Gibson's Folly Formation basalts. In this scenario the early volcanism is generated from subduction modified mantle, whereas the later magmatism is derived from mantle that has not experienced significant modification by subduction processes. Stolz (1995) proposed a similar model to explain a change in the composition of the basalts of the Cambrian Mt Windsor Volcanic Belt with time from relatively low-Ti basalts characterised by a marked subduction signature to relatively high-Ti basalts and andesites with many similarities to the Bumble Creek rocks. Oceanic back-arc basin basalts (e.g. Mariana Trough, Stern et al., 1990) commonly display a similar change in compositions from early eruptives with a well-developed subduction signature to more normal MORB compositions as the site of back-arc basin magma generation becomes more remote from the subduction zone. A significant difference between the relatively high- and low-Ti rocks from the Cowombat Rift and the Mt Windsor belt is that the latter are characterised by similar Nd isotopic signatures, whereas the Bumble Creek rocks have substantially different ε_{Nd} values to the Gibson's Folly Formation. This could reflect in the source of the Bumble Creek Volcanics a smaller contribution to a depleted mantle source of a subduction component with a relatively low ε_{Nd} value. However, the

preferred interpretation is that the Bumble Creek volcanics are of Ordovician age due to the restricted and different ranges of isotopic characteritsics for the Ordovician and Silurian volcanics evident from other studies, and because of the lack of gradational chemical and isotopic characteristics between the Bumble Creek and Gibson's Folly suites.

As the Ordovician shoshonitic volcanics in southern New South Wales are no longer considered the remnants of an Ordovician arc (Wyborn, 1992), the earliest post-Cambrian evidence of arc magmatism in eastern Australia is provided by the Late Silurian-Early Devonian Calliope Arc volcanics in the northern New England Fold Belt (Murray, 1986). However, the compositions of the Calliope volcanics suggest they were erupted in an oceanic island arc setting, and the arc was subsequently accreted onto the eastern Australian margin (Day et al., 1978; Powell, 1984). Continental margin arc volcanism does not appear to have been established in the New England Fold Belt until the Carboniferous when the Connors Arch volcanics were produced. Although there was widespread silicic volcanism and intrusive activity in the LFB during the Silurian, Devonian and Carboniferous, this is spread over the entire 800km width of the LFB (Chappell et al., 1988; Coney et al., 1990), and does not appear to be related to concurrent subduction activity. However, Fergusson and Vandenberg (1990) argued for the existence of a Silurian arc located close to the present coast of southeastern Australia based on the presence of an apparent subduction complex in the Bungonia-Goulburn area. The deformation in these apparent forearc rocks was originally interpreted in terms of a west dipping subduction zone (Powell, 1984; Fergusson and Vandenberg, 1990; Fergusson and Coney, 1992a), although subsequently it has also been interpreted as related to an east dipping subduction zone (Fegusson and Coney, 1992b). A model involving a west dipping subduction zone near the present continental margin may be consistent with the distribution of granitoids in southeastern Australia. The north–south oriented I–S line separates dominantly S-type granitoids in the west from exclusively I-type granitoids to the east (White et al., 1976). The concentration of I-type magmatism in a discrete linear belt may be reflecting the roots of a Silurian arc that has been removed by erosion, or the remobilisation of material that was underplated during Silurian subduction-related magmatic activity.

The characteristic subduction-related geochemical signature of the basalts in the Gibson's Folly Formation indicates they were derived from a subduction-modified mantle source. However, there is good evidence both from modern arcs (Johnson et al., 1978; Stolz et al., 1993) and ancient volcanic packages (Wyborn, 1992) that a subduction modified source may be tapped well after subduction has ceased, most likely during a period of post-collisional extension. Hence the geochemical data for the volcanics from the Cowombat Rift do not provide clear support for either a transtensional margin or a back-arc setting during the Silurian, although it is difficult to explain the periodic strong episodes of deformation within the LFB from the Lower Silurian to Lower Devonian in the absence of a proximal convergent margin (Fergusson and Coney, 1990). The considerable uncertainty that surrounds the existence of an arc in the LFB during the Silurian attests to the difficulty in producing a coherent tectonic model for this complex terrane.

Basement to the Lachlan Fold Belt

There has been considerable debate in the literature regarding the composition of the basement to the LFB (e.g. McCulloch and Chappell, 1982; Cas, 1983; Crawford et al., 1984; Chappell et al., 1988; Coney et al., 1990; Fergusson and Coney, 1992a). Early models that envisaged deposition of the Ordovician turbidites on oceanic lithosphere are inconsistent with Nd isotope and P–T constraints on subsequent derivation of S- and I-type granitoids by partial melting of the middle to lower crust (Chappell et al., 1988; Coney et al., 1990). The relatively large negative ε_{Nd} values of the S-type granitoids (ε_{Nd} = –5 to –13; McCulloch and Chappell, 1982), and coeval eruptives such as the Thorkidaan Volcanics (Table 5), indicate derivation from relatively old crustal material with a substantial time-integrated history of LREE enrichment. Depleted mantle model ages suggest that this crustal material is of Upper Proterozoic age (McCulloch and Chappell, 1982). Estimates of the maximum thickness of the sedimentary package are typically ~10 km, and segregation of the S-type melts probably occurred at a depth of about 20–25km. This suggests that the source for the S-type granitoids was not the Ordovician turbidite package, although it was probably similar late Proterozoic crustal material to that from which the Ordovician sediments were derived. Crawford et al. (1984) suggested that a wedge of continental crust may have been thrust westward under oceanic crust providing the basement source for the S-type granitoids. However, Fergusson and Coney (1992a) suggest this is unlikely as it does not explain the complex deformation pattern in the LFB.

The substantial overlap between the Nd isotope ratios of the S- and I-type granitoids is somewhat problematic if they are considered to be derived from discrete sedimentary and igneous sources, respectively (Chappell and White, 1974; Chappell and Stephens, 1988; White and Chappell, 1988). This problem is highlighted by the large negative ε_{Nd}

values (ε_{Nd} = –8.2 to –9.1) and depleted mantle model age of 1100 Ma for the source of the hornblende-phyric dacitic (I-type) volcanics from the Bluey's Creek Formation. If the I-type granitoids were derived from an igneous source, their relatively large negative ε_{Nd} values must be attributed to continuous underplating and aging of the igneous source materials over a considerable time interval (McCulloch and Chappell, 1982), or they were inherited from igneous lower crustal material that was characterised by a substantial subduction component (Chappell and Stephens, 1988). Gray (1984) proposed that the geochemical and isotopic character of many of the LFB granitoids and volcanics could be explained by a simple mixing model involving contamination of mantle-derived magmas by Ordovician turbidites. However, although much of the Nd, Sr and O isotopic data of the S- and I-type granitoids can be modelled in terms of mixing of a depleted mantle component and an older continental crustal component, the very large crustal component in many I-type magmas inferred from the isotopic data is inconsistent with many of their major and trace element characteristics (McCulloch and Chappell, 1982; Chappell and Stephens, 1988; White and Chappell, 1988).

An alternative explanation is that the underplated I-type source materials assimilated substantial amounts of Proterozoic lower crustal material at the time of their emplacement. This could have occurred at any time between the late Proterozoic and Early Silurian, depending on the amount of material assimilated. An early Silurian age for the emplacement of the I-type souce rocks would be consistent with the inferred extensional tectonic environment and associated mafic magmatism. However, this model would require substantial assimilation of Upper Proterozoic lower crustal material by the underplating magmas as there would be negligible time for isotopic evolution of unmodified mantle-derived compositions to produce the relatively radiogenic Sr and unradiogenic Nd isotope compositions that characterise the I-type granitoids. Assimilation of crustal material during crystal fractionation (DePaolo, 1981) has been proposed to explain the relatively radiogenic Sr and unradiogenic Nd isotopic characteristics of continental flood basalts and intrusives (Carlson et al, 1981). Chemical and isotopic variations in lower crustal mafic xenoliths have also been explained by this mechanism (Rudnick et al., 1986; Rudnick and Goldstein, 1990), and substantial changes in the isotope signature can accompany relatively small changes in the bulk composition of the magma. Partial melting of mafic to intermediate lower crustal rocks modified in this manner may explain the I-type chemistry coupled with the more continental crust-like Nd, Sr and O isotope characteristics of the I-type granitoids and volcanics in the LFB.

Pb isotope data for the I- and S-type granitoids from the LFB (McCulloch and Woodhead, 1993) indicate a very restricted range of compositions with substantial overlap between the granitoid suites and the Ordovician sedimentary rocks which they have intruded. McCulloch and Woodhead (1993) proposed that the limited range in Pb isotope ratios coupled with the relatively large range in Sr and Nd isotope ratios for the granitoids reflected homogenisation of the Pb in their source regions by deep crustal-scale fluid advection systems. However, assimilation of relatively Pb-rich sedimentary material (6–33 ppm, McCulloch and Woodhead, 1993) with a restricted range of Pb isotope ratios during fractional crystallisation of relatively Pb-poor basic magma (~1–2 ppm) could also produce an igneous source with a fairly uniform Pb isotope composition and yet maintain a significant range in the Sr and Nd isotope ratios due to the substantially greater difference in Pb (compared with the Sr and Nd) concentrations between the assimilating magma and the assimilate.

The importance of silicic magmatism to mineralisation

Considerable importance has been attributed to the rhyolitic rocks associated with massive sulphide deposits in influencing the development of mineralisation. The implied role of the silicic magmatism differs depending on the preferred model for the genesis of these deposits and either involves (1) a passive role whereby the metals are leached from footwall silicic volcanics by seawater-dominated hydrothermal fluids (e.g. Spooner and Fyfe, 1973; Franklin et al., 1981; Ohmoto et al., 1983), or (2) a more direct role through exhalation of base metal-rich fluids from crystallising high-level silicic magma bodies (Urabe and Sato, 1978; Sawkins and Kowalik, 1981; Urabe, 1987; Stanton, 1990, 1994). Solomon (1976) made the important observation that about 50 percent of massive sulphide deposits have a footwall package dominated by rhyolitic volcanics and volcaniclastic rocks. These were predominantly Zn–Cu and Zn-Pb-Cu type deposits, the names reflecting the relative metal concentrations in the deposits. In contrast, the Cu-Fe or Pb-poor Cyprus-style deposits are apparently never associated with rhyolitic volcanics (Solomon, 1976). These relationships were interpreted as indicating derivation of the Pb in the Zn-Pb-Cu deposits from relatively Pb-rich rhyolites (12–20 ppm Pb), whereas ocean-floor basalts with < 1ppm Pb are incapable of providing significant Pb to spatially associated deposits regardless of the mechanism by which metals are enriched.

An additional feature of many of the rhyolite hosted VHMS deposits is that there is commonly no basic or intermediate (mantle-derived) volcanism occurring as a precursor to the silicic volcanism (Sillitoe, 1982;

Large, 1992), and the mineralisation is located either at the interface between the silicic volcanics and overlying sequence or within the overlying mixed basalt-andesite-dacite package as in the case of the deposits from Benambra and the Mt Windsor Volcanic belt (Stolz, 1995). This relationship suggests that the basic magmatism exerts a more important influence on the mineralisation process than the silicic magmatism.

Stanton (1985, 1990, 1994) has been one of the most enthusiastic proponents of a magmatic source for the metals in VHMS deposits and argued for a close relationship between the magmatic evolution of the calc-alkaline rock series in island arc settings and the type of associated mineralisation, the Zn-Cu type deposits being related to the basalt-andesite stage of fractionation, and the Zn-Pb-Cu-type more closely related to the dacite-rhyolite stages of volcanism. In addition, Urabe (1987) argued on the basis of the close spatial relationship between massive sulphide deposits and dacitic to rhyolitic domes in the Hokuroko district, as well as other chemical features of the ores, that subvolcanic silicic magmas are an important source of metals in the deposits via an exsolved volatile phase. There is also fluid inclusion and isotopic evidence from modern hydrothermal systems (de Ronde, 1995) and the Cambrian Hellyer deposit from western Tasmania (Khin Zaw et al., 1995) that suggest a significant component of the mineralising fluids may be derived from a magmatic source. However, there seems to be general agreement that relatively small intrusions of silicic magma of the type that occur in the footwall to many VHMS deposits (cf. Campbell et al., 1981) would not have sufficient latent heat of crystallisation to drive a hydrothermal convection cell of the size necessary to leach the quantity of metals occurring in even a small VHMS deposit (Cathles, 1978, 1983; Lydon, 1989). Thermal balance calculations indicate that relatively large, shallow and hot convecting magma bodies are necessary to provide sufficient heat to drive a hydrothermal convection system of the magnitude required to produce a reasonable size massive sulphide deposit (Cann et al., 1985; Strens and Cann, 1986).

The results of this study provide no direct support for either a leaching or magmatic source for the metals in the deposits. However, the recognition from the isotopic and trace element data for the Benambra volcanics and also the Mt Windsor Volcanic belt (Stolz, 1995) that there are two chemically and isotopically discrete suites of silicic volcanics associated with massive sulphide deposits in some of these belts is important. It enables us to distinguish silicic volcanic packages derived by partial melting of older sedimentary rocks that are unlikely to be mineralised from those produced by fractionation of basaltic or andesitic magmas. Blevin and Chappell (1992) demonstrated a close relationship between highly fractionated, relatively reduced S-type granitoids and Sn-W mineralisation in the Lachlan Fold Belt, whereas Cu-Au mineralisation appears to be associated with relatively unfractionated and oxidised, intermediate I-type magmas. Due to the relatively reduced character of the sediment-derived S-type magmas, sulphides are precipitated early, depleting the melt in sulphur and base metals. The preference of the Sn-W mineralisation for S-type magmas and Cu-Au mineralisation with more oxidised systems is also supported by experimental work discussed by Candela (1989).

Perhaps most important from the exploration perspective is the observation that in some belts the appearance of the VHMS mineralisation can be correlated with a marked change in the composition and style of the volcanism from these crustal-derived silicic eruptives to a mantle derived basalt-andesite-dacite suite. Moreover, where a thick package of S-type silicic volcanics is erupted prior to any basaltic, andesitic or dacitic volcanics, the rhyolitic package is unlikely to be mineralised. The appearance of the basaltic magmatism seems necessary to either provide the heat to initiate a substantial hydrothermal convection cell, or the fractionating basalt-andesite-dacite suite is necessary as a direct magmatic source of metal-rich hydrothermal fluids (e.g. Fig. 14). If on the other hand, the mafic magmatism has preceded or been active concurrently with the S-type silicic magmatism, mineralisation may potentially occur anywhere within the sequence, and the recognition of these discrete magma types will be of limited use in exploration.

The broader significance of these conclusions to other mineral fields is uncertain because the data necessary to distinguish these different groups of silicic rocks is generally lacking. Sillitoe (1982) noted that a substantial proportion of VHMS deposits with a felsic footwall package do not have an earlier phase of mafic magmatism, and some of these sequences may include crustal derived silicic melts. For the well studied Kuroko deposits where some isotopic data is available, the general stratigraphic relationships indicate both pre-ore and post-ore phases of basaltic volcanism, but the pre-ore basalts apparently do not occur in close association with the deposits (Urabe, 1987). The Sr isotopic data for the host volcanics to the Kuroko deposits does not indicate the presence of two isotopically distinct suites of silicic volcanics. The rhyolites all have significantly less radiogenic Sr than the analysed basement rocks from the district (Farrell and Holland, 1983), and are therefore probably comagmatic with the basalts. However, Sr isotope data for subaqueously erupted volcanics are particularly susceptible to modification by seawater, and Nd istope studies similar to those undertaken in

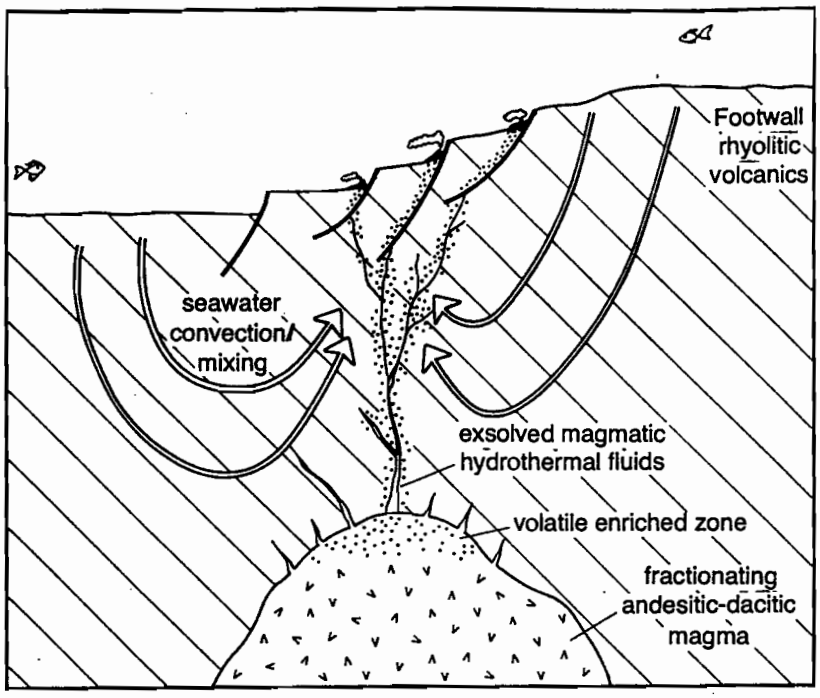

Fig. 14. A hypothetical model showing how a fractionating basic to intermediate magma body may provide heat to drive a hydrothermal convection cell and periodically contribute metal-rich hydrothermal fluids to a mineralising system.

this study may prove more fruitful in elucidating the source characteristics and mineralised potential of other ancient submarine volcanic sequences.

Conclusions

Middle to Upper Silurian volcanics that host the Wilga and Currawong Cu-Zn massive sulphide deposits in northeastern Victoria can be grouped into four chemically and isotopically distinct suites with discrete origins. The earliest manifestation of volcanism in the Cowombat Rift comprises minor I-type dacites, closely followed by voluminous rhyolitic and rhyodacitic lavas and volcaniclastic deposits. The rhyolitic rocks, which form the dominant footwall sequence to the massive sulphide deposits, have a Nd isotope signature that suggests they were derived by partial melting of Late Proterozoic lower crustal rocks, and they display at least two chemically discrete suites that have evolved by crystal fractionation processes in separate magma chambers.

The hangingwall and host volcanic sequence is a basalt-andesite-dacite suite with a uniform Nd isotope signature that indicates they represent a cogenetic suite related by fractional crystallisation. Spatially associated, relatively high-Ti andesites and dacites have a different Nd isotopic signature as well as other trace element features which distinguish them from the hangingwall volcanics. The volcanism and related VHMS mineralisation in the Cowombat Rift developed in a restricted extensional basin concomitant with similar features further north in the LFB. The geochemical characteristics of the mafic volcanics from the Cowombat Rift are similar to those from the Okinawa Trough; a modern back-arc basin developing on attenuated continental lithosphere adjacent to the Ryuku arc. A similar tectonic setting is the preferred model for the Cowombat Rift, although the limited evidence for an active arc to the east of the Cowombat Rift during the Middle to Upper Silurian means that development of the basin adjacent to a dextral transtensional margin remains a possibility.

Comparisons with mineralisation styles associated with S-type granitoids, coupled with thermal constraints on the ability of small silicic magma bodies to generate significant hydrothermal convection cells suggest that the thick rhyolitic footwall package at Benambra and in similar volcanic belts are unlikely to contain VHMS deposits. Exploration for this style of deposit should be focussed where there is a change to mantle-derived basalt-andesite-dacite volcanism, or within these mixed volcanic suites.

Acknowledgements

We are grateful to Bob Singer of Denehurst Ltd for access to drill core from the Wilga and Currawong prospects. AJS is supported by an Australian Research Fellowship.

References

Allen, R.L., 1987, Subaqueous volcanism, sedimentation and the geological setting of Zn-Cu-Pb massive sulphide deposits, Benambra, S.E. Australia: Unpub. Ph.D. thesis, Clayton, Victoria, Monash Univ., 284p.

Allen, R.L., 1992, Reconstruction of the tectonic, volcanic, and sedimentary setting of strongly deformed Zn-Cu massive sulfide deposits at Benambra, Victoria: Economic Geology, v. 87, p. 825–854.

Allen, R.L. and Barr, D.J., 1990, Benambra copper-zinc deposits: Australasian Inst. Mining Metallurgy Mon. 14, p. 1311–1318.

Allen, R.L. and Vandenberg, A.H.M., 1988, Limestone Creek graben and associated outliers (Silurian-Middle Devonian), *in* Douglas, J.G. and Ferguson, J.A., eds., Geology of Victoria: Melbourne, Geol. Soc. Australia, Victorian Div., p. 125–129.

Bain, J.H.C., Wyborn, D., Henderson, G.A.M., Stuart-Smith, P.G., Abell, R.S. and Solomon, M., 1987, Regional geological setting of the Woodlawn and Captains Flat massive sulphide deposits, N.S.W., Australia: Pacrim 87, p. 25–28.

Berry, R.F. and Crawford, A.J., 1988, The tectonic significance of Cambrian allochthonous mafic-ultramafic complexes in Tasmania: Australian Journal of Earth Sciences, v. 35, p. 523–533.

Blevin, P.L. and Chappell, B.W., 1992, The role of magma sources, oxidation states and fractionation in determining the granite metallogeny of eastern Australia: Trans. Roy. Soc. Edinburgh, Earth Sci., v. 83, p. 305–316.

Boden, S.B. and Valenta, R.K., 1995, Primary and tectonic features of the Currawong Zn-Cu-Pb (-Au) massive sulfide deposit, Benambra, Victoria: implications for ore genesis: Economic Geology, in press.

BVSP, 1981, Basaltic Volcanism on the Terrestrial Planets, Pergamon Press, New York, 1286p.

Campbell, I.H., Franklin, J.M., Gorton, M.P., Hart, T.R. and Scott, S.D., 1981, The role of subvolcanic sills in the generation of massive sulfide deposits: Economic Geology, v. 76, p. 2248–2253.

Candela, P.A., 1989, Felsic magmas, volatiles, and metallogenesis, in, Whitney, J.A. and Naldrett, A.J., eds., Ore Deposition Associated with Magmas: Reviews in Economic Geology, v. 4, p. 223–233.

Cann, J.R., Strens, M.R. and Rice, A., 1985, A simple magma-driven thermal balance model for the formation of volcanogenic massive sulfides: Earth Planet. Sci. Lett., v. 76, p. 123–134.

Carlson, R.W., Lugmair, G.W. and MacDougall, J.D., 1981, Columbia River volcanism: the question of mantle heterogeneity or crustal contamination: Geochimica Cosmochimica Acta, v. 45, p. 2483–2499.

Cas, R.A.F., 1983, A review of the palaeogeographic and tectonic development of the Palaeozoic Lachlan fold belt of southeastern Australia: Geol. Soc. Australia Spec. Pub. 10, 104p.

Cathles, L.M., 1978, Hydrodynamic constraints on the formation of Kuroko deposits: Mining Geology, v. 28, p. 257–265.

Cathles, L.M., 1983, An analysis of the hydrothermal system responsible for massive sulfide deposition in the Hokuroko Basin of Japan, in Ohmoto, H. and Skinner, B.J. eds., Kuroko and Related Volcanogenic Massive Sulphide Deposits: Economic Geology, Monograph 5, p. 439–487.

Chappell, B.W., 1984, Source rocks of I- and S-type granites in the Lachlan Fold Belt, southeastern Australia: Philos. Trans. R. Soc. London, Ser. A, v. 310, p. 693–707.

Chappell, B.W. and White, A.J.R., 1974, Two contrasting granite types: Pacific Geology v. 8, p. 174–174.

Chappell, B.W. and Stephens, W.E., 1988, Origin of infracrustal (I-type) granite magmas: Trans. R. Soc. Edinburgh Earth Sci. v. 79, p. 71–86.

Chappell, B.W., White, A.J.R. and Hine, R., 1988, Granite provinces and basement terranes in the Lachlan Fold Belt, southeastern Australia: Aust. J. Earth Sci., v. 35, p. 505–521.

Collins, W.J. and Vernon, R.H., 1992, Palaeozoic arc growth, deformation and migration across the Lachlan Fold Belt, southeastern Australia: Tectonophysics v. 214, p. 318–400.

Coney, P.J., Edwards, A., Hine, R., Morrison, F. and Windrim, D., 1990, The regional tectonics of the Tasman orogenic system, eastern Australia: J. Structural Geology, v. 12, p. 519–543.

Cox, R., Ebsworth, G.B. and Forsythe, D.L., 1990, The Wilga base-precious metals deposit, Benambra, Victoria, Australia: Terra Nova, v. 2, p. 264–272.

Crawford, A.J., Cameron, W.E. and Keays, R.R., 1984, The association of boninite low-Ti andesite-tholeiite in the Heathcote Greenstone Belt, Victoria; ensimatic setting for the early Lachlan Fold Belt: Aust. J. Earth Sci. v. 31, p. 161–175.

Crook, K.A.W., Bein, J., Hughes, R.J. and Scott, P.A., 1973, Ordovician and Silurian history of the southeastern part of the Lachlan Geosyncline: J. Geol. Soc. Aust. v. 20, p. 113–138.

Davis, L.W., 1990, Silver-lead-zinc-copper mineralisation in the Captains Flat–Goulburn Synclinorial Zone and the Hill End Synclinorial Zone. In: Hughes, F.E. (ed.) Geology of the Mineral Deposits of Australia and New Guinea. The Australasian Institute of Mining and Metallurgy, Melbourne, p. 1375–1384.

Day, R.W., Murray, C.G. and Whitaker, W.G., 1978, The eastern part of the Tasman orogenic zone: Tectonophysics, v. 48, p327–364.

Degeling, P.R., Gilligan, L.B., Scheibner, E. and Suppel, D.W., 1986, Metallogeny and tectonic development of the Tasman Fold Belt System in New South

Wales: Ore Geology Reviews, v. 1, p. 259–313.

DePaolo, D.J., 1981, Trace element and isotopic effects of combined wallrock assimilation and fractional crystallization: Earth and Planetary Science Letters, v. 53, p. 189–202.

de Ronde, C.E.J, 1995, Fluid chemistry and isotopic characteristics of seafloor hydrothermal systems and associated VMS deposits: potential for magmatic contributions, In Thompson, J.F.H. (ed.) Magmas, Fluids, and Ore Deposits: Mineral. Soc. Assoc. Canada, Short Course Ser., v. 23, p. 479–509.

Ewart, A., 1982, The mineralogy and petrology of Tertiary-Recent orogenic volcanic rocks: with special reference to the andesite-basaltic composition range, In: Thorpe, R.S. (ed.) Andesites : Orogenic Andesites and Related Rocks, John Wiley and Sons, p. 25–95.

Farrell, C.W. and Holland, H.D., 1983, Strontium isotope geochemistry of the Kuroko deposits: Economic Geology, Monogr., 5, p. 302–319.

Fergusson, C.L. and Coney, P.J., 1992a Convergence of intraplate deformation in the Lachlan Fold Belt of southeastern Australia: Tectonophysics, v. 214, p. 417–439.

Fergusson, C.L. and Coney, P.J., 1992b, Implications of a Bengal Fan-type deposit in the Paleozoic Lachlan fold belt of southeastern Australia: Geology, v. 20, p. 1047–1049.

Fergusson, C.L. and Vandenberg, A.H.M., 1990, Middle Palaeozoic thrusting in the eastern Lachlan Fold Belt, southeastern Australia: J. Structural Geology, v. 12, p. 577–589.

Fergusson, C.L., Gray, D.R. and Cas, R.A.F., 1986, Overthrust terranes in the Lachlan fold belt, southeastern Australia: Geology v. 14, p. 519–522.

Fouquet, Y. et al., 1991, Hydrothermal activity and metallogenesis in the Lau back-arc basin: Nature, v. 349, p778–781.

Franklin, J.M., Sangster, D.F. and Lydon, J.W., 1981, Volcanic associated massive sulfide deposits: Economic Geology 75th Anniv. Vol., p. 485–627.

Gill, J.B., 1981, Orogenic Andesites and Plate Tectonics: Berlin, Springer-Verlag, 390p.

Gray, C.M., 1984, An isotopic mixing model for the origin of granitic rocks in southeastern Australia: Earth Planet. Sci. Lett., v. 70, p. 47–60.

Halbach, P., Nakamura, K., Wahsner, M., Lange, J., Sakai, H., Käselitz, L., Hanse, R.-D., Yamano, M., Post, J., Prause, B., Seifert, R., Michaelis, W., Teichmann, F., Kinoshita, M., Märten, A., Ishibashi, J., Czerwinski, S. and Blum, N., 1989, Probable modern analogue of Kuroko-type massive sulphide deposits in the Okinawa Trough back-arc basin: Nature, v. 338, p. 496–499.

Honma, H., Kusakabe, M., Kagami, H., Iizumi, S., Sakai, H., Kodama, Y. and Kimura, M., 1991, Major and trace element chemistry and D/H, $^{18}O/^{16}O$, $^{87}Sr/^{86}Sr$ and $^{143}Nd/^{144}Nd$ ratios of rocks from the spreading center of the Okinawa Trough, a marginal back-arc basin: Geochemical Journal, v. 25, p. 121–136.

Ishizuka, H., Kawanobe, Y. and Sakai, H., 1990, Petrology and geochemistry of volcanic rocks dredged from the Okinawa Trough, an active back-arc basin: Geochemical Journal, v. 24, p. 75–92.

Johnson, R.W., Mackenzie, D.E. and Smith, I.E.M., 1978, Delayed partial melting of subduction-modified mantle in Papua New Guinea: Tectonophysics v. 46, p. 197–216.

Jones, J.A., Carr, P.F., Fergusson, C.L. and McDougall, I., 1995, Silurian volcanism in the Wollondilly Basin, eastern Lachlan Fold Belt, New South Wales: Aust. J. Earth Sci., v. 42, p. 25–34.

Khin Zaw, Gemmell, J.B., Large, R.R., Mernagh, T. and Ryan, C.G., 1995, Microthermometry and geochemistry of fluid inclusions in the stringer zone, Hellyer VHMS deposit, Tasmania, Australia: Mineralium Deposita, in press.

Large, R.R., 1992, Australian volcanic-hosted massive sulfide deposits: features, styles, and genetic models: Economic Geology v. 87, p. 471–810.

Letouzey, J. and Kimura, M., 1985, Okinawa Trough genesis: structure and evolution of a back-arc basin developed in a continent: Marine and Petroleum Geology, v. 2, p. 111–130.

Lydon, J.W., 1989, Volcanogenic massive sulphide deposits Part 2: genetic models, in, Roberts, R.G. and Sheahan, P.A. eds. Ore Deposit Models, Geoscience Canada, Reprint Series 3, p. 155–181.

MacLean, W.H. and Barrett, T.J., 1993, Lithogeochemical techniques using immobile elements: Journal of Geochemical Exploration, v. 48, p. 109–133.

Macquarie Oil NL, 1987, Quarterly report 30th September, 1987: Melbourne, Macquarie Oil NL, 7p.

McCulloch, M.T. and Chappell, B.W., 1982, Nd isotopic characteristics of S- and I-type granites: Earth Planet. Sci. Lett., v. 58, p. 51–64.

McCulloch, M.T. and Woodhead, J.D., 1993, Lead isotopic evidence for deep crustal-scale fluid transport during granite petrogenesis: Geochim. Comochim. Acta, v. 57, p. 659–674.

McKay, W.J. and Hazeldene, R.K., 1987, Woodlawn Zn-Pb-Cu sulfide deposit, New South Wales, Australia: an interpretation of ore formation from field observations and metal zoning: Economic Geology v. 82, p. 141–164.

Miller, C.F. and Mittlefehldt, D.W., 1982, Depletion of light rare earth elements in felsic magmas: Geology v. 10, p. 129–133.

Murray, C.G., 1986, Metallogeny and tectonic development of the Tasman fold belt system in Queensland: Ore Geology Reviews, v. 1, p. 315–400.

Norrish, K. and Chappell, B.W., 1977, X-ray fluorescence spectrometry: In: Zussman, J. (ed.) Physical Methods in Determinative Mineralogy (2nd ed). Academic Press, London, p. 201–272.

Ohmoto, H., Mizukami, M., Drummond, S.E., Eldridge, C.S., Pisutha-Arnond, V. and Lenagh, T.C., 1983, Chemical processes of kuroko formation: Econ. Geol. Monogr., v. 5, p. 570–604.

Owen, M and Wyborn, D., 1979, Geology and geochemistry of the Tantangara and Brindabella

1:100,000 sheet areas: Bur. Mineral. Res. Geol. Geophys. Bull. 204, 52p.

Peccirillo, A. and Taylor, S.R., 1976, Geochemistry of Eocene calcalkaline volcanic rocks from the Kastamonu area, northern Turkey: Contributions to Mineralogy and Petrology, v. 58, p. 63–81.

Petersen, M.D., Lambert, I.B. and Ayres, D.E., 1977, Results of analyses of country rocks around the Woodlawn copper-lead-zinc orebody, southeastern New South Wales: Technical Communication 63, Minerals Research Laboratories, CSIRO.

Powell, C. McA., 1984, Ordovician to earliest Silurian: marginal sea and island arc; Silurian to mid-Devonian dextral transtensional margin; Late Devonian and Early Carboniferous: continental magmatic arc along the eastern edge of the Lachlan Fold Belt, In: Veevers, J.J. (ed.) Phanerozoic Earth History of Australia. Oxford University Press, Oxford, p. 290–340.

Ramsay, W.R.H. and Vandenberg, A.H.M., 1986, Metallogeny and tectonic development of the Tasman Fold Belt system in Victoria: Ore Geology Reviews, v. 1, p. 213–257.

Rapp, P.R. and Watson, E.B., 1986, Monazite solubility and dissolution kinetics: implications for the Th and LREE chemistry of felsic magmas: Contributions to Mineralogy and Petrology v. 94, p. 304–316.

Robinson, P., Higgins, N.C. and Jenner, G.A., 1986, Determination of rare earth elements, yttrium and scandium in rocks by an ion-exchange–X-ray fluorescence technique: Chemical Geology, v. 55, p. 121–137.

Rudnick, R.L. and Goldstein, S.L., 1990, The Pb isotopic compositions of lower crustal xenoliths and the evolution of lower crustal Pb: Earth Planet. Sci. Lett. v. 98, p. 192–207.

Rudnick, R.L., McDonough, W.F., McCulloch, M.T. and Taylor, S.R., 1986, Lower crustal xenoliths from Queensland, Australia: evidence for deep crustal assimilation and fractionation of continental basalts: Geochim. Cosmochim. Acta v. 50, p. 1099–1115.

Sawkins, F.J. and Kowalik, J., 1981, The source of ore metals at Buchans: Magmatic versus leaching models: Geol. Assoc. Canada Spec. Pap., v. 22, p. 255–267.

Scheibner, E., 1974, A plate tectonic model of the Palaeozoic tectonic history of New South Wales: J. Geol. Soc. Aust., v. 20, p. 405–426.

Scheibner, E., 1987, Palaeozoic tectonic development of eastern Australia in relation to the Pacific region, *in* Monger, J.W.H. and Francheteau, J. eds., Circum-Pacific Orogenic Belts and the Evolution of the Pacific Ocean Basin: Am. Geophys. Union, Geodynamic Ser., v. 18, p. 133–165.

Sillitoe, R.H., 1982, Extensional habitats of rhyolite-hosted massive sulfide deposits: Geology v. 10, p. 403–407.

Solomon, M., 1976, "Volcanic" massive sulphide deposits and their host rocks - a review and an explanation, in, Wolf, K.A., ed., Handbook of stratbound and stratiform ore deposits, II. Regional studies and specific studies, Amsterdam, Elsevier, p. 21–50.

Spooner, E.T.C. and Fyfe, W.S., 1973, Sub-sea floor metamorphism, heat and mass transfer: Contrib. Mineral. Petrol., v. 42, p. 287–304.

Stanton, R.L., 1985, Stratiform ores and geological processes: Roy. Soc. N.S.W., v. 118, p. 77–100.

Stanton, R.L., 1990, Magmatic evolution and the ore type-lava affiliations of volcanic exhalative ores: Aust. Inst. Mining Metallurgy Monogr. v. 15, p. 101–107.

Stanton, R.L., 1994, Ore Elements in Arc Lavas, Clarendon Press, Oxford, 391p.

Stern, R.J., Lin, P-N., Morris, J.D., Jackson, M.C., Fryer, P., Bloomer, S.H. and Ito, E., 1990, Enriched back-arc basin basalts from the northern Mariana Trough : implications for the magmatic evolution of back-arc basins: Earth and Planetary Science Letters, v. 100, p. 210–225.

Stolz, A.J., 1995, Geochemistry of the Mount Windsor Volcanics: Implications for the tectonic setting of Cambro-Ordovician volcanic-hosted massive sulfide mineralization in northeastern Australia: ECON. GEOL. in press.

Stolz, A.J., Davies, G.R., Crawford, A.J. and Smith, I.E.M., 1993, Sr, Nd and Pb isotopic compositions of calc-alkaline and peralkaline silicic volcanics from the D'Entrecasteaux Islands, Papua New Guinea, and their tectonic significance: Mineralogy and Petrology v. 47, p. 103–126.

Strens, M.R. and Cann, J.R., 1986, A fracture-loop thermal balance model of black smoker circulation: Tectonophysics, v. 122, p. 307–324.

Sun, S.-S. and McDonough, W.F., 1989, Chemical and isotopic systematics of oceanic basalts: implications for mantle composition and processes. In: Saunders, A.D. and Norry, M.J. (eds.) Magmatism in the Ocean Basins: Geological Society Special Publication No. 42, p. 313–345.

Sun, S.-S. and Wyborn, D., 1994, Source character and magmatic processes in some Au, Cu and Sn provinces: a trace element and isotope approach: Geol. Soc. Aust., Abstr., 12, p. 421.

Talent, J.A., Berry, W.B.N. and Boucot, A.J., 1975, Correlation of the Silurian rocks of Australia, New Zealand, and New Guinea: Geol. Soc. America Spec. Paper 150, 108 p.

Urabe, T., 1987, Kuroko deposit modeling based on magmatic hydrothermal theory: Mining Geology v. 37, p. 159-176.

Urabe, T. and Sato, T., 1978, Kuroko deposits of the Kosaka mine, northeast Honshu, Japan—products of submarine hot springs on the Miocene sea floor: Economic Geology v. 73, p. 161–179.

Vandenberg, A.H.M. and O'Shea, P.J., 1981, Explanatory notes on the Bairnsdale 1:250, 000 geological map: Victoria Geol. Survey, rept. 65, 61 p.

Vandenberg, A.H.M., Bolger, P.F. and O'Shea, P.J., 1984, Geology and mineral exploration of the Limestone Creek area, northeast Victoria: Victoria Geol. Survey, rept. 72, 59 p.

Volpe, A.M., Macdougall, J.D. and Hawkins, J.W., 1988, Lau Basin basalts (LBB): trace element and Sr-Nd isotopic evidence for heterogeneity in back-arc basin mantle: Earth and Planetary Science Letters, v. 90, p. 174–186.

Wark, D.A. and Miller, C.F., 1993, Accessory mineral behaviour during differentiation of a granite suite: monazite, xenotime and zircon in the Sweetwater Wash Pluton, southeastern California, U.S.A.: Chem. Geol. v. 110, p. 49–67.

White, A.J.R. and Chappell, B.W., 1988, Some supracrustal (S-type) granites of the Lachlan Fold Belt: Trans. R. Soc. Edinburgh Earth Sci. v. 79, p. 169–181.

White, A.J.R., Williams, I.S. and Chappell, B.W., 1976, The Jindabyne thrust and its tectonic, physiographic and petrogenetic significance: J. Geol. Soc. Aust. v. 23, p. 105–112.

Whitford, D.J., McPherson, W.P.A. and Wallace, D.B., 1989. Geochemistry of the host rocks to the volcanogenic massive sulfide deposit at Que River, Tasmania: Economic Geology, v. 84, p. 1–21.

Wilson, M., 1989, Igneous Petrogenesis: London, Unwin-Hyman, 466p.

Winchester, J.A. and Floyd, P.A., 1977, Geochemical discrimination of different magma series and their differentiation products using immobile elements. Chemical Geology, v. 20, p. 325–344.

Wyborn, D., 1992, The tectonic significance of Ordovician magmatism in the eastern Lachlan Fold Belt: Tectonophysics, v. 214, p. 177–192.

Geochemistry of the Mt Windsor Volcanics : implications for the tectonic setting of Cambro–Ordovician VHMS mineralisation in northeastern Australia.

A.J. Stolz

(submitted for publication in *Economic Geology*)

Abstract

The Mt Windsor Subprovince is an important relic of Upper Cambrian to Lower Ordovician sedimentation and volcanism in the northern part of the Tasman Orogenic Zone. Volcanic-hosted massive sulfide mineralisation occurs at several stratigraphic horizons within the volcano-sedimentary package and one major mine is operational within the belt. Major and trace element data and Nd isotope ratios are presented for the least altered coherent units from the three major volcanic-bearing formations in the Mt Windsor Subprovince. The data are used to discriminate four major phases of volcanism and related intrusive activity derived from three isotopically discrete sources, and to assess the geodynamic setting in which the volcanism occurred.

The earliest phase of mafic volcanism has minor and trace element characteristics suggesting an alkaline intraplate or rift association, and was probably produced by partial melting of attenuated subcontinental lithospheric mantle. The overlying Mt Windsor Formation silicic volcanics have Nd isotope characteristics (εNd (480Ma) = –4.7 to –12.8) which suggest they were produced by partial melting of underlying Precambrian crustal rocks. Mafic volcanics of the overlying Trooper Creek Formation include a low-TiO_2 suite and a high-TiO_2 suite with a range of distinguishing chemical characteristics, but similar Nd isotopic ratios (εNd (480Ma) = +3.8 to +2.3) which indicate derivation from relatively depleted asthenospheric mantle variably modified by subduction processes. The high-TiO_2 suite is also represented by abundant intrusives within the underlying volcanic package. The more silicic volcanics in the Trooper Creek Formation appear to be cogenetic with their mafic associates, but have varying Nd isotope ratios which suggest progressive crustal interaction with increasing SiO_2 content.

Comparisons with modern volcanic compositions and ore depositional environments suggest that the volcanic and sedimentary units within the Mt Windsor Subprovince were deposited in a back-arc basin developed by extension of continental lithosphere along the eastern Australian margin in the late Cambrian and early Ordovician. Mineralisation and volcanic deposits of similar age further north in the Tasman Orogenic Zone suggest that this basin may have had a north–south orientation, although there is no clear evidence remaining of the original arc front deposits.

Introduction

The Mt Windsor Subprovince is an important relic of Upper Cambrian to Lower Ordovician volcanism and sedimentation in the northern section of the Tasman Orogenic Zone (Fig. 1). It is host to one significant massive sulfide deposit (Thalanga) as well as a number of smaller deposits, and has substantial exploration potential for this style of deposit (Berry et al., 1992). Lithogeochemical studies of ancient volcanic belts are largely under-utilised during exploration for volcanic-hosted massive sulphide (VHMS) deposits. However, when integrated with basic geological mapping and an appreciation of the

Centre for Ore Deposit and Exploration Studies, University of Tasmania, G.P.O. Box 252C, Hobart, Tasmania 7001, Australia.

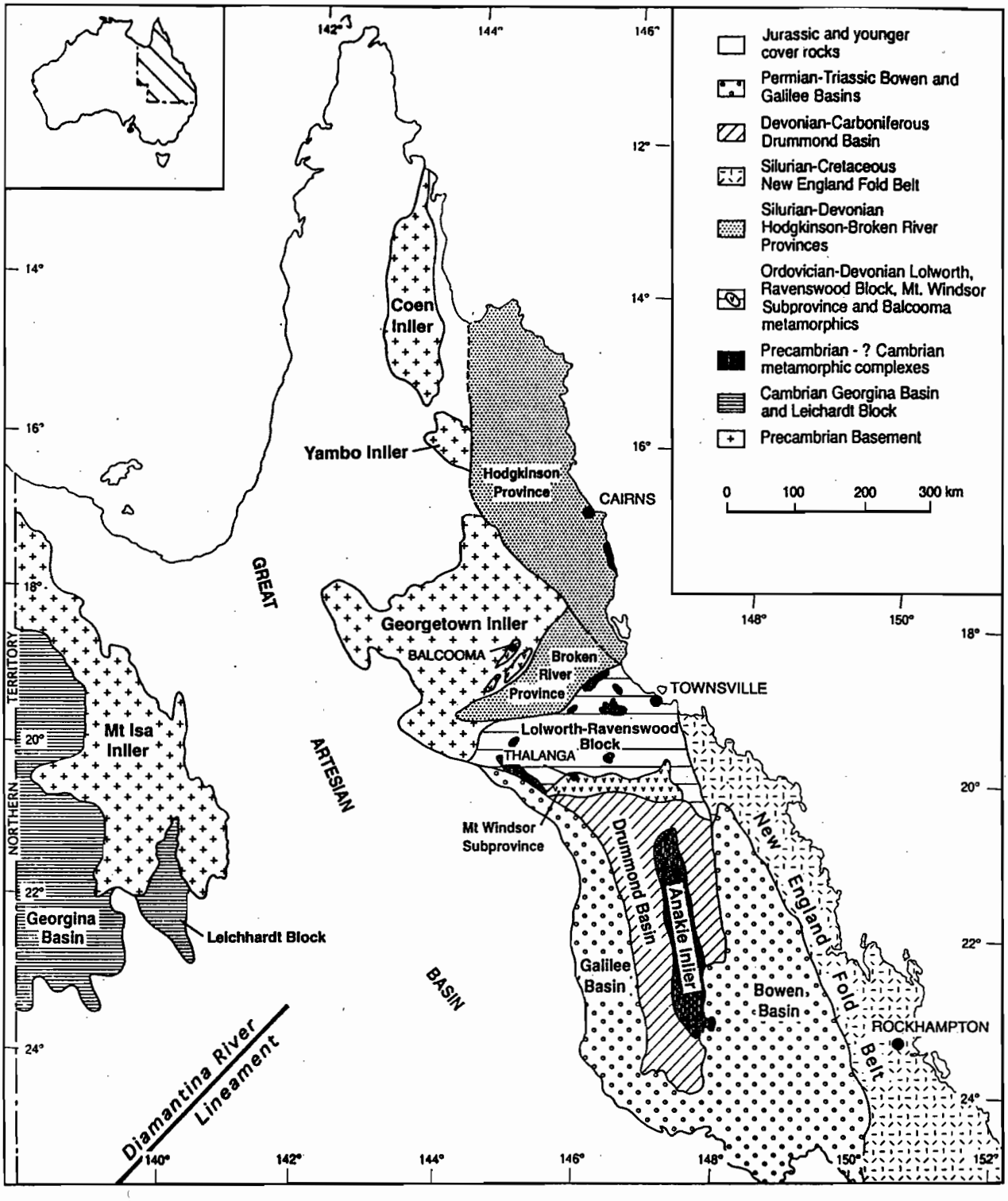

Fig. 1. Simplified geological map of northern Queensland showing the distribution of Precambrian basement rocks and major Cambrian to Devonian structural blocks in the region.

volcanic facies architecture, the geochemical data can be used to facilitate stratigraphic correlations as well as provide basic information about precursor lithologies where secondary mineral assemblages predominate. The geochemistry of the least altered mafic volcanic units in such sequences can also provide useful information about the geodynamic setting at the time of deposition and the tectonic evolution of the belt.

When coupled with our rapidly advancing knowledge of the depositional environment and tectonic setting of modern exhalative seafloor massive sulfide deposits, the geochemical data for ancient sequences comprise an important aid in the selection of regional exploration targets. This study builds on earlier studies of the geology, structure and mineralisation of the Mt Windsor Subprovince (Henderson, 1986; Berry et al., 1992; Duhig et al., 1992) and aims to use geochemical and Nd isotopic data for the volcanics to help clarify stratigraphic relationships, and to assess the likely tectonic setting of the volcanism at the time of mineralisation.

Regional Setting and Geology of the Mt Windsor Subprovince

The Mt Windsor Subprovince is part of the early Palaeozoic Lolworth–Ravenswood Block (Fig. 1). It comprises a linear belt of volcano-sedimentary units which principally occur as a subvertical, south-facing limb of an east–west trending fold (Berry et al., 1992). The volcano-sedimentary belt outcrops discontinuously over a distance of about 160 km and has been extensively intruded along its northern margin by Ordovician–Devonian granitoids of the Lolworth–Ravenswood batholith (Richards, 1980).

The Lolworth–Ravenswood Block is separated from the Ordovician Broken River Province to the north by the Clarke River Fault (Fig. 1; Day et al., 1978; Murray, 1986), and is covered to the south by Devonian to Carboniferous rocks of the Drummond Basin, and various alluvial and ferricrete deposits of Tertiary age. The Balcooma metamorphic belt which occurs about 250 km to the north of the Mt Windsor belt also hosts several small massive sulfide deposits (Huston et al., 1992) and has been correlated with the Mt Windsor Subprovince despite substantially higher grade (amphibolite facies) metamorphism in the former (Henderson, 1986; Withnall et al., 1991).

There are four major stratigraphic subdivisions in the Mt Windsor Subprovince (Fig. 1; Henderson, 1986; Berry et al., 1992). The Puddler Creek Formation (PCF), which is the oldest exposed part of the sequence, comprises a thick sedimentary package of mixed continental and volcanic provenance, and a small volume of basaltic to intermediate volcanics which occur predominantly in upper two hundred meters of the package. Mafic sills and dykes comprise a volumetrically important part of the PCF (10–15%), and silicic dykes are also locally abundant in the upper part of the sequence. The base of the PCF is nowhere exposed due to the extensive granitoid intrusives.

The overlying and broadly conformable Mt Windsor Formation (MWF) is composed of a thick sequence of rhyolitic volcanics and associated volcaniclastic rocks. These are occasionally intruded by mafic sills and dykes similar to those which are abundant in the PCF. The transition to the conformably overlying Trooper Creek Formation (TCF) is delineated by the first appearance of dacitic or andesitic volcanics which typically occur as thin flows and display relatively rapid facies variations with associated volcaniclastic units. The Rollston Range Formation (RRF) represents the youngest part of the sequence and is composed almost exclusively of volcanic-derived sedimentary rocks.

The age of the volcanics within the TCF is reasonably well constrained by fossiliferous units within the TCF and RRF which indicate a Lower Ordovician age for those formations (Henderson, 1983). The conformably underlying MWF and PCF have been interpreted as Upper Cambrian by Henderson (1986), although both formations are devoid of fossils, and they could be of similar age to the TCF rocks if they were deposited in a rapidly subsiding basin.

These volcanic and sedimentary units have experienced low to moderate grade regional metamorphism. Metamorphic grades range from prehnite–pumpellyite facies in the eastern part of the belt to greenschist facies in the central part of the belt (Berry et al., 1992). Further west, close to the Thalanga mine (Fig. 2), the regional metamorphism has been substantially overprinted by contact metamorphic

effects of the nearby Devonian granitoids resulting in hornblende hornfels assemblages. The metamorphic grades are amphibolite facies at Waddy's Mill (Fig. 2) and are characterised by higher strain, possibly resulting from recrystallisation in response to simultaneous regional deformation and granitoid emplacement.

Sampling and Analytical Techniques

The analytical data in this paper relates to a suite of the least altered, coherent volcanic and intrusive units selected from approximately four hundred samples collected along ten detailed traverses across the belt from Waddy's Mill in the west to Sunrise Spur in the east (Fig. 2). Outcrop samples were supplemented by drillcore material in the vicinity of the major prospects or mines, particularly Thalanga and Waterloo. Samples were crushed initially in a jaw crusher, and a hand-picked sub-sample of chips free of vein material and vesicles was powdered in a tungsten carbide disc mill. Major and trace elements were determined on a Philips automated XRF spectrometer at the University of Tasmania using standard fused bead and pressed pellet techniques (Norrish and Chappell, 1977). Concentrations of Th and Nb in some of the basaltic rocks are close to or below the detection limits (2 and 1ppm, respectively), and although relatively imprecise at these levels, they provide an indication of the abundances for comparison with less depleted rocks. Rare earth elements were determined by an ion-exchange XRF technique at the University of Tasmania (Robinson et al., 1986). Precision of the REE analyses is typically in the range 1–4%, and usually 1–2% for Sm and Nd (Robinson et al., 1986). Accuracy of the REE analyses was monitored by concurrent analysis of standard rocks. Nd isotope ratios were measured on a Finigan MAT261 TIMS operated in peak switching mode at the Geology Department, Adelaide University, following chemical separation in the Geology Department, University of Tasmania. Sample powders (~0.1 g) were dissolved in a mixture of 8M HNO_3 and 40% HF in a screw-top teflon beaker at 80°C for 36hrs. Nd was separated in a three-column procedure. This involved initial separation of the REE on ion-exchange columns eluting with 2.5M HCl and collecting the REE fraction with 6M HCl. This was followed by separation of Ba from the REE on a smaller set of columns; eluting with 1.5M HNO_3 and collecting the REE with 8M HNO_3. Final separation of Nd from the other REE was achieved using PTFE columns and eluting with 0.25M HCl. The routine total blank was about 0.2 ng, hence no blank corrections are necessary.

Constraints on the Data

Variable mobility of the chemical components of ancient volcanics during hydrothermal alteration and low grade regional metamorphism is now a well known and documented phenomenon (e.g. Wood et al., 1976; MacLean and Kranidiotis, 1987; Gemmell and Large, 1992). Samples with obvious evidence of hydrothermal alteration and rocks with excessively high loss on ignition values were avoided for this study, but all volcanics in the belt have experienced regional metamorphism at prehnite–pumpellyite or greenschist facies conditions. Under these conditions the least mobile elements are likely to be the high field strength elements (HFSE) such as Ti, Zr, Nb, and the rare earth elements (Whitford et al., 1989). A number of other minor and trace elements (including P, Sc, V, Cr, Ni and Th) probably also have concentrations which closely approximate their original values. However, the measured concentrations of the large-ion lithophile elements (LILE) such as K, Rb, Ba and also Sr are not likely to provide reliable estimates of pre-eruptive magmatic abundances. Rocks subjected to intense hydrothermal alteration may display substantial mobility of the LREE and most other elements (Campbell et al., 1984), although Zr, Ti, Al and the HREE appear to remain essentially immobile (MacLean and Barrett, 1993).

There are numerous tests for element immobilty based on coherence of inter-element correlations (e.g. Zr vs Nb; cf. Whitford et al., 1989; MacLean and Barrett, 1993). However, these are only useful for individual suites of rocks. If several discrete suites are represented, a spread in the data may be a primary feature rather than a result of differential element mobilisation during metamorphism or hydrothermal alteration. In general, there is a strong negative correlation between Ti/Zr values and SiO_2 contents of the Mt Windsor volcanics (Berry et al., 1992) indicating that silica mobility has been quite limited

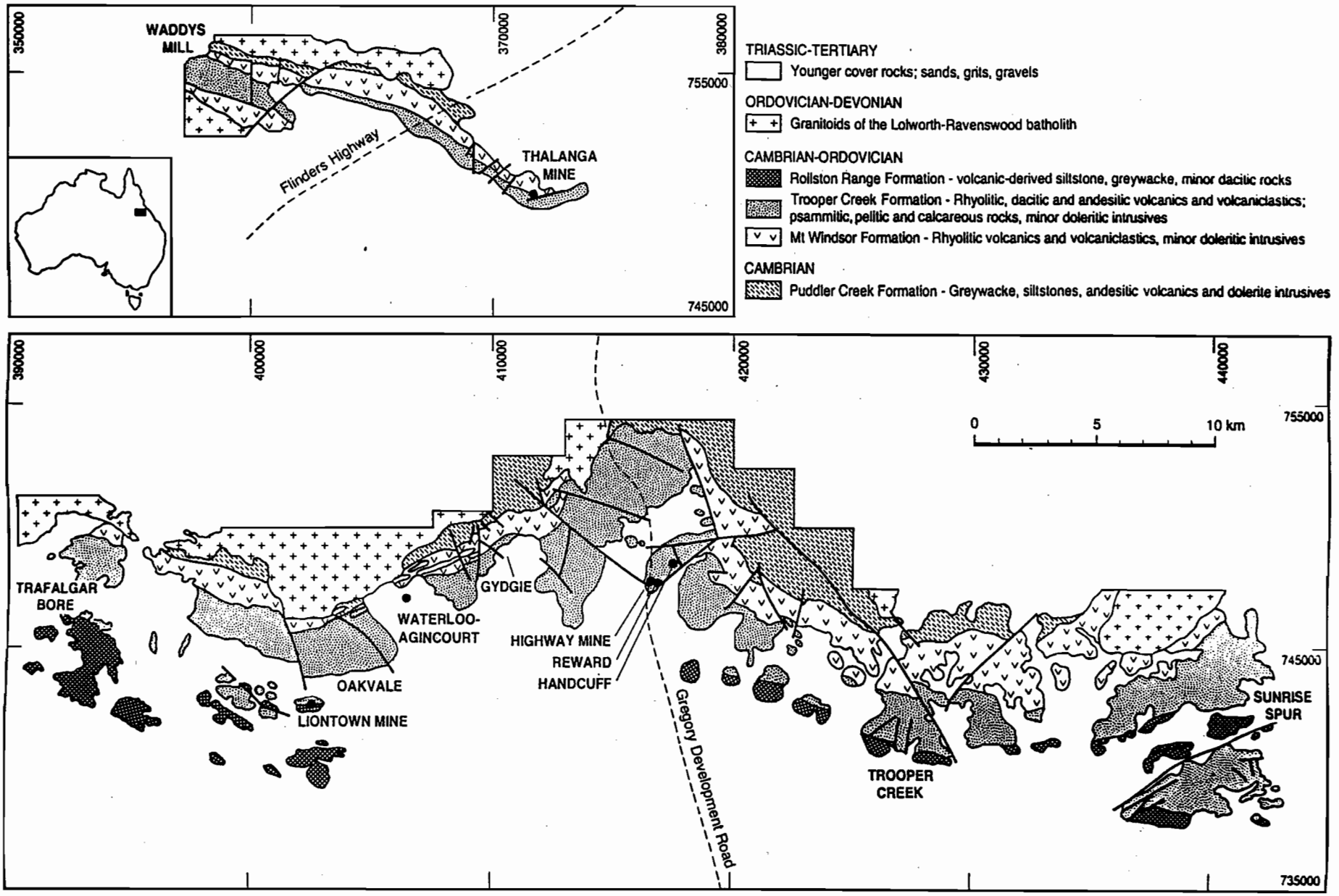

Fig. 2. Geological map of the Mt Windsor Subprovince between Waddy's Mill and Sunrise Spur showing the distribution of the principal units and younger granitoid intrusives.

during the metamorphism. The rocks have therefore been classified primarily on the basis of their silica contents (e.g. Peccirillo and Taylor, 1976; Gill, 1981), although the Ti/Zr (Berry et al., 1992) and Zr/TiO_2 values (Fig. 3) result in comparable classification.

Chemistry

The chemical data for the volcanics and dykes (Tables 1 to 3) are presented according to their stratigraphic designation based on mapping and the lithological constraints discussed above. The major element analyses have been recalculated to 100% anhydrous to remove variations due to different loss on ignition values. From a total data set of about 180 whole-rock analyses four discrete suites can be distinguished in the Mt Windsor Volcanic belt that can be related to stratigraphic position and timing of emplacement.

Puddler Creek Formation Volcanics

Volcanics from the upper part of the PCF range from basaltic andesite to dacite in composition based on their silica concentrations and Ti/Zr values. The mafic variants are characterised by moderate TiO_2 (>1.2 wt. %), high P_2O_5 (>0.60 wt. %), high concentrations of incompatible elements (e.g. Zr, Nb and Th), high Nb/Y, and low Zr/Nb values (Figs 3 to 6) typical of intraplate volcanics (e.g. Sun and McDonough, 1989). In addition, they are characterised by relatively low MgO (< 5wt. %), Cr and Ni contents, and low Ti/Zr values (Figs 5, 7), suggesting they are moderately fractionated. The PCF volcanics also have high LREE concentrations (La 300 X chondrite) and are strongly enriched in LREE relative to the HREE (La/Yb ~ 17) in chondrite-normalised REE diagrams (Fig. 8), with only minor evidence of relative Eu depletion in the more evolved samples. The strong enrichment in incompatible elements in these rocks (e.g. Zr, Nb, Th, P and LREE) coupled with low Zr/Nb (4.4–6.7), La/Nb (0.9–1.7), and high Nb/Y values suggests they represent an alkaline intraplate association. They would therefore be more accurately termed trachy-andesites and trachytes, despite their low alkali contents which are probably due to post-depositional alteration processes. Alkaline volcanics from convergent margin settings may also be strongly enriched in incompatible elements, but they are characterised by substantially higher Zr/Nb (typically > 15) and La/Nb (typically > 5–8), and lower Nb/Y values reflecting their generation in a subduction setting (Foley et al., 1987; Stolz et al., 1990).

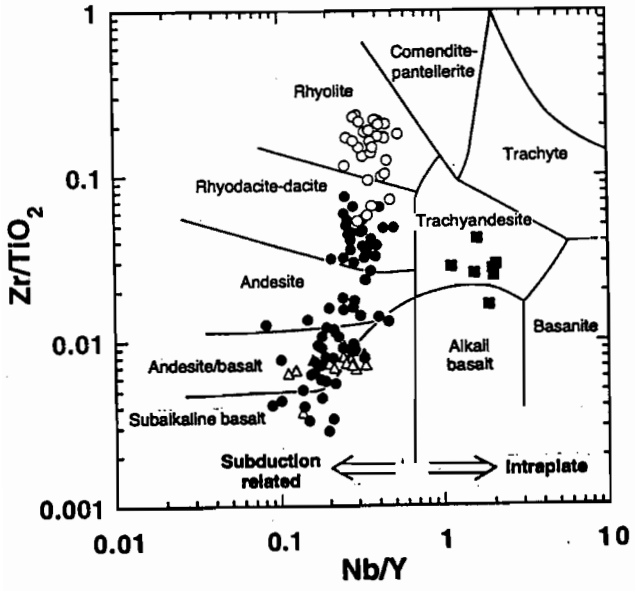

Fig. 3. Plot of Nb/Y versus Zr/TiO_2 (after Winchester and Floyd, 1977) for the Mt Windsor volcanics (symbols as for Fig. 4).

Trooper Creek Formation Volcanics

In contrast, most basaltic to andesitic volcanics within the TCF have a clear subduction-related geochemical signature with low TiO_2 (<1 wt. %; Fig. 4), low incompatible element concentrations (including P, Zr, Nb and Th), high Zr/Nb (~14; Fig. 6) and La/Nb, and low Nb/Y values (Fig. 3) compared with volcanics from divergent margin or intraplate settings. This results in the characteristic negative Nb anomaly displayed by subduction-related volcanics in mantle- or MORB (mid-ocean ridge basalt)-normalised multi-element plots. The most mafic rocks extend to relatively high MgO contents (up to 10 wt. %) with correspondingly high Cr, and to a lesser extent, Ni concentrations (Fig. 7). The TCF basaltic rocks have low total REE contents (La 10–30 X chondrite) and they are characterised by straight, slightly LREE-enriched patterns (Fig. 9). The andesitic rocks generally have subparallel patterns with slightly higher total REE concentrations.

The more silicic rocks of the TCF are predominantly dacites and high-silica dacites. The latter are distinguished as having greater than 70 wt. %

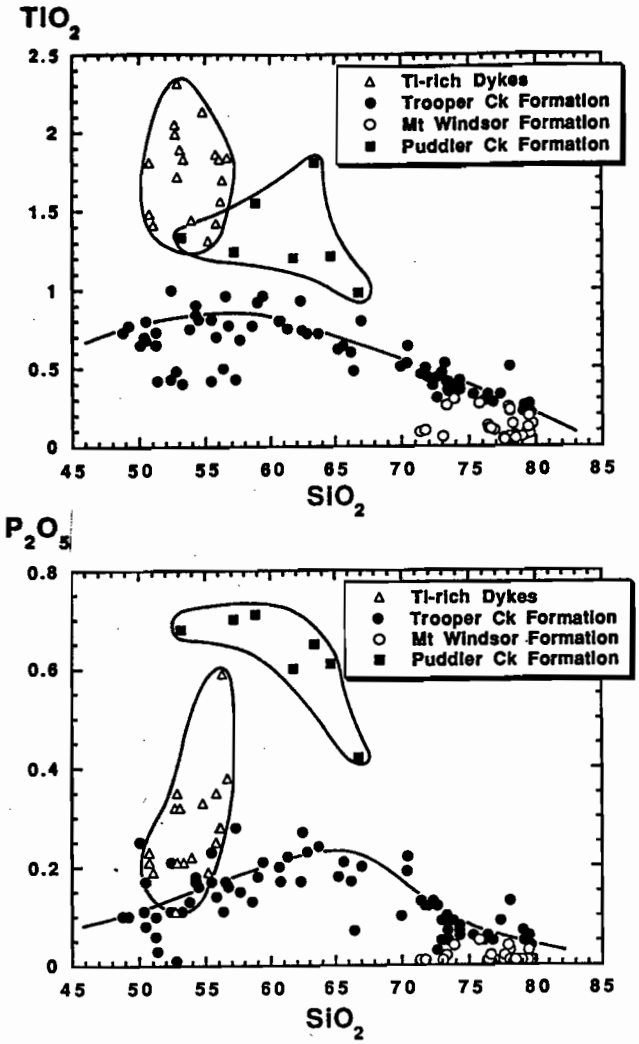

Fig. 4. Plots of SiO_2 versus (a) TiO_2 and (b) P_2O_5 for the Mt Windsor volcanics showing the four major suites.

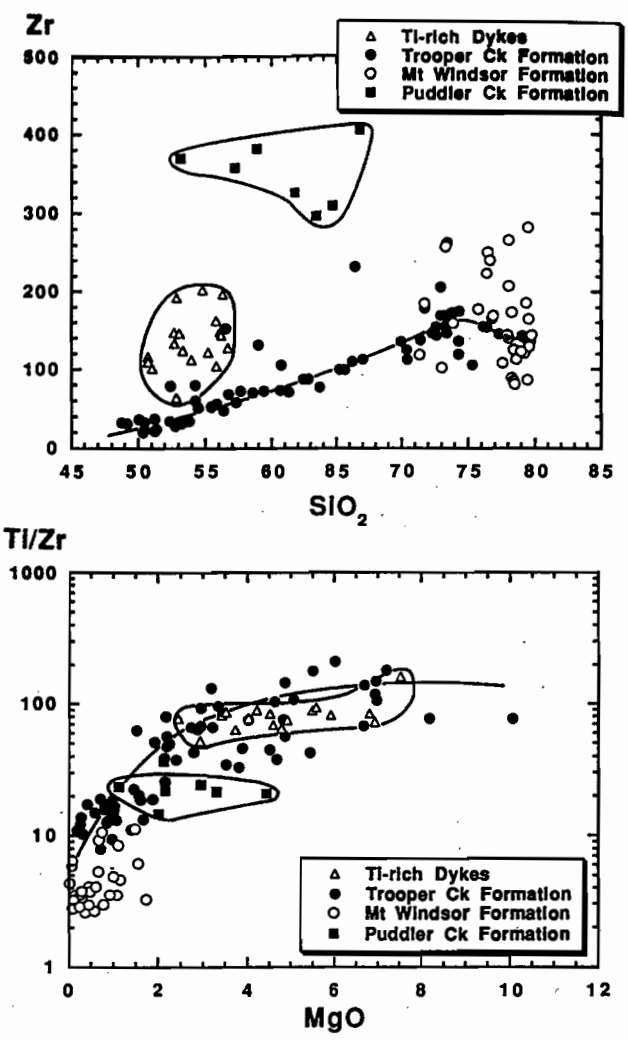

Fig. 5. Plots of a) SiO_2 versus Zr and b) MgO versus Ti/Zr for the Mt Windsor volcanics.

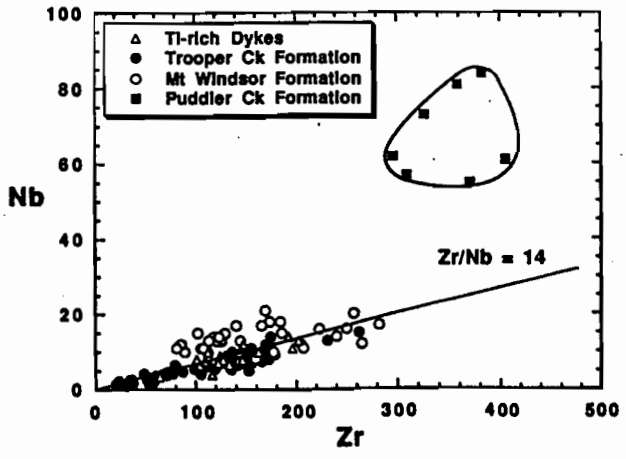

Fig. 6. Plot of Zr versus Nb for the Mt Windsor volcanics showing the different Zr/Nb values for the PCF andesites compared with the other suites.

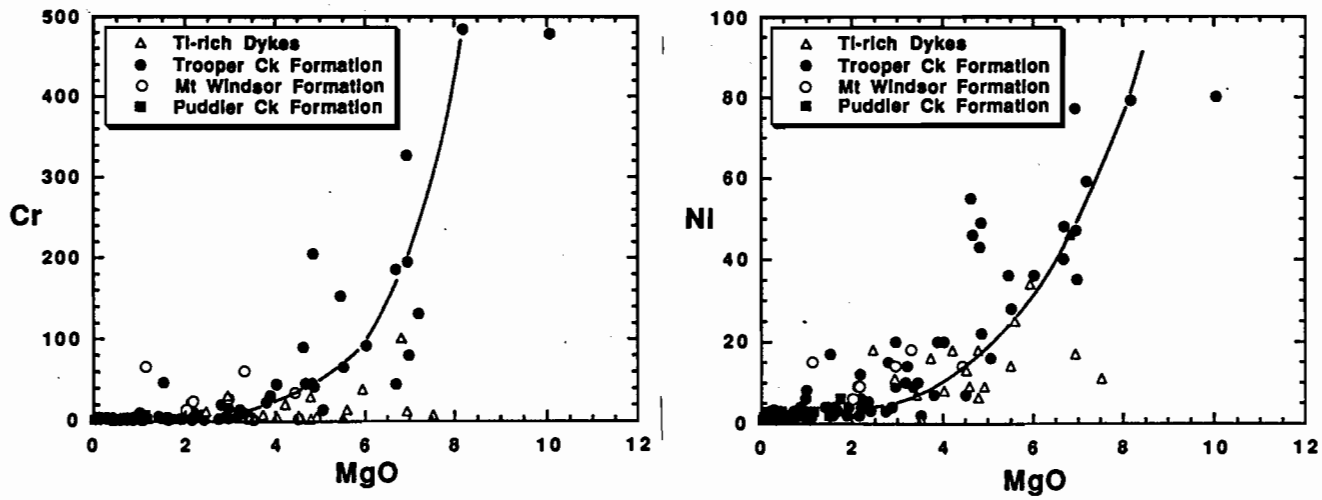

Fig. 7. Plots of MgO versus (a) Cr and (b) Ni for the Mt Windsor volcanics.

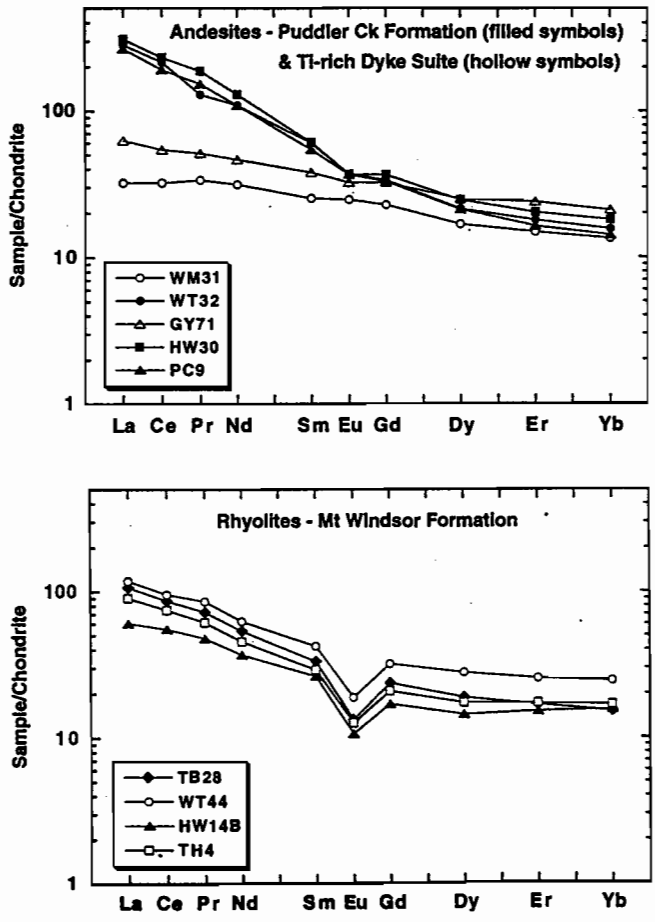

Fig. 8. Chondrite normalised REE plots for (a) PCF andesites and the TCF Ti-rich dyke suite, and (b) rhyolitic volcanics from the MWF.

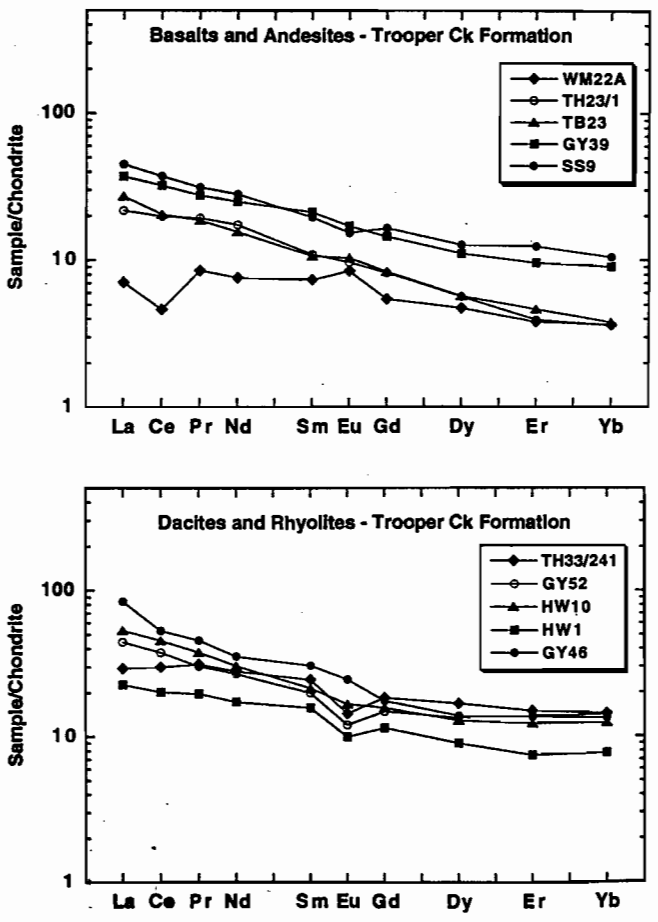

Fig. 9. Chondrite normalised REE plots for (a) basalts and andesites from the TCF, and (b) dacites and rhyolites from the TCF.

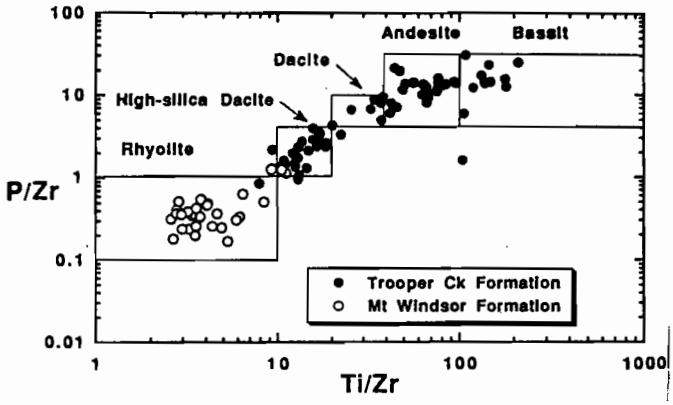

Fig. 10. Plot of Ti/Zr versus P/Zr used to discriminate MWF silicic rocks from TCF volcanics.

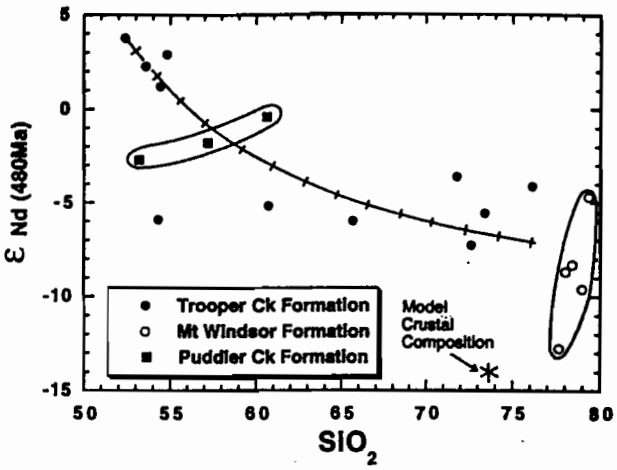

Fig. 13. Plot of $\varepsilon_{Nd\ (480Ma)}$ versus SiO_2 for volcanics from the three major volcanic-bearing formations within the Mt Windsor Subprovince. A calculated AFC (assimilation fractional crystallisation) trend is shown for comparison with the TCF volcanics (see text for details).

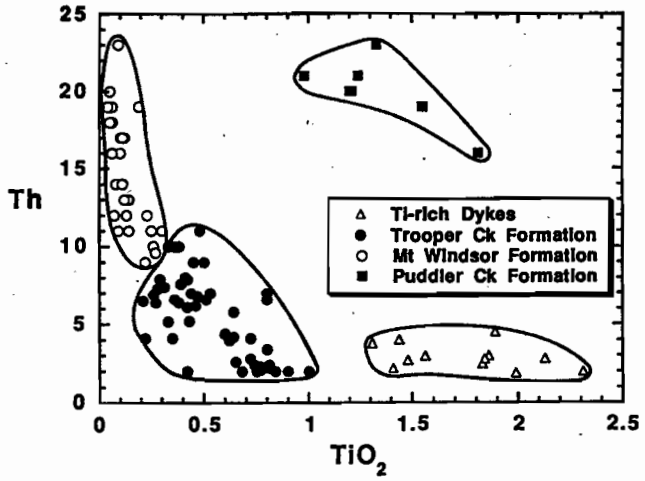

Fig. 11. Plot of TiO_2 versus Th for the Mt Windsor volcanics which most effectively discriminates the four major suites.

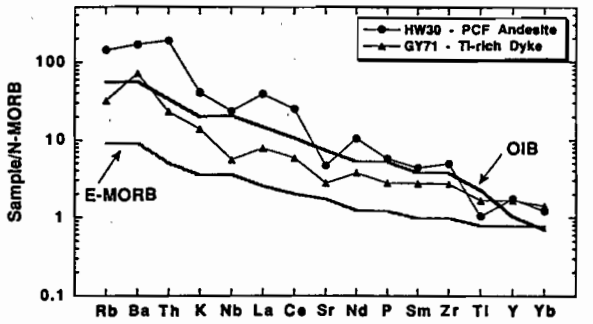

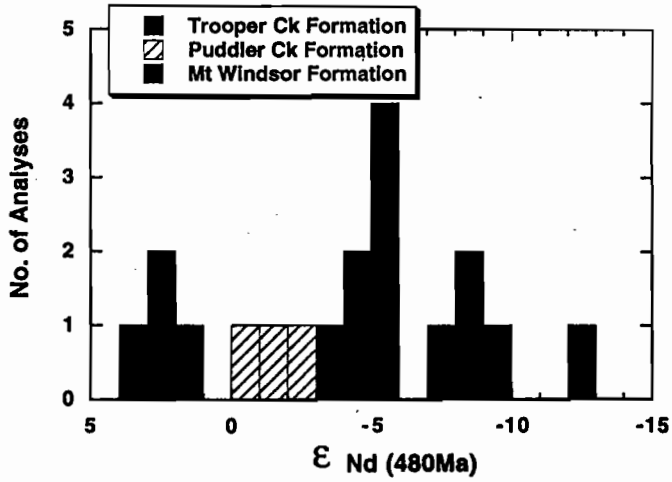

Fig. 12. Histogram showing the ranges of $\varepsilon_{Nd\ (480Ma)}$ values in PCF, MWF and TCF volcanics.

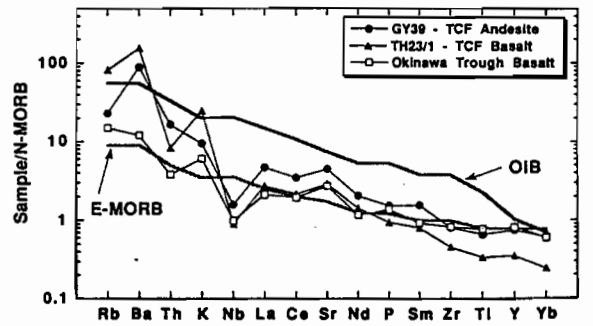

Fig. 14. N-MORB-normalised multi-element plots comparing typical E-MORB and OIB compositions with: a) mafic representatives of the PCF and Ti-rich TCF suite, and b) low-Ti TCF mafic volcanics, and a young back-arc basalt from the Okinawa Trough.

SiO_2, but with consistently higher Ti/Zr values than the clearly rhyolitic rocks of the MWF (Fig. 10). These high-silica dacites generally contain plagioclase phenocrysts and less than 1 modal percent quartz phenocrysts, in contrast to the rhyolitic rocks in which quartz is generally the dominant phenocryst phase. They are also characterised by high Na_2O/K_2O values, which despite the likelihood of some alkali mobilisation during metamorphism, may broadly reflect the original values. REE abundances in the TCF silicic rocks are generally higher than in associated andesites (although exceptions include HW1, Fig. 9), and the patterns are essentially parallel except for the presence of small negative Eu anomalies in a few samples.

A feature of the volcanics in the TCF is the continuous and coherent nature of the geochemical variation from basalt to high-silica dacite. This is best illustrated in plots of SiO_2 vs TiO_2, P_2O_5 and Zr (Figs 4, 5), although the SiO_2–TiO_2 variation suggests the possibility of a separate very low TiO_2 (~0.5 wt. %) basalt–andesite group which is distinct from the main basalt–andesite suite. Overall these coherent chemical variations appear to be consistent with the TCF lavas being a cogenetic suite related by low pressure fractional crystallisation.

The systematic decreases in MgO, Cr, and CaO with increasing SiO_2 content are consistent with fractionation of olivine + clinopyroxene or amphibole and plagioclase. In contrast, TiO_2 is relatively constant over the silica range 50–60 wt.% and only decreases to very low levels at higher silica contents. This suggests fractionation of a Ti-bearing accessory phase such as magnetite became more important in the more silicic compositions reflecting the diminishing solubility of Ti with increasing SiO_2 (Ryerson and Watson, 1987). P_2O_5 increases systematically with SiO_2 to a maximium of ~0.25 wt.% at 62% SiO_2, and decreases quite rapidly following apatite saturation to very low concentrations (<0.05 wt.%) in the high-silica dacites. Evidence for the fractionating phases, apart from plagioclase, has generally been obscured by the effects of subsequent metamorphism.

Mt Windsor Formation Volcanics

The MWF volcanics span a relatively narrow silica range (71–79 wt. %) and are characterised by very low P_2O_5 and low TiO_2 (Fig. 4), CaO and MgO. They display a broad range in Na_2O and K_2O values with widely varying Na_2O/K_2O values. This suggests some samples have had their alkali contents significantly modified, possibly due to exchange with seawater immediately following eruption. The MWF rhyolites are characterised by LREE-enriched patterns with distinct negative Eu anomalies (Fig. 8), and their total REE concentrations are generally higher than rocks of equivalent silica content from the TCF.

The silicic rocks of the MWF are most readily discriminated from the siliceous TCF rocks by their lower Ti/Zr and P/Zr values (Fig. 10), and generally higher Th and lower TiO_2 in a plot of TiO_2 vs Th (Fig. 11). Indeed the latter plot is probably the most effective in discriminating all the major volcanic types of the Mt Windsor Subprovince. The MWF rhyolites also typically have higher total REE and more pronounced negative Eu anomalies that are rare or only weakly developed in the TCF dacites.

Ti-rich Dykes and Volcanics

The mafic dykes that are abundant in the PCF also occur within the MWF and TCF, but not the RRF. In the TCF, this magmatic event appears to be represented by both minor intrusives and highly vesicular extrusives with very similar chemistry. These rocks have SiO_2 contents in the range 50.8 to 58.6 wt. %, and are characterised by moderate to high TiO_2 (1.4–2.3 wt. %), coupled with low to moderate P_2O_5 (0.19–0.35 wt. %; Fig. 4). Their high Ti contents clearly distinguish them from the main low-Ti TCF suite, and their lower P_2O_5, Zr, Nb and Th (Figs 4, 5, 6, 11), and higher Zr/Nb distinguish them from the PCF volcanics.

The Ti-rich dykes and volcanics have similar or slightly higher LREE concentrations (La 30–60 X chondrite) to the TCF andesitic rocks, but they have significantly higher HREE contents resulting in somewhat flatter, only slightly LREE-enriched patterns (Fig. 8) with no relative depletion of Eu.

Nd Isotopes

Nd isotope analyses were undertaken of representative samples from the geochemically distinguishable groups with the aim of assessing possible source differences between the different volcanic suites. Nd isotopes are probably the most useful isotopic system for this purpose in ancient volcanics as the REE are

Table 1. Major and trace element analyses of volcanics from the Puddler Creek Formation, and Ti-rich dykes and associated volcanics

	Puddler Ck Formation Volcanics							Ti-rich Dykes and Volcanics								
	HW30	WT32	WT22	PC9	WT23	WT53	PC12	HW27	TC47	PC4	WT46	GY26	TB25	SS9	GY71	WM31
	Andesite	Andesite	Andesite	Andesite	Dacite	Dacite	Dacite	Basalt	Basalt	Basalt	Basalt	Andesite	Andesite	Andesite	Andesite	Andesite
SiO2	53.16	57.18	58.85	61.76	63.41	64.68	66.81	50.75	50.76	51.05	52.87	53.34	53.54	54.39	54.80	55.82
TiO2	1.33	1.24	1.55	1.20	1.81	1.21	0.98	1.81	1.48	1.41	2.31	1.63	1.78	1.20	2.13	1.42
Al2O3	17.95	19.91	18.60	16.80	15.37	16.68	14.80	14.01	15.34	15.77	14.91	14.55	14.81	16.07	14.29	15.12
Fe2O3#	8.97	7.22	8.71	8.42	8.16	5.82	6.96	14.31	12.12	11.89	13.72	13.82	12.66	10.69	13.72	10.91
MnO	0.20	0.03	0.12	0.12	0.23	0.12	0.12	0.22	0.23	0.20	0.34	0.24	0.18	0.16	0.19	0.18
MgO	3.31	4.44	2.96	2.17	2.13	1.13	2.02	5.59	5.93	6.82	6.94	5.50	2.82	5.27	3.73	3.42
CaO	7.81	1.04	1.27	3.17	2.51	1.40	2.57	9.57	9.88	8.35	4.01	6.98	9.03	8.88	5.39	7.07
Na2O	3.67	8.14	6.67	5.17	4.50	3.49	3.94	2.78	3.79	4.22	2.50	2.91	4.63	2.82	4.43	5.27
K2O	2.93	0.11	0.55	0.59	1.23	4.86	1.36	0.73	0.26	0.30	2.06	0.82	0.27	0.54	1.01	0.42
P2O5	0.68	0.70	0.71	0.60	0.65	0.61	0.42	0.23	0.21	0.19	0.35	0.21	0.28	0.19	0.33	0.35
Total *	100.00	100.00	100.00	100.00	100.00	100.00	100.00	100.00	100.00	100.00	100.00	100.00	100.00	100.00	100.00	100.00
LOI	7.86	2.79	2.69	2.95	3.33	1.25	2.40	4.51	1.01	3.40	8.87	8.10	0.81	2.28	4.97	0.39
Sc	25	13	19	13	21	18	13	41		41	37	39	35		34	
V	101	79	124	95	127	105	82	325	318	254	378	415	398	278	314	279
Cr	81	35	27	24	22	66	14	14	39	102	12	4	2	67	8	3
Ni	18	14	14	9	9	15	6	25	34	46	17	14	8	32	16	7
Cu	7	2	43	13	4	2	4	82	27	93	42	58		52	56	13
Zn	129	2	21	44	14	81	92	117	95	88	223	121		93	141	130
Pb	15	2	4	8	4	18	8	6	35	3	48	3	7	4	6	11
Rb	80	1	17	19	36	124	44	33	8	9	54	22	4	8	18	7
Sr	423	123	248	433	141	159	253	786	288	304	103	224	734	303	251	234
Y	49	39	42	37	33	37	38	36	30	29	43	31	54	27	47	33
Zr	370	358	382	326	296	309	405	116	109	101	192	124	132	104	202	104
Nb	55	81	84	73	62	57	61	4	8	8	14	9	9	8	13	7
Ba	1081	30	554	260	1377	1625	567	1178		209	807	1024	388		453	
Th	23	21	19	20	16	20	21	<2	3	2	2	<2	4	3	3	<2
Ti/Zr	21.8	20.8	24.3	22.1	36.7	23.4	14.5	93.5	81.4	83.7	72.2	88.5	80.7	89.4	63.2	82.0
Zr/Nb	6.7	4.4	4.5	4.5	4.8	5.4	6.6	29.0	14.3	12.8	13.7	13.8	14.7	13.0	15.5	14.9
Zr/Y	7.8	9.2	9.1	8.8	9.0	8.4	10.7	3.2	3.6	3.5	4.5	4.0	2.4	3.9	4.3	3.2
Nb/Y	1.12	2.08	2.00	1.97	1.88	1.54	1.61	0.11	0.25	0.28	0.33	0.29	0.17	0.30	0.28	0.21
La	97.1	74.8	76	63.2	55	74	65	5	11	10	19	11	18.2	14.2	19.7	10.2
Ce	188	135	146	155	111	140	129	20	23	19	41	24	37.9	30.4	44.2	26.3
Pr	21.5	15.2		17.6									5.75	3.6	5.9	3.87
Nd	77.3	55	60	65.1	47	54	54	13	16	10	20	15	25.4	18.8	27.7	18.7
Sm	11.7	9.73		10.45									6.71	3.77	7.3	4.87
Eu	2.66	2.42		2.65									2.67	1.11	2.34	1.79
Gd	9.45	7.81		8.5									8.49	4.27	8.35	5.91
Dy	8.02	8.38		6.88									8.33	4.12	8.14	5.45
Er	4.29	4.27		3.46									4.95	2.63	5.07	3.16
Yb	3.74	3.89		2.94									4.11	2.18	4.36	2.8
(La/Yb)N	17.1	13.4		18.7									2.9	4.3	3.0	2.4

Total Fe as Fe2O3; * Analyses recalculated to 100% anhydrous

Table 2. Major and trace element analyses of volcanics from the Mt Windsor Formation.

	TH5 Rhyolite	TH2 Rhyolite	TH26/304 Rhyolite	TH4 Rhyolite	TB26 Rhyolite	TB19 Rhyolite	TB31 Rhyolite	WT44 Rhyolite	WT27 Rhyolite	HW14B Rhyolite	HW35 Rhyolite	HW12 Rhyolite	TC25 Rhyolite	TC28 Rhyolite	SS17 Rhyolite
SiO2	76.39	78.26	79.21	79.33	77.44	76.58	78.71	76.02	79.44	77.59	77.66	78.06	76.64	78.96	78.40
TiO2	0.13	0.06	0.07	0.09	0.09	0.17	0.10	0.06	0.12	0.05	0.04	0.23	0.11	0.06	0.04
Al2O3	12.05	12.05	11.57	11.66	12.16	11.60	11.24	11.27	11.65	12.08	11.80	11.78	12.41	12.14	12.32
Fe2O3#	2.17	1.33	1.02	1.79	1.29	2.62	1.51	1.62	1.28	1.37	1.25	3.15	1.14	1.57	0.65
MnO	0.08	0.03	0.01	0.04	0.02	0.01	0.06	0.03	0.01	0.01	0.02	0.02	0.03	0.05	0.00
MgO	1.09	0.45	0.15	0.76	0.81	0.13	0.52	0.37	1.12	0.07	0.38	0.67	0.10	0.45	0.25
CaO	1.75	0.17	0.37	0.10	0.34	0.24	0.88	0.73	0.14	0.09	0.10	0.07	0.04	0.12	0.03
Na2O	2.49	2.22	3.99	2.31	3.06	6.25	2.20	2.68	5.70	1.96	2.64	5.90	1.83	5.87	2.27
K2O	3.65	5.42	3.60	3.88	4.97	0.40	4.77	5.21	0.33	6.78	6.09	0.09	7.67	0.78	6.02
P2O5	0.01	0.01	0.01	0.01	0.01	0.01	0.01	0.01	0.01	0.01	0.02	0.01	0.02	0.01	0.01
Total *	100.00	100.00	100.00	100.00	100.00	100.00	100.00	100.00	100.00	100.00	100.00	100.00	100.00	100.00	100.00
LOI	0.77	0.86	0.18	0.99	0.51	1.58	1.23	0.83	0.90	0.46	0.64	1.26	0.52	0.74	0.93
Sc	10	4	8	7	5	10	4	12	5	8		10	7		
V	4	5	1	2	4	4	2	3	14	4	3	12	1	4	3
Cr	3	3	3	4	4	2	2	2	7	5	4	4	4	1	3
Ni	2	3	3	2	1	1	1	3	2	2	3	2	3	1	3
Cu	2	20	2	3	1		7	2	1	5	6	13	4	25	2
Zn	41	99	25	39	13		42	31	2	15	14	62	22	57	23
Pb	5	66	13	4	15	10	16	10	2	11		3	16	3	5
Rb	98	57	60	108	108	7	126	141	7	162		3	136	20	168
Sr	91	53	86	50	72	71	81	50	60	60		109	57	81	45
Y	36	32	32	33	37	66	39	56	25	27		47	36	34	38
Zr	223	89	121	165	112	302	162	140	86	108		265	240	123	85
Nb	16	10	13	15	10	21	11	17	12	11		12	14	14	12
Ba	500	1386	955	494	669	165	822	595	82	1038		241	2397		
Th	12	16	12	11	16	14	16	18	17	20		12	14	19	19
Ti/Zr	3.5	4.1	3.5	3.0	4.8	3.4	3.8	2.6	8.4	2.8		5.3	2.8	3.0	2.9
Zr/Nb	13.9	8.9	9.3	12.3	11.2	14.4	14.7	8.2	7.2	9.8		22.1	17.1	8.8	7.1
Zr/Y	6.2	2.8	3.8	5.6	3.0	4.6	4.2	2.5	3.4	4.0		5.6	6.7	3.6	2.2
Nb/Y	0.44	0.31	0.41	0.45	0.27	0.32	0.26	0.30	0.48	0.41		0.26	0.39	0.41	0.32
La	25	26	21	26.43	33.7	44	34	37.3	22	19.1	16.9	24.7	34	33	40.2
Ce	52	52	43	60.7	70.2	95	62	77.7	45	45	44.5	54.1	74	75.1	40.5
Pr				7.06	6.32			9.63		5.49	5.46	6.6		9.38	13.7
Nd	23	23	20	27.14	32	45	28	37.3	21	22	22.6	26.4	32	38.5	51.4
Sm				5.59	6.37			6.12		5.04	6.97	6.6		8.73	8.99
Eu				0.91	0.96			1.36		0.77	1.68	1.64		1.28	1.42
Gd				5.4	6.13			8.26		4.41	5.67	6.96		7.66	6.32
Dy				5.62	6.11			9.03		4.88	5.66	7.11		6.54	6.06
Er				3.66	3.58			5.4		3.23	3.53	4.6		3.56	3.98
Yb				3.49	3.15			5.09		3.23	3.14	4.46		3.51	3.78
(La/Yb)N				5.4	7.1			4.8		3.9	4.0	3.7		6.2	7.1

Total Fe as Fe2O3; * Analyses recalculated and normalised to 100% anhydrous

Table 3. Representative major and trace element analyses of volcanics from the Trooper Ck Formation

	TH57/12 Basalt	TB23 Basalt	TH23/1 Basalt	GY39 Andesite	WT16/8 Andesite	WT16/10 Andesite	GY20 Andesite	GY37 Andesite	GY59 Dacite	WT13 Dacite	TH33/241 Dacite	HW10 Dacite	GY52 Dacite	HW1 Dacite	TB26 Dacite	GY46 Dacite
SiO2	48.78	50.49	52.38	54.25	56.74	58.58	60.66	62.82	65.64	69.93	71.75	73.36	73.78	75.28	75.48	78.11
TiO2	0.73	0.88	0.43	0.84	0.77	0.77	0.80	0.72	0.64	0.51	0.50	0.36	0.38	0.33	0.65	0.29
Al2O3	17.14	18.96	14.81	17.91	18.30	18.35	15.33	15.40	15.06	14.44	14.50	13.57	14.31	12.95	11.69	13.40
Fe2O3#	11.05	9.96	8.78	11.08	9.28	10.05	8.92	8.71	7.14	4.65	3.14	3.21	2.62	3.07	3.87	2.30
MnO	0.49	0.18	0.18	0.18	0.13	0.12	0.18	0.19	0.11	0.06	0.05	0.07	0.06	0.03	0.07	0.07
MgO	6.70	5.51	10.06	3.45	2.96	3.22	2.74	2.26	2.15	1.47	0.81	0.59	1.07	0.72	0.43	1.41
CaO	10.58	10.88	8.38	8.50	8.94	4.87	6.00	4.71	4.23	1.37	0.69	1.55	0.16	0.44	1.04	1.13
Na2O	3.26	3.13	3.32	4.92	2.43	3.24	3.58	4.74	3.39	6.65	6.22	5.45	7.21	6.92	5.86	4.05
K2O	1.15	0.37	1.79	0.89	0.29	0.67	1.59	0.23	1.43	0.81	2.21	1.75	0.12	0.19	0.78	1.19
P2O5	0.10	0.08	0.11	0.18	0.16	0.13	0.20	0.23	0.21	0.10	0.12	0.07	0.09	0.06	0.13	0.05
Total *	100.00	100.00	100.00	100.00	100.00	100.00	100.00	100.00	100.00	100.00	100.00	100.00	100.00	100.00	100.00	100.00
LOI	1.06	1.12	1.42	1.47	4.53	5.40	6.74	3.35	5.42	1.60	0.38	1.18	1.01	0.96	0.52	1.58
Sc	51	43	44	39	32	30	32	25	24	12	17	14	15	9	14	9
V	309	284	237	320	273	255	173	116	94	67	38	27	16	18	4	31
Cr	186	68	478	5	16	14	3	6	2	4	2	2	4	3	2	6
Ni	48	28	80	10	20	14	3	4	2	4	2	2	1	2	3	4
Cu	3	65	164	84	97	84	1	118	4	1	2	3	34	3	2	23
Zn	204	63	68	102	100	136	102	124	88	40	89	45	83	32	60	81
Pb	24	5	13	7	10	10	7	12	9	14	3	9	3	10	6	4
Rb	22	7	48	13	5	13	31	5	24	10	43	43	1	6	12	27
Sr	197	354	261	404	644	437	166	222	193	153	46	170	97	191	87	226
Y	15	11	10	21	15	17	23	25	22	25	34	26	29	17	65	27
Zr	32	23	34	60	68	70	73	87	99	135	178	146	172	105	383	155
Nb	2	2	2	4	4	4	4	5	5	9	9	7	8	4	26	7
Ba	112	424	978	564	115	400	1047	173	219	348	778	430	183	123	580	486
Th	<2	<2	<2	2	2	2	3	3	4	7	9	7	10	5	11	8
Ti/Zr	137.7	178.2	78.5	83.9	67.7	66.3	88.1	49.4	38.7	22.6	16.9	14.9	13.1	18.9	10.3	11.1
Zr/Nb	16.0	11.5	17.0	15.0	15.8	17.1	18.3	17.4	19.8	15.0	19.8	20.9	21.5	26.3	14.7	22.1
Zr/Y	2.1	2.1	3.4	2.9	4.5	4.1	3.2	3.5	4.5	5.4	5.2	5.8	5.9	6.2	5.9	5.7
Nb/Y	0.13	0.18	0.20	0.19	0.29	0.24	0.17	0.20	0.23	0.36	0.26	0.27	0.28	0.24	0.40	0.26
La	4	8.58	6.85	11.74	7	12	10.4	13	20	25	9.24	16.9	14.0	7.16	17.7	26.5
Ce	11	18.7	16.2	28.3	21	17	23.9	29	33	44	24.5	37.1	30.7	16.5	44.2	43.4
Pr		2.14	2.23	3.18			3.06				3.61	4.37	3.50	2.28	6.02	5.27
Nd	4	9.32	10.4	15.0	11	9	14.1	16	16	17	16.8	18.3	16.1	10.4	28.0	21.2
Sm		2.05	2.10	4.09			3.50				4.73	4.14	3.84	3.05	7.75	5.91
Eu		0.75	0.70	1.23			0.91				1.04	1.21	0.87	0.72	1.97	1.78
Gd		2.18	2.12	3.74			3.70				4.77	4.08	3.84	2.97	7.88	4.54
Dy		1.88	1.84	3.6			3.49				5.45	4.17	4.36	2.92	9.27	4.51
Er		0.99	0.84	2.04			2.14				3.18	2.6	2.94	1.58	6.35	2.88
Yb		0.79	0.75	1.88			1.92				2.99	2.58	2.93	1.61	6.26	2.78
(La/Yb)N		7.2	6.0	4.1			3.6				2.0	4.3	3.2	2.9	1.9	6.3

Total Fe as Fe2O3; * Analyses recalculated and normalised to 100% anhydrous

Table 4. Nd isotope data for the Mt Windsor volcanics

		$^{147}Sm/^{144}Nd$	$(^{143}Nd/^{144}Nd)_m$	$\varepsilon_{Nd(480Ma)}$
Puddler Ck Formation				
WT32	Andesite	0.106969	0.512263	-1.81
HW30	Andesite	0.091517	0.512168	-2.72
PC9	Andesite	0.097106	0.512304	-0.16
Mt Windsor Formation				
WT44	Rhyolite	0.131621	0.511990	-8.67
HW35	Rhyolite	0.186467	0.511953	-12.75
SS17	Rhyolite	0.165989	0.512117	-8.29
TH4	Rhyolite	0.124537	0.512171	-4.69
TC28	Rhyolite	0.137062	0.511961	-9.60
Trooper Ck Formation				
TH23/1	Basalt	0.122103	0.512596	+3.76
TB25	Basalt	0.159747	0.512638	+2.27
SS9	Andesite	0.135695	0.512508	+1.21
TH33/241	Dacite	0.170243	0.512368	-3.65
GY39	Andesite	0.164868	0.512235	-5.92
GY46	Dacite	0.168565	0.512338	-4.13
HW10	Dacite	0.136788	0.512164	-5.58

Table 5. Comparison of the average metal contents of some modern and ancient massive sulfide deposits

	Pb (wt. %)	Zn (wt. %)	Cu (wt. %)	Au (g/t)
Thalanga	3.9	12.3	2.2	0.6
Okinawa Trough	14.3	22.0	1.8	4.6
East Pacific Rise	0.05	8.2	7.8	0.26
Lau Basin	0.6	10.9	3.3	1.7

relatively immobile during low grade regional metamorphism (Wood et al., 1976; Menzies et al., 1979; Ludden et al., 1982). In addition, there is a large amount of Nd isotope data now available for modern volcanics from a variety of tectonic settings where contributions from different mantle and crustal source materials are commonly inferred.

Nd isotope data for the four chemically distinguishable suites in the Mt Windsor Volcanic belt (Table 4, Fig. 12) suggest at least three isotopically discrete sources for the volcanism. Firstly, the LREE-enriched PCF volcanics have $\varepsilon_{Nd\ (480Ma)}$ values which span a relatively narrow range (–0.2 to –2.7) close to the predicted Bulk Earth value. This is consistent with their derivation from a relatively undepleted or slightly enriched mantle source, interpreted in this case to be subcontinental lithosphere. The MWF rhyolites have a relatively restricted range of $\varepsilon_{Nd\ (480Ma)}$ values (–4.7 to –12.8) suggesting they were derived from a long-term LREE-enriched source such as old continental crust. In contrast, the TCF rocks display a broad range of $\varepsilon_{Nd\ (480Ma)}$ values from +3.8 to –7.3. The basaltic to andesitic rocks are mostly characterised by positive values, whereas the dacites and rhyolites have negative values. The positive $\varepsilon_{Nd\ (480Ma)}$ values for the TCF basaltic rocks reflect their mantle source which was depleted in LREE for a substantial period compared with the source of the PCF volcanics. A model depleted mantle composition similar to the source of modern MORB would have had $\varepsilon_{Nd\ (480Ma)} \sim +8.6$. This is somewhat higher than the values of the TCF volcanics. However, modern island arc and back-arc basin volcanics frequently have relatively unradiogenic Nd isotope values when compared with MORB (e.g. Morris and Hart, 1983; Loock et al., 1990; Stern et al., 1990), and this is attributed to modification of a depleted MORB-source by a subduction-related fluid phase which may in part have an older crust-like Nd isotope signature. A high-Ti basaltic andesite from the TCF (Table 4, TB25) and a likely intrusive equivalent from the Ti-rich dyke suite (e.g. Table 4, GY71) have similar $\varepsilon_{Nd\ (480Ma)}$ values to the low-Ti subduction-related variants, indicating that the mantle source for the Ti-poor and Ti-rich magmas was isotopically similar.

In a plot of $\varepsilon_{Nd\ (480Ma)}$ versus SiO_2 (Fig. 13) there is a general decrease in $\varepsilon_{Nd\ (480Ma)}$ with increasing silica content for the TCF volcanics. If it is accepted that these rocks comprise a cogenetic suite (as suggested by their coherent chemical variations), this relationship is best explained by assimilation of continental crust during fractional crystallisation where the crust had a similar isotopic signature to that which is considered to have undergone partial melting to produce the MWF rhyolites. The assimilation-fractional crystallisation (AFC) process can be modelled using the equation of DePaolo (1981) after making a number of assumptions about the nature of the contaminant and the degree of interaction. However, given the large uncertainties in the isotopic and chemical composition of the contaminant, as well as possible post-crystallisation modification of SiO_2 values in the volcanics, this exercise is only intended to demonstrate that the broad compositional and isotopic variations in the TCF suite are consistent with the AFC model. Firstly, the basaltic rock with the highest positive ε_{Nd} value (TH23/1; $\varepsilon_{Nd(480Ma)}$ = +3.8, Nd = 10.4ppm; SiO_2 = 52.4 wt.%) was assumed to be the least contaminated parental magma composition. The contaminant was assumed to have a similar isotopic composition to felsic granulite xenoliths from North Queensland ($\varepsilon_{Nd(480Ma)} \sim -14.0$, Nd ~ 25ppm; SiO_2 = 74 wt.%) which may be indicative of the nature of the Proterozoic crust in the region (Stolz and Davies, 1989).

The ratio of the mass of contaminant to the mass of crystals was set at 0.4 although somewhat higher values may be justifiable at relatively deep crustal levels due to reduced temperature contrast between the magma and wall-rock. At higher values of r the composition of the melt more rapidly approaches the composition of the contaminant for a given degree of crystallisation. The modelled variation of ε_{Nd} as a function of SiO_2 for these conditions is shown in Fig. 13. The trend is in general agreement with the variations in the natural rocks, although there are several andesitic rocks which appear to have lower $\varepsilon_{Nd\ (480Ma)}$ values than predicted for their SiO_2 contents (e.g. Table 4, GY39). This may reflect enhanced assimilation by some magmas, or variability in the composition of the contaminant. The silica content used in the calculations is higher than that of the xenoliths, and a range of contaminant compositions can be used to calculate a variety of mixing trends that span the variations in the natural data.

Comparable Modern Volcanic Associations and Tectonic Settings

Modern Analogues

The strong enrichment in incompatible elements (e.g. Zr, Nb, Th, P and LREE), the low Zr/Nb and high Nb/Y values of the PCF volcanics suggest similarities to intraplate or continental rift-related alkaline volcanics. Their incompatible element abundances and the La/Nb values (average 1.2) are somewhat higher than typical alkali basalts (La/Nb generally < 1; Sun and McDonough, 1989), and their TiO_2 contents are generally lower than rift-related mafic alkaline volcanics or typical OIB (ocean island basalts) resulting in slight relative depletions of Nb and Ti in a N-MORB normalised plot (Fig. 14). Although the strong enrichment in incompatible elements may in part be explained by their relatively evolved nature (evident from their low MgO, Cr and Ni), the elevated La/Nb and low TiO_2 values suggest the involvement of an enriched lithospheric mantle component in their origin. Similar (although less enriched) geochemical signatures characterise many continental flood basalts and have been explained either by derivation from ancient subduction-modified lithospheric mantle (Hergt et al., 1991; Lightfoot et al., 1993), or by crustal contamination of asthenospheric-derived melts (e.g. Carlson et al., 1981; Brandon et al., 1993). Given the relatively evolved nature of these volcanics, interaction with continental crust during fractional crystallisation is feasible. However, this would be expected to produce a decrease in the $\varepsilon_{Nd\ (480Ma)}$ value with increasing SiO_2, as is the case for the TCF volcanics, but the reverse trend is observed for the PCF volcanics (Fig. 13).

In a MORB-normalised plot (Fig. 14) the basalts and andesites of the TCF display patterns typical of many modern subduction-related volcanics with a marked relative depletion of Nb and similar or lower abundances of the HREE and Ti to N-MORB. This pattern is partly controlled by the enrichment in LILE (e.g. Rb, Ba and K) and although the abundances of these elements are not reliable in ancient volcanics, the relatively high Th abundances support the validity of these patterns. In addition to island arc and continental margin arc volcanics, this geochemical signature is frequently a feature of back-arc basin (BAB) basalts formed during the early stages of back-arc basin evolution (e.g. Fig. 14, Okinawa Trough; Ishizuka et al., 1990; Honma et al., 1991). With progressive opening of a basin, the basalts generally evolve toward N-MORB compositions (e.g. Stern et al., 1990) possibly due to the dilution of subduction-modified mantle material by upwelling asthenospheric mantle as the subduction zone becomes more remote from the principal site of BAB magma generation.

The presence of quite primitive compositions (i.e. high MgO, Cr and Ni) within the TCF further supports the interpretation that these rocks were erupted in a BAB setting. Island arc basalts generally have lower MgO (average 5 to 6 wt. %; BVSP, 1981), Cr and Ni than BAB, although there are some exceptions (e.g. New Britain arc, BVSP, 1981). It could be argued that the negative Nb anomalies that characterise these rocks may have been imposed on them as a result of the interaction between basaltic magma and continental crust. However, the very low Zr concentrations (20–30 ppm) and positive $\varepsilon_{Nd\ (480Ma)}$ values which characterise the more primitive compositions suggest this is unlikely.

The Ti-rich dykes and volcanics have relatively smooth MORB-normalised patterns characterised by only a slight relative depletion of Nb, and abundances intermediate between E-MORB and OIB for most minor and trace elements (Fig. 14). Their compositions closely resemble those of continental flood basalts and also basalts from some back-arc basins (e.g. South Sandwich spreading axis, Tarney et al., 1977; Lau Basin, Hawkins, 1977; Volpe et al., 1988).

Therefore the chemistry of the more mafic volcanics in the Mt Windsor Subprovince reflects their derivation from a range of mantle sources, including subcontinental lithosphere, subduction modified asthenospheric material, and asthenospheric mantle that has not been affected by subduction processes, but which displays isotopic evidence of moderately long-term depletion in LREE compared with model Bulk Earth estimates.

Tectonic Model for the Mt Windsor Subprovince

Murray and Kirkegaard (1978) interpreted the Mt Windsor Subprovince as a volcanic arc separated from the Precambrian craton of the Georgetown Inlier to the north by a marginal sea of unknown extent. Subsequently, Henderson (1986) interpreted the sequence as the fill of a back-arc basin which developed on the Precambrian craton west of a

continental margin volcanic arc. The idea that the basin developed on stretched continental lithosphere was based on the relative abundance of silicic volcanics in the Mt Windsor Formation compared with mafic volcanics in the Mt Windsor Belt as a whole. This is supported by the Nd isotope data presented in this study which suggests these rocks were derived by partial melting of older (Precambrian) crustal rocks.

The Mt Windsor Subprovince appears to comprise a relatively thick (possibly in excess of 12 km; Henderson, 1986) volcano-sedimentary package indicative of substantial basin subsidence. The overall thickness of the package is not well constrained given the poor level of understanding of the structural relationships in the PCF. However, such thicknesses may not be unrealistic as seismic evidence suggests that about 10 km of sediment and volcanics have accumulated in the northern Okinawa Trough since the Miocene (Letouzey and Kimura, 1985).

Volcanological studies of the Mt Windsor Subprovince (Stolz, 1991) also indicate that the large majority of the volcanic and volcaniclastic units have been deposited in a subaqueous environment. Some of the mafic volcanics display relic pillow structures, and hyaloclastite deposits, whereas the silicic volcaniclastic units include abundant hyaloclastite material and some insitu, quench-fragmented deposits. A considerable proportion of the silicic volcaniclastic units have been redeposited as mass-flow units. In addition, the presence of exhalative sea-floor massive sulfide deposits within the sequence (Berry et al., 1992) supports the interpretation that the host package was deposited in a deep submarine environment.

A model for the tectonic evolution of the belt based on the stratigraphic, geochemical and isotopic relationships discussed above is summarised in Fig. 15. Evidence from recent supercontinent reconstructions (e.g. Moores, 1991; Brookfield, 1993) suggests that Australia and Antarctica rifted off from western North America in the Neoproterozoic resulting in a passive margin along much of eastern Australia. The late Proterozoic to Lower Cambrian margin of northeastern Australia may therefore have been an attenuated passive margin upon which continental-derived sedimentation was occurring. Quartz-rich and micaceous metasedimentary rocks of the Puddler Creek Formation are probably representative of the material derived from an exposed Precambrian crustal source and deposited on the passive margin.

At some stage early in the Cambrian it is suggested that westerly dipping subduction of oceanic crust was initiated. This may have involved foundering of cold, relatively dense oceanic crust close to the old passive margin. However, current models (e.g. Mueller and Phillips, 1991) favour the view that passive margin boundaries become annealed with time and that subduction is more likely to be initiated along old intra-oceanic transform structures in response to attempted subduction of buoyant material at a mature trench. An alternative mechanism for achieving a westerly dipping subduction zone is by subduction polarity reversal following collision of an island arc with the continental margin due to subduction of the intervening oceanic crust along an easterly dipping subduction zone. This model has been invoked to explain relationships between Neoproterozoic and Cambrian rocks in western Tasmania (Berry and Crawford, 1988; Crawford and Berry, 1992). However, the lithological and structural evidence for a collision of this type that has been well documented in western Tasmania is not as well developed in the Mt Windsor Subprovince.

After subduction of oceanic lithosphere was initiated, there would have been a lag period of approximately 2 to 5 Ma (depending on convergence rate and subduction geometry) before significant subduction-related volcanism was generated due to metasomatism of the mantle wedge above the subsiding slab. Extension of this active continental margin arc, possibly due to rollback of the subducting slab, subsequently initiated development of a back-arc basin. Although there is considerable debate about the mechanisms by which BAB opening is initiated, the evidence from currently developing marginal basins such as the Hachijo and Aoga Shima Rifts behind the Izu–Bonin arc (Klaus et al., 1992), suggests that extension causes the arc to split longitudinally along the volcanic front as it represents the hottest and mechanically weakest part of the lithosphere.

Subsidence of the attenuated continental lithosphere appears to have been followed initially by rapid deposition of the PCF sediments. These were largely derived from the adjacent Precambrian craton, particularly in the western part of the basin suggesting a westerly landward provenance. Further

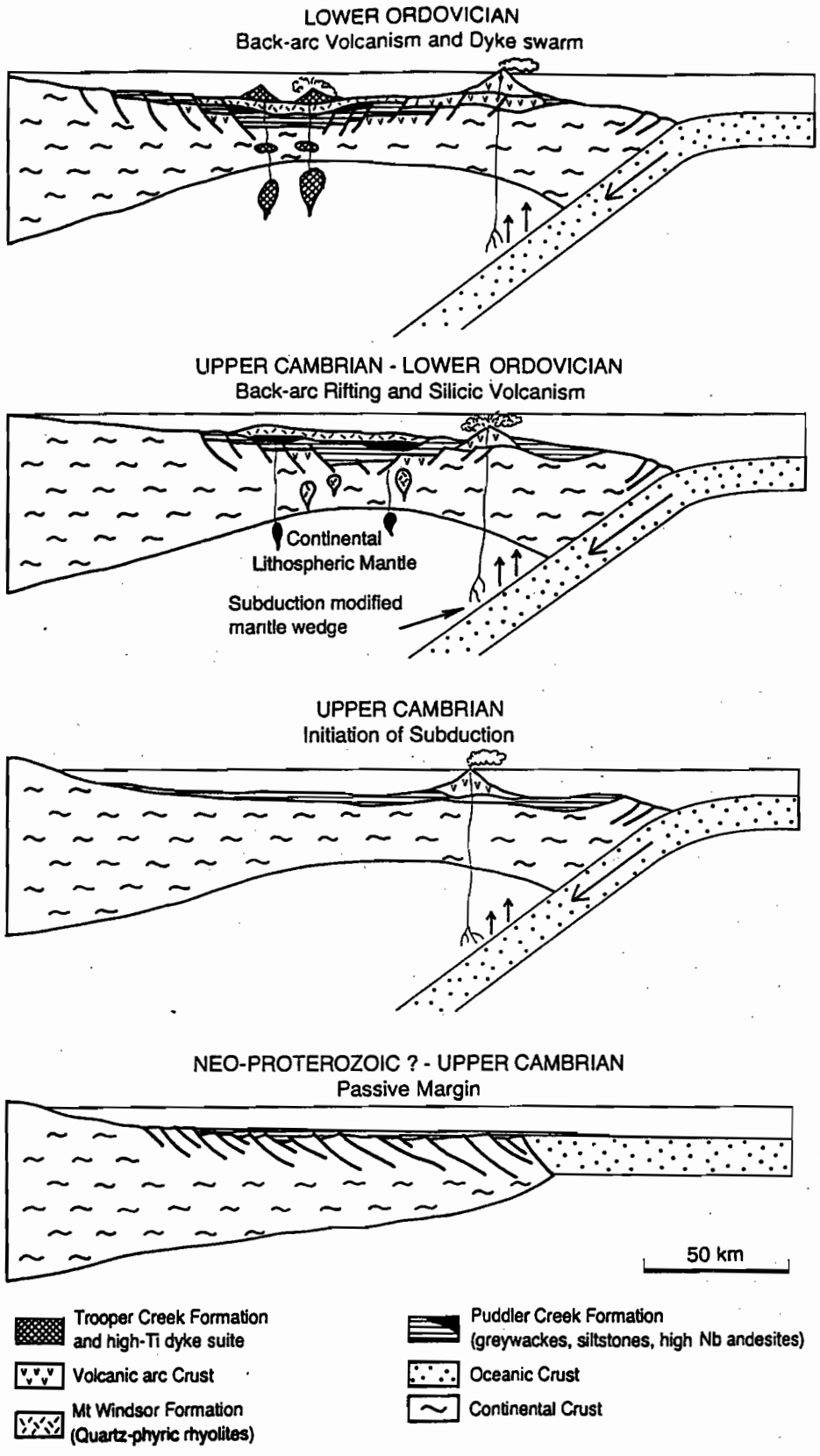

Fig. 15. Model for the tectonic development of the Mt Windsor Subprovince in northeastern Australia from the late Proterozoic to the Lower Ordovician.

east in the PCF, particularly in the upper portions of the sequence, there is substantial evidence of an increased volcanic component which was most likely derived from the frontal arc that was probably located toward the east. The orientation of the original depositional basin is uncertain and a matter of some debate. Henderson (1986) argued that the arc and adjacent back-arc basin were oriented north–south, roughly parallel to the broad structural grain of the Tasman Orogenic Zone. The present east–west orientation of the belt is regarded by Henderson (1986) as due to disruption and folding associated with the emplacement of the Ravenswood Granodiorite Complex. The preliminary observations regarding the provenance of sedimentary and volcanic components within the PCF noted above lend some support to Henderson's model. However, these observations would also be broadly consistent with a northeast–southwest oriented arc that was aligned parallel to the Precambrian cratonic margin as inferred from gravity and magnetic data, and defined by the Diamantina Lineament (Fig. 1).

The small volume of PCF basaltic andesites and andesites generated in response to continued lithospheric thinning and increased heat-flow resulting from upwelling mantle appears to be the first manifestation of volcanism in the basin. At the same time the increased heat-flow is probably responsible for substantial crustal melting, the products of which were subsequently erupted as the MWF rhyolites. This phase of silicic volcanism appears to have been completed by the onset of volcanism produced by melting of variably subduction-modified mantle sources (i.e. TCF). The earliest low-Ti basalts and andesites reflect contributions from the most extensively subduction-modified mantle, whereas the relatively high-Ti dyke swarm and related volcanics reflect the input of progressively less modified asthenospheric mantle material into the melting regime.

Following the eruption of the TCF volcanics, evidence of volcanic activity is rare, and the youngest Rollston Range rocks probably represent mainly reworked TCF volcaniclastic material, but may also contain contributions from an active arc further east. The Mt Windsor Subprovince contains no volcanic sequences that are MORB-like in composition, and hence it is inferred that lithospheric extension did not proceed to the stage of developing new oceanic crust.

It is uncertain what proportion of the back-arc basin sequence is represented by the presently exposed window of Cambro-Ordovician units, and what tectonic events led to basin uplift and preservation. However, the relatively low levels of strain and recrystallisation which characterise deformation within the Mt Windsor Subprovince (Berry et al., 1992) do not suggest a major collision event. Instead the convergent margin may have been converted to a major transform structure due to more oblique plate convergence.

Correlation with other Sequences in the Tasman Orogenic Zone

A volcano-sedimentary package of essentially identical age (478 to 471 ± 5 Ma; Withnall et al., 1991), but characterised by substantially higher metamorphic grade (amphibolite facies) than the Mt Windsor Subprovince occurs about 250km to the northwest at Balcooma (Fig. 1; Henderson, 1986; Huston, 1990; Withnall et al., 1991). This sequence, which hosts several small massive sulfide bodies (Huston, 1990; Huston et al., 1992), is separated from the Mt Windsor Subprovince by Ordovician to Carboniferous rocks of the Broken River Province, and Ordovician–Devonian granitoids of the Lolworth–Ravenswood batholith. The northwestern margin of the Balcooma Metavolcanics is a mylonite zone, and the dominantly Proterozoic basement rocks of the Georgetown Inlier are considered to have been thrust westward over the Ordovician–Devonian sequences (Withnall et al., 1991).

The Balcooma Metavolcanics are dominated by silicic volcanic and volcaniclastic rocks with apparently only a small package of andesitic rocks. The lack of published geochemical data for these more mafic rocks precludes any comparison with the volcanics from the Mt Windsor Subprovince. However, the abundance of silicic volcanic compositions, and the recognition of inherited zircons with Archean ages in some of these units (Withnall et al., 1991) suggests that the silicic magmatism in the Balcooma area may have had a similar origin to the Mt Windsor Formation rhyolites, by partial melting of older crustal rocks. The close overlap in age, and the lithological similarities of the Balcooma and Mt Windsor sequences supports the model that they were both deposited in a back-arc basin with a broadly north–south orientation. There is no obvious

evidence for the location of the frontal arc to this basin and presumably the majority of the arc deposits were eroded and have been covered by younger deposits.

A number of studies have argued that the Ordovician to Devonian metasedimentary rocks of the Hodgkinson and Broken River Provinces (Fig. 1) were deposited in a back-arc basin (e.g. Murray, 1986), and it has recently been argued that the Devonian to Carboniferous deposits of the Drummond Basin are back-arc basin deposits (Davis and Henderson, 1994) . If these interpretations are correct, it suggests the repeated development of back-arc basins in this region of northeastern Australia over a considerable time interval.

Development of the Mt Read Volcanic Belt in western Tasmania has also been interpreted as being broadly coeval with the Mt Windsor Subprovince (Henderson, 1986). However, $^{39}Ar/^{40}Ar$ and U–Pb zircon (SHRIMP) ages (Perkins and Walshe, 1993) indicate the Mt Read Belt is slightly older (~500 Ma) than the Mt Windsor Subprovince, and their respective locations at the southern and northern extremities of the Tasman Orogenic Zone make correlations more tenuous. The Mt Read Volcanic Belt records evidence of a substantially more complex tectonic history than the Mt Windsor Subprovince with the main phase of calcalkaline volcanism (the Central Volcanic Complex) apparently following the allochthonous emplacement of an ophiolite sheet due to collision of the Precambrian continent with an island arc (Berry and Crawford, 1988; Crawford and Berry, 1992). In addition, several volcanic centres within the Mt Read Belt are characterised by post-collisional volcanics with distinctive geochemical characteristics (e.g. the hangingwall sequence to the Hellyer and Que River VHMS deposits, Crawford et al., 1992) which have no correlates in the Mt Windsor Subprovince.

Despite the differences between these volcano-sedimentary belts, there are substantial similarities in the character of many of the volcanic products and the style of mineralisation. There is also limited Nd and Sr isotopic data for the Mt Read Volcanics (Whitford et al., 1990) which suggests that some of the silicic volcanics were produced by partial melting of older (Precambrian) crustal rocks. This supports a continental margin arc or back-arc depositional environment for both the Mt Read and Mt Windsor belts, and suggests that during the Middle Cambrian to Lower Ordovician the eastern Australian margin was characterised by active subduction associated with periods of extension.

Relationship between Mineralisation and Volcanism

Studies of modern seafloor massive sulfide deposits and their associated volcanic rocks have added substantially to our understanding of the spatial relationships between ancient massive sulfide deposits and their host volcanic sequences. Tectonic settings for the ancient deposits can also be inferred from comparisons with compositionally similar sulfide deposits and volcanics from the modern ocean basins.

Massive sulphide mineralisation within the Mt Windsor Subprovince occurs at the boundary between the MWF and TCF (e.g. Thalanga) and at stratigraphically higher levels within the TCF (e.g. Waterloo and Liontown prospects, Fig. 2; Berry et al., 1992). The main mineralising events follow the eruption and deposition of the MWF silicic magmas, and are synchronous with the onset of back-arc volcanism produced by partial melting of subduction-modified sub-arc mantle. Although there is evidence for weak hydrothermal activity prior to the initiation of the MWF silicic magmatism, it is noteworthy that there are no mineralised horizons within the MWF despite the existence of a thick sequence of silicic eruptives. One possibility is that the eruption rate for the MWF rhyolites was too high to permit the deposition of significant thicknesses of exhalative massive sulfides on the seafloor. Alternatively, it could be argued that the presence of more mafic magma was necessary, either to provide a more substantial heat source to drive the hydrothermal circulation cells, or as a direct source of metals.

A close modern analogue to the Mt Windsor Volcanics and the associated style of VHMS mineralisation is provided by the Okinawa Trough (Letouzey and Kimura, 1985; Halbach et al., 1989). This is a back-arc basin currently developing by extension of continental lithosphere behind the Ryukyu trench-arc system. Seafloor massive sulphide deposits from the Okinawa Trough are relatively rich in Pb and Zn and closely comparable with the

Cambro-Ordovician deposits in the Mt Windsor Subprovince (Table 5). The basic volcanics which host the Okinawa deposits are also geochemically very similar to the TCF lavas (cf. Fig. 14). However the mafic and silicic rocks in the Okinawa Trough have essentially identical Nd and Sr isotope signatures (Honma et al., 1991) suggesting little or no interaction of the magmas with underlying continental crust as has clearly occurred during emplacement of the Mt Windsor volcanics. It is unknown if the footwall sequence to the Okinawa massive sulfide deposits includes a suite of crustal derived melts similar to the MWF rhyolites due to the limited portion of the stratigraphy available for inspection.

The relatively Pb-rich VHMS deposits from the Okinawa Trough and Mt Windsor Subprovince contrast with the Pb-poor Fe–Cu (± Zn) type deposits from the major ocean spreading ridges (e.g. East Pacific Rise, Table 5), and mature back-arc basins which are developed on oceanic lithosphere (e.g. North Fiji Basin, Grimaud et al., 1991; Lau Basin, Fouquet et al., 1991). Deposits in the southern part of the Lau Basin also have relatively low Pb contents (Table 5) despite being hosted by volcanics with a distinctive subduction-related geochemical signature (Fouquet et al., 1991). This illustrates the close relationship that exists between host volcanic and massive sulfide compositions. Pb-poor VHMS deposits are hosted by N-MORB or similar oceanic basalts with extremely low Pb concentrations (<1 ppm), whereas Pb-rich VHMS deposits are hosted by calcalkaline silicic or andesitic volcanics which have substantially higher Pb concentrations. Although the Lau Basin deposits are associated with calcalkaline volcanics, the host rocks are likely to have very low Pb concentrations, based on the data for the associated Tonga–Kermadec arc volcanics (Ewart and Hawkesworth, 1987), probably reflecting the nature of the subduction component added to their mantle source.

Despite the close relationship that exists between host volcanic and massive sulfide compositions, it remains unclear whether the metals in these deposits have a magmatic origin, as exsolved fluids from crystallising subvolcanic magma chambers (e.g. Stanton and Ramsay, 1980; Urabe, 1987; Stanton, 1990), or if this association simply reflects the metals available for leaching in the footwall volcanics by circulating hydrothermal fluids (e.g. Large, 1992).

Acknowledgements

This research was supported by an ARC Research Fellowship to AJS, and funding provided by Pancontinental Mining, Outokumpu Australia and Agip Australia.

References

Berry, R.F. and Crawford, A.J., 1988. The tectonic significance of Cambrian allochthonous mafic-ultramafic complexes in Tasmania. *Australian Journal of Earth Sciences* 35: 523–533.

Berry, R.F., Huston, D.L., Stolz, A.J., Hill, A.P., Beams, S.D., Kuronen, U. and Taube, A., 1992. Stratigraphy, structure, and volcanic-hosted mineralisation of the Mount Windsor Subprovince, north Queensland, Australia. *Economic Geology* 87: 739–763.

Brandon, A.D., Hooper, P., Goles, G.G. and Lambert, R. St J., 1993. Evaluating crustal contamination in continental basalts: the isotopic composition of the Picture Gorge Basalt of the Columbia River Basalt Group. *Contributions to Mineralogy and Petrology* 114: 452–464.

Brookfield, M.E., 1993. Neoproterozoic Laurentia–Australia fit. *Geology* 21: 683–686.

BVSP, 1981. *Basaltic Volcanism on the Terrestrial Planets*. Pergamon Press, New York: 1286 pp.

Campbell, I.H., Lesher, C.M., Coad, P., Franklin, J.M., Gorton, M.P. and Thurston, P.C., 1984. Rare-earth element mobility in alteration pipes below massive Cu–Zn sulphide deposits. *Chemical Geology* 45: 181–202.

Carlson, R.W., Lugmair, G.W. and MacDougall, J.D., 1981. Columbia River volcanism: the question of mantle heterogeneity or crustal contamination. *Geochimica Cosmochimica Acta* 45: 2483–2499.

Crawford, A.J. and Berry, R.F., 1992. Tectonic implications of Late Proterozoic-Early Palaeozoic igneous rock associations in western Tasmania. *Tectonophysics* 214: 37–56.

Crawford, A.J., Corbett, K.D. and Everard, J., 1992. Geochemistry of the Cambrian VHMS-rich Mount Read Volcanics, Tasmania, and some tectonic implications. *Economic Geology* 87: 597–619.

Davis, B.K. and Henderson, R.A., 1994. Syn-rift magmatic assemblages of the Drummond Basin. *In* R.A. Henderson and B.K. Davis (eds.): *New Developments in Geology and Metallogeny*. Northern Tasman Orogenic Zone, Ext. Conf. Abstr.: 103–104.

Day, R.W., Murray, C.G. and Whitaker, W.G., 1978. The eastern part of the Tasman orogenic zone. *Tectonophysics* 48: 327–364.

DePaolo, D.J., 1981. Trace element and isotopic effects of combined wallrock assimilation and fractional crystallization. *Earth and Planetary Science Letters* 53: 189–202.

Duhig, N.C., Stolz, A.J., Davidson, G.J. and Large, R.R., 1992. Cambrian microbial and silica gel textures in silica iron exhalites from the Mount Windsor Volcanic belt, Australia : their petrography, chemistry and origin. *Economic Geology* 87: 764–784.

Ewart, A. and Hawkesworth, C.J., 1987. The Pleistocene–Recent Tonga–Kermadec arc lavas : interpretation of new isotopic

and rare earth data in terms of a depleted mantle source model. *Journal of Petrology* 28: 495–530.

Foley, S.F., Venturelli, G., Green, D.H. and Toscani, L., 1987. The ultrapotassic rocks : characteristics, classification and constraints for petrogenetic models. *Earth Science Reviews* 24: 81–134.

Fouquet, Y. et al., 1991. Hydrothermal activity and metallogenesis in the Lau back-arc basin. *Nature* 349: 778–781.

Gemmell, J.B. and Large, R.R., 1992. Stringer system and alteration zones underlying the Hellyer volcanic-hosted massive sulfide deposit, Tasmania, Australia. *Economic Geology* 87: 620–649.

Gill, J.B., 1981. *Orogenic Andesites and Plate Tectonics*. Berlin, Springer–Verlag: 390 pp.

Grimaud, D., Ishibashi, J-I., Lagabrielle, Y, Auzende, J-M. and Urabe, T., 1991. Chemistry of hydrothermal fluids from 17°S active site on the North Fiji Basin Ridge (SW Pacific). *Chemical Geology* 93: 209–218.

Halbach, P., Nakamura, K., Wahsner, M., Lange, J., Sakai, H., Käselitz, L., Hanse, R.-D., Yamano, M., Post, J., Prause, B., Seifert, R., Michaelis, W., Teichmann, F., Kinoshita, M., Märten, A., Ishibashi, J., Czerwinski, S. and Blum, N., 1989. Probable modern analogue of Kuroko-type massive sulphide deposits in the Okinawa Trough back-arc basin. *Nature* 338: 496–499.

Hawkins, J.W., 1977. Petrologic and geochemical characteristics of marginal basin basalts. *In* Talwani, M. and Pitman, W.C. III (eds.): *Island Arcs, Deep Sea Trenches and Back-Arc Basins*. American Geophysical Union, Washington, DC: 355–365.

Henderson, R.A., 1983. Early Ordovician faunas from the Mount Windsor Subprovince, northeastern Queensland. *Memoirs of the Association of Australasian Palaeontologists* 1: 145–175.

Henderson, R.A., 1986. Geology of the Mount Windsor subprovince - a lower Palaeozoic volcano-sedimentary terrane in the northern Tasman orogenic zone. *Australian Journal of Earth Sciences* 33: 343–364.

Hergt, J. M., Peate, D.W. and Hawkesworth, C.J., 1991. The petrogenesis of Mesozoic Gondwana low-Ti flood basalts. *Earth and Planetary Science Letters* 105: 134–148.

Honma, H., Kusakabe, M., Kagami, H., Iizumi, S., Sakai, H., Kodama, Y. and Kimura, M., 1991. Major and trace element chemistry and D/H, $^{18}O/^{16}O$, $^{87}Sr/^{86}Sr$ and $^{143}Nd/^{144}Nd$ ratios of rocks from the spreading center of the Okinawa Trough, a marginal back-arc basin. *Geochemical Journal* 25: 121–136.

Huston, D.L., 1990. The stratigraphic and structural setting of the Balcooma volcanogenic massive sulphide lenses, northern Queensland. *Australian Journal of Earth Sciences* 37: 423–440.

Huston, D.L., Taylor, T., Fabray, J. and Patterson, D.J., 1992. A comparison of the geology and mineralization of the Balcooma and Dry River South volcanic-hosted massive sulfide deposits, northern Queensland. *Economic Geology* 87: 785–811.

Ishizuka, H., Kawanobe, Y. and Sakai, H., 1990. Petrology and geochemistry of volcanic rocks dredged from the Okinawa Trough, an active back-arc basin. *Geochemical Journal* 24: 75–92.

Klaus, A., Taylor, B., Moore, G.F., Murakami, F. and Okamura, Y., 1992. Back-arc rifting in the Izu-Bonin island arc: structural evolution of Hachijo and Aoga Shima rifts. *The Island Arc* 1: 16–31.

Large, R.R., 1992. Australian volcanic-hosted massive sulfide deposits : features, styles, and genetic models. *Economic Geology* 87: 471–510.

Letouzey, J. and Kimura, M., 1985. Okinawa Trough genesis: structure and evolution of a back-arc basin developed in a continent. *Marine and Petroleum Geology*, 2: 111–130.

Lightfoot, P.C., Hawkesworth, C.J., Hergt, J.M., Naldrett, A.J., Gorbachev, N.S., Fedorenko, V.A. and Doherty, W., 1993. Remobilisation of the continental lithosphere by a mantle plume: major-, trace-element, and Sr-, Nd-, and Pb-isotope evidence from picritic and tholeiitic lavas of the Noril'sk District, Siberian Trap, Russia. *Contributions to Mineralogy and Petrology* 114: 171–188.

Loock, G., McDonough, W.F., Goldstein, S.L. and Hofmann, A.W., 1990. Isotopic composition of volcanic glasses from the Lau Basin. *Marine Mining* 9: 235–245.

Ludden, J., Gelinas, L. and Trudel, P., 1982. Archean metavolcanics from the Rouyan–Noranda district, Abitibi greenstone belt, Quebec. 2. Mobility of trace elements and petrogenetic constraints. *Canadian Journal of Earth Sciences* 19: 2276–2287.

MacLean, W.H. and Barrett, T.J., 1993. Lithogeochemical techniques using immobile elements. *Journal of Geochemical Exploration* 48: 109–133.

MacLean, W.H. and Kranidiotis, P., 1987. Immobile elements as monitors of mass transfer in hydrothermal alteration: Phelps Dodge massive sulfide deposit, Matagami, Quebec. *Economic Geology* 82: 951–962.

Menzies, M., Seyfried, W. and Blanchard, D., 1979. Experimental evidence of rare earth element immobility in greenstones. *Nature* 282: 398–399.

Moores, E.M., 1991. Southwest US–East Antarctic (SWEAT) connection: an hypothesis. *Geology* 19: 425–428.

Morris, J.D. and Hart, S.R., 1983. Isotopic and incompatible element constraints on the genesis of island arc volcanics from Cold Bay and Amak Island, Aleutians, and implications for mantle structure. *Geochimica Cosmochimica Acta* 47: 2015–2030.

Mueller, S. and Phillips, R.J., 1991. On the initiation of subduction. *Journal of Geophysical Research* 96: 651–665.

Murray, C.G., 1986. Metallogeny and tectonic development of the Tasman fold belt system in Queensland. *Ore Geology Reviews* 1: 315–400.

Murray, C.G. and Kirkegaard, A.G., 1978. The Thomson orogen of the Tasman orogenic zone. *Tectonophysics* 48: 299–325.

Norrish, K. and Chappell, B.W., 1977. X-ray fluorescence spectrometry. *In* Zussman, J. (ed.): *Physical Methods in Determinative Mineralogy* (2nd ed). Academic Press, London: 201–272.

Peccirillo, A. and Taylor, S.R., 1976. Geochemistry of Eocene calcalkaline volcanic rocks from the Kastamonu area, northern Turkey. *Contributions to Mineralogy and Petrology* 58: 63–81.

Perkins, C. and Walshe, J.L., 1993. Geochronology of the Mount Read Volcanics, Tasmania, Australia. *Economic Geology* 88: 1176–1197.

Richards, D.N.G., 1980. Palaeozoic granitoids of northeastern Australia. *In* Henderson, R.A. and Stephenson, P.J. (eds.) *The Geology and Geophysics of Northeastern Australia*. Geological Society of Australia, Queensland Division: 229–246.

Robinson, P., Higgins, N.C. and Jenner, G.A., 1986. Determination of rare earth elements, yttrium and scandium in rocks by an ion-exchange–X-ray fluorescence technique. Chemical Geology 55: 121–137.

Ryerson, F.J. and Watson, E.B., 1987. Rutile saturation in magmas : implications for Ti–Nb–Ta depletion in island arc basalts. Earth and Planetary Science Letters 86: 225–239.

Stanton, R.L., 1990. Magmatic evolution and the ore type - lava type affiliations of volcanic exhalative ores. Australasian Institute of Mining and Metallurgy Monograph 14: 101–107.

Stanton, R.L. and Ramsay, W.R.H., 1980. Exhalative ores, volcanic loss, and the problem of the island arc calcalkaline series: a review and an hypothesis. *Norges geologiske undersokelse* 360: 9–57.

Stern, R.J., Lin, P-N., Morris, J.D., Jackson, M.C., Fryer, P., Bloomer, S.H. and Ito, E., 1990. Enriched back-arc basin basalts

from the northern Mariana Trough : implications for the magmatic evolution of back-arc basins. *Earth and Planetary Science Letters* 100: 210–225.

Stolz, A.J., 1991. Stratigraphy and geochemistry of the Mt Windsor volcanics and associated exhalites. *In* Mt Windsor Project Research Report No. 2, CODES, University of Tasmania: 23–83.

Stolz, A.J. and Davies, G.R., 1989. Metasomatised lower crustal and upper mantle xenoliths from north Queensland: Chemical and isotopic evidence bearing on the composition and source of the fluid phase. *Geochimica Cosmochimica Acta* 53: 649–660.

Stolz, A.J., Varne, R., Davies, G.R., Wheller, G.E. and Foden, J.D., 1990. Magma source components in an arc-continent collision zone : the Flores–Lembata sector, Sunda arc, Indonesia. *Contributions to Mineralogy and Petrology* 105: 585–601.

Sun, S.-S. and McDonough, W.F., 1989. Chemical and isotopic systematics of oceanic basalts: implications for mantle composition and processes. In: Saunders, A.D. and Norry, M.J. (eds.) Magmatism in the Ocean Basins. *Geological Society Special Publication* 42: 313–345.

Tarney, J., Saunders,A.D. and Weaver, S.D., 1977. Geochemistry of volcanic rocks from the island arcs and marginal basins of the Scotia arc region. *In* Talwani, M. and Pitman, W.C. III (eds): *Island Arcs, Deep Sea Trenches and Back-Arc Basins.* American Geophysical Union, Washington, DC: 367–377.

Urabe, T., 1987. Kuroko deposit modeling based on magmatic hydrothermal theory. *Mining Geology* 37: 159–176.

Volpe, A.M., Macdougall, J.D. and Hawkins, J.W., 1988. Lau Basin basalts (LBB): trace element and Sr–Nd isotopic evidence for heterogeneity in back-arc basin mantle. *Earth and Planetary Science Letters* 90: 174–186.

Whitford, D.J., McPherson, W.P.A. and Wallace, D.B., 1989. Geochemistry of the host rocks to the volcanogenic massive sulfide deposit at Que River, Tasmania. Economic Geology 84: 1-21.

Whitford, D., Crawford, T., Korsch, M. and Craven, S., 1990. The Mt Read Volcanics; strontium and neodymium isotope geochemistry. CSIRO Division of Exploration. *Geoscience Exploration Research News* 4: 11.

Winchester, J.A. and Floyd, P.A., 1977. Geochemical discrimination of different magma series and their differentiation products using immobile elements. *Chemical Geology* 20: 325–344.

Withnall, I.W., Black, L.P. and Harvey, K.J., 1991. Geology and geochronology of the Balcooma area: part of an early Palaeozoic magmatic belt in north Queensland. *Australian Journal of Earth Sciences* 38: 15–29.

Wood, D.A., Gibson, I.L. and Thompson, R.N., 1976, Element mobility during zeolite facies metamorphism of the Tertiary basalts of eastern Iceland. *Contributions to Mineralogy and Petrology* 55: 241–254.

Mineralisation and Alteration Module

Team members

J. Bruce Gemmell
Robina Sharpe
Mark Doyle
Russell Fulton
Garry Davidson
Anthea Hill
Karin Orth

Introduction

In the past there has been considerable research on alteration geochemistry of VHMS systems. Our research is not to repeat previous work but to break new ground, utilising a multi-disciplinary approach at the ore deposit scale, with emphasis on selective geochemical techniques.

The specific aims of this module are:

- To undertake case studies of alteration halos related to specific VHMS deposits with particular emphasis on footwall and hangingwall alteration zonation, and the relationship between alteration patterns and volcanic facies.

- To develop a set of vectors towards ore, based on the ore deposit specific studies, that can be applied in the exploration for VHMS deposits in submarine volcanic sequences throughout Australia. The vector matrix will include:
  - hangingwall alteration vectors
  - exhalite vectors
  - vectors based on mineral chemistry (e.g. chlorite, sericite, carbonate)
  - vectors based on whole-rock oxygen isotopes
  - vectors based on sulfur isotopes
  - vectors based on C/O isotopes in carbonates.
  - vectors based on volcanic facies factors

Deposit case studies

Case studies will be conducted on selected ore deposits from the Mount Read Volcanics, Mount Windsor Volcanics and Murchison Province of Western Australia in order to develop alteration halo models and integrate these with the vectors analysis.

The deposits for study in the MRV:

- **Hellyer**
  Bruce Gemmell and Cliff Stanley (MDRU-UBC). This new research will focus on determining subtle geochemical and isotopic halos in the hangingwall basalt and black shale sequence and the footwall andesite—extending up to several kilometres from the deposit. This study will involve interpretation of whole rock geochemistry using Pearce Element ratios.

  Russell Fulton and Bruce Gemmell. Investigation of the mineral chemical variation in hydrothermal minerals (in particular sericite, carbonate, chlorite) of the hangingwall alteration.

- **Rosebery**
  A project on the mineralogy and mineral chemistry of the carbonate alteration is proposed.

- **Henty**
  No published data are available on alteration associated with the Henty gold deposit. A detailed halo study is under negotiation.

- **Mount Lyell**
  See Bill Wyman's section in the Regional Geochemistry/Petrology Module (p. 57).

The deposits for study in the MWV:

- **Thalanga**
  Two studies are currently underway at Thalanga.:
  1. Anthea Hill is completing her PhD research entitled "Geology and geochemistry of the Thalanga massive sulfide deposit, Queensland"
  2. Holger Paulik has just returned from his initial field season at Thalanga where he is undertaking "a comparison of volcanic facies architecture and alteration styles of felsic and mafic volcanic host sequences to massive sulfide deposits —Thalanga, North Queensland and Teutonic Bore, Western Australia".

- **Highway–Reward**
  These are unusual pyrite–chalcopyrite pipes that may show different alteration patterns and vectors when compared with other VHMS deposits. This work could form part of the on-going PhD study by Mark Doyle entitled "Volcanic facies and mineralisation, Highway–Reward Cu–Au deposit, Queensland".

- Garry Davidson and Joe Stolz. Geology and geochemistry of volcanic associated Fe formations, vectors to VHMS mineralisation. Field work will be conducted in the Mount Windsor Volcanics in late 1995.

The deposits for study in the Archean Murchison province:

- **Gossan Hill**
  Robina Sharpe is currently in the second field season of her PhD research entitled "Mineralisation, alteration and structure of the Gossan Hill Cu-Zn VHMS deposit, WA: implications for ore genesis and exploration".

- **Teutonic Bore**
  Although Holger Paulik's PhD thesis will be investigating the alteration associated with the Teutonic Bore deposit, no field work has been undertaken to date. It is anticipated that Holger will begin field work at Teutonic Bore in mid 1996.

Collaboration with other research groups

This project will involve collaboration with two other research groups working on hydrothermal alteration in Canada.

1. Mineral Deposit Research Unit (MDRU) at the University of British Columbia which has an industry/NSERC funded project on "Lithogeochemical exploration for metasomatic alteration zones associated with hydrothermal mineral deposits". Principal investigators are Professor A.J. Sinclair and Dr C.R. Stanley.

2. Geological Survey of Canada based in Ottawa, which has a Mining Industry Technology Council in Canada (MITEC) funded research project on "The roles of regional-scale alteration zones and subvolcanic intrusions on the generation of volcanic-associated massive sulfide deposits". Principal investigators are Drs A.G. Galley, H.L. Gibson, M.D. Hannington, B.E. Taylor and D.H. Watkinson.

Discussions have been held with the principal representatives of these two groups in order to develop a framework for collaboration in the areas of overlap within our three projects. It is planned that during the course of the three projects, joint meetings will be held to exchange research results and models. Dr Cliff Stanley visited CODES in May, 1995 and conducted two days of field work with Bruce Gemmell at Hellyer. Drs Mark Hannington and Allan Galley hope to visit Australia in mid to late 1996.

In addition to the international collaboration, collaboration will also occur with Industry, Safety and Mines (formerly Mineral Resources Tasmania) in the mapping, collection and analysis of rocks from the Mount Read Volcanics and with the Key Centre for Strategic Minerals, UWA, in the studies on Archean VHMS deposits in the Golden Grove district.

Lithogeochemical Exploration for Metasomatic Alteration Zones using Pearce Element Ratios: Hellyer Case Study

Clifford R. Stanley and J. Bruce Gemmell

Mineral Deposit Research Unit, Department of Geological Sciences, University of British Columbia; and Centre for Ore Deposit and Exploration Studies, Geology Department, University of Tasmania

Many mineral deposits have associated hydrothermal alteration zones that envelop the mineralization and thus are larger than the deposits themselves. As a result, these zones constitute ideal intermediate exploration targets that may be used as guides to mineralization. This study intends to improve lithogeochemical exploration methods to enhance a geologist's ability to locate, identify and understand these hydrothermal alteration zones, and thus improve their chances of discovering associated mineral deposits. This will be accomplished by (i) developing a numerical methodology, founded on simple yet sound theory, that may be used to quantify the metasomatism that accompanied the hydrothermal reactions responsible for the alteration zones and (ii) investigate the Hellyer alteration system in order to test the lithogeochemical exploration methodology. In short, the goal of this project is to provide an improved exploration tool for the AMIRA participants, supply them with the means to use this tool, and equip them with the geological criteria and knowledge to effectively direct its use.

Background

The principal sources of geochemical variation observed in host rocks of VHMS deposits are (i) measurement error, including error during sampling (nugget effect) and analysis, (ii) closure, a mathematical artifact caused by the requirement that a rock composition sum to 100%, preventing the manifestation of differences in rock composition from directly reflecting the actual changes that have occurred in the rock, (iii) fractionation, systematic geochemical variations produced by crystal or volatile separation from a melt, and by crystal sorting; present before mineralising fluids alter these rocks, (iv) compositional mixing, mechanical mixing of rocks of different genesis and composition (e.g. volcaniclastics with exotic clasts) and (v) metasomatism, material transfer associated with chemical reactions between mineralising fluids and host rocks.

Lithogeochemistry has traditionally been used in mineral exploration to locate hydrothermal alteration zones associated with volcanic-hosted massive sulphide (VHMS) deposits. Examples include the numerous Na and Ca depletion anomalies identified in the volcanic footwalls to many VHMS deposits. In many cases, these anomalous zones contributed to the discovery of the deposits. Unfortunately, these lithogeochemical anomalies may sometimes be difficult to identity. This is because (i) the processes that produce these lithogeochemical anomalies are not restricted to only those responsible for hydrothermal mineral deposits, (ii) pre-existing lithogeochemical variations in the host rocks can obscure these anomalous patterns and prevent their identification, (iii) many elements do not necessarily display consistent lithogeochemical patterns in the alteration zones (e.g. K in VHMS footwalls), and (iv) the effect of closure, a mathematical peculiarity that introduces spurious numerical variations to concentration data. can obscure any real lithogeochemical pattern that does exist. All of these factors can make it difficult to confidently identity anomalous lithogeochemical patterns associated with the alteration zones related to hydrothermal mineral deposits.

A number of numerical approaches, all of which avoid the spurious effects of closure in concentration data, have been developed to quantity the effects of

metasomatism (Akella, 1966; Gresens, 1967; Grant, 1986; MacLean and Barrett, 1993). Recently, theoretical advances in Pearce element ratioanalysis (PER) (Russell and Stanley, 1990; Stanley and Madeisky, 1993) have also allowed its use to study various types of material transfer processes, including metasomatic processes associated with hydrothermal alteration and mineral deposit genesis. Whereas PER was originally used to study fractionation processes in igneous systems (e.g. Russell and Stanley 1990), Stanley and Madeisky (1993) have demonstrated how PER can also be used effectively in lithogeochemical exploration for several types of hydrothermal mineral deposits. One of their significant discoveries was that the magnitude of pre-existing lithogeochemical variability in VHMS deposit host rocks (i.e. the background variations caused by phenocryst sorting in the host volcanics) may, in many cases. be as large as the variations produced by the metasomatism that accompanied deposit genesis. Previous numerical approaches that lack the ability to model and remove the pre-existing lithogeochemical variability are unable to accurately quantity the effects of metasomatism because of this background 'noise'. The ability to avoid the effects of closure and to model and remove the effects of pre-existing lithogeochemical variations (fractionation) make PER analysis a superior tool in lithogeochemical exploration for igneous rock-hosted hydrothermal mineral deposits. With this methodology, even subtle metasomatic effects that would otherwise be obscured by the background lithogeochemical variability can readily be identified.

Preliminary application of the PER methodology to VHMS deposits has already resulted in several new observations with significant exploration import. in the Rio Tinto VHMS camp, the most evolved portions of the footwall rhyolite appear to be spatially associated with the deposits, and are the most metasomatized. This suggests that the degree of petrologic evolution, along with the degree of metasomatism, may constitute important exploration parameters for VHMS deposits (Stanley and Madeisky 1993). Furthermore, explanations for common observations made during lithogeochemical exploration have also been discovered using PER's. In VHMS footwalls, K is known to generally be a less effective exploration tool for discovering footwall alteration zones to VHMS deposits than Na or Ca (personal communication, Dr. Steve Juras, 1993). This is because K can be added or lost during the formation of a quartz-muscovite-pyrite alteration zone. PER analysis has demonstrated that this variable lithogeochemical behavior is dependent on the original feldspar composition and (Na+K)/Al ratio of the volcanic host rocks (Stanley and Madeisky, unpublished work). Because it is unlikely that these discoveries could be made using a numerical methodology that could not remove the effects of pre-existing background lithogeochemical variation, significant advantages can be gained through use of the PER technique in lithogeochemical exploration.

The theoretical basis for PER analysis requires that (1) at least one conserved element be present (an element that is "incompatible" during igneous fractionation and "immobile" during hydrothermal alteration), (2) the rocks be related to a common parent that was at one time homogeneous (at least with respect to the conserved element) and (3) at least one material transfer process has acted to create the geochemical variability observed in these rocks. The PER approach uses a ratio formulation (computer spreadsheet) where the material transfer equation is expressed in molar terms using a conserved constituent (element) in the ratio denominator. This causes the PER to be directly proportional to the amount of material transfer in the numerator element. By using a mole instead of mass concentrations in PER analysis the resulting material transfers can be related directly to mineral formulae and chemical reactions (Stanley and Madeisky, 1993). This allows solid-solution mineral composition variations to be accommodated and allows development of linear fractionation models which can represent the geochemical heterogeneity in volcanic rocks before the advent of hydrothermal alteration. PER analysis overcomes the effects of closure and also allows geochemical variations associated with fractionation and crystal sorting to be recognised and accommodated. It has been demonstrated that the magnitude of pre-existing lithogeochemical variability in VHMS deposit host rocks (i.e. background variations caused by phenocryst sorting in host volcanics) may, in many cases, be as large as the variations produced by the alteration).

A study of alteration in a variety of felsic hosted VHMS deposits (Archean to Mesozoic, zeolite to middle amphibolite metamorphic grades) by PER

analysis by Madeisky and Stanley (1994) concluded that the patterns of metasomatic additions and losses in both quartz-sericite and quartz-chlorite alteration zones are surprisingly consistent among deposits. Fluid-rock (buffered) reactions include the common Na and Ca metasomatic losses as well as the addition of K, an often erratic behaviour that is controlled by the primary K/Na ration (alkali feldspar) and Al budget of the host rocks, and the stability of sericite. The behaviours of chalcophile elements (Cu, Pb, Zn, Ag, Au) can be explained in terms fluid only (unbuffered) reactions within specific alteration mineral stability fields, and the mass transfer of other trace elements (Sr, Rb, Ba, Cr, Ni, Mn) corresponds with camouflaging major element behaviour. Environments where Al is mobile in the hydrothermal fluids appear to be restricted (Madeisky and Stanley, 1994). To date there has not been a study using PER to a VHMS system hosted by intermediate to mafic volcanics, this is why Hellyer was choosen and will make an excellent case study.

The recent development of the above numerical methodologies to study material transfer processes provides a unique opportunity to (i) study metasomatic processes at a level of rigor previously unattainable, leading to a better geological and geochemical understanding of hydrothermal mineral deposits and the processes that formed them, and (ii) develop effective, theoretically-based strategies, methodologies and models for use in lithogeochemical exploration for hydrothermal mineral deposits. The ability of PER analysis to avoid the effects of closure and to model and remove the effects of pre-existing lithogeochemical variations (fractionation) make PER analysis a superior tool in lithogeochemical exploration for igneous rock-hosted VHMS deposits (Stanley and Madeisky, 1993).

Research

This research project can be divided into three basic objectives. These are: (i) to develop a new, effective lithogeochemical exploration methodology, (ii) to produce dedicated computer software with which to implement this methodology, and (iii) to test this methodology, expand its application, improve its results, and identify sound strategies for its use in exploration.

Hellyer Case Study

As the lithogeochemical signature of the footwall (Gemmell and Large, 1992) and hangingwall (Jack, 1989) alteration at Hellyer has previously been investigated and is well charcterised this study will concentrate on the lithologies surrounding the deposit to detect a regional lithogeochemical signature. At Hellyer, data from Jack (1989), Gemmell (1990), Gemmell and Large (1992), Sinclair (1994) and unpublished Aberfoyle data will be used in conjunction with new analyses for the Pearce Element lithogeochemical study. In May, 1995 Cliff and Bruce made a field visit to Aberfoyle's Burnie exploration office to collect drill logs and geochemical data, including the pulps from Jack's Masters thesis. This project will be broken down into two parts: (i) previous data from both the footwall and hangingwall alteration zones will be interpreted to determine the systematics of the intense alteration and (ii) new samples and previous data from the immediate footall and hangingwall lithologies away from the alteration zones will be analysed to determine vectors towards the alteration and mineralisation. In addition ninety new samples were collected from the Hellyer basalt, Que River Shale and the footwall andesite in drill holes up to 4 km away surrounding Hellyer (Table 1). For the purpose of this investigation no footwall polymict debris flow material will be analysed.

These samples are currently being crushed in a W carbide pulverizer and will be analysed by lithium mets borate frisioll XRF whole rock analysis for SiO_2, TiO_2, Al_2O_3, Fe_2O_3, MnO, MgO, CaO, Na_2O, K_20, P_20_5 and LOI and by pressed pellet or fused disk for Ni, Cr, V, Zr, Y, Sc, La, Sr, Rb, Ba, Cu, Pb, Zn, Au, Ag, Nb, TI, Se, Sb, Cd and Mo. In addition both H_2O+ and CO_2 contents will be determined. The samples will be analysed at the University of Tasmania.

Initial results and interpretations will be presented at the next AMIRA meeting.

References

Akella, J., 1966. Calculation of material transport in some metasomatic processes. *Neues Jahrbuch ftr Mineralogische Abhandlungen* 104, pp. 316-329.

Gemmell, J.B., 1990. Hellyer Stringer Zone Project: Progress Report 3. Unpublished report, Aberfoyle Resources Ltd (Australia), 76 pp.

Gemmell, J.B. and Large, R.R., 1992. Stringer system and alteration zones underlying the Hellyer volcanogenic massive sulphide deposit, Tasmania, Australia. *Economic Geology* 87(3): 620-649.

Grant, J.A., 1986. The isocon diagram — A simple solution to Gresens' equation for metasomatic alteration. *Economic Geology* 81: 1976-1982.

Gresens, R.L. (1967): Composition-Volume Relationships in Metasomatism. Chemical Geology, Vol. 2, pp. 47-55.

Jack, D.J., 1989, Hellyer host rock alteration: Unpublished MSc thesis, University of Tasmania: 182 pp.

MacLean, W.H. and Barrett, T.J., 1993. Lithogeochemical techniques using immobile elements. *Journal of Geochemical Exploration* 48: 109-133.

Russell, J.K. and Stanley, C.R., 1990. Theory and application of Pearce Element Ratios to geochemical data analysis. Geological Association of Canada, Short Course 8, Vancouver, BC: 310 pp.

Sinclair, B.J., 1994. Geology and geochemistry of the Que River Shale, western tasmania. Unpublished BSc (Hons) thesis, University of Tasmania.

Stanley, C.R. and Madeisky, H.E., 1993. Pearce Element ratio analysis: Applications in lithogeochemical exploration. Mineral Deposit Research Unit, Dept. of Geological Sciences, Univ. of British Columbia, Short Course 13, Vancouver, British Columbia: 540 pp.

Table 1. Drill holes sampled for the Hellyer Pearce Element Ratio Study

HL 14	HAT 4*
	HAT 8*
HL 15	HAT 9*
HL 26*	
HL 30	MAC 4*
HL 31	MAC 10*
HL 35A	MAC 11*
HL 39	MAC 15
HL 50	MAC 17
HL 57	MAC 19*
HL 61	MAC 21*
HL 80*	MAC 25*
HL 246*	MAC 31*
HL 306	
HL 345	
HL 345A	MC 12*
HL 469	
HL 469B	
HL 469C	
HL 541*	

* New samples collected from these holes. Pre-existing lithogeochemical data from the other holes by Aberfoyle, Jack (1989), Gemmell (1990), Gemmell and Large (1992) and Sinclair (1994) will also be analysed in this study.

Hellyer Hangingwall Alteration Study

Russell Fulton and J. Bruce Gemmell
Centre for Ore Deposit and Exploration Studies, Geology Department, University of Tasmania

Hangingwall alteration has only been documented in a few Australian VHMS deposits (e.g. Hellyer — Jack, 1989; Scuddles — Ashley et al., 1988; Mt Chalmers — Large, 1992). In general the effects of hangingwall alteration is subtle and can extend for tens to hundreds of metres into post-ore volcanics.

In this project we will focus on the mineralogy, mineral chemistry and whole rock geochemistry of hangingwall alteration at Hellyer in order to develop a more complete database and determine vectors to mineralisation.

Jack (1989) studied the hangingwall alteration at Hellyer based on the initial surface exploration drilling. His study documented the alteration mineralogy and the gross geochemical signature of this alteration. Little mineral chemistry data was generated in Jack's (1989) study.

Our study will focus on the detail of the alteration mineralogy, mineral chemistry of specific phases (fuchsite-sericite, carbonate and chlorite) and a re-evaluation of the whole-rock geochemistry. To begin with we will utilise Jack's (1989) thesis thin section collection of the hangingwall alteration (Table 1) for a detailed investigation of the alteration mineralogy, paragenesis, zonation and mineral chemistry. Jack's (1989) whole rock data will then be re-evaluated inlight of the results of the mineralogical study. Jack's thin section collection and whole-rock geochemical data was collected from Aberfoyle's Burnie Exploration office in August, 1995. It is anticipated that additional samples will be collected from the initial surface drilling and subsequent underground drilling in 1996.

This study will be the thesis project for Russell Fulton's Master of Economic Geology degree. Russell will begin this research in November 1995 and initial results from this research will be presented at the next AMIRA meeting.

References

Ashley, P.M., Dudley, R.J., Lesh, R.H., Marr, J.M., and Ryall, A.W., 1988. The Scuddles Cu–Zn prospect, an Archean volcanogenic massive sulfide deposit, Golden Grove district, Western Australia. *Economic Geology* 83: 918–951.

Jack, D.J., 1989. Hellyer host rock alteration: Unpublished MSc thesis, University of Tasmania: 182 pp.

Large, R.R., 1992. Australian volcanic-hosted massive sulphide deposits: features, styles and genetic models. *Economic Geology* 87: 471-510.

Table 1. Hellyer hangingwall alteration samples.

SAMPLE #	HOLE	DEPTH	SAMPLE TYPE	NORTHING	EASTING	R.L.	THIN SECTION
272844	HL7	66.4	TC	10600.3	5567.8	642.3	
333916	HL14	85.0-89.6	AG	10500.1	5408	618.3	
333917	HL14	89.6-92.0	AG	10500	5409.5	616.5	
333918	HL14	92.0-112.0	AG	10499.4	5422	600.9	
333919	HL14	112.0-118.0	AG	10499.2	5425.8	596.2	
333920	HL14	118.0-121.0	AG	10499	5427.6	593.9	
333921	HL14	121.0-144.8	AG	10498	5442.6	575.4	
333922	HL14	144.8-187.0	AG	10495.8	5469.5	543	
333923	HL14	187.0-189.0	AG	10495.6	5470.8	541.5	
333924	HL14	189.0-199.0	AG	10495.1	5477.2	533.8	
333925	HL14	199.0-201.8	AG	10494.9	5479	531.6	
333926	HL14	201.8-213.0	AG	10494.3	5486.2	523.1	
333927	HL14	213.0-223.0	AG	10493.7	5492.7	515.5	
333928	HL14	223.0-225.4	AG	10493.5	5494.2	513.7	
333929	HL14	225.4-230.87	AC	10493.2	5497.8	509.6	
333930	HL14	230.87-234.1	AC	10493	5499.9	507.1	
333969	HL14	49	MC	10500.8	5381.9	649.4	√
333970	HL14	75.81	MC	10500.4	5399.2	629	√
333971	HL14	106.97	MC	10499.6	5418.9	604.8	√
333973	HL14	139.27	MC	10498.2	5439.1	579.7	√
333974	HL14	177.38	MC	10496.3	5463.3	550.4	√
333975	HL14	198.66	MC	10495.1	5477	534.1	√
333976	HL14	224.5	MC	10493.6	5493.6	514.4	√
333977	HL14	226.5	MC	10493.4	5495	512.9	√
333978	HL14	234	MC	10493	5499.9	507.2	√
333994	ADIT	857	MR	10718.6	6105.3	390.8	√
333995	ADIT	823	MR	10708.4	6137.8	390.5	√
333996	ADIT	805	MR	10703	6155	390.3	√
333997	ADIT	805	MR	10703	6155	390.3	√
333998	ADIT	790	MR	10698.5	6169.3	390.1	√
333999	ADIT	782	MR	10696.1	6176.9	390.1	√
334001	HL55	64.0-91.2	TG	10896	5895.1	603	
334002	HL55	91.2-145.0	TG	10893.9	5876.6	552.5	
334003	HL55	145.0-152.8	TG	10893.6	5874	545.1	
334004	HL55	152.8-259.1	TG	10893	5865.2	519.9	
334005	HL55	179.5-210.3	TG	10892.7	5854.6	491	
334006	HL55	210.3-225.0	TG	10892.8	5849.4	477.3	
334007	HL55	225.0-233.8	TG	10892.8	5846.3	469	
334008	HL55	233.8-241.0	TG	10892.9	5843.7	462.3	
334009	HL55	241.0-258.0	TG	10893.1	5837.6	446.5	
334010	HL55	258.95-259.1	TG	10893.1	5837.2	445.4	
334011	HL55	73.5	TC	10896.8	5901.3	619.5	
334012	HL55	83.3	TC	10896.3	5897.9	610.3	√
334013	HL55	89.5	TC	10896	5895.7	604.5	
334014	HL55	92	TC	10895.9	5894.8	602.2	
334015	HL55	100.05	TC	10895.6	5892	594.7	
334016	HL55	100.7	TC	10895.5	5891.8	594.1	√
334017	HL55	101.8	TC	10895.5	5891.4	593	
334018	HL55	102.9	TC	10895.4	5891.1	592	
334019	HL55	112	TC	10895	5887.9	583.5	
334020	HL55	116.45	TC	10894.9	5886.4	579.3	√
334021	HL55	116.7	TC	10894.9	5886.3	579.1	
334022	HL55	123.5	TC	10894.6	5883.9	572.7	
334023	HL55	125.05	TC	10894.5	5883.4	571.2	
334024	HL55	129.2	TC	10894.4	5882	567.3	
334025	HL55	129.65	TC	10894.4	5881.8	566.9	
334026	HL55	133.7	TC	10894.2	5880.5	563.1	√

Table 1 cont.

334027	HL55	141.2	TC	10894	5877.9	556.1	
334028	HL55	151.7	TC	10893.7	5874.4	546.2	
334029	HL55	153.6	TC	10893.6	5873.7	544.4	
334030	HL55	154.2	TC	10893.6	5873.5	543.8	
334031	HL55	157.85	TC	10893.5	5872.3	540.4	√
334032	HL55	165.5	TC	10893.3	5869.8	533.2	
334033	HL55	167.1	TC	10893.3	5869.3	531.7	
334034	HL55	176	TC	10893	5866.3	523.3	√
334035	HL55	183.55	TC	10892.9	5863.9	516.1	
334036	HL55	189.6	TC	10892.7	5861.9	510.4	√
334037	HL55	191.15	TC	10892.7	5861.4	508.9	
334038	HL55	193.5	TC	10892.8	5860.4	506.8	√
334039	HL55	198.4	TC	10892.8	5858.8	502.2	
334040	HL55	203	TC	10892.8	5857.2	497.9	
334041	HL55	207.85	TC	10892.7	5855.5	493.3	
334042	HL55	218.5	TC	10892.8	5851.7	483.3	
334043	HL55	223.35	TC	10892.8	5850	478.8	
334044	HL55	227.9	TC	10892.8	5848.4	474.6	
334045	HL55	232.2	TC	10892.8	5846.9	470.5	√
334046	HL55	239.4	TC	10892.9	5844.3	463.8	
334047	HL55	247	TC	10893	5841.6	456.7	
334048	HL55	257.5	TC	10893.1	5837.8	446.9	
334099	HL79	379.1	TC	11060.8	5971.4	313.3	
334067	HL30	188	TC	10902.9	5513.6	506.5	√
334068	HL30	204.4	TC	10902.8	5519.4	491.2	
334069	HL30	218.1	TC	10902.7	5524.3	478.4	
334070	HL30	243	TC	10902.4	5533.2	455.2	
334071	HL30	268.5	TC	10901.8	5542.5	431.4	
334072	HL30	274.5	TC	10901.7	5544.7	425.8	
334072	HL30	274.4	TC	10901.7	5544.7	425.9	
334072	HL30	274.5	TC	10901.7	5544.7	425.8	
334073	HL30	275.3	TC	10901.6	5545	425.1	
334074	HL30	278.7	TC	10901.5	5546.2	421.9	
334108	HL30	186.9-200.0	TG	10902.8	5517.9	495.3	
334109	HL30	200.0-263.0	TG	10902	5540.5	436.5	
334110	HL30	263.0-272.4	TG	10901.7	5543.9	427.8	
334111	HL30	272.4-278.3	TG	10901.5	5546.1	422.3	
334112	HL30	278.3-278.8	TG	10901.5	5546.3	421.8	
334113	HL30	278.8-283.4	TG	10901.4	5548	417.6	
334134	HL31	102.0-105.0	TG	10889.8	6009.5	588.3	
334135	HL31	105.0-126.8	TG	10887.8	6001.2	568.3	
334136	HL31	126.8-142.0	TG	10886.2	5995.4	554.3	
334137	HL31	142.0-172.5	TG	10883.1	5983.5	526.4	
334138	HL31	172.5-188.0	TG	10881.4	5977.3	512.2	
334139	HL31	188.0-195.0	TG	10880.7	5974.5	505.9	
334140	HL31	195.0-205.0	TG	10879.6	5970.4	496.8	
334141	HL31	205.0-220.9	TG	10877.9	5963.8	482.5	
334142	HL31	220.9-284.0	TG	10872.2	5937.2	425.5	
334143	HL31	284.0-288.4	TG	10871.9	5935.4	421.5	
334144	HL31	288.4-308.6	TG	10870.8	5926.8	403.3	
334145	HL31	308.6-324.2	TG	10870	5920.1	389.2	
334049	HL31	316.15	TC	10870.4	5923.6	396.5	√
334162	HL6	208.4	TC	10498.4	5830.1	563.9	
334171	HL5	284.5	TC	10707.1	5746.9	466	√
334172	ADIT	697	MR	10670.7	6258	389.2	√
334174	ADIT	717	MR	10676.6	6238.9	389.4	√
334175	ADIT	737	MR	10682.6	6219.8	389.6	√
334176	ADIT	755	MR	10688	6202.7	389.8	√
334177	ADIT	719	MR	10677.2	6237	389.4	√

Table 1 cont.

334191	HL50	243.83	AC	10743	5775.1	494.9	√
334192	HL50	262.22	AC	10742.4	5765.4	479.3	√
334193	HL50	282.9	AC	10741.7	5754.5	461.8	√
334194	HL50	299.09	AC	10741.1	5745.9	448	√
334195	HL28	139.6	AC	10901.6	5760	562.8	√
334196	HL28	145.5	AC	10901.2	5762.6	557.5	√
334197	HL28	157.96	AC	10900.2	5768.1	546.4	√
334198	HL28	169.61	AC	10899.3	5773.3	536	√
334199	HL28	170.32	AC	10899.2	5773.6	535.3	√
334200	HL28	173.32	AC	10899	5774.9	532.6	√
334201	HL28	187.96	AC	10897.7	5781.3	519.6	√
334202	HL28	208.27	AC	10895.9	5790.3	501.4	√
334203	HL28	228.87	AC	10894.2	5799.6	483.1	√
334204	HL28	234.63	AC	10893.7	5802.2	478	√
334205	HL28	249.14	AC	10892.4	5808.8	465.1	√
334206	HL28	265.76	AC	10891.1	5816.5	450.5	√
334207	HL57	222.58	AC	10746.2	5752.4	538.8	√
334208	HL57	229.19	AC	10746.2	5747.7	534.1	√
334209	HL57	245.43	AC	10746.2	5736.3	522.6	√
334210	HL57	271.3	AC	10745.7	5718.1	504.2	√
334211	HL57	286.82	AC	10745.3	5707.3	493.1	√
334212	HL57	296.5	AC	10745	5700.5	486.2	√
334213	HL57	305.14	AC	10744.8	5694.4	480	√
334214	HL57	312.88	AC	10744.6	5689	474.5	√
334215	HL57	317.68	AC	10744.5	5685.6	471.1	√
334216	HL57	322.25	AC	10744.4	5682.4	467.9	√
334222	HL57	323.53	AC	10744.4	5681.5	467	√
334223	HL57	326.62	AC	10744.4	5679.3	464.8	√
334217	HL24	217.43	AC	10744.5	5685.8	471.3	√
334218	HL24	232.62	AC	10909.3	5764.3	464.5	√
334219	HL24	246.1	AC	10909	5768.3	451.6	√
334220	HL24	249.31	AC	10908.9	5769.2	448.6	√
334221	HL24	252.8	AC	10908.8	5770.3	445.2	√
334265	HL24	183.0-187.9	AG	10910.1	5751.3	507.3	
334266	HL24	187.9-199.5	AG	10909.9	5754.7	496.2	
334267	HL24	199.5-203.9	AG	10909.8	5755.9	492	
334268	HL24	203.9-211.2	AG	10909.7	5758.1	485	
334269	HL24	211.2-220.0	AG	10909.5	5760.6	476.6	
334270	HL24	220.0-251.6	AG	10908.9	5769.9	446.4	
334271	HL24	251.6-253.9	AG	10908.8	5770.6	444.2	

The following data is available for all samples

Whole Rock Chemistry

SiO_2, TiO_2, Al_2O_3, FeO, MnO, MgO, CaO, Na_2O, K_2O, P_2O_5, L.O.I.

Trace Element Chemistry

Cu, Pb, Zn, Sr, Y, Zr, Ni, Cr, Ba, Sc, La, As, Ag, Rb, V, Nb, S,

Key:

Sample type - M = Tasmanian Mines Dept, Launceston. XRF
T = Geology Dept, Universuty of Tasmania. XRF
A = AMDEL. ICP, AAS, XRF

G = continuous core grind
C = split core sample
R = rock grab sample

Rosebery Site Study

Ross Large
Centre for Ore Deposit and Exploration Studies, Geology Department, University of Tasmania

Aim

- To determine distribution and geochemistry of carbonate alteration related to the Rosebery VHMS deposit
- To develop geochemical and isotope vectors to ore in carbonate altered volcanics; hangingwall, footwall and along strike.

Research plan

- Summarise the results of previous work on the geochemistry of host rocks and related hangingwall and footwall volcanics at Rosebery — from PhD, MSc and Honours theses and available non-confidential company reports.
- Sampling of drill core to give a three-dimensional data set of alteration in the hangingwall, footwall and along-strike from one of the Northern ore lenses.
- Whole-rock and selected trace element analyses of samples in order to relate carbonate trends to whole-rock geochemical trends.
- Analyses of selected acid digests to study carbonate chemistry.
- Microprobe analyses of carbonate minerals.
- Carbon and oxygen isotope analyses on selected samples.
- Compilation of analytical data on cross section and plan to relate chemical variations to the ore lens position..
- Development of an alteration vector matrix.

Ore lens for study

The ore lens selected for study will ideally have the following characteristics:

- be at the north end of the mine away from the effects of the Devonian granite
- be known to have associated carbonate alteration
- be a mineable ore lens of typical Rosebery grade and significant tonnage
- have boundaries defined by relatively close spaced drilling
- have a number of drill holes which intersect the barren 'ore position' along-strike for a considerable distance (say, ideally, 100–500 m)

Who will do the study

The study will be undertaken by a post-graduate research student or a post-doctoral fellow in collaboration with Professor Ross Large.

When

Depending on the availability of a suitable student, or Research Fellow, the project will commence in about August 1995.

Support required from Pasminco

- Access to previous non-confidential geochemical data on the Rosebery deposit
- Logistics support on-site
- Accommodation at Rosebery as part of the in-kind support for the ARC-AMIRA Collaborative project

Reporting

It is expected that the project will take 12 months to complete. Six-monthly reports will be provided to Pasminco as part of the reporting schedule required by AMIRA.

Textures and origins of carbonate associated with the volcanic-hosted massive sulfide deposit at Rosebery, Tasmania

Anthea Hill and Karin Orth

Introduction

Carbonate-bearing rocks are commonly associated with volcanic-hosted massive sulfide (VHMS) deposits but have been overlooked in many ore genesis models (e.g. Lydon, 1988). Numerous deposits in Australia are associated with carbonate including Scuddles (Archaean), Hellyer, Que River, Hercules, and Rosebery (Cambrian), Thalanga (Cambrian–Ordovician), Captain's Flat, Mt Bulga, Breadalbane (Upper Ordovician-Lower Devonian), and Mt Chalmers (Permian). The carbonates have been interpreted either as exhalative (e.g. Large and Both, 1980; McLeod and Stanton, 1984; Ashley et al., 1988; Gregory et al., 1990), or the result of hydrothermal alteration associated with massive sulfide mineralization (e.g. Gemmell and Large, 1992; Khin Zaw and Large, 1992; Hill and Orth, 1994).

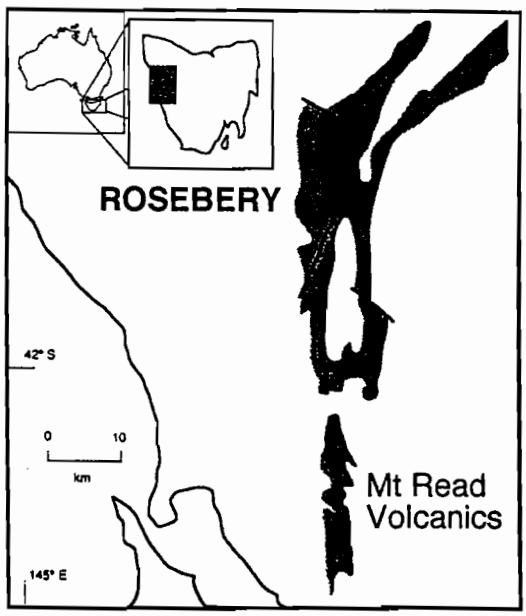

FIG. 1. Location of Rosebery in the Mount Read Volcanics, western Tasmania (after Large, 1992).

Centre for Ore Deposit and Exploration Studies, Geology Department, GPO Box 252C, Hobart, Tasmania, Australia 7001

Dixon (1980) described the mineralogy, textures, and distribution of carbonates at Rosebery in western Tasmania. Our study rexamines and re-interprets the Rosebery carbonate textures in the light of recent volcanological studies (Allen and Cas, 1990; McPhie and Allen, 1992) which demonstrate that the deposit occurs in the upper part of a graded pumiceous mass-flow deposit. This textural study shows that the pumice clasts are altered to carbonate and we suggest that Rosebery is partly a subsea-floor replacement deposit.

The Rosebery deposit is hosted by the Middle to Late Cambrian Mount Read Volcanics, a 200 × 20 km volcanic belt of dominantly felsic lavas and volcaniclastic rocks (Corbett, 1989, 1992) (Fig. 1). Corbett (1992) and McPhie and Allen (1992) outline the stratigraphy, volcanic facies associations, and geological setting of the Mount Read Volcanics. The Mount Read Volcanics host several important VHMS deposits, including Mount Lyell, Hellyer, Que River, Hercules, and South Hercules. The geology of these deposits is reviewed by Large (1992).

Geology of the Rosebery deposit

The geology and geological setting of the Rosebery VHMS deposit are documented by Brathwaite (1972, 1974), Green et al. (1981), Green (1983), Corbett and Lees (1987), Corbett (1992), and Allen and Cas (1990). Recent textural studies by Allen and Cas (1990) have

shown that the thick footwall units were emplaced by subaqueous pumiceous and variably crystal-rich mass flows sourced from nearby subaerial or shallow water environments. The graded top of the youngest thick pumiceous mass flow deposit and other thinner graded pumiceous mass-flows (the "host rocks") host the orebody (Fig. 2), and are overlain by pyritic black mudstone ("black slate") and thinner, quartz-bearing volcaniclastic mass-flow units ("hangingwall pyroclastics").

The stratiform Rosebery orebody is composed of multiple tabular massive sulfide lenses that dip at 45° to the east and have strike lengths of up to 1500 m (Brathwaite 1974; Green et al., 1981) (Fig. 3). Massive to blebby carbonate forms a halo around and between the ore lenses. The multiple ore sheets are considered to represent either an original blanket-like syn-volcanic deposit that has been structurally repeated (Brathwaite, 1972; Khin Zaw et al., 1988; Berry, 1990; Large, 1990), or, alternatively, structurally controlled dilatant zones that filled with sulfides mobilized from the footwall during Devonian deformation and metamorphism (Aerden, 1990, 1991).

Carbonate distribution and composition

Dixon (1980) documented the textural features of the carbonates and described the main textural groups as blebby, massive, colloform, and diagenetic carbonate. Carbonate occurs in the "host rock" immediately along strike from the sp-gn-cp lens, and interfingers with the sulfides (Fig. 3). A siliceous zone typically separates the sulfides and massive carbonate, and there is a gradation away from mineralization to blebby or poddy carbonate (Brathwaite, 1974; Dixon, 1980). Carbonate varies from calcite—kutnohorite—rhodochrosite in composition, with minor Mg and Fe substitution (Khin Zaw, 1991).

Carbonate is always associated with sericite–quartz–chlorite ± albite assemblages in the "host rocks". Minor sulfides, including sphalerite and pyrite, occur in the carbonate as small veins and replacement areas.

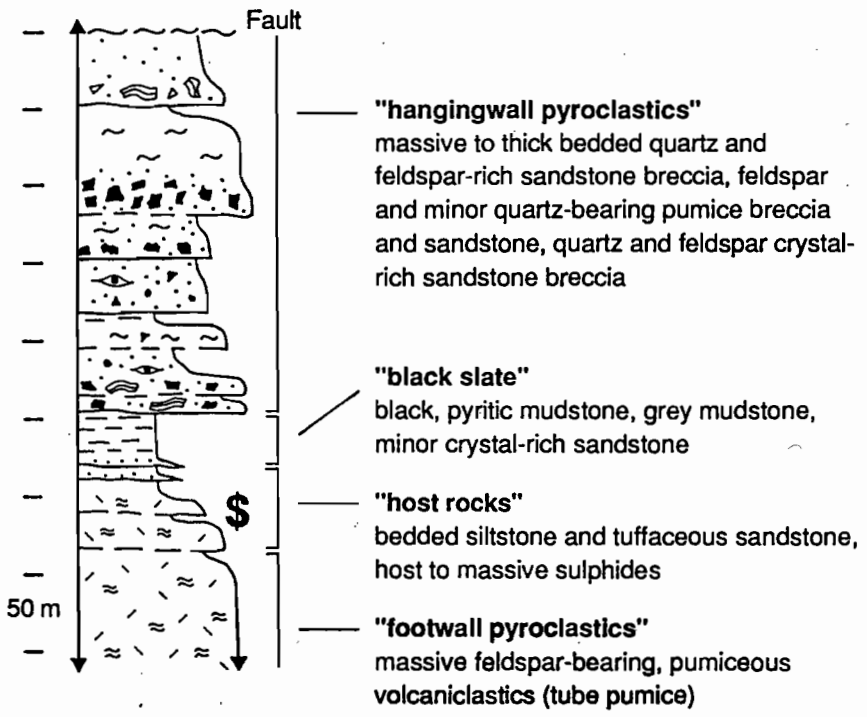

FIG. 2. Simplified stratigraphic column of the volcaniclastic sequence that hosts the Rosebery deposit (after McPhie and Allen, 1992).

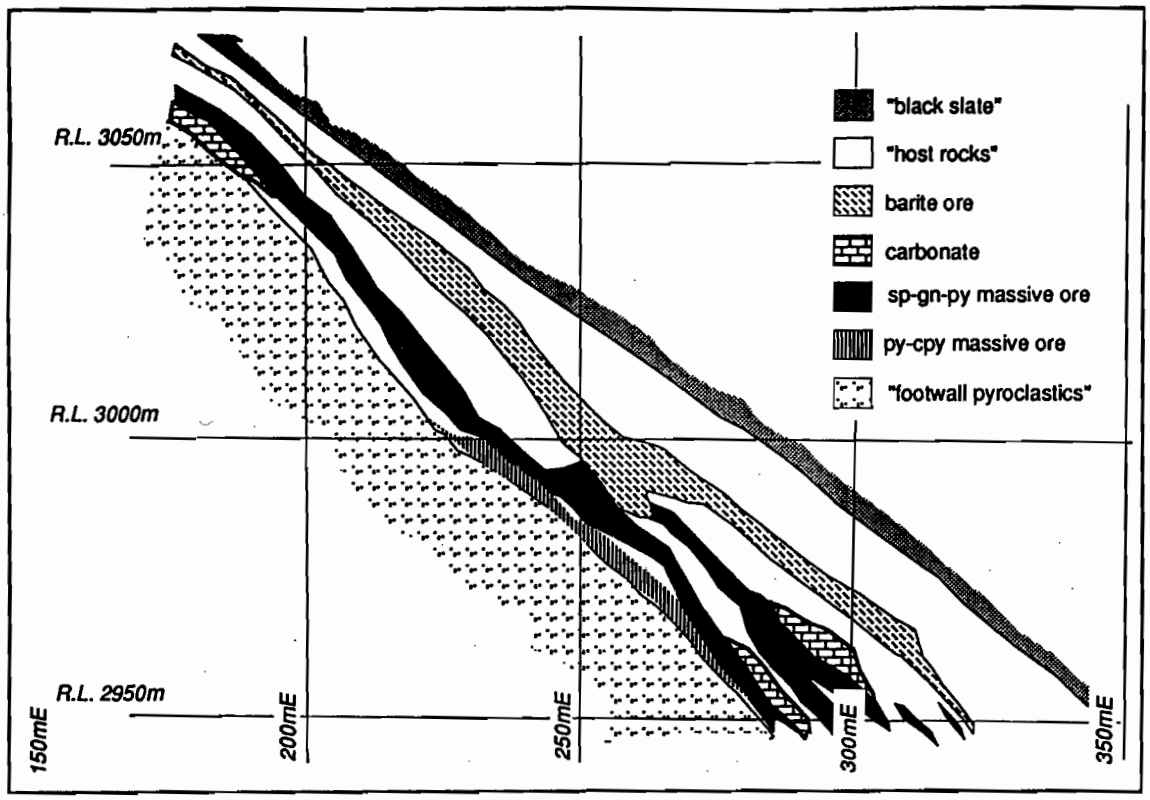

FIG. 3. Geology of the northern ore lenses at Rosebery, section 1113 mN (from Huston and Large, 1988). Note carbonate lenses below, above, and lateral to the ore lenses.

Textures in the Rosebery carbonates

In this study detailed petrographic and cathodoluminescence (CL) analyses of the carbonate at Rosebery have been undertaken in the light of recent developments in the understanding of the volcanic setting of the area (Allen and Cas, 1990; McPhie and Allen, 1992; McPhie et al., 1993).

Methods

Cathodoluminescence is the emission of light from a material under electron bombardment (Nickel, 1978; Pierson, 1981). Crystal lattice imperfections and substituted ions in the crystal structure act as luminescent centres and absorb energy from the electron beam, either activating or inhibiting luminescence. Transition metal ions are common impurities causing luminescence, and in carbonates, Mn^{2+} is an activator of luminescence and Fe^{2+} is a quencher of luminescence (Sommer, 1972; Nickel, 1978; Pierson,. 1981). Luminescence in carbonate rocks is typically yellow-orange-red, and the intensity of luminescence is controlled by the balance of activator and quencher centres. Fe^{2+} will quench luminescence in carbonate as its concentration reaches 10,000 ppm, and above concentrations of 15,000 ppm Fe^{2+}, carbonate is non-luminescent regardless of Mn^{2+} content (Pierson, 1981).

Cathodoluminescence studies were conducted on a Nudide ELM-2B Luminoscope using 6–8 kV and about 0.5 mA current and a focussed beam 8-12 mm in diameter generated by a cold cathode electron gun. The residual gas and chamber pressure was maintained around 100 mTorr during operation. Glass-mounted polished thin sections were placed within the sample chamber prior to evacuation and observed through a binocular microscope.

Textures

Spheroidal and blebby textures are typical of most carbonate at Rosebery, and vary from dispersed to close-packed. Massive and poddy carbonate are common where spheroids are closepacked and intergrown. Macroscopic carbonate forms and distinctive microscopic textural criteria are summarised in Table 1. The categories defined here are an

Table 1. Textures of the carbonate at Rosebery.

Carbonate texture	Core	Rim
Spheroidal: (i) large spheroids (Fig.4a)	Spherical to nodular shape Up to 20 mm diameter Mosaic of anhedral carbonate grains Non-luminescent to dull and speckled brown-red under CL	0.2-0.4 mm thick Radial, euhedral grains Non-luminescent
(ii) small spheroids (Type A; Fig. 4a, b)	Spherical shape Up to 10 mm diameter Mosaic of anhedral grains Non-luminescent to speckled, dark blood-red to red-brown under CL	0.2-0.4 mm thick Radial, euhedral grains (Fig.5a,c) Fine dark red to bright red-orange bands under CL (Fig. 6a,c)
(iii) small spheroids (Type B)	Irregular shape Small, 0.2-2 mm Mosaic of anhedral grains luminescent to dull brown-red under CL	0.5-1 mm thick Zoned, coarse, radial, euhedral grains (Fig. 5b) Fine bands of alternating dark and bright red luminescent carbonate
Blebs	Irregular shape, some rectangular (possibly carbonate after feldspar) Variable size up to 10 mm Mosaic of fine anhedral grains	Rare rims of radial, euhedral carbonate rhombs Dark red under CL
Pods (Fig. 4c,d)	Irregular shape Up to 100 mm in length Mosaic of anhedral carbonate grains or intergrown spheroids	Irregular margins, no distinctive rim
Rhombs (Fig. 4e)	Dusty, inclusion-rich in transmitted light Dull to non-luminescent under CL	Zoned, <1.5 mm thick Alternating bands of blood-red and dull red-brown luminescent carbonate (Fig. 6a)
Massive (Fig. 4f)	Mosaic of anhedral to euhedral carbonate grains, or intergrown carbonate spheroids	Intergranular sericite, quartz and chlorite is common

interpretation of those described by Dixon (1980).

The carbonate occurs in a matrix of fine grained sericite with quartz, minor albite and chlorite. Feldspar crystals are strongly quartz, sericite, and calcite altered, and this calcite is irregular in shape, bright orange under CL, and extends along the feldspar cleavage planes.

Carbonate spheroids have a wide variation in grainsize and packing (Fig. 4a, b). Large, small and rhombic spheroids (Table 1) can all occur together, with small rhombs interstitial to many carbonate spheroids. Type-B spheroids appear similar to the small type-A spheroids in handspecimen, but contain a small, irregular core and zoned, radially intergrown euhedral rhombs visible in thinsection (Fig. 5b). Poddy carbonate has gradual contacts with the surrounding spheroidal or blebby carbonate (Fig. 4c,d). Scattered spheroids become massive carbonate where late carbonate overprints and fills the spaces between spheroids. This is clearly seen under CL (Fig. 6e).

Textures within carbonate

Carbonate–sericite–quartz aggregates form pseudomorphs after feldspar phenocrysts in some spheroidal carbonate. The phenocrysts appear highly corroded and sub to anhedral under plane polarized light, but are clearly euhedral under CL (Fig. 6c). Most feldspar crystals occur in the spheroid cores (Fig. 5d), although altered feldspar crystals also occur near the margins of the larger nodular spheroids. Carbonate grains radiate out from the feldspar crystals, indicating that the carbonate nucleated on the feldspar and enveloped other feldspar crystals as it grew.

Circular and arcuate shapes occur in the fine grained, anhedral cores of many carbonate spheroids, but have not been observed in the recrystallized cores or euhedral rims of spheroids (Fig. 5e,f,g). In most samples, these features are now completely replaced by single carbonate crystals which remain optically continuous across the 'circles' and 'arcs'. Rare arcuate features are rimmed by a thin layer of fine grained sericite-chlorite. Allen and Cas (1990) have demonstrated that the Rosebery "host rocks" are the fine top of a purniceous mass-flow deposit. We therefore interpret the circular and arcuate features within the carbonate to be uncompacted pumice replaced and preserved by carbonate.

Timing of carbonate deposition

Cathodoluminescence shows that carbonate at Rosebery is composed of several generations of carbonate (Fig. 7). The earliest carbonate (I) occurs in the cores of spheroids, replacing pumice walls and filling vesicles, and is dark red to brown and speckled in texture under CL (Fig. 6a). Euhedral carbonate rims (II) are highly zoned with alternating light red to yellow and dark red to brown bands visible under CL. Some vesicles in pumice are filled with this zoned carbonate (Fig. 6b). The interstitial carbonate rhombs have the same luminosity and zonation under CL as the euhedral overgrowths on spheroidal carbonate (Fig. 6a) indicating that both are the same generation. An overprinting carbonate phase (III), blood red under CL, partly replaces the core and rims, preserving zonation in the euhedral carbonate (Fig. 6c). Non-luminescent carbonate (IV) partly replaces the earlier spheroids, in places forming massive carbonate (Fig. 6d). Successive phases of carbonate deposition are likely to have occurred during one episode of carbonate alteration, and differences in timing probably reflect the distribution of carbonate within the deposit and proximity to major fluid pathways.

Cleavage wraps around the spheroids, rhombs and pods of carbonate (Fig. 4a), indicating that most carbonate formation at Rosebery pre-dates Devonian deformation. However, in some samples, calcite occupies pressure shadow regions of spheroids, indicating either remobilization and recrystallization of earlier carbonate, or secondary carbonate precipitation during deformation.

Sulfides occur in all carbonate samples, either disseminated in the "host rock", or within spheroids and rhombs. Sulfides rim pumice fragments preserved in some carbonate spheroids (Fig. 5g). Sulfides also occur as veinlets subparallel to the cleavage, wrapping around spheroids or uncommonly crosscutting carbonate blebs. On the mine scale, sulfides replace carbonate (Fig. 4g). Carbonate formation appears to be part of the early stages of hydrothermal activity, rather than a post-sulfide event as interpreted at South Hercules (Khin Zaw and Large, 1992). The concentration of carbonates laterally along strike from the massive sulfides, suggests that ore fluids may have replaced part of the carbonate altered "host rocks" with sulfides. We suggest that Rosebery may be partly a sub-seafloor replacement VHMS deposit. However, further work is necessary to relate this replacement style mineralization to other parts of the deposit. This research is part of ongoing work that aims to establish how sulfide mineralization and carbonate formation occurred at Rosebery.

Discussion

Origin of spheroidal textures

Previous workers have interpreted the spheroidal carbonates at Rosebery as ooids that precipitated on the sea floor (Brathwaite, 1974; Dixon, 1980). Spheroidal carbonate textures elsewhere (e.g. Hercules, Lees, 1987; South Hercules, Khin Zaw and Large, 1992; Mattabi, Franklin et al., 1975) are

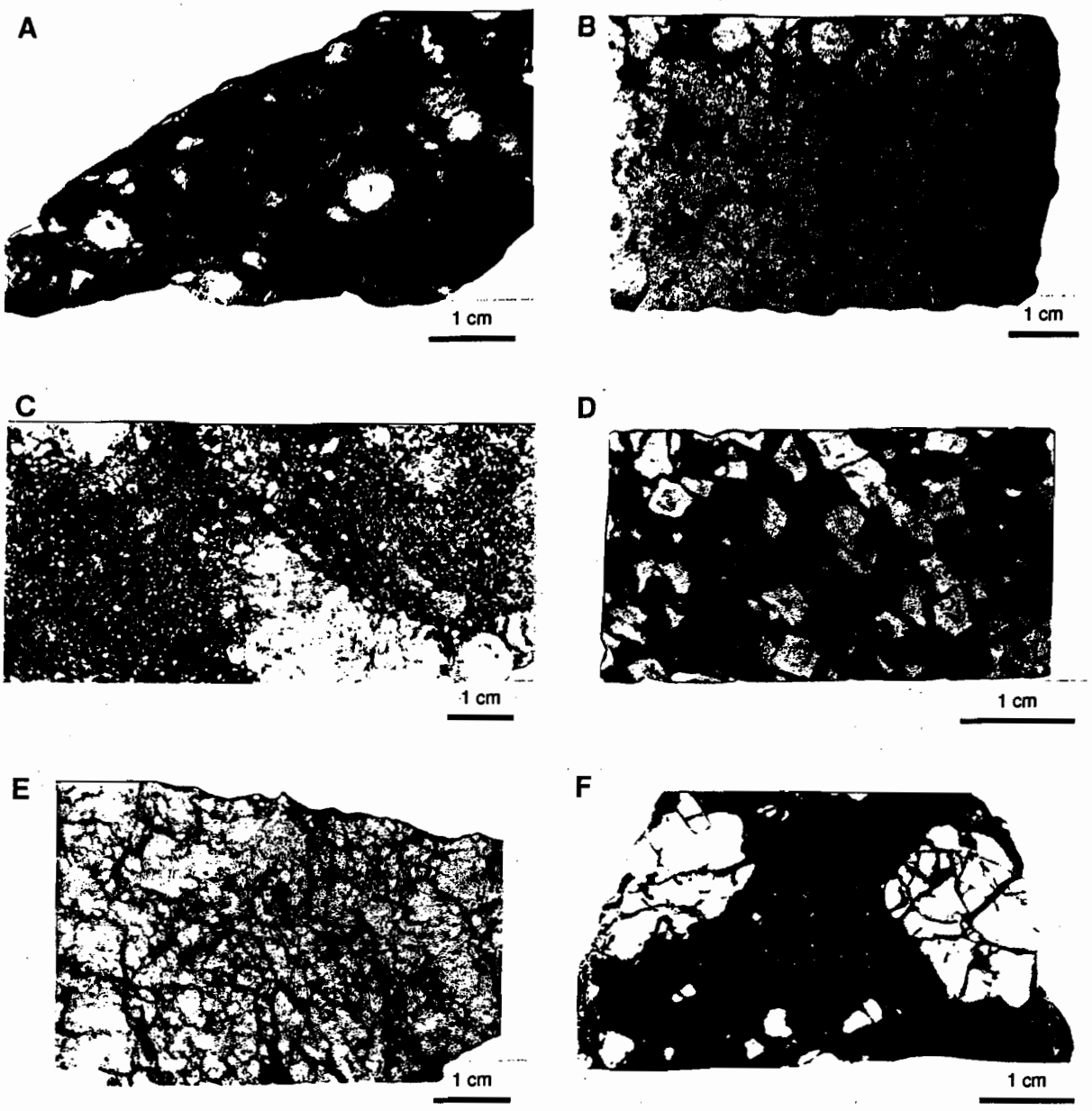

FIG. 4. Carbonate handspecimen textures. A. Large spheroids and small carbonate blebs after feldspar, in foliated sericite-chlorite-quartz-albite matrix. B. Close-packed small spheroids displaying some zonation in sericite-chlorite-quartz-albite matrix. Spheroids are partly coalesced into more massive carbonate on the left. C. Irregular pods of carbonate with intervening small rhombs and spheroids in sericitechloriteuartz-albite matrix. D. Zoned carbonate rhombs in a foliated matrix of sericite-chlorite-quartz-albite. E. Massive carbonate, partly composed of intergrown spheroids, with chlorite and crosscutting silica veinlets. F. Pods of carbonate surrounded and cross-cut by massive sulfides (sphalerite-galena-pyrite).

FIG. 5 (opposite). Photomicrographs of carbonate textures. A. Typical small spheroid (type A), with core of fine grained anhedral carbonate surrounded by radiating coarse rhombs. Crossed nicols. B. Small spheroids (type B), composed of radiating carbonate rimmed by clear carbonate, in a chlorite-quartz matrix. Interstitial sphalerite occasionally replaces carbonate. Plane light. C. Carbonate spheroids (type A) displaying zones of radiating carbonate with an overgrowth of coarse rhombs (arrow). Carbonate may have nudeated on a pumice vesicle wall. Crossed nicols. D. Pumice vesicles and glass walls preserved by carbonate and a fine layer of sericitechiorite. Coarse carbonate rhombs occur at the edge of the pumice fragment. Plane light. E. Pumice textures clearit preserved in carbonate. Plane light. F. Feldspar crystals in core of carbonate spheroid. Crossed nicols. G. Pyrite repladng carbonate. Fine-grained pyrite forms a coating on some pumice walls (arrow). Crossed nicols.

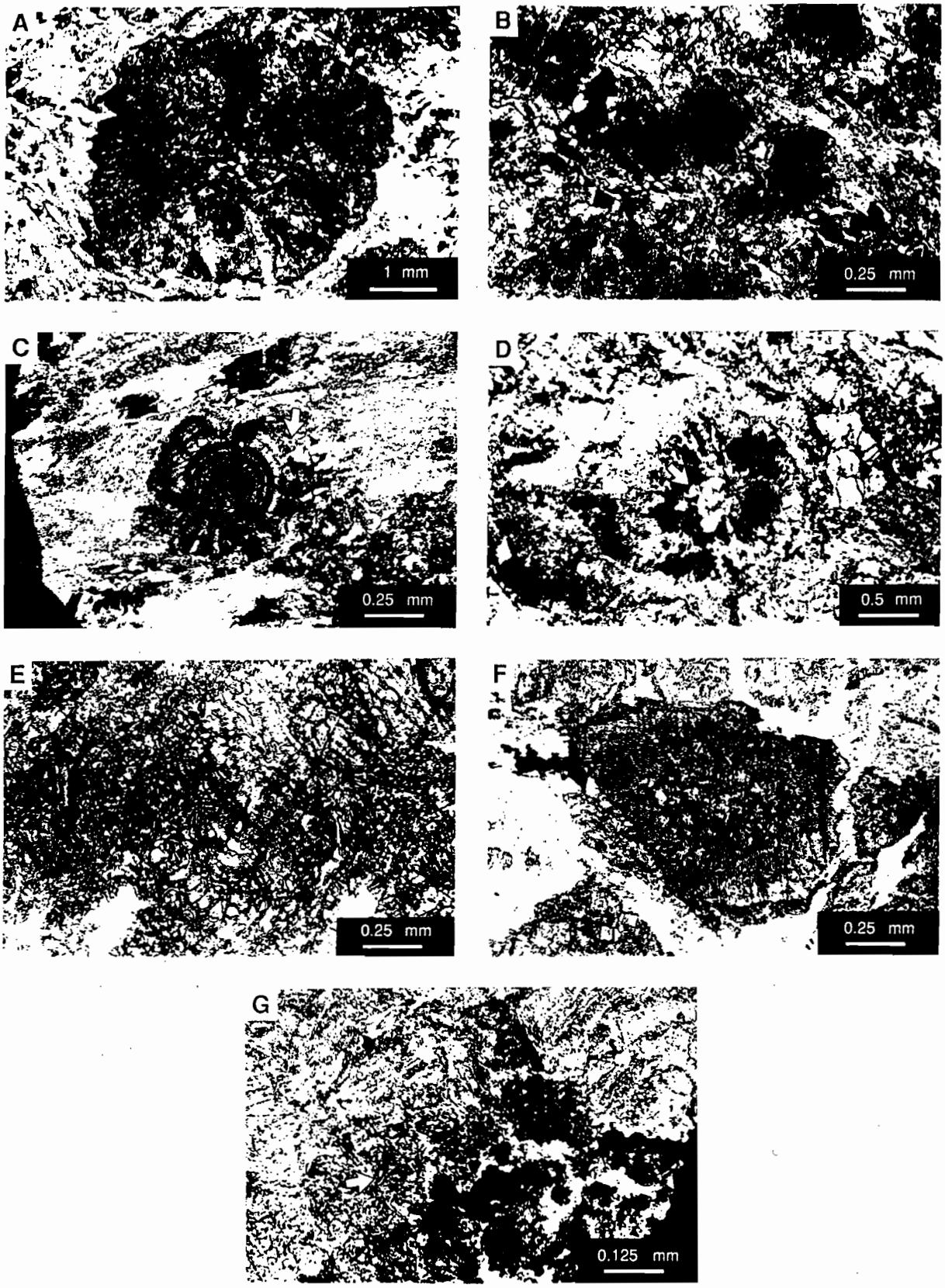
A
1 mm
B
0.25 mm
C
0.25 mm
D
0.5 mm
E
0.25 mm
F
0.25 mm
G
0.125 mm

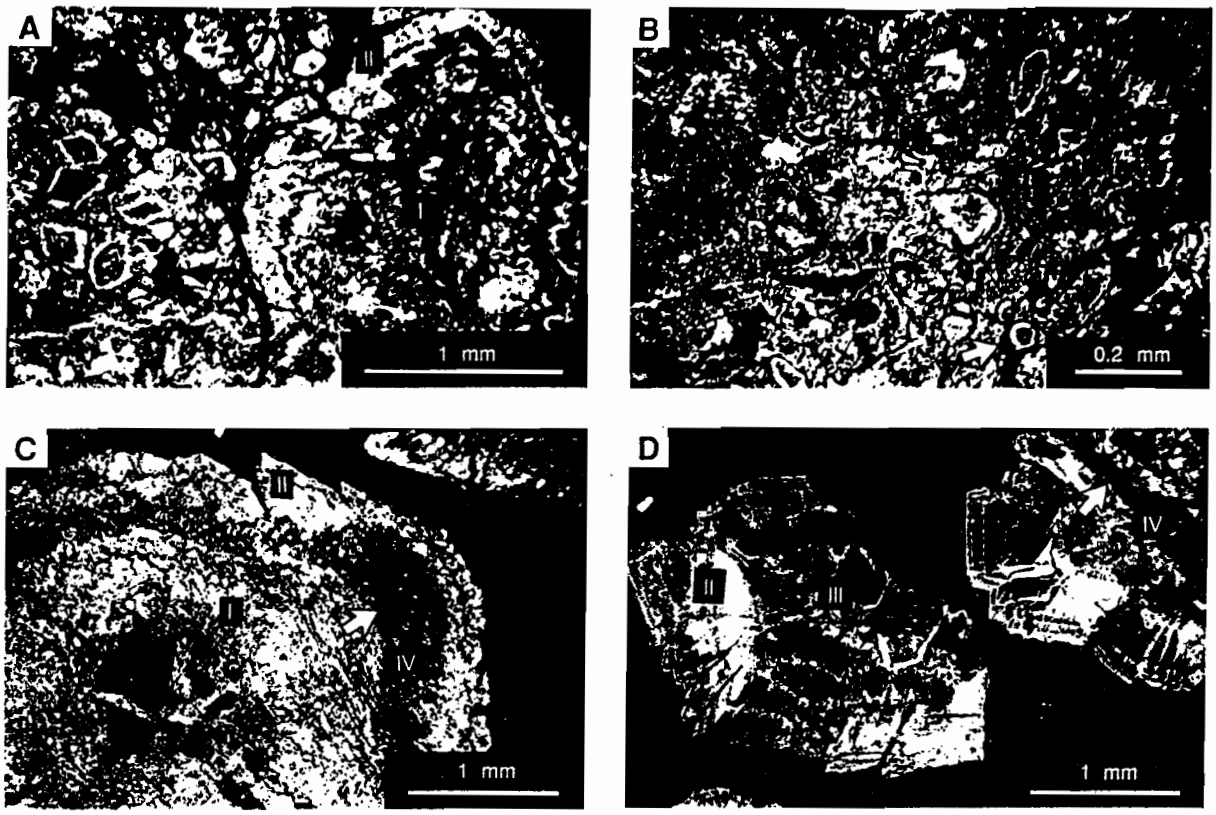

FIG. 6. Photomicrographs of Rosebery carbonate under cathodoluminescence. A. Under CL the spheroid core is dark red and speckled (I), with bands of blood red and yellow luminesdng carbonate at the rim (11). Adjacent small rhombs have similar zonation and are probably contemporaneous with the spheroid rim. B. Pumice textures in the spheroid core are partly defined by non-luminescent sericite-chlorite. Zoned carbonate (11) in some vesicles indicates open-space growth. C. Euhedral feldspar crystals in spheroid core are replaced by non-luminescent sericite, quartz and carbonate. The zoned spheroid rim (11) is also partly replaced by the non-luminescent carbonate (IV) (arrow). D. Red luminescing carbonate (III) partly replaces yellow and brown banded spheroids (I and II) and mimics the preexisting zoning in places. Veins of non-luminescent carbonate (W) crosscut the spheroid (arrow).

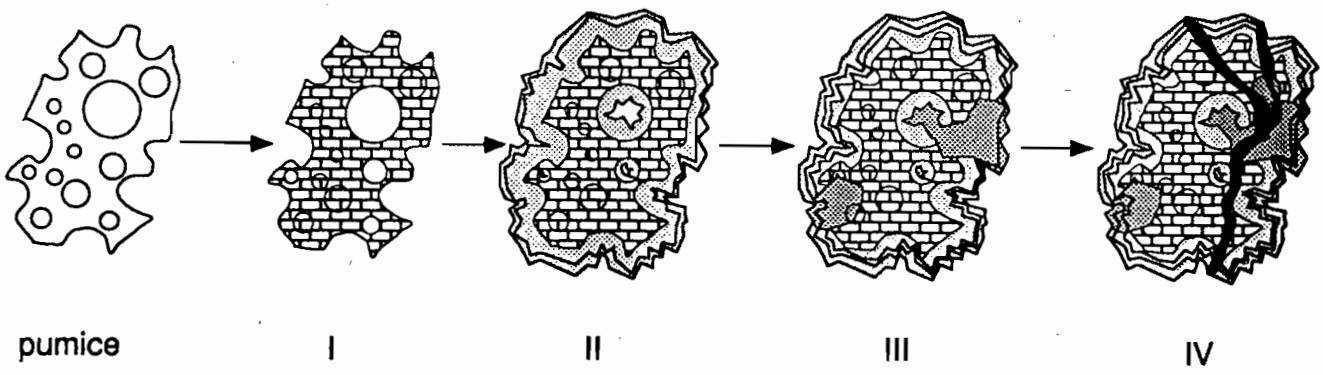

FIG. 7. Cartoon illustrating the episodes of carbonate alteration. I: pumice walls replaced and some vesicles infilled, II: spheroids rimmed and remaining vesicles infilled, III: cores and rims of spheroids and blebs partly replaced, W: carbonate veins crosscut and partly replace spheroids and blebs.

considered to result from alteration associated with VHMS formation. In many sedimentary environments spheroidal carbonate textures are diagenetic (e.g. Floran and Papike, 1975; Carrigan and Cameron, 1991), and most workers attribute the spherical habit to unrestricted or displacive growth in soft sediments (Talbot and Kelts, 1986; Brown and Kingston, 1993; Gibson et al., 1994). However, at Rosebery carbonate replaces glass rather than displaces unconsolidated pumice clasts.

Carbonate formation may have been initiated by nucleation on feldspar phenocrysts in pumice, free feldspar crystals, or pumice fragments in the upper part of the host mass-flow deposit. Abundant nucleation sites may allow preservation of pumiceous textures in the carbonate. Euhedral carbonate does not retain any preexisting textures and this may reflect fewer nucleation sites and subsequent overprinting of pumice. Spheroidal or blebby growth is possibly a natural habit for carbonate growing in a porous environment. Closely packed spheroids or blebs reflect numerous nucleation sites.

Preservation of pumiceous textures

Preservation of primary volcanic textures indicates a replacement origin for the carbonate, rather than sea-floor precipitation. At Rosebery, most pumice textures in carbonate are pristine and we suggest that carbonate has directly replaced the pumice fragments in these sites. Replacement of felsic glass by carbonate has been recognized in other volcanic sequences (Browne and Ellis, 1970; Carrigan and Cameron, 1991; Howells et al., 1991). Furthermore, in some geothermal areas calcite is an important component of the hydrothermal alteration assemblage (Muffler and White, 1969; Browne 1978; Browne and Ellis, 1970; Henley and Ellis, 1983), whereas zeolite and clay minerals are typical of diagenetic alteration of volcanic glass (Bargar and Beeson, 1981; Fisher and Schmincke, 1984; Noh and Boles, 1993). In addition, the close spatial association of carbonate with the Rosebery orebody strongly supports a genetic relationship with the hydrothermal system.

Fine grained sericite-chlorite mark vesicles and tube walls in some samples, but in most cases submicroscopic minerals or inclusions define the pumice walls. As both pumice walls and vesicles are now carbonate, an early stage of alteration may be necessary to coat the pumice clasts in order to preserve the volcanic textures through the carbonate replacement. Prior to the deposition of the "footwall pyroclastics" and "host rocks" the edges of the pumice clasts may have been oxidized or reacted with seawater, especially if the pumiceous mass flows were hot before encountering seawater. Alternatively, diagenetic zeolite or clay minerals may line the pumice walls, similar to the rims of glass shards in other volcaniclastic deposits (Boles and Coombs, 1975; Noh and Boles, 1993). Evidence of oxidation or the reaction of pumice clasts with seawater should be recognized throughout the mass flow deposit, whereas diagenesis is likely to be controlled by porosity and permeability and would explain the patchy distribution of the pumice clasts recognized in carbonate.

Allen (1991) recognized an early silica and feldspar alteration at Rosebery that preserves the pumice fragments. He considers carbonate alteration to be later, replacing the secondary feldspar, but retaining the pumice textures. In the samples we have examined there is no evidence that carbonate is after secondary feldspar, but further work is required to determine the overall alteration timing relationships.

Mechanisms of carbonate deposition

Carbonate deposition occurred early in the formation of the Rosebery deposit, similar to some other VHMS deposits (Large and Both, 1980; Galley et al., 1993), suggesting that carbonate formation may represent a cooler temperature or distal equivalent to the massive sulfides (Large and Both, 1980). Calcite has reverse solubility (Ellis, 1963) and could be deposited directly from seawater oversaturated in $CaCO_3$ if rising high temperature fluids mixed with the overlying seawater. Galley et al. (1993) propose that carbonate associated with VHMS mineralization was precipitated on the seafloor from the overlying seawater and dolomitized during hydrothermal alteration. We have found that the carbonate at Rosebery shows no evidence of seafloor deposition.

Acidic CO_2-rich hydrothermal fluids will deposit calcite in open spaces at elevated temperatures (Ellis, 1963) and replace plagioclase with calcite and clays (Giggenbach, 1981). We suggest that at Rosebery, hot, acidic CO_2-bearing fluids reacted with felsic glass

within the porous top of the pumiceous mass flow (Fig. 10) replacing the pumice with carbonate and eventually precipitating carbonate in the vesicles and pore spaces. At the time of carbonate deposition, the sea floor was either at the top of the pumiceous "host rock" or equivalent to a level within the accumulating "black slate". Indeed, the pumiceous "host rock" may have behaved as an aquifer beneath the fine grained top of the mass flow or the overlying "black slate" aquitard (Fig. 8). The period of quiescence represented by the "black slate" may infact correspond to the episode of carbonate and sulfide mineralization.

Possible sources of CO_2 in hydrothermal fluids at Rosebery include decarbonation of limestone or dolomite or reactions with organic matter dispersed in rocks lower in the stratigraphy, from solution in seawater, or magma tic fluids. Galley et al. (1993) suggests that carbonate in the lower part of the footwall alteration zone at the Chisel Lake and North Chisel deposits could have been deposited from either a boiling hydrothermal fluid, or a hydrothermal fluid mixed with seawater. At Hercules, oxygen and carbon isotopic studies combined with fluid inclusion research by Khin Zaw and Large (1992) suggests that the carbonate was sourced from seawater modified during circulation through the volcanic pile. Mixing of a hot CO_2-bearing hydrothermal fluid with seawater in the permeable pumiceous "host rocks" at Rosebery probably triggered carbonate formation.

Conclusions

Carbonate occurs along strike from the massive sulfide deposit at Rosebery and is overprinted by the sulfides. Spheroidal and blebby carbonate textures are common and comprise radial carbonate rims overgrowing cores of anhedral grains. Massive to poddy carbonate reflects variations in the spacing and number of nucleation sites. Arcuate and circular textures in cores of carbonate spheroids are similar to pumice textures in unaltered "host rocks" along strike from the orebody. In some cases, altered feldspar crystals occur in the spheroid cores. We conclude that carbonate nucleated on pumice clasts and feldspar crystals.

Carbonate alteration is confined to the upper part of a graded pumiceous mass-flow deposit. Uncompacted pumice textures indicate that glassy pyroclasts were replaced and infilled by carbonate either immediately below the seafloor position, or if the "black slate" was an aquitard, at some shallow depth beneath the seafloor during the accumulation of the mud. Carbonate probably precipitated when hot CO_2-bearing hydrothermal fluids mixed with cold seawater, and replaced the felsic glass and eventually infilled spaces within and between pumice clasts.

Compositional zonation in carbonate overgrowths and carbonate veins replacing spheroids and blebs indicate many stages of carbonate alteration. Nevertheless, the stages may have been more or less concurrent but at different positions relative to the source of hydrothermal fluids. Euhedral rhombs and rims on spheroids postdate replacement of pumice clasts, but formed prior to the onset of sulfide mineralization. Sulfides deposition at Rosebery postdates carbonate formation, replacing the carbonate in places. This evidence suggests that Rosebery is partly a subseafloor replacement VHMS deposit.

Acknowledgments

David Cooke, Ross Large, and Jocelyn McPhie kindly reviewed various drafts of the manuscript. Critical comments and discussions with Rod Allen, Mark Doyle, David Green from the Rosebery Mine, Steven Hunns, and Khin Zaw were very helpful and greatly appreciated. The rocks we examined were collected by Grant Dixon, and thanks go to Kathi Stait for helping to locate them. Simon Stevens assisted in thinsection preparation and Peter Cornish got the CL machine up and running.

References

Aerden, D.G.A.M., 1990, Formation of a massive sulfide orebody by syneformational host rock replacement in a ductile shear zone, Rosebery, Tasmania [abs.]. Geol. Soc. Australia Abstracts, no. 25: 174-175.

Aerden, D.G.A.M., 1991, Foliation boudinage control on the formation of the Rosebery PZn orebody, Tasmania. J. Struct. Geol. 13: 759-775.

Allen, R. L., 1991, Structure, stratigraphy and volcanology of the Rosebery-Hercules Zn-PbCu-Au massive sulphide district, Tasmania. Unpub. report to Pasminco Mining and Exploration, Rosebery, results 1988-1990.

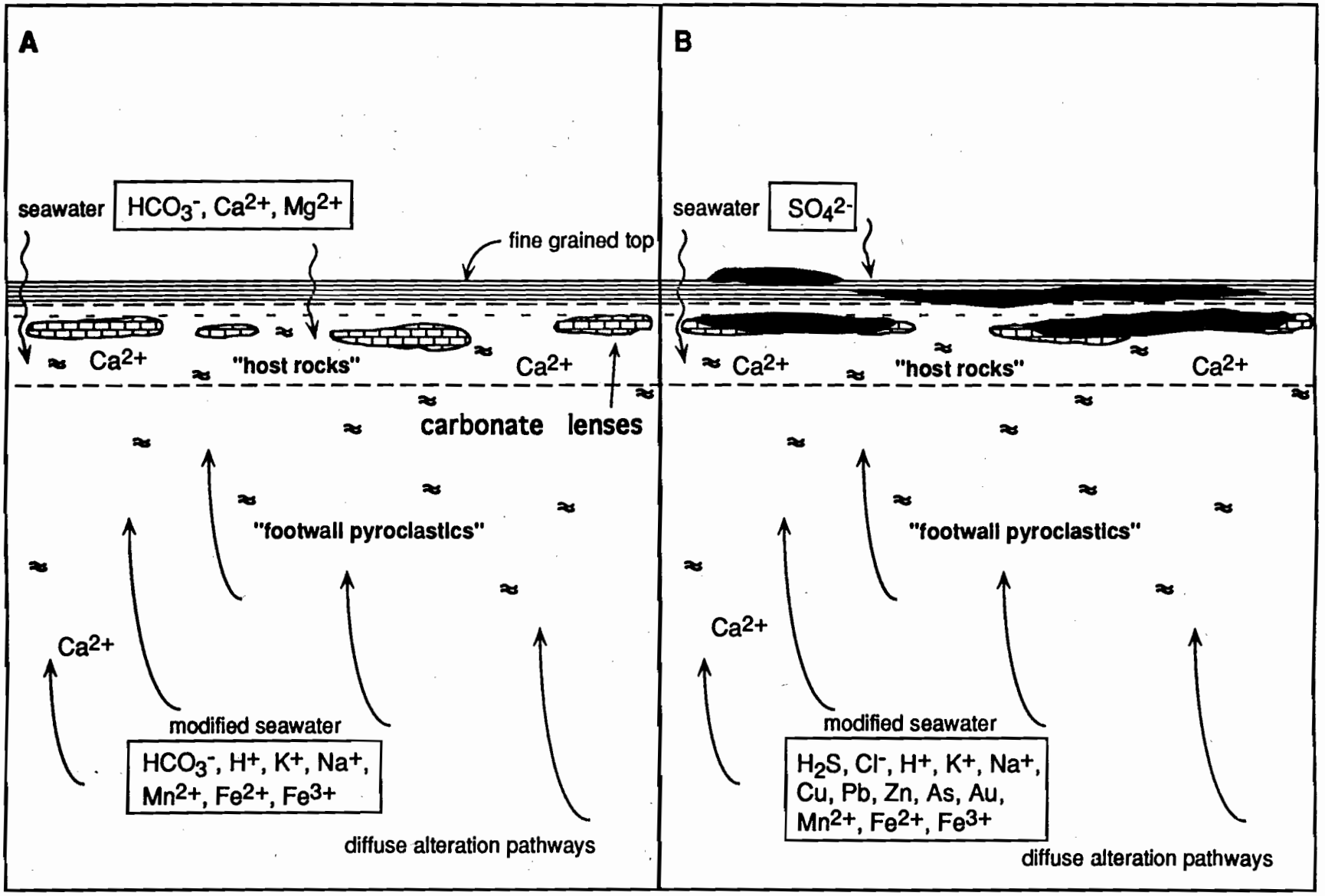

FIG. 8. Sketch illustrating the model for carbonate formation in the porous parts of the host pumiceous mass-flow. Hot hydrothermal fluids ascend through the porous pumiceous footwall and reacts with seawater trapped in pore spaces near the top of the mass-flow deposits. Carbonate nucleates on pumice fragments and feldspar crystals. Subsequent sulfide mineralization partly replaces the carbonate.

Allen, R. L., and Cas, R.A.F., 1990, The Rosebery controversy: Distinguishing prospective submarine ignimbrite-like units from true subaerial ignimbrites in the Rosebery-Hercules ZnCu-Pb massive sulphide district, Tasmania tabs.]. Geol. Soc. Australia Abstracts, no. 25: 31-32.

Ashley, P. M., Dudley, R.J., Lesh, R.H., Marr, J.M., Ryall, A.W., 1988, The Scuddles Cu-Zn prospect, and Archaean volcanogenic massive sulfide deposit, Golden Grove district, Western Australia. Econ. Geol. 83: 918-951.

Bargar, K. E., and Beeson, M.L., 1981, Hydrothermal alteration in research drill hole Y-2, Lower Geyser Basin, Yellowstone National Park, Wyoming. Am. Miner. 66: 473-490.

Berry, R. F., 1990, The structure of the Rosebery mine sequence, Western Tasmania [abs.]. Geol. Soc. Australia Abstracts, 25: 278.

Boles, J. R., and Coombs, D.S., 1975, Mineral reactions in zeolitic Triassic tuff, Hokonui Hills, New Zealand. Geol. Soc. Amer. Bull. 86: 163-173.

Brathwaite, R. L., 1972, The structure of the Rosebery ore deposit, Tasmania. Australasian Inst. Mining Metallurgy Proc. 241: 1-13.

Brathwaite, R. L., 1974, The geology and origin of the Rosebery ore deposit, Tasmania. Econ. Geol., v.69: 1081101.

Brown, G. H., and Kingston, D.M., 1993, Early diagenetic spherulitic siderites from Pennsylvanian palaeosols in the Boss Point Formation, Maritime, Canada. Sod. 40: 467A74.

Browne, P. R. L., 1978, Hydrothermal alteration in active geothermal fields. Ann. Rev. Earth Planet. Sci. 6: 229-250.

Browne, P. R. L., and Ellis, A.J., 1970, The Ohaki-Broadlands hydrothermal area, New Zealand: Mineralogy and related geochemistry. Amer. J. Sci. 269: 97-131.

Carrigan, W. J., and Cameron, E.M., 1991, Petrological and stable isotope studies of carbonate and sulfide minerals from the Gunflint Formation, Ontario: evidence for the origin of early Proterozoic iron-formation. Precambrian Res. 52: 347-380.

Corbett, K. D., 1989, Stratigraphy, palaeogeography and geochemistry of the Mt Read Volcanics. Geol. Soc. Australia Spec. Pub. 15: 86119.

Corbett, K. D., 1992, Stratigraphic-volcanic setting of massive sulfide deposits in the Cambrian Mount Read Volcanics, Tasmania. Econ. Geol., v.87: 56586.

Corbett, K. D., and Lees, T.C., 1987, Stratigraphic and structural relationships and evidence for Cambrian deformation at the western margin of the Mount Read Volcanics, Tasmania. Australian Jour. Earth Sci. 34: 457.

Dixon, G. H., 1980, Geological, geochemical and stable isotope studies of the carbonates at Rosebery. Unpub. B.Sc. Honours thesis, University of Tasmania, 173 p.

Ellis, A. J., 1963, The solubility of calcite in sodium chloride solutions at high temperatures. Arm Jour. Sci. 261: 259-267.

Fisher, R. V., and Schmincke, H.U., 1984, Pyroclastic rocks. Berlin, Springer-Verlag, 472 p.

Floran, R. J., and Papike, J.J., 1975, Petrology of the low-grade rocks of the Gunflint Iron-Formation, OntarioMinnesota. Geol. Soc. Amer. Bull. 86: 1169-1190.

Franklin, J. M., Kasarda, J., and Poulsen, K.H., 1975, Petrology and chemistry of the alteration zone of the Mattabi massive sulphide deposit. Econ. Geol. 70: 63-79.

Galley, A. G., Bailes, A.H., and Kitzler, G., 1993, Geological setting and hydrothermal evolution of the Chisel Lake and North Chisel Zn-Pb-Cu-Ag-Au massive sulfide deposits, Snow Lake, Manitoba. Explor. Mining Geol. 2: 271-295.

Gemmell, J. B., and Large, R.R., 1992, Stringer system and alteration wnes underlying the Hellyer volcanic-hosted massive sulfide deposit, Tasmania, Australia. Econ. Geol. 87: 620-649.

Gibson, P. J., Shaw, H.F., and Spiro, B., 1994, The nature and origin of sideritic ironstone bands in the Tertiary Lowmead and Duaringa Basins, Queensland. Australian J. Earth Sci. 41: 255-263.

Giggenbach, W. F., 1981, Geothermal mineral equilibria. Geochim. Cosmochim. Acta, v. 45: 393410.

Green, G. R., 1983, The geological setting and formation of the Rosebery volcanic-hosted massive sulfide orebody, Tasmania. Unpub. Ph.D. thesis, University of Tasmania, 288 p.

Green, G. R., Solomon, M., and Walshe, J.L., 1981, The formation of the volcanic-hosted massive sulfide deposit at Rosebery, Tasmania. Econ. Geol. 76: 304—338.

Gregory, P. W., Hartley, J.S., and Wills, Kj.A., 1990, Thalanga zinc-lead-copper-silver deposit. Australasian Inst. Mining Metallurgy Mon. 14: 1527-1537.

Henley, R. W., and Ellis, A.J., 1983, Geothermal systems ancient and modern: A geochemical review. Earth Sd. Rev. 19: 1-50.

Hill, A. P., and Orth, K., 1994, Textures and origin of carbonate associated with some Australian VHMS deposits [abs.]. AMF Symposium:

Howells, M. F., Reedman, Aj., and Cambell, S.D.G., 1991, Ordovician (Caradoc) marginal basin volcanism on Snowdonia (northwest Wales): London, HMSO for the British Geological Survey, 191 p.

Huston, D. L., and Large, R.R., 1988, Distribution, mineralogy, and geochemistry of gold and silver in the north end orebody, Rosebery, Tasmania. Econ. Geol. 83: 1181-1192.

Khin Zaw, 1991, The effect of Devonian metamorphism and metasomatism on the mineralogy and geochemistry of the Cambrian VMS deposits in the Rosebery-Hercules district, western Tasmania. Unpub. Ph.D. thesis, University of Tasmania, 302 p.

Khin Zaw and Large, R. R., 1990, 18O and a13C isotopic variation of hydrothermal carbonates from the Rosebery, Hercules and South Hercules deposits, western Tasmania: Interplay of Cambrian vs Devonian systems labs.]. Geol. Soc. Australia Abstracts, no. 27: 114.

Khin Zaw and Large, R. R., 1992, The precious metal-rich South Hercules mineralization, western Tasmania: A possible subsea-floor replacement volcanic-hosted massive sulfide deposit. Econ. Geol. 87: 931-952.

Khin Zaw, Huston, D.L., and Large, R.R., 1988, Ore metal distribution, zonation and structural relationships at Rosebery, western Tasmania. Unpub. rept to E.Z. Company, University of Tasmania, 26 p.

Large, R. R., 1990, The gold-rich seafloor massive sulphide deposits of Tasmania. *Geol. Rundschau* 79: 2278.

Large, R. R., 1992, Australian volcanic-hosted massive sulfide deposits: features, styles and genetic models. *Econ. Geol.* 87: 471-510.

Large, R. R., and Both R.A., 1980, The volcanogenic sulfide ores at Mount Chalmers, eastern Queensland. *Econ. Geol.*, v.75: 992-1009.

Lees, T., 1987, Geology and mineralization of the Rosebery-Hercules area, Tasmania. Unpub. M.Sc. thesis, University of Tasmania, 164 p.

Lydon, J. W., 1988, Volcanogenic massive sulphide deposits, Part 2. Genetic models, *in* Roberts, R. G. and Sheahan, P.A., eds, *ORE DEPOSIT MODELS. Geoscience Canada*: 43-65.

McLeod, R. L., and Stanton, R.L., 1984, Phyllosilicates and associated minerals in some Paleozoic stratiform sulfide deposits of southeastern Australia. Econ. Geol. 79: 1-22.

McPhie, J., and Allen, R.L., 1992, Facies architecture of mineralized submarine volcanic sequences: Cambrian Mount Read Volcanics, western Tasmania. *Econ. Geol.* 87: 587-596.

McPhie, J., Doyle, M., and Allen, R.L., 1993, Volcanic textures: a guide to the interpretation of textures in volcanic rocks. Hobart, CODES Key Centre, University of Tasmania, 196 p.

Muffler, L. J. P., and White, D.E., 1969, Active metamorphism of Upper Cenozoic sediments in the Salton Sea geothermal field and the Salton Trough, southeastern California. *Geol. Soc. Am. Bull.* 80: 157-182.

Nickel, E., 1978, The present status of cathode luminescence as a tool in sedimentology. *Minerals Sci. Engng* 10: 73-100.

Noh, J. H., and Boles, J.R., 1993, Origin of zeolite cements in the Miocene sandstones, North Tejun oilfields, California. *J. Sed. Petrol.* 63: 248-260.

Pierson, B. J., 1981, The control of cathodoluminescence in dolomite by iron and manganese. *Sededimentology* 28: 601–610.

Sommer, S. E., 1972, Cathodoluminescence of carbonates, 2. Geological applications. Chem. Geology 9: 257-273.

Talbot, M. R., and Kelts, K., 1986, Primary and diagenetic carbonates in the anoxic sediments of Lake Bosumtwi, Ghana. *Geology* 14: 912-916.

Volcanic facies relationships and hydrothermal modification of primary volcanic textures at the Thalanga deposit

Anthea P. Hill

Centre for Ore Deposit and Exploration Studies, Geology Department, University of Tasmania

The Thalanga Zn–Pb–Cu–Ag–Au deposit is located at the contact between rhyolitic volcanics of the Mount Windsor Formation, and the overlying dacitic to andesitic volcanics and volcaniclastics of the Trooper Creek Formation in the Cambrian to Ordovician Mount Windsor Volcanics, northern Queensland. The ore and enclosing volcanics are locally strongly deformed and metamorphosed to upper greenschist facies. Bedding is now subvertical and the ore horizon has been divided into four main lenses by post-tectonic normal faults: West, Central, and East Thalanga and the Vomacka Zone (Fig. 1).

Sulfide mineralisation at Thalanga is spatially, and probably genetically associated with subaqueous felsic intrusions and mass-flow deposits, that together constitute the ore horizon. The main ore minerals are sphalerite, chalcopyrite, pyrite and galena, and in most places the sulfides are coarse-grained with annealed grain boundaries. Banding in the massive sulfide lenses is interpreted to be mainly tectonic in origin. Chalcopyrite, and to a lesser degree, sphalerite and galena have been remobilised during deformation and now occupy fault zones and sites of dilation. Metal zonation is erratic and mainly reflects the widespread remobilisation of sulfides at Thalanga, although there is a general variation from pyrite–chalcopyrite-rich sulfides at the base of the ore horizon, to sphalerite–galena ± barite towards the stratigraphic top of the ore horizon. Quartz–magnetite lenses along strike from the massive sulfides are interpreted as distal, low temperature exhalites contemporaneous with sulfide mineralisation (Duhig et al., 1992).

Rhyolites (Rhyolitic Volcanics) with both coherent and clastic textures are present in the footwall at Thalanga. However, variable quartz ± sericite ± chlorite ± pyrite alteration makes identification of facies relationships difficult. The least altered coherent rhyolite at Thalanga is feldspar- and quartz-phyric with microcrystalline quartzo-feldspathic groundmass, and is present down dip and along strike from the sulfide lenses. Rare spherulites and perlitic fractures demonstrate that the groundmass was originally glassy.

Perlitic fractures in the altered rhyolites are replaced by fine grained white mica (sericite), and the kernels are replaced by recrystallised quartz. With increasing quartz–sericite±pyrite alteration, a network of sericite envelopes circular or polygonal quartz kernels. Textures comprising isolated kernels of recrystallised quartz in pervasive sericite may result from intense alteration of perlite.

Monomict rhyolitic breccias that have gradational contacts with coherent rhyolite were probably generated by autoclastic (quenching, flow fragmentation) processes. Single flow-banded rhyolite clasts in pervasive quartz ± sericite ± chlorite ± pyrite alteration are possibly relicts of rhyolitic hyaloclastite or autobreccia. In intensely altered parts of the footwall, textural domains comprising abundant, irregularly distributed, poorly sorted quartz crystals are interpreted as originally volcaniclastic, whereas domains of evenly distributed, well sorted quartz crystals are interpreted as altered coherent rhyolite.

Syn-volcanic quartz–feldspar–porphyry (QFP) sills, with peperitic contacts with enclosing siltstones, are present within the ore horizon in East Thalanga. QFP sills also occur at the ore horizon position in the Thalanga Range to the northwest of the deposit. The QFP sills are coarsely porphyritic and contain 25–35% distinctive rounded and embayed blue quartz (maximum = 8 mm) and white feldspar (maximum =

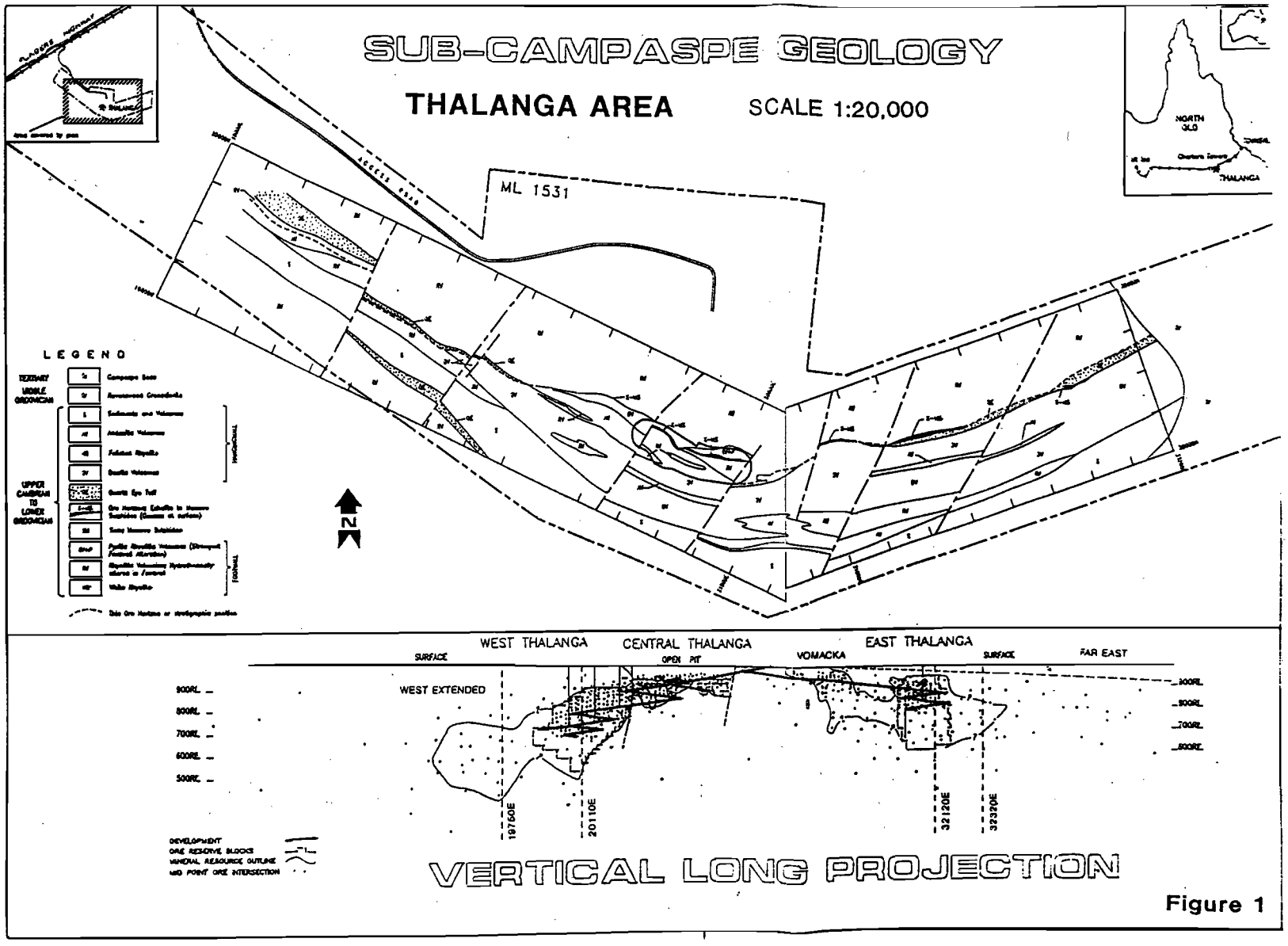
SUB-CAMPASPE GEOLOGY
THALANGA AREA
SCALE 1:20,000
ML 1531
LEGEND
N
WEST THALANGA
CENTRAL THALANGA
EAST THALANGA
SURFACE
OPEN PIT
VOMACKA
SURFACE
FAR EAST
WEST EXTENDED
900RL
800RL
700RL
600RL
500RL
19760E
20110E
32120E
32320E
DEVELOPMENT
ORE RESERVE BLOCKS
MINERAL RESOURCE OUTLINE
MID POINT ORE INTERSECTION
VERTICAL LONG PROJECTION

Figure 1

4 mm) phenocrysts. Typically, the groundmass is composed of fine grained, recrystallised equant quartz, with minor sericite. Mega-clasts of QFP (>20 m) in Central Thalanga contain recrystallised spherulites, indicating that the microcrystalline, sericite-rich groundmass was formerly glassy.

Poorly sorted, polymict, normally graded quartz crystal-rich breccias (locally, quartz 'eye' volcaniclastics; QEV) occur in both West and East Thalanga, and rarely in Central Thalanga. Components of the QEV are listed in Table 1. The blue quartz crystals, feldspar crystals, and crystal fragments in the QEV have no glassy selvages. QFP clasts are non-vesicular and are the largest and most abundant clasts in the QEV, suggesting proximity to source. Rare QFP clasts with sericite-rich groundmass and wispy terminations may be altered pumice.

The abundant coarse quartz and feldspar crystals in the QEV are interpreted to have been liberated from of a highly porphyritic QFP magma by explosive eruption. The small volume of clasts interpreted as altered pumice or glass shards suggests that some of the pumiceous fraction produced by such an explosive eruption was separated from the crystals during eruption and/or transportation. The site of eruption is poorly constrained, but was probably located in shallow water (≤ 1 km deep; cf. McBirney, 1963) or in a subaerial environment at the basin margin. The internal organisation of units of the QEV is consistent with transport to the site of final deposition by subaqueous mass flows (cf. Cas, 1983). The mass flows collected clasts from the substrata, including clasts from massive sulfide lenses which must have been exposed on the seafloor.

Large, angular to blocky QFP clasts are more common at the base of the QEV, and apparently grade into coherent QFP in East Thalanga. Non-vesicular QFP magma is interpreted to have been emplaced as shallow sills while the QEV was wet and unconsolidated, resulting in blocky peperite comprising QFP clasts in QEV matrix. In West Thalanga, where QFP sills are absent, the QEV may include clasts generated by quench-fragmentation of QFP clasts. Perhaps QFP intrusions broke through the seafloor, quenched and fragmented, and the resulting hyaloclastite was incorporated by subsequent crystal-rich mass flows.

The Hanging Wall Fragmental (HWF) has sharp, depositional contacts with the underlying QEV and massive sulfides, and is composed of multiple beds of unaltered, graded to massive siltstones and sandy siltstones, with fresh feldspar crystal fragments. Perlitic dacite clasts are dispersed through the siltstones, and minor rhyolite clasts are common at the base of graded beds. Dacite clasts in the HWF are more common in East and Central Thalanga, where the HWF is up to 18 m thick, compared to West Thalanga where the HWF is <2 m thick.

Coherent dacite overlies the HWF in all parts of the Thalanga deposit, with sparsely (2–5%) feldspar-phyric dacite common in East Thalanga, and 5–8% feldspar-phyric dacite present in West Thalanga. The basal contact varies from sharp and planar, to disrupted and peperitic with clasts of perlitic sparsely feldspar-phyric dacite within the HWF. Perlitic fractures are present towards the stratigraphic top of the dacite. The dacite has gradational contacts with overlying poorly sorted dacite breccia thought to be in situ hyaloclastite. The dacite is interpreted to have flowed over and foundered into partly consolidated HWF.

A gradational contact occurs between the in situ dacite hyaloclastite and overlying, normally graded, poorly-sorted dacite breccias. White, siliceous dacite clasts with angular to cuspate margins are the most abundant clast-type in this breccia, and are interpreted as resedimented dacite hyaloclastite. Coherent andesite overlies and partly intrudes the resedimented dacite hyaloclastite in Central Thalanga. Elsewhere, either dacite or andesite overly the resedimented hyaloclastite.

Massive sulfide lenses in West Thalanga are interpreted to partly replace carbonate- and chlorite-rich alteration that is restricted to a narrow interval (<30 m thick) at the stratigraphic top of the Rhyolitic Volcanics. The QEV overlies the massive sulfides in West Thalanga. In Central Thalanga and the Vomacka Zone, a single lens of massive sulfides, interpreted as exhalative in origin, directly overlies the Rhyolitic Volcanics. QEV and QFP do not occur in the Vomacka Zone, but pods of QEV and QFP are present in the western parts of Central Thalanga. Two main ore lenses are present in East Thalanga, the footwall lens and the hangingwall lens, and each is interpreted to

be exhalative and to represent a seafloor position. The QEV and QFP sills occur between the ore lenses, and are interpreted to have been synchronous with mineralisation, interrupting but also preserving the ore lenses.

References

Cas, R.A.F., 1983. Submarine 'crystal tuffs': their origin using a Lower devonian example from southeastern Australia. *Geological Magazine* 120: 471–486.

Duhig, N.C., Stolz, J., Davidson, G.J., and Large, R.R., 1992. Cambrian microbial and silica gel textures in silica iron exhalites from the Mount Windsor volcanic belt, Australia: their petrography, chemistry, and origin. *Economic Geology* 87: 764–784.

McBirney, A.R., 1963. Factors governing the nature of submarine volcanism. *Bulletin Volcanologique* 26: 455–469.

Table 1 Components of the Quartz 'Eye' Volcaniclastic deposit

Components	Size Range	Shape	Abundance
Quartz crystals and crystal fragments – blue to grey	<1 mm to 12 mm, average = 6 mm	rounded crystals to angular fragments	variable, up to 60%, common towards top of QEV
Feldspar crystals – partly albitised plagioclase, minor K-feldspar crystals	<1 mm to 4 mm	subhedral crystals to angular fragments	variable, absent in places, common towards stratigraphic top
QFP clasts	1 cm to 5 m, commonly 10–20 cm	angular and blocky, irregular, to rounded	common, up to 80% of QEV in places
Rhyolite clasts– siliceous, quartz-phyric	<1 cm to 60 cm, commonly 5–10 cm	rounded to blocky and cuspate in places	minor component, overall <10% of QEV
Chloritic wisps – patches of chlorite	< 1 cm	angular to wispy, elongate parallel to cleavage	patchy distribution, about 5–10% of QEV (after biotite)
Sericitic streaky wisps – quartz-phyric with intergrown quartz-sericite groundmass	<5 cm	wispy, irregular clasts	patchy distribution about 5–10 % of QEV
Massive sulfide clasts – massive py to sp–gn±cp	<10 cm, possibly up to 1 m	rounded to elongate parallel to cleavage	rare
Quartz–magnetite clasts	up to 30 cm	blocky to rounded and irregular	rare

A comparison of volcanic facies architecture and alteration styles of felsic and mafic volcanic host sequences to massive sulphide deposits — Thalanga, northern Queensland and Teutonic Bore, Western Australia

Holger Paulick

Centre for Ore Deposit and Exploration Studies, Geology Department, University of Tasmania

The supervisors of project are Dr J. McPhie and Dr Bruce Gemmell (CODES), and Prof. Dr Gerhard Franz (TU, Berlin)

The aim of this project is to compare two distinct volcanic sequences which share the common feature of hosting sighnificant volcanic-hosted massive sulfide (VHMS) mineralisation. The Archean volcanics at Teutonic Bore form part of a greenstone belt in the Yilgarn cratonic complex while the Cambro-Ordovician volcanics at Thalanga belong to a deformed volcano-sedimentary sequence deposited in a continental backarc basin. The main purposes are to unravel the volcanic facies architecture in both areas and to define their style of alteration.

The project commenced in June 1995 with field work at the Thalanga mine, which is located at the western end of the volcano-sedimentary Mount Windsor Subprovince, approximately 180 km west of Townsville (northern Queensland). During a visit from Dr J. McPhie, a number of representative diamond drill holes were examined and several aspects concerning the direction of the study were discussed with on-site geologists. In conclusion, diamond drill holes from three cross sections through the Thalanga orebody have been selected for detailed logging. These are located at the western margin of the western ore lens of Thalanga (19460E), through the central part of the western lens (20080E) and in the central part of the Thalanga deposit (10860E). This selection was guided by the availability of core intersecting considerable stratigraphic thickness of the host rock volcano-sedimentary sequence and the intention to map individual stratigraphic unit and alteration phenomena in three-dimensional space. Logging of these drill holes has been carried out from June to October 1995.

This work revealed several major consistent differences between the hangingwall and the footwall strata of the Thalanga orebody concerning volcanic facies and alteration. The footwall consists almost entirely of coherent rhyolites and associated monomict volcaniclastic deposits. The alteration of these units is pervasive and two dominant end-member textures can be defined: (1) strongly foliated sericite-chlorite assemblages, and (2) "flooding" by white silica replacing the entire groundmass.

The major textural differences between alteration styles appear to be their pervasive or their dominantly vein-controlled character. To date, the following distinctions seem to be reasonable:

I. Pervasive alteration, dominantly siliceous groundmass

(a) homogeneously while silica

(b) dark grey and pale grey silica phases with dark grey, silica domains appearing as pseudoclasts (e.g. TH410 @ 322.8 m)

Gradational contact between Ia and Ib in TH410 @ 322.8 m.

II. Pervasive alteration, phyllosilicate-rich groundmass

(a) sericite/chlorite assemblages in well defined layers of irregular domains to networks of a few millimetres to centimetres thickness

(b) sericite/chlorite 'blotches' usually not foliated or deformed, appearing as pseudoclasts (e.g. TH410 @169.90 m)

Gradational contadct between Ib and IIa in TH410 @ 192.8 m, and gradational contact between Ia and IIa in TH410 @ 131.0 m)

III. Vein controlled to patchy alteration — SiO_2
(a) silica veins
(b) silica-calcite veins (TH410 @503.0 m)
(c) silica veins with chlorite patches (with or without calcite) (TH410 @337.80 m)

IV. Epidote and/or feldspar-hematite (?) assemblages in veins and patches

Usually associated with pinkish and/or yellow-greenish staining of surrounding volcanic groundmass material (this alteration style seems to be confined to coherent volcanics — dacites and rhyolites — that have not been affected by phyllosilicate forming alteration.

(a) Pinkish staining along veins penetrating into the surrounding volcanic groundmass for up to 2 cm with fussy/gradational terminations. Colour dyes: hematite? Red-pink material in veins: feldspar with hematite inclusions?

(b) Yellow-greenish staining of groundmass in patches and along veins penetrating into the surrounding volcanic groundmass for up to 1 cm with fussy/gradational terminations. Colouring of grondmass: dispersed epidote. Yellow-green material in veins: epidote.

V. Patches/veins of actinolite-sericite (TH410 @ 295.0 m)

VI. Calcite veins
(a) white calcite (TH410 @ 503.0 m)
(b) purple/pinkish calcite

Alteration process and according mineral reactions may only be possible to determine by detailed observations in thin sections, whole-rock geochemistry and microprobe analysis. However, in one sample the successive replacement of feldspar by biotite through a transitional contact from alteration style Ib to IIa could be observed (TH410A @ 278.0 m).

The composition of the hangingwall sequence is much more diverse but coherent dacites and associated feldspar-rich volcaniclastic sedimentary deposits are volumetrically dominant. Laminated shales occur at several stratigraphic levels but appear to be more abundant from 100 m stratigraphically above the favourable horizon onwards. A quartz-feldspar-phyric, coarse rhyolite variety and associated volcaniclastic deposits — which have previously been considered to be exclusive to the favourable horizon — have been encountered in the hangingwall sequence. Furthermore, coherent andesites with unclear emplacement characteristics are present.

This succession of volcanic and sedimentary rocks has been affected by dominantly vein-controlled to 'patchy' alteration, except for the feldspar-rich volcaniclastic units which usually have a groundmass consisting of strongly foliated sericite and chlorite. This characteristic may be attributable to the reseumably high content of volcanic glass in these deposits. The coherent dacites frequently show alteration by yellow-green epidote and pink Fe^{3+}-bearing feldspar (?) vein-filling assemblages. These veins are surrounded by 1–2 cm wide, 'fussy-edged' haloes of pink or green staining of the volcanic groundmass. Furthermore, veins may contain white silica sometimes associated with white calcite and/or chlorite or may be entirely filled with white or pale purple calcite.

The whole volcano-sedimentary host succession of the Thalanga orebody experienced metamorphism of apparently upper greenschist facies conditions. These may be responsible for the frequenly observed transformation of feldspar into biotite, which may have occurred in accordance with the reaction: K-feldspar + chlorite → biotite + muscovite + quartz + H_2O. Bright red garnets (presumably rich in almandine and/or pyrope endmember composition) occasionnally occur in chlorite-rich domains and may be attributable to a reaction such as : chlorite + muscovite → garnet + biotite + quartz + H_2O.

Sampling of the examined cross sections has been chiefly directed by the following aims:
- unravel the metamorphic influence on mineral assemblages and textures
- characterise the alteration assemblages and clarify the sequential order of specific reactions
- determine the original emplacement characteristics of the volcanic units and their distribution in time and space.

Consequently, the analytical work currently underway will include detailed petrographic studies of thin sections and whole-rock geochemical analyses, which will be followed-up by electron microprobe analyses of the most important mineral phases. Possibly isotopic studies will bne conducted at a later stage of the project.

Preliminary investigation of alteration at the Highway and Reward deposits, Mount Windsor Volcanics, Queensland

Mark Doyle

Centre for Ore Deposit and Exploration Studies, Geology Department, University of Tasmania

Geological setting

The Mount Windsor subprovince comprises an Upper Cambrian to Lower Ordovician volcano-sedimentary terrain which hosts several major VHMS-style deposits (Fig. 1). The belt extends for around 160 km discontinuously from Ravenswood in the east to Pentland in the west. The current stratigraphic nomenclature for the Mt Windsor subprovince was proposed by Henderson (1986). The four principal components are:

Puddler Creek Formation (Late Cambrian)
Mt Windsor Formation (Late Cambrian–Early Ordovician)
Trooper Creek Formation (Basal Ordovician)
Rolston Range Formation (Bendigonian–Late Lancefieldian)

The Puddler Creek Formation consists primarily of lithic sandstone, greywacke, and sandstone. Quartz, feldspar, phyllite grains, polycrystalline quartz, and detrital mica are the main components. The Puddler Creek Formation is overlain conformably by the Mount Windsor Formation. The latter Formation was defined by Henderson (1986) as a thick sequence of rhyolitic volcanics and pyroclastics with minor dacites and rare andesites, and which lacks interlayered sediments. The conformably overlying Trooper Creek Formation was interpreted to comprise siltstones, mudstones, andesitic to rhyolitic tuff, and lesser basaltic andesite and andesite flows, andesitic lapilli tuff, and volcaniclastic sandstone and conglomerate. In contrast, the conformably overlying Rolston Range Formation is characterised by a dominance of sandstone and siltstone, and rare volcaniclastic unis. Sandstones and siltstones are dominated by volcanically sourced material, but contain basement-derived muscovite and phyllite grains.

Objectives

The principal objective of this study is to delineate between alteration associated with lava domes and syn-sedimentary intrusions from hydrothermal alteration accompanying formation of the Highway and Reward volcanic-hosted massive sulfide deposits. Secondly, to examine the characteristics of footwall and hanging wall alteration associated with a sub-seafloor replacement style volcanic-hosted massive sulfide deposit and to compare these patterns with alteration associated with known exhalative deposits. Thirdly, to establish an evolutionary trend for textures and mineralogy in volcanic host rocks (coherent, volcaniclastic) to mineralisation in response to high temperature devitrification, hydration, diagenetic alteration and hydrothermal alteration.

Graphic lithological logs and detailed cross-sections incorporating facies and alteration characteristics have been constructed for the deposits. Detailed mapping between Coronation homestead and Trooper Creek prospect provide examples of hydrothermal alteration unrelated to massive sulfide mineralisation, and progressive stages in the textural evolution of lavas, syn-sedimentary intrusions and volcaniclastic deposits. Analysis of mineralogical and geochemical characteristics of alteration are to be undertaken in Jan 1996.

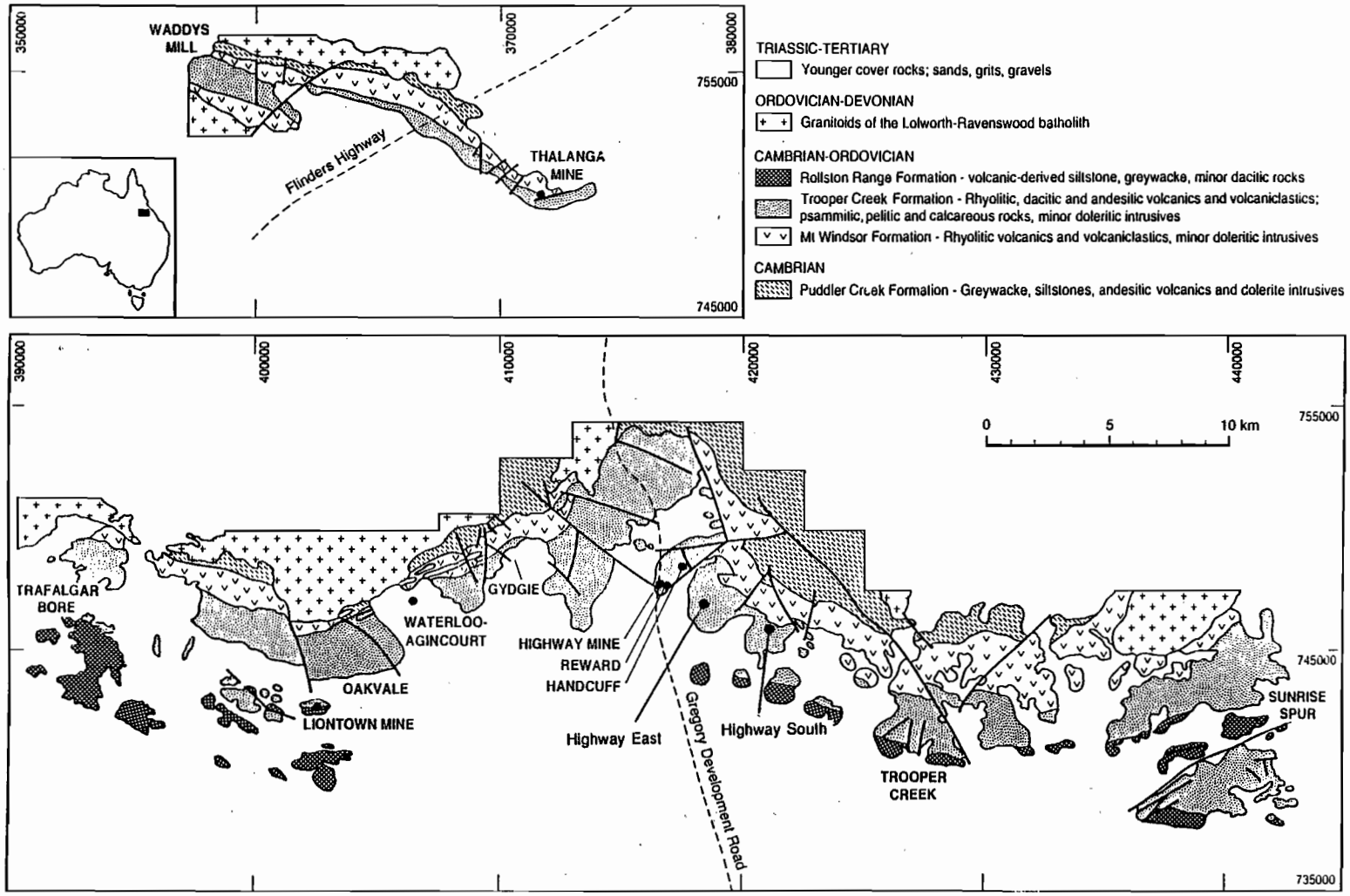

Figure 1: Simplified geological map of the Mt Windsor subprovince between Waddy's Mill and Sunrise Spur showing the distribution of the principal units and younger granitoids. Modified from Berry et al. (1992).

Stratigraphy

Mapping of the current study supports Henderson's (1986) four part division of the Mt Windsor subprovince however has considerably refined the interpretation of component lithologies.

As this investigation focuses on alteration in the Trooper Creek Formation further discussion of the stratigraphy is limited to this formation. The Trooper Creek Formation is well exposed in the Seventy Mile Range between the Highway mine and Trooper Creek prospect. The Trooper Creek Formation is characterised by rapid variations between volcanic and sedimentary facies associations (Henderson 1986, Berry et al. 1992, Doyle 1994a,b). The sedimentary facies association consists of massive to thinly laminated siltstone and minor massive and graded sandstone. This facies contains fossil evidence which constrains the age of the formation to Lower Ordovician (Henderson 1986). The volcanic facies association comprises rhyolitic to andesitic lavas and related autoclastic breccia, peperite, syn-sedimentary intrusions, pumice–crystal–lithic sandstone–breccia and scoria–lithic breccia.

There are regional variations in the proportion of sedimentary versus volcanic facies and in lavas and intrusions to volcaniclastic facies in the Trooper Creek Formation. In the Highway–Reward to Highway East area the volcanic facies association is dominant and represented by: rhyolitic, dacitic and andesitic lavas, syn-sedimentary intrusions, autoclastic breccia and peperite; and lesser graded rhyolitic–dacitic pumice–crystal–lithic sandstone–breccia and scoria–lithic breccia. To the west, sedimentary facies are more abundant and the volcanic facies contains a higher proportion of pumiceous, crystal-rich, and scoriaceous high-concentration turbidity-current deposits. Original volcanic textures are well preserved in all but the most deformed and hydrothermally altered areas.

Highway and Reward deposits

The Trooper Creek Formation at Highway–Reward hosts two spatially associated gold- and copper-rich massive sulfide orebodies. After Thalanga the Reward deposit is the largest known volcanic-hosted massive sulfide deposit in the Mount Windsor Volcanics. The Highway pipe is located approximately 200m grid west of the Reward pipe beneath the abandoned Highway open pit.

Facies and facies architecture

The Highway and Reward massive sulfide deposits are hosted by both volcanic and sedimentary facies associations. A sedimentary facies association dominated by suspension-settled and turbiditic siltstone of immature volcanic provenance forms a minor component of the sequence. The characteristics of the sedimentary facies suggest that volcanism took place in a below-storm-wave-base (250 m), quiet water, submarine environment. Contact relationships and phenocryst mineralogy, size and percentages indicate the presence of eleven distinct porphyritic units in an area of 1 x 1 x 0.5 km (Fig. 2). Massive coherent lava and associated in situ or resedimented hyaloclastite and peperite are the principal facies in the environment of mineralisation. The distribution and arrangement of these facies are the basis for determining the mode of emplacement. Upper contact relationships are critical in evaluating intrusive versus extrusive emplacement as basal contacts can be similar. The peperitic upper margins to many porphyries records the fragmentation of large volumes of the magma during intrusion into wet unconsolidated sediment. Syn-sedimentary intrusions, partly extrusive cryptodomes, and lava domes have been recognised. These are dominant in the environment of mineralisation and represent a proximal facies association from intrabasinal, intrusive-extrusive, non-explosive volcanism. Individual porphyries have sheet or squat shapes, vary from <10 m to 350 m in thickness, and some are less than 200 m in diameter. Their small volume contrasts with silicic lavas, domes and cryptodomes emplaced in modern and ancient subaerial (eg. Clough 1982, Cortese et al 1986), and subaqueous environments (eg. Pichler 1965, Cas 1978,). The shape, distribution, and emplacement mechanisms of porphyritic units are, in part, a reflection of the subaqueous depositional environment. Rising magma that encountered unconsolidated water-saturated sediment commonly remained subsurface and was emplaced as syn-sedimentary intrusions rather than erupting as lava flows or domes. Intrusion

of magma is favoured where its density exceeds that of the surrounding host, and/or the hydrostatic pressure of the magma is low (McBirney 1963, Walker 1989). Within submarine sedimentary basins the water column can contribute significantly to the confining pressure (lithostatic and hydrostatic pressure) exerted on the magma promoting intrusion at shallow levels beneath the sea floor (eg. Yamamoto 1991). Progressive dewatering of host sediments by early intrusions favours the eruption of subsequent magma as lavas and domes. The positions of previously or concurrently emplaced porphyries strongly influenced their shape and distribution. Magma preferentially invaded sediment, avoiding earlier porphyries or conforming to their margins. Syn-volcanic faults may have acted as conduits for magma as well as for concurrent and later hydrothermal fluids. Lava domes, partly emergent cryptodomes, and deposits of resedimented hyaloclastite and peperite are important indicators of palaeo-seafloor positions at Highway–Reward. Sills and cryptodomes may have influenced seafloor topography and therefore sedimentation, but do not mark seafloor positions.

The volcanic facies association also includes graded turbiditic sandstone, monomictic to polymictic rhyolitic-dacitic lithic breccia and thick, non-welded pumice- and crystal-rich sandstone–breccia. Pumiceous and crystal-rich deposits were sourced from explosive silicic eruptions but emplaced by cold, water-supported, high-concentration turbidity currents. The implied eruptive style is likely to have been limited to intrabasinal volcanic centres shallower than 1000 m, or basin margin or subaerial settings.

Mineralisation

The Highway and Reward massive sulfide deposits consist of pipe-like bodies of massive pyrite–chalcopyrite with minor marginal zones of massive to semi-massive and disseminated sphalerite–galena–barite (Fig. 2). The Highway pipe is a sub-vertical, grid ENE trending, chalcopyrite-rich massive pyrite body that is approximately 50m x 175m in plan, and 150 m in depth. This amounts to a resource of 1.2 million tonnes at 5% Cu. The Reward deposit consists of one main and several smaller subvertical massive pyrite pipes that are discordant to bedding and associated with minor Pb–Zn mineralisation. The largest pipe has horizontal dimensions of up to 100 m x 150 m and a vertical length of 200 m. It contains around 5 m.t. of massive pyrite (Beams et al., 1989), which includes a small chalcopyrite-rich zone.

Figure 3 is a schematic reconstruction showing successive stages in the development of the Highway–Reward volcanic centre. By the time of massive sulfide mineralisation the centre had the configuration shown in frame four. Pyrite–chalcopyrite pipes represent high-temperature feeder zones at the centre of a large hydrothermal system and are subseafloor replacements of the host sediment, syn-sedimentary intrusions, lava domes and autoclastic breccia. The pipes occur at the contacts between distinct porphyritic units suggesting a permeability control on the migration of hydrothermal fluids. Fluids which passed from the pipes into the surrounding sediment, and coherent interior and peperitic base of the porphyries formed a weak halo of disseminated and patchy sphalerite–galena–barite mineralisation.

Alteration

Alteration is defined as a change in the mineralogy or texture of a rock facilitated by the action of hot or cold aqueous solutions or gases. Different alteration minerals and textures in a rock result from different processes acting on the pre-alteration texture. Devitrification, hydration, hydrothermal and diagenetic alteration, diagenetic compaction, and metamorphism act to modify primary textures. Each represents an *alteration stage* although the time between each stage may be very short or even overlap and several stages may be unimportant or not affect all parts of a volcanic deposit/rock. Several *steps*, each recorded by a characteristic mineral assemblage, are often involved in forming the alteration texture which characterises each stage.

The characteristics of hydrothermal alteration associated with mineralisation cannot be satisfactorily understood without determining the role of preceding alteration stages in modifying the mineralogy and texture of the host rocks. Preliminary studies suggest that the textural evolution of rhyolites, dacites and volcaniclastics hosting the Highway and Reward deposits is determinable in all but the most highly altered areas. Detailed drill core logging of alteration and volcanic facies allow for investigation of the interplay between primary volcanic texture,

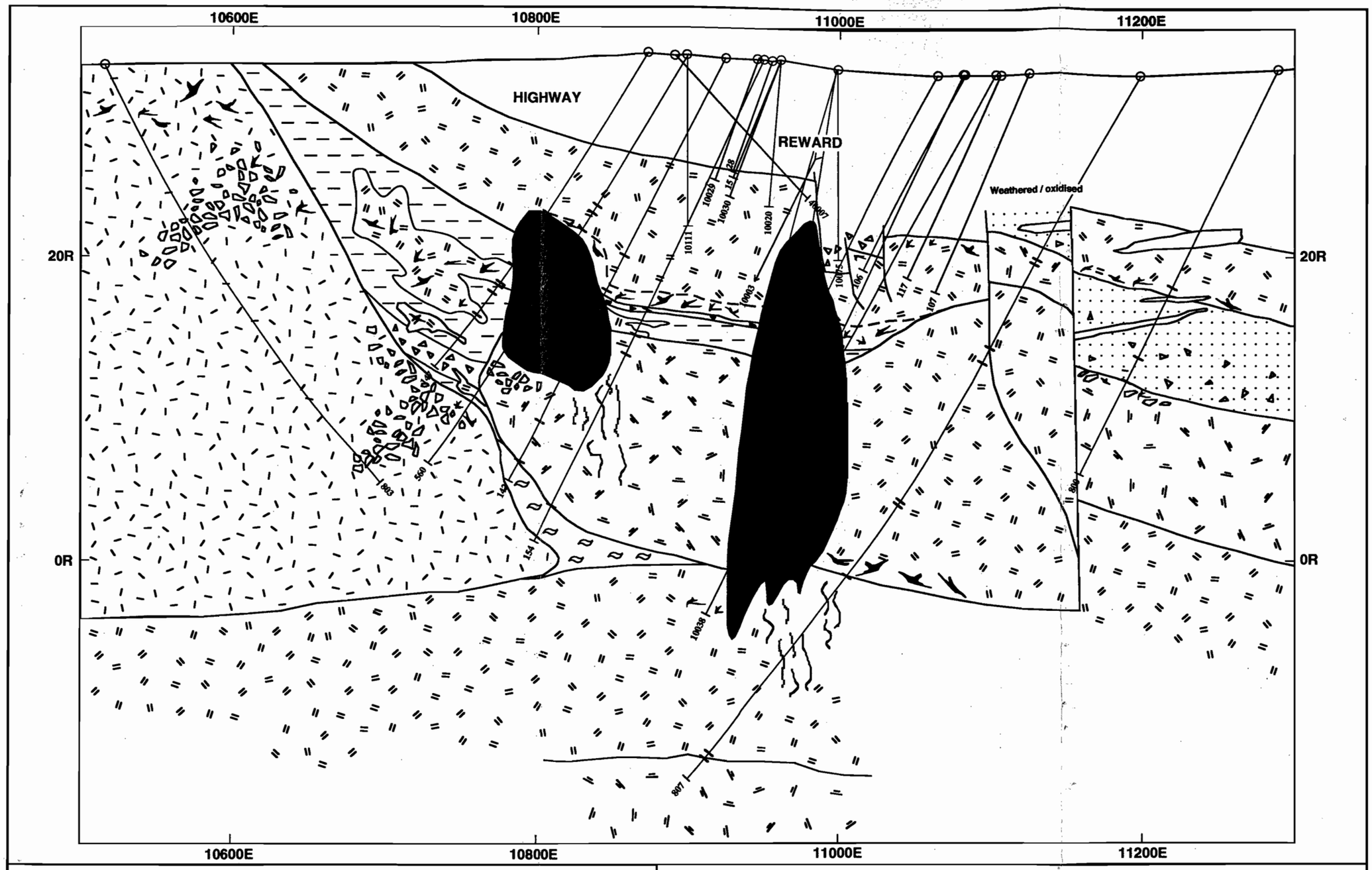

	CODES, University of Tasmania		
	Mapped: M. Doyle	**Mount Windsor Volcanics, Queensland**	**Scale: 1: 2500**
	Date: 20 / 10 / 95	**Highway-Reward**	**Figure: 2**
		Geological X-Sect 10150N ± 15 m	

Sericite

Sericite-silica

Silica-sericite

Silica ± pyrite

Sericite-silica-chlorite

Sericite-chlorite

Chlorite

Chlorite-silica ± sericite

Chlorite-sericite

Chlorite-sericite-silica

Silica - K-feldspar

K-feldspar-chlorite

K-feldspar-sericite

K-feldspar-sericite-silica-chlorite

Hematite

Hematite-sericite

Hematite-chlorite

Sericite (± silica)-hematite

Silica-hematite

Chlorite (± sericite)-carbonate

Sericite-carbonate

Clay

Andesite

Dacite

Rhyolite

Rhyodacite

Flow banding

Hyaloclastite

Peperite

Polymict lithic breccia

Monomict lithic breccia

Crystal-rich sandstone

Crystal-pumice breccia-sandstone

Crystal-lithic breccia-sandstone

Pumice breccia

Siltstone clasts, intraclasts

Siltstone

Stringer veins

Massive sulfide

Intensely altered

Fault

Key to figures 2, 4a-c and 5: Distribution of alteration and volcanic facies along section 10150N, Highway-Reward, Mount Windsor Volcanics.

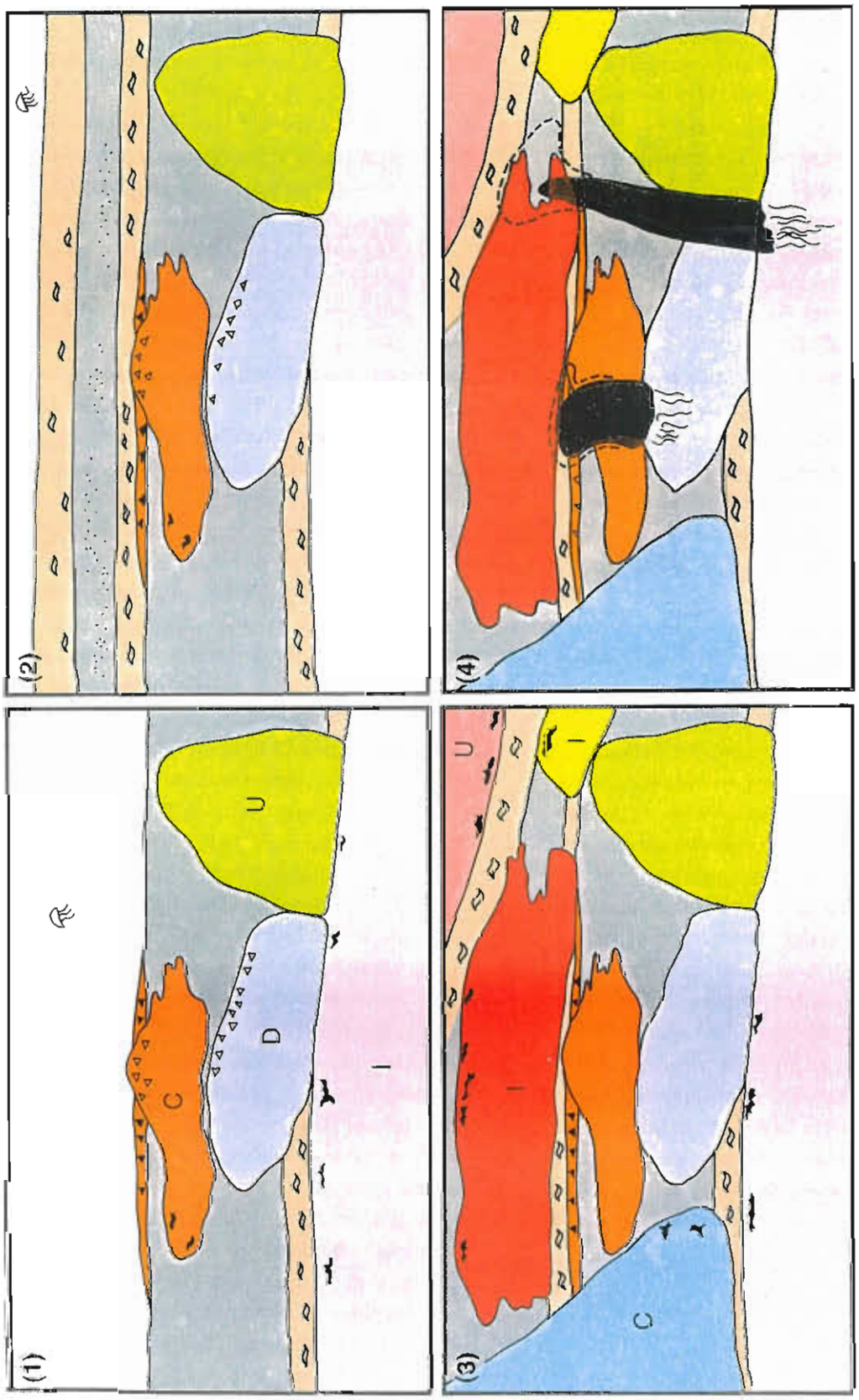

Figure 3: Schematic reconstruction showing successive stages (1–4) in the development of the Highway–Reward volcanic centre. Pyrite–chalcopyrite pipes are subseafloor replacements of the host sediment, syn-sedimentary intrusions, lava domes, and autoclastic breccia.

the texture and mineralogy of each alteration stage, and mineralisation. Graphic lithological logs are an effective way of presenting this information as the nature and positions of contacts, volcanic textures and facies, alteration mineralogy, and mineralisation are visible at a glance (Fig. 4a–c). Textural relationships between each alteration stage and the pre-alteration texture, and mineral abundances and associations, have been recorded using a code system which is detailed in appendix 1. Three alteration styles are identifiable: (a) alteration associated with domes and syn-sedimentary intrusions; (b) diagenetic alteration of pumiceous and crystal-rich volcaniclastics; (c) hydrothermal alteration concurrent with mineralisation. Detailed investigations of each are scheduled for early 1996. Following are some preliminary observations concerning alteration associated with mineralisation.

- The Highway and Reward pyrite–chalcopyrite pipes are underlain by zones of intense sericite–silica alteration resulting from the upward flow of mineralising fluids through the volcanic pile. They enclose domains (pipes ?) of intense silicic alteration interpreted to represent regions of more focussed flow (Fig. 5).
- Quartz–pyrite stringer veins up to 15 cm in width extend beneath the pipe within the sericite–silica zone and represent mineralised feeders.
- Small zones of intense chlorite alteration occur within the sericite–silica zones beneath the Highway and Reward deposits. At the margin of the Reward pipe, pods of cleaved pervasive chlorite alteration contains euhedral anhydrite crystals to 1.5 cm. Anhydrite may have been deposited during the waning stages of the hydrothermal system as hydrothermal fluids interacted with seawater in the enclosing volcanosedimentary package.
- Sericite–silica alteration gives way laterally and vertically to pervasive and patchy sericite–chlorite±silica and chlorite–sericite alteration. Included are small zones and large domains of pervasive chlorite alteration, which along the margins of the pyrite pipes contain disseminations, patches and spots of sphalerite–galena–barite.
- Weak to moderate sericite–silica alteration extends into a hangingwall intrusive rhyolite above the Highway and Reward pyrite pipes on some sections. These alteration zones record pathways for high-temperature mineralising fluids which progressed towards the seafloor position(s) at the time of mineralisation.
- Poorly focussed fluid flow to the west and east of the Highway and Reward deposits produced zones of weak to moderate sericite–silica alteration.
- Albite–silica–chlorite (± carbonate) alteration of pumice breccia and perlitic rhyolite–dacite is interpreted to be unrelated to mineralisation. This alteration style is the product of early diagenetic or hydrothermal alteration of volcanic glass.
- Patchy and pervasive hematite and silica–hematite–geothite alteration are common throughout the Trooper Creek Formation at the margins of, and within, lava domes and syn-sedimentary intrusions. They also occur as stratiform lenses enclosed by volcaniclastics. Many of these occurrences are interpreted as unrelated to mineralisation and record hydrothermal alteration/replacement/exhalation concurrent with volcanism (cf. Sigurdsson 1977).

Conclusions

The Highway and Reward massive sulfide deposits are hosted in the proximal facies association of a submarine (below-wave-base), non-explosive, silicic volcanic centre dominated by intrusive-extrusive porphyries. Pyrite–chalcopyrite pipes and marginal sphalerite–galena–barite mineralisation are subseafloor replacements of the host sediment, synvolcanic intrusions, lavas, and volcaniclastics. Alteration associated with mineralisation is zonally arranged around the pyrite–chalcopyrite pipes. High temperature mineralising fluids transgressed lithologies above the pipes so that alteration in the footwall and hangingwall is similar. Graphic lithological logs are and effective way of examining interrelationships between alteration and the nature and positions of contacts, volcanic textures and facies, and mineralisation.

References

Beams, S.D., Laing, W.P. and O'Neill, D.M., 1989. The exploration history and geology of the polymetallic Reward deposit, Mount Windsor volcanic belt, north Queensland. In: North Queensland Gold 89, Townsville, Australia: 95–102

Berry, R.F., Huston, D.L., Stolz, A.J., Hill, A.P., Beams, S.D., Kuronen, U. and Taube A., 1992. Stratigraphy, structure and volcanic-hosted mineralisation of the Mount Windsor subprovince, North Queensland, Australia. *Economic Geology* 87: 739–763

Cas, R.A.F., 1978. Silicic lavas in Paleozoic flysch-like deposits in New South Wales, Australia: Behaviour of deep subaqueous silicic flows. *Geological Society of America Bulletin* 89: 1708–1714

Clough, B.J., Wright, J.V. and Walker, G.P.L., 1982. Morphology and dimensions of the young comendite lavas of La Primavera volcano, Mexico. *Geological Magazine* 5: 477–485

Cortesse, M., Frazzetta, G. and La Volpe, L., 1986. Volcanic history of Lipari (Aeolian Islands, Italy) during the last 10,000 years. *Journal of Volcanological and Geothermal Research* 27: 117–133

Doyle, M.G., 1994. Facies architecture of a submarine volcanic centre: Highway–Reward, Mount Windsor Volcanics, Cambro-Ordovician, Northern Queensland. *In* Henderson RA and Davis BK, *New developments in geology and matallogeny: Northern Tasman Orogenic Zone*: 149–150

Doyle, M.G. and McPhi,e J., 1994. A silicic submarine syn-sedimentary intrusive-dome-hyaloclastite host sequence to massive sulfide mineralisation: Mount Windsor Volcanics, Cambro-Ordovician, Australia. *IAVCEI International Volcanological Congress, Ankara, Turkey, Abstracts*

Henderson, R.A., 1986. Geology of the Mt Windsor Subprovince-a lower Palaeozoic volcano-sedimentary terrain in the north Tasman Orogenic Zone. *Australian Journal of Earth Science* 33: 343–364

McBirney, A.R., 1963. Factors governing the nature of submarine volcanism. *Bulletin Volcanologique* 26: 455–469

Walker, G.P.L., 1989. Gravitational (density) controls on volcanism, magma chambers and intrusions. *Australian Journal of Earth Science* 36: 149–165

Pichler, H., 1965. Acid hyaloclastites. *Bulletin Volcanologique* 28: 293–310

Sigurdsson, H., 1977. Chemistry of the crater lake during the 1971–72 Soufrière eruption. *Journal of Volcanological and Geothermal Research* 2: 165–186

Yamamoto, T., Soya, T., Suto, S., Uto, K., Takada, A., Sakaguchi, K.and Ono, K., 1991. The 1989 submarine eruption off eastern Izu Peninsula, Japan: ejecta and eruption mechanisms. *Bulletin Volcanologique* 53: 301–308.

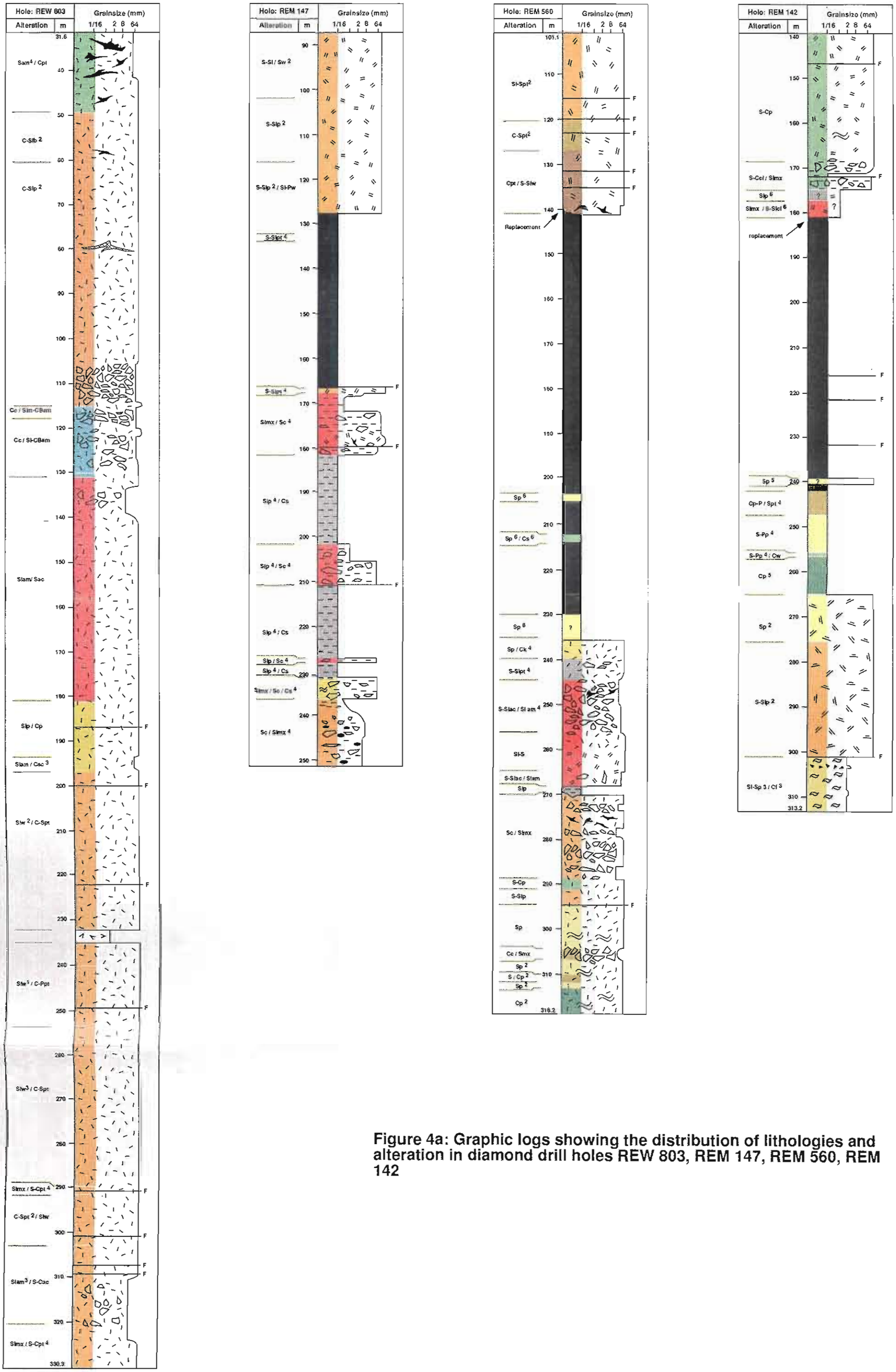

Figure 4a: Graphic logs showing the distribution of lithologies and alteration in diamond drill holes REW 803, REM 147, REM 560, REM 142

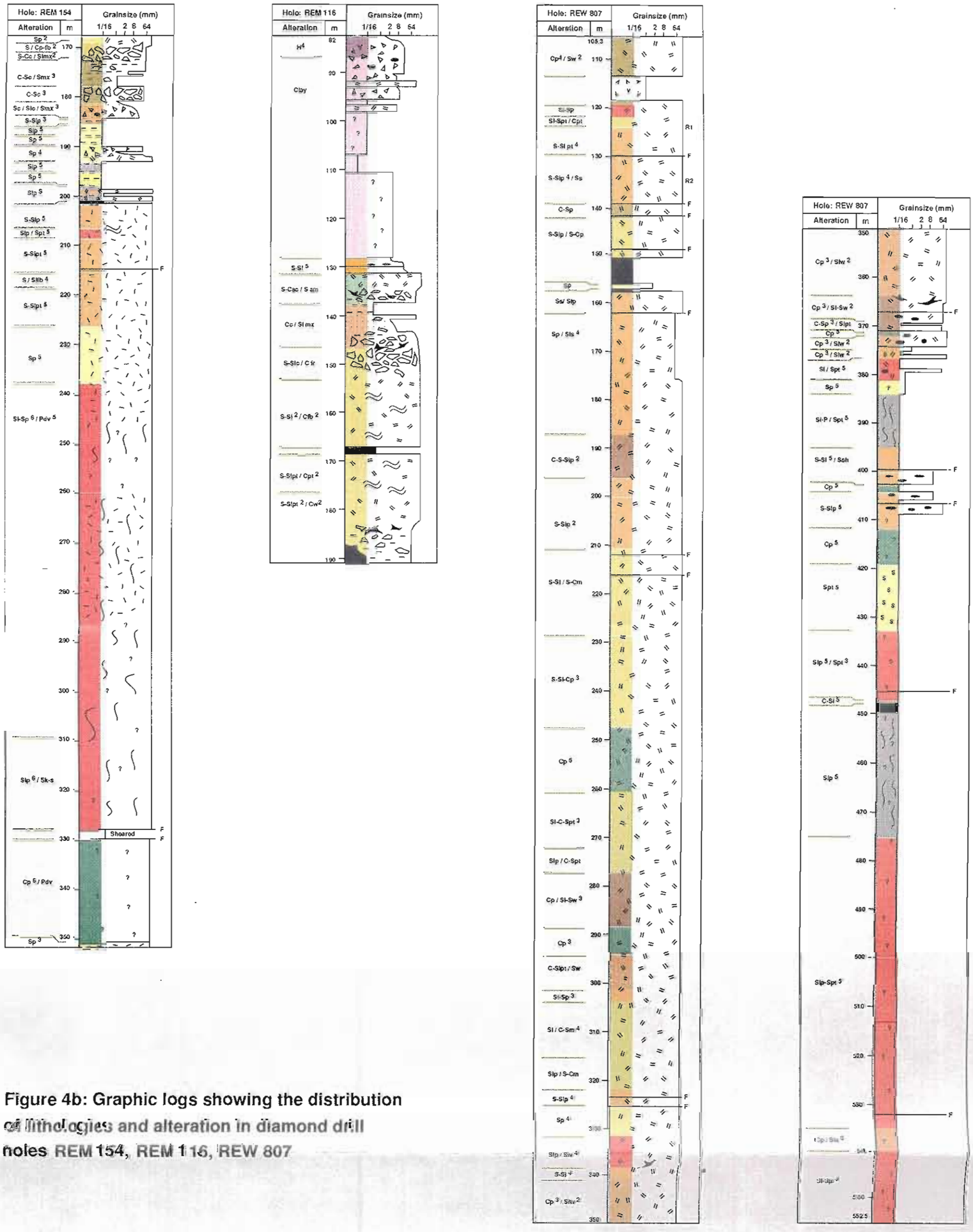

Figure 4b: Graphic logs showing the distribution of lithologies and alteration in diamond drill holes REM 154, REM 116, REW 807

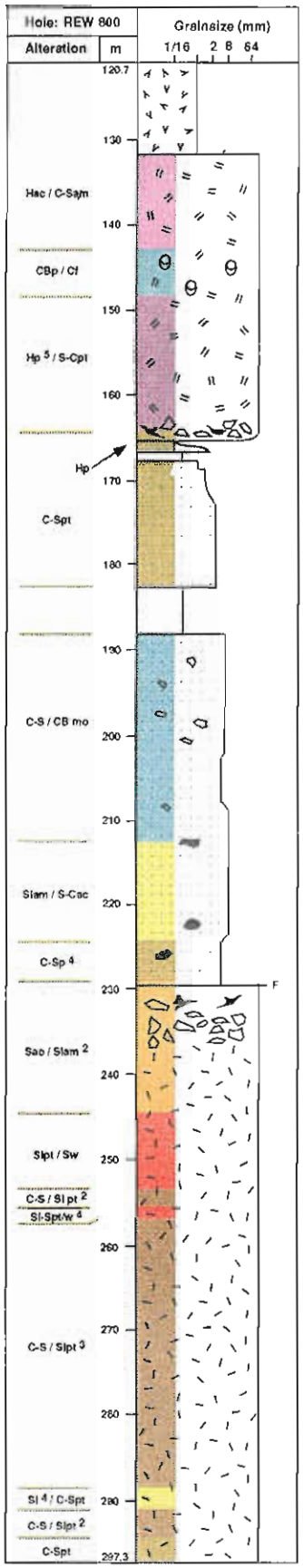

Figure 4c: Graphic log showing the distribution of lithologies and alteration in diamond drill hole REW 800

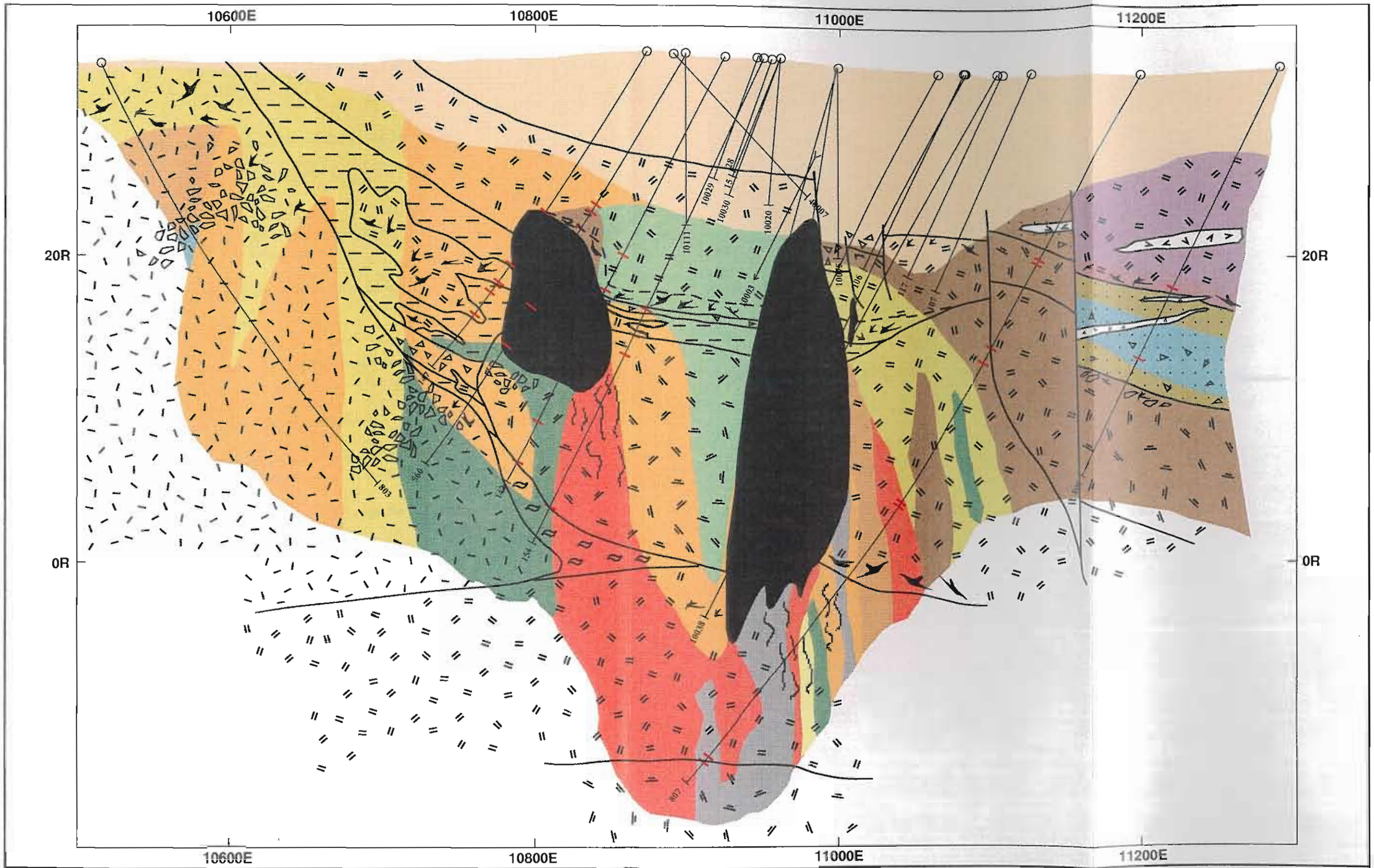

CODES, University of Tasmania

Mapped: M. Doyle	Mount Windsor Volcanics, Queensland	Scale: 1: 2500
	Highway-Reward	
Date: 16 / 10 / 95	Simplified geology & alteration x-section 10150N ± 15 m	Figure: 5

Appendix 1: Facies codes for alteration in volcanic rocks

(a) Phase(s)

- phase or phases comprising each alteration domain; e.g. chlorite, sericite–silica.
- capital letters
- substitute code for colour

C — chlorite	S — sericite
SI — silica	K — potassium feldspar
H — haematite	CB — carbonate

S–SI silica–sericite (two-phase alteration comprising an alteration domain)

(b) Relative abundance (phases - domains)

- the least abundant phase within an alteration domain is presented on the RHS, and the most abundant phase on the LHS.

e.g. S-SI (sericite–silica) dominant phase–subordinate phase

- in a rock comprising two or more alteration domains the phase(s) comprising the most significant domain are presented on the LHS and those of remaining domains on the RHS in ascending order.

e.g. C/S–SI (chlorite and sericite–silica) dominant ⇒ subordinate domain

(c) Intensity

- allocation of a number to describe the intensity each alteration domain

Low	(1-2)
Medium	(3-4)
High	(5-6)

e.g. C^5 ; $S\text{-}SI^3$; $C^2/S\text{-}SI^5$

(d) Controls/textures

- lower case

mx - matrix	x - crystal / phenocryst	sh - shear
c - clasts	p - pervasive	fi - fiamme
f - fracture (perlite, quench)	m - motley	ac - apparent clast
hf - hydraulic fracture	w - wash	am - apparent matrix
fb - flow banding	s - spotty	k - fleck

e.g. C_m^5 ; $S\text{-}SI_f^3$; C_p^2 / $S\text{-}SI_f^5$